ADDIS ABABA UNIVERSITY

ETHIOPIAN INSTITUTE OF WATER RESOURCES

HYDROLOGICAL SIGNIFICANCE OF ENSET-BASED LAND USE SYSTEM AND ITS ROLE IN WATER RESOURCES AND WATERSHED MANAGEMENT IN MEKI RIVER WATERSHED, LAKE ZIWAY SUB-BASIN, CENTRAL RIFT VALLEY OF ETHIOPIA

ALEMU BEYENE WOLDESENBET

PRESENTED IN FULFILLMENT OF THE REQUIREMENTS FOR THE DEGREE OF DOCTOR OF PHILOSOPHY (PH.D) IN WATER RESOURCES ENGINEERING AND MANAGEMENT

SUBMITTED

TO

ETHIOPIAN INSTITUTE OF WATER RESOURCES

WATER RESOURCES ENGINEERING AND MANAGEMENT PROGRAM

SEPTEMBER, 2023

ADDIS ABABA, ETHIOPIA

Hydrological Significance of Enset-Based Land Use System and its Role in Water resources and Watershed Management in Meki River Watershed, Lake Ziway Sub-Basin, Central Rift Valley of Ethiopia

Alemu Beyene Woldesenbet GSR/0070/07

Presented in Fulfillment of the Requirements for the Degree of Doctor of Philosophy (Ph.D) in Water Resources Engineering and Management

Submitted

To

Ethiopian Institute of Water Resources (EIWR)

Water Resources Engineering and Management (Surface water Management Specialization)

Supervisors:

Prof. Sebsibe Demisew, Professor, Addis Ababa University, Ethiopia

Prof. Mekuria Argaw, Professor, Addis Ababa University, Ethiopia

Dr. Azage Gebreyohannes, Ass. Professor, Addis Ababa University, Ethiopia

Addis Ababa University,

Addis Ababa, Ethiopia

September, 2023

Declaration

I, Alemu Beyene Woldesenbet, declare that this Doctoral dissertation entitled **“**Hydrological Significance of Enset-Based Land Use System and its Role in Water resources and Watershed Management in the Meki River Watershed, Lake Ziway Sub-Basin, Central Rift Valley of Ethiopia**”** is my own original work and the work has not been presented elsewhere for assessment other than for peer reviewed publication. Sources, aides and advisors that herein have been used and/or consulted are properly cited and noted.

Alemu Beyene ________________ September, 2023

Signature Date

Dissertation Approval

This is to certify that the thesis prepared by Alemu Beyene entitled *"Hydrological Significance of Enset-Based Land Use System and its Role in Water resources and Watershed Management in Meki River Watershed, Lake Ziway Sub-Basin, Central Rift Valley of Ethiopia"* and submitted in fulfillment of the requirements for the Degree of Doctor of Philosophy in Water Resources Engineering and Management complies with the regulations of the University and meets the accepted standards with respect to originality and quality.

Approved by Board of Examiners:

Hydrological Significance of Enset-Based Land Use System and its Role in Water resources and Watershed Management in Meki River Watershed, Lake Ziway Sub-Basin, Central Rift Valley of Ethiopia

Alemu Beyene Woldesenbet GSR/0070/07

Presented in Fulfillment of the Requirements for the Degree of Doctor of Philosophy (Ph.D) in Water Resources Engineering and Management

Submitted

To

Ethiopian Institute of Water Resources (EIWR)

Water Resources Engineering and Management (Surface water Management Specialization)

Approved by Board of Examiners:

Name	Signature	Date
Sebsebe Demisew (Professor) Main Advisor	Signature	date
Mekuria Argaw (Professor) Main - Advisor	Signature	date
Azage Gebreyohannes (PhD) Co - Advisor	Signature	date
Alemseged Tamiru (PhD) Internal Examiner	Signature	date
Gebremedhin Tesfaye (PhD) Internal Examiner	Signature	date
Adane Abebe (PhD) External Examiner	Signature	date
Mamo Kasegn Chair Person	Signature	date
Tilahun Derib (PhD) EIWR Education Coordinator	Signature	date
Zeleke Agide (PhD) EIWR Director	Signature	date

Abstract

Modeling the hydrological significance of Enset-Based Land Use System is critical for estimation, planning, management and sustainability of current and future water resources. The main objective of this study is to model the hydrological significance of EBLUS and its contribution for water resources and watershed management in Meki River Watershed, Lake Ziway Sub-Basin, central Rift Valley of Ethiopia. This work pursued: EBLULC change detection and dynamics analysis using Remote sensing softwares and evaluated it's significance on soil erosion control using RUSLE model and Geo-statistical and statistical tools; it invoved measurement and analysis of infiltration rate of the soil using Amozi-meter and collection of organic carbon stock data; it seeks to interpolate the Curve Number matrix for EBLUS with respect to other land use systems with predetermined CN matrix; it presents the impact of EBLUS on magnitude of surface runoff using HEC-HMS and it evaluates the implications of EBLUS for the water resources and watershed management for sustainability of water bodies. As a result an increase in EBLUS over the last thirty years by 11.2% was observed without much loss (stable), the difference in soil loss for non-enset growing zones and enset growing zones were evaluated as 1.405t $ha^{-1}yr^{-1}$. Higher mean infiltration rate in EBLUS (12.8125 $mmhr^{-1}$) next to Forests (12.9675 $mmhr^{-1}$) caused in the lowest average CN of EBLUS (52.6). Calibration (NSE=76.25) and validation (1990-1994) (NSE=62%) results confirmed that the adequacy of the HEC-HMS model for runoff simulation. 11.26% of surface runoff infiltrated due to the presence of EBLUS. The high surface runoff in the lower sub-watersheds than the upper sub-watersheds indicates the contribution of EBLUS is high in the watershed despite the area coverage of EBLUS was low (10%). Generally, EBLUS increases the canopy cover of the watershed, decrease the truction power of rainfall, reduce the soil loss in the watershed, increase infiltration rate of the soil and reduce the magnitude of surface runoff and contribute to the sustainability of water bodies. Therefore, expanding the coverage of the EBLUS can improve the hydrological components to enhance water absorption into the ground water system and contribute to the water resources and ecological sustainability of the surrounding in addition to its social, economic, food security, environmental and microclimatic importance of the watershed which have a direct influence on water resources and watershed management in Meki river watershed.

Keywords: Enset, Infiltration, CN, Amozi-meter, Geostatistics

Acknowledgements

I would like to thank my Almighty God, for his endless love, for he gives me strength, health and healthy mind to complete my PhD dissertation work properly and great thanks be to him forever.

It gives me great pleasure to share my gratitude to Professor Sebsibe Demissew for his deep sympathy and it is not easy to express the role and contribution of Professor Mekuria Argaw in words that I can only want to say thank you for that you have built my life. I would like also to thank Dr Dessie Nidaw and Dr Solomon Gebrehiwot for reviewing the curve number and flow modeling portion of my desertation. I have kept Dr Azage Gebreyohanes in my heart for his extremely positive, innocent, loving, very kind, hard working, supportive, committed and genuine cooperation and help on my needs. Unfortunately, I feel so troubled whenever I remember his sudden pass away. I gratefully acknowledge the great contributions of Dr Feleke Zewge and Dr. Bikila from Addis Ababa University, College of Natural and Computational Sciences and Dr Zeleke Agide, Dr Sirak Tekleab and Mr Mamo Kassegn from Ethiopian institute of water resources for their cooperation on my needs. Thank you my families and friends who shared my good or bad feelings.

I show gratitude to the keen cooperation of College of Natural and Computational Sciences, Department of Plant Biology and Biodiversity Management (AAU) thematic research fund and Ethiopian Institute of Water Resources (AAU) for financial support. I would also like to thank the Ministry of Water and Energy (MOWE) of Ethiopia, National Meteorology Agency (NMA), Central Statistical Agency (CSA) of Ethiopia, Geospatial & Mapping Agency (GSMA) of Ethiopia, Ethiopian Institute of Water Resources (EIWR) of Addis Ababa University and United States Geological Survey (USGS) for providing necessary data, materials, equipment and information for this study.

Table of Contents

Contents **Page**

Lists of Figures

Lists of Tables

Abbreviations

AOI	Area of Interest
CASC2D	CASCade of planes in 2-Dimensions
CRV	Central Rift Valley
CSA	Central Statistical Agency of Ethiopia
DEM	Digital Elevation Model
DWSM	Dynamic Watershed Simulation Model
EBLUS	Enset-Based Land Use System
EGZ	Enset Growing Zone
ERA	Ethiopian oad Authority
ERDAS	Earth Resources Data Acquisition System
FAO	Food and Agriculture Organization of the United Nations
GPS	Geographical Positioning System
GSIA	Geospatial information agency of Ethiopia
HBV	Hydrologisika Bayraans Vattenbalans-avediling
HEC-GEOHMS	Hydrologic Engineering Center’s Geospatial Hydrologic Modeling System
HEC-HMS	Hydrologic Engineering Center’s Hydrologic Modeling System
HSG	Hydrologic Soil Group
HSPF	Hydrological Simulation Program-FORTRAN
HWSD	Harmonized World Soil Data

IIASA	International Institute for Applied Systems Analysis
IPCC	Intergovernmental Panel on Climate Change
ISRIC	International Soil Reference and Information Centre
IWRM	Integrated Water Resource Management
JRC	Joint Research Centre of the European Commission
LULCC	Land Uses and Land Cover Change
m.a.s.l.	Meter above Sea Level
MIKE SHE	European Hydrological System model (From Danish Hydraulic Institute)
MOA	Ministry of Agriculture
MOWIE	Ministry of Water and Energy of Ethiopia
WR	Water Resources
MRWS	Meki river watershed
NEGZ	Non-Enset Growing Zone
NMA	National Meteorology Agency of Ethiopia
PRMS	Precipitation-Runoff Modeling System
RUSLE	Revised Universal Soil Loss Equation
SCS-CN	Soil Conservation Services Curve Number
SWAT	Soil and Water Assessment Tool
TOPMODEL	Topographic Model
USDA	United State Department of Agriculture
USGS	United States Geological Survey
WASIM	Water balance Simulation Model

1. Introduction

1.1. Background and Justification

Enset (*Ensete ventricosum*, Musaceae) is an African crop that currently provides the staple food for approximately 20 million Ethiopians. Whilst wild enset grows over much of East and Southern Africa and the genus extends across Asia to China, it has only ever been domesticated in the Ethiopian Highlands where smallholder farmers cultivate hundreds of landraces across diverse climatic and agroecological systems (Borrell, *et al*, 2019).

Despite a widespread distribution in eastern, central and southern tropical Africa (Baker and Simmonds, 1953; Lock, 1993), enset has only been domesticated in Ethiopia (Brandt *et al.*, 1997). Here, hundreds of landraces are found in diverse climatic and agroecological systems (Birmeta *et al.*, 2002; Tesfaye and Lüdders, 2003). Analysis of data from ECSA (CSA, 1995–2017) shows the area of land under enset production has increased approximately 46% over the past twenty years, whilst yield has been reported to increase twelve fold (Borrell, *et al*, 2020).

South and southwestern parts of Ethiopia are among the potential producers of enset as a staple and co-staple source of food (Ambachew, *et al*, 2018; Spring *et al*. 1996). Enset is widely accepted and adopted by rural community because it is rich in carbohydrate and mineral substances (calcium and iron) (Ambachew, *et al*, 2018) and also it help to prevent soil erosion (Ambachew, *et al*, 2018; Shigeta 1990).

According to Tesfaye and Bongers (2012), households on average have roughly one quarter of their homegarden area devoted to enset; there are large variations across sites and between households within a site. Various socioeconomic factors (e.g. farm size, access to markets) and biophysical factors (e.g. altitude) influence how much land farmer's use for enset production. Farmers with large farms have a lower proportion of their land under enset and poor farmers generally have small land holdings and need to produce early maturing crops for their subsistence, as they cannot afford to wait four or more years after planting before the enset crop can be harvested (Tesfaye and Bongers, 2012). Farmers with good market access devote a smaller proportion of their land to growing enset and a higher proportion to cash crops (Tesfaye and Bongers, 2012).

The most important biophysical factor influencing the area share of enset is altitude. In the intermediate highland (Woyna dega) agroecological zone where altitude ranges from 1,500 to 2,200 m, the share of enset increases with altitude (Tesfaye and Bongers, 2012). In the warmer and relatively drier low altitude sites (1,500-1,750 m) farmers grow more of other food crops, mainly maize (Abebe, 2005). According to Tesfaye and Bongers, 2012; Abebe *et al.*, 2010, the variation among farmers and the impacts of such drivers show that the landuse systems in southern region are dynamic: farmers make individual choices and respond to emerging challenges and opportunities that forces the system to be coined as Enset-based land use system (EBLUS).

The Enset-based land use system (EBLUS) where Enset (*Enset ventricosum*) is cultivated as the main staple or co-staple food with other crops is one of the major farming systems in our country (Fetta , 2019; Almaz, 2001; Westphal, 1975). Central statistics agency of Ethiopia has reported that, 302,000 ha of land are covered by enset plant in Ethiopia. Out of the total enset plant production, 211,000 ha of land covered by enset plant found in South Nations and Nationalities of People Regional State (SNNPR). In general, around 75% of enset plant production is located in southern part of the country (Ambachew, *et al*, 2018) including Meki River Watershed although sufficient information was not available.

Eventhough some studies were conducted about enset and EBLUS, the hydrological components are missing. According to Beven (2001), techniques for the analysis of the impact of LULCC on modeled hydrological responses are still very much at early stage and the prediction of the effect of future change has hardly even started. Analogically, the effect of EBLUS change on hydrological and watershed processes was not formerly been recognized and quantified. Therefore, Modeling the hydrological significance of EBLUS was critical for estimation, planning, and management of current and future water resources and watershed sustainability in the watershed.

1.2. Problem statement

In Enset-based land use system (EBLUS), enset grows as an indigenous and herbaceous monocot banana-like perennial plant that grows best at an altitude of 1600 to 3100 m.a.s.l., average temprature of 16°C to 20°C, a relative humidity of 60 to 80%, annual rainfall of 1100 mm to 1500 mm and its leaves reaches a height of 5 to 13 m (Borrell *et al.*, 2020; Uloro & Mengel, 2014).

The enlarged pseudo-stem and underground corm (carbohydrates) of enset is used for human consumption (Michael, 2002) and its products are used for everything from food wrapping to medicinal purposes throughout the southern part of Ethiopia (Uloro & Mengel, 2014). The production of Enset is attractive to farmers due to the resistance to relatively prolonged soil moisture stress or drought, higher yield compared to other cultivated crops in the region and the minimum input required to produce it.

The anti-famine, anti-drought and food security enhancing nature of Enset-based farming systems (Anita, *et al.,* 1996) that was constrained mainly by land degradation (Tilahun & Robert, 2006) points to the need for further consideration of Enset to research, development and policy although very little attention has been paid to it and there was a lack of appreciation of the number of people who depend on this root crop and the number of lives that have been saved during drought and the resulting famine (Uloro & Mengel, 2014) by policymakers and researchers as most of their efforts have been concentrated on cash crops or the more familiar grains (Anita, *et al.,* 1996).

Some studies were conducted by different scholars regarding the socio-economic (Shiferaw, 2003), yield and inputs required (Uloro & Mengel, 2014), the sources of income (Mbow, *et al.*, 2014; Tilahun & Robert, 2006), physiology (Admasu and P.C.Struik, 2003), ecosystem services (Mesfin, *et al.*, 2017), agronomy (Admasu, 2007), breeding (James Harrison, 2014), pathology (Bridge, 1992), postharvest (Yirmaga, 2013) and soil nutrition (Elias, 2011) aspect of enset and EBLUS but the hydrological and watershed components are missing (Beven, 2001). Analogically, the effect of EBLUS change on hydrological processes was not formerly been recognized and quantified: the EBLUS change and dynamics (stability) was not studied; the impact of EBLUS on soil erosion was not well conducted; the impact of EBLUS on surface water resources were not fully understood (Nejadhashem, et al., 2011; Wang, et al., 2007).

The contribution of EBLUS to ecological stability, watershed management, infiltration rate of the soil, surface runoff and other hydrological componenets was not studied well in the Meki river watershed (MRWS). In addition, curve number (CN) matrix was previously developed for all land use systems (LUSs) except for EBLUS (ERA, 2013; Oliver et al., 2006; Anita, et al., 1996) thence, it forces us to focus on developing a CN matrix for EBLUS as a contribution for science community.

Considering the importance of Meki river watershed to the sustainability of lake Ziway and absence of hydrological studies in the watershed, detailed watershed and hydrological modeling and analysis were needed at different scales. Therefore, Modeling the hydrological significance of EBLUS was critical for estimation, planning, and management of current and future water resources and watershed sustainability in the watershed. Hence, the aim of this study was initiated to examine the significance of Enset-Based land use system (EBLUS) on Curve Number, infiltration rate, surface runoff and soil erosiom vis-a-vis other land use systems with established hydrological characteristics at both landscape unit and watershed scales, under finer and more detailed resolution than existing studies and also to quantify its contribution for water resources and watershed management.

1.3. Research Questions

The core research question for this study is "**What are the hydrological significance of EBLUS and its contribution to water resources and watershed management?**"

List of specific research questions:

1. How the EBLUSC & its dynamics (stability analysis) over the last 30 years in Meki river watershed (MRWS) looks like?
2. What is the effect of EBLUS change on soil loss over 30 years in MRWS?
3. What is the influence of EBLUS on infiltration rate and CN of the soil in MRWS?
4. How can we interpolate the curve number of EBLUS relative to other LUS in MRWS?
5. What is the effect of EBLUS on magnitude of surface runoff, water resources and watershed management in MRWS?

1.4. Research Objectives

1.5. General Objective

The main objective of this study is to model the hydrological significance of Enset-Based land use system (EBLUS) and its contribution for water resources and watershed management in Meki river watershed (MRWS).

1.5.1. Specific objectives:

1. Assessment of land use land cover change and dynamics (stability) for different land use land covers;
2. To determine the effect of EBLUS on the magnitude and rate of soil erosion;
3. To identify the contribution of EBLUS on infiltration rate of the soil;
4. To interpolate the CN matrix of EBLUS and to quantify the effect of EBLUS on CN of the soil;
5. To model the effect of EBLUS on magnitude of surface runoff and to discuss its effect on water resources and watershed management in Meki river watershed.

1.6. Significance of the study

The upper most part of MRWS with very steep slopes are being cultivated for cereal based crops, which exposes the surface of the soil to rain drop impacts that aggravates erosion in the area in addition to the topographic factors. EBLUS is expanding in the middle portion of the watershed which helps in erosion control and other hydrological importance.

Therefore, detail study of EBLUS has vital importance in controlling the hydrological components of the watershed to contribute for sustainable water resources and watershed management. The research fills a gap in knowledge of hydrological implication of EBLUS and its role in water resources and watershed management, which has not been studied before. Altogether, this study provides important information for climate change mitigation motivators, planners, researchers, decision makers, conservationists, foresters, land administrators, sustainability motivators and other stakeholders in the MRWS.

1.7. Limitation of the study

This study was planned to the level of demonstration site establishment but it was interrupted by policy change of US during 2017G.C. In addition, the financial stress was a significant dragging factor which limited the work to the current detail that required further additional details. In addition to cancelation of demonstration level research planned due to US policy change, conflicts at different portion of the watershed created inconvinience for the easy movement and data collection works.

1.8. Structure of the Thesis

Chapter one pursues the background, research questions, research objectives, limitation of the study while the second chapter discusses the literature review regarding the study gaps in Hydrological Significance of EBLUS and its Role in WR and WSM in Meki river watershed. In the third chapter, materials and methods of study was discussed while the fourth chapter covers the result and discussion part that addresses: 1) Enset-Based land use land cover change (EBLULCC) detection, dynamics (stability) analysis and its impact on soil erosion 2) Interpolation of Curve Number matrix for EBLUS with respect to other land use systems with predetermined CN matrix 3) Modeling the contribution of EBLUS to modify the magnitude of surface runoff, WR and WS management in MRWS. Conclusion and Recommendations are presented in the fifth chapter.

2. Literature Review

2.1. Enset distribution, production and sustainability in Ethiopia

Enset (*Ensete ventricosum*, Musaceae) is an African crop that currently provides the staple food for approximately 20 million Ethiopians. Whilst wild enset grows over much of East and Southern Africa and the genus extends across Asia to China, it has only ever been domesticated in the Ethiopian Highlands where smallholder farmers cultivate hundreds of landraces across diverse climatic and agroecological systems (Borrell, *et al*, 2019).

Despite a widespread distribution in eastern, central and southern tropical Africa (Baker and Simmonds, 1953; Lock, 1993), enset has only been domesticated in Ethiopia (Brandt *et al.*, 1997). Here, hundreds of landraces are found in diverse climatic and agroecological systems (Birmeta *et al.*, 2002; Tesfaye and Lüdders, 2003). Analysis of data from ECSA (CSA, 1995–2017) shows the area of land under enset production has increased approximately 46% over the past twenty years, whilst yield has been reported to increase twelve fold (Borrell, *et al*, 2020).

South and southwestern parts of Ethiopia are among the potential producers of enset as a staple and co-staple source of food (Ambachew, *et al*, 2018; Spring *et al*. 1996). Enset is widely accepted and adopted by rural community because it is rich in carbohydrate and mineral substances (calcium and iron) (Ambachew, *et al*, 2018) and also it help to prevent soil erosion (Ambachew, *et al*, 2018; Shigeta 1990).

2.2. Land Use and Land Cover Change Studies in Ethiopia

Land cover is defined as the physical materials on the surface of a given parcel of land (e.g. grass, concrete, tarmac, water) and Land use is defined as the human activity that takes place on or makes use of that land (e.g. residential, commercial, industrial). Land use can consist of varied land covers, (i.e. a mosaic of biogeophysical materials found on the land surface). For instance, a single family residential area consists of a pattern of land – cover materials (e.g. grass, pavement, shingled rooftops, trees, etc.) (Treitz & Rogan, 2003). The aggregate of these surfaces and their prescribed designations (e.g. Park) determines land use (Anderson *et al*., 1976).

Land use is an abstract concept, constituting a mix of social, cultural, economic and policy factors, which have little physical importance with respect to reflectance properties, and hence has a limited relationship to remote sensing. Remote sensing data record the spectral properties of surface materials, and hence, are more closely related to land cover (Treitz & Rogan, 2003).

The Changes in land cover driven by land use can be modification and conversion (Mekuria, 2005 and Ermias *et al.,* 2013) which can be detected using remote sensing (Treitz and Rogan, 2003). Information derived from RS data has often been used to assist in the formulation of policies and provide insight in to LCLU patterns (Loveland *et al.,* 2002).

Studies that have been carried out at different parts of Ethiopia indicated that croplands have expanded at the expense of natural vegetation, including forests and shrublands; for instance Solomon, 1994 (West Ethiopia); Gete and Hurni 2001(North-Western Ethiopia); Belay 2002 (North Ethiopia); Girmay 2003 (North-Eastern Ethiopia); Gregor *et al.*, 2004 (South Ethiopia); Selamyihun 2004; Bewket, 2004 (North Ethiopia); Mekuria, 2005 (South-Western Ethiopia); and Solomon, 2005 (North Ethiopia).

Shibru *et al.* (2003) and Selamyihun (2004,) reported the effect of LULC change in causing major gullies and quantified the rate of expansion and their effects on the livelihoods of people in eastern and central highlands of Ethiopia but EBLUS was not considered in all former studies.

2.3. Land-use dynamics in enset-based agroforestry in Ethiopia

The long-term sustainability of agricultural production and the environmental consequences of the current intensification of agricultural systems are crucial elements to resolve the need to protect and conserve decreasing biodiversity with the need to feed, clothe and shelter a growing human population (Tesfaye and Bongers, 2012; Padoch and Pinedo-Vasquez, 2010). According to Tesfaye and Bongers, 2012; Kumar and Nair, 2006, attention needs to be given to achieve stability in the use of land in the long term like tropical homegarden integrated agroforestry land-use system which are better than the modern technologies in many remote areas for achieving sustainable agriculture (Tesfaye and Bongers, 2012; Abebe *et al.*, 2006; Godfray *et al.*, 2010), while at the same time meeting the needs of the local population (Tesfaye and Bongers, 2012; Godfray *et al.*, 2010; Matson *et al.*, 2002; Swift and Ingram, 1996; Tilman *et al.*, 2002).

The decomposition of litter and manuring (Tesfaye and Bongers, 2012; Hoogerbrugge and Fresco, 1993) maintain soil fertility which are generally considered to be economically efficient, ecologically sound and biologically sustainable agroforestry systems (Tesfaye and Bongers, 2012; Kumar and Nair, 2006).

The enset-coffee homegarden in Southern Ethiopia (Tesfaye and Bongers, 2012; Abebe, 2005; Abebe *et al.*, 2006, 2010) is characterised by a unique combination of two native perennial crops. Enset (Enset ventricosum Welw Cheesman) is the staple food in the region and coffee (Coffea arabica L.) the main cash crop. The homegardens are located at altitudes of 1,500-2,300 m, where moisture and temperature conditions are favourable for agriculture. The sites are characterized by a moist to sub-humid warm subtropical climate with average annual rainfall of 1000-1,800 mm and a mean temperature of 15-20 °C. Unlike most homegardens in the tropics, which are supplementary food production systems in addition to farm fields located elsewhere, the enset-coffee homegardens are 'integral' or complete farm systems from which farmers derive almost all their subsistence and cash needs (Tesfaye and Bongers, 2012; Abebe *et al.*, 2006).

Most of the homegardens in the area have evolved from forests. Farmers maintain the upper storey trees and clear the undergrowth to open up space for planting enset, coffee and other crops that contain three main components of agricultural biodiversity: crops, trees and livestock. The diversity and density of the crops vary spatially and temporally (Tesfaye and Bongers, 2012).

The high diversity with different uses and production cycles, is considered an essential component of sustainable agriculture that plays different roles in these systems like year-round production of food and wood products, decreased risks of production failure, increased productivity over time (Tesfaye and Bongers, 2012; Netting and Stone, 1996), maintenance of genetic diversity and landscape protection (Tesfaye and Bongers, 2012; Perfecto *et al.*, 2009). Hence, regarding the dynamics's hydrological implication is still a question in those areas including MRWS.

2.4. Dynamics in enset area composition and it's implication

According to Tesfaye and Bongers (2012), households on average have roughly one quarter of their homegarden area devoted to enset; there are large variations across sites and between households within a site. Various socioeconomic factors (e.g. farm size, access to markets) and biophysical factors (e.g. altitude) influence how much land farmer's use for enset production.

Farmers with large farms have a lower proportion of their land under enset and poor farmers generally have small land holdings and need to produce early maturing crops for their subsistence, as they cannot afford to wait four or more years after planting before the enset crop can be harvested (Tesfaye and Bongers, 2012). Farmers with good market access devote a smaller proportion of their land to growing enset and a higher proportion to cash crops (Tesfaye and Bongers, 2012).

The most important biophysical factor influencing the area share of enset is altitude. In the intermediate highland (Woyna dega) agroecological zone where altitude ranges from 1,500 to 2,200 m, the share of enset increases with altitude (Tesfaye and Bongers, 2012). In the warmer and relatively drier low altitude sites (1,500-1,750 m) farmers grow more of other food crops, mainly maize (Abebe, 2005).

According to Tesfaye and Bongers, 2012; Abebe *et al.*, 2010, the variation among farmers and the impacts of such drivers show that the landuse systems in southern region are dynamic: farmers make individual choices and respond to emerging challenges and opportunities.

2.5. Computing Change Detection Statistics

Use Change Detection Statistics to compile a detailed tabulation of changes between two classification images. The changes detected using this routine differs significantly from a simple differencing of the two images (ITT Industries, Inc., 2006). While the statistics report does include a class-for-class image difference, the analysis focuses primarily on the initial state classification changes; that is, for each initial state class, the analysis identifies the classes into which those pixels changed in the final state image (ITT Industries, Inc., 2006).

ENVI can report changes as pixel counts, percentages, and areas. In addition, you can produce a special type of mask image (classification masks) that provides a spatial context for the tabular report. The class masks are ENVI classification images with class colors matching the final state image, making it easy to identify not only where changes occurred but also the class into which the pixels changed.

The input images must be coregistered or georeferenced. For the most accurate results, carefully coregister the images before processing. If the input images are not coregistered, ENVI uses the available map information to automatically coregister the images, using the initial state image as the base if re-projection or resampling is required (ITT Industries, Inc., 2006).

The Change Detection Statistics window contains all of the statistics tables that you selected from the Report Type field in the Change Detection Statistics Output dialog box, separated by tabs. It also contains a Reference tab, which includes additional information about the analysis, such as the names of the input images and the equivalent class pairings (ITT Industries, Inc., 2006). Note that the initial and final state images do not have the same number of classes, and that only four of the five initial state classes are included in the Equivalent Class Pairings list (lakes & ponds is not used).

The statistics tables list the initial state classes in the columns and the final state classes in the rows. However, the columns include only the selected (paired) initial state classes, while the rows contain all of the final state classes. This is required for a complete accounting of the distribution of pixels that changed classes (ITT Industries, Inc., 2006).

2.6. Effect of Land Use Change and soil conservation intervention on Soil Properties and Processes

Land use is one of the main drivers of many processes of environmental change, as it influences basic resources within the landscape, including the soil resources (Antonio *et al.*, 2014). Poor soil management can rapidly deteriorate vast amounts of land, which frequently becomes a major threat to rural subsistence in many developing and developed countries (Antonio *et al.*, 2014).

Conversion of forest to cultivated land significantly influence soil properties and modify soil forming processes and it can affect soils and soil processes (Rezaei *et al.*, 2012; Chen *et al.*, 2000). Conversion from native forest to plantation forests altered the amount of soil organic carbon (SOC) (Rezaei *et al.*, 2012 and Smith *et al*., 2002) and it can also alter the chemical nature of soil organic carbon (Rezaei *et al.*, 2012; Quideau *et al.*, 2000). Several scientists reported that soil aggregate size distribution and stability were important indicators of soil physical quality which reflect the impact of land use and soil management (Rezaei *et al.*, 2012; Castro Filho *et al.*, 2002).

Conversion of forest to other land uses could result in higher bulk density, lower hydraulic conductivity, reduced in infiltration and higher susceptibility to soil erosion, thereby exacerbating soil degradation and decline in SOC concentration (Rezaei *et al.*, 2012; Lal, 2003; Taimeh *et al.*, 2015; Lal, 1988).

Socio-economic factors, including poverty, land fragmentation, low standards of living and earning, a low level of education, and health condition, were cited as drivers contributing to an increased risk of degradation during the last few decades (Taimeh *et al.*, 2015; Wakindiki and Ben-Hur, 2002).

Deforestation is considered a major cause of cover loss, which accelerates land degradation, increases erosion, and exacerbates degradation of the physical and chemical properties of soil (Taimeh *et al.*, 2015; Benneh *et al.*, 1996) and the transition from forest to another agricultural use leads to a significant reduction in organic matter in the topsoil, or may induce substantial modifications in the quality and quantity of soil organic matter (Taimeh *et al.*, 2015; Kocyigit and Demirci, 2012; Yimer and Abdelkadir, 2011; Riezebos and Loerts, 1998) as well as changes in soil properties (Taimeh *et al.*, 2015; Wang *et al.*, 2011; Tesfahunegn, 2013).

2.7. Land use land cover change and soil erosion

Vegetation cover is important for the protection of the soil surface from the beating action of raindrops (rain splash) and erosion by surface runoff. Studies in West Africa have shown annual erosion under natural forest cover lower than 500 kg/ha even on slopes up to 65 %, while rates were up to 1000 times higher from bare soil on similar slopes (Roose, 1986).

Morgan (1995) has insisted that soil erosion estimate of 10 t ha-1yr-1 was a proper level at which the agricultural experts should have an interest. Hurni (1993) estimated that soil loss due to erosion from cultivated fields in Ethiopia amounts to about 42 t ha-1yr-1. According to Herweg and Ludi (1999) soil erosion rates measured in the Anjeni is 17 t ha-1yr-1 to 176 t ha-1yr-1.

According to Hurni (1985) "tolerable" soil loss of about 2-18 t ha-1 yr-1 estimated for Ethiopia. The soil loss rates are also beyond the rate of soil generation or formation of 3-7 t ha-1 yr-1 (Hurni, 1985). The mean global rate of soil loss is 15 t ha-1yr-1 and mean rate of soil loss for Africa is 9 t ha-1yr-1 (Lulseged and Paul, 2008). The findings of Gunten (1993) and Eyasu (2002) as cited in Mekuria (2005) from the Gununo (Wolayta) area of southern Ethiopia is reported. Gunten (1993) reported a soil erosion rate of 13 t ha-1yr-1 in cultivated fields from runoff plot measurements on a slope gradient of 10-13%.

Eyasu (2002) reported 6-13 t $ha^{-1}yr^{-1}$ from cultivated fields and Mersha *et al.*, (2018) also reported annual soil loss of 31 t $ha^{-1}yr^{-1}$ in 1973 and 56 t ha^{-1} in 2006 in the Central Rift Valley of Ethiopia which is attributed to conversion of forests or woodlands to croplands. The range of soil loss rate in the central rift valley should not be beyond its formation rate of 10 t $ha^{-1}yr^{-1}$ (Table 2.1).

Table 2.1: Zonal variability of soil formation rates (Sources: Hurni, 1993)

Zone	Soil Formation Rates (t ha-1yr-1)
Gonder, Rift Valley	6-10
Gojam, Arsi Regions, Gemo Gofa	10-14
Welega, Kefa, Shewa	18-22
Kenya border	6-10

2.8. The Driving Forces of LULC change and Land Degradation in CRV

The major causes of LULC change and land degradation in the Ethiopian CRV are growth in human population and livestock in a region of limited natural resources, unsustainable and/or poor farming techniques, a land tenure system that discourages land conservation, and poverty. In addition, there is rising concern about climate change, salinization, and low soil fertility that promote LULC change in the CRV (Derege *et al.*, 2012).

In the past 33 years (1973–2006), land degradation had been expanding by about 60 km2 every year. However, more detail study of the degradation amount in relation to soil erosion, sediment yield to the lakes and catchment characteristics should be made using adaptable models; so as to guide the implementation of comprehensive and sustainable land use management by giving more attention to erosion prone areas (Derege *et al.,* 2012).

Population growth

Steady growth in human and livestock populations is occurring in the CRV without changes in agricultural and economic systems. Rapidly increasing human populations need more agricultural land, so clearing of forests and woodland has increased. As the population grows, more fragile, marginal lands are used, such as areas of steep slope and protected areas. Another outcome of population growth in some areas is a reduction in fallow periods, from four or five-year rotations to 2 years or fewer (Derege *et al.,* 2012; FAO, 2007).

A strong local tendency to hold wealth as livestock creates further impact on LULC change, particularly land degradation (Derege *et al.,* 2012; Jansen *et al.,* 2007; Scholten, 2007), as does a rising rate of livestock density on limited grazing land.

Beside the animals from mixed farming system, nomadic pastoralists periodically graze their animals in the CRV. As vegetation cover declines under heavy stocking rates, the water infiltration rate decreases and sediment production (soil erosion) increases (Derege *et al.,* 2012; Legesse *et al.,* 2004). The enhanced action of animal hooves on limited grazing land damages the surface soil as it destroys vegetation cover. Footpaths used by humans and cattle develop into rills and then gullies, exacerbating erosion.

Arable land management

The most common farming system in the CRV is small-scale mixed rain-fed agriculture, primarily grain cropping and livestock production. Most of the arable land is covered by teff, barley, maize, and wheat grains (Derege *et al.*, 2012; Legesse and Ayenew, 2006). Production of all these crops exposes the soil to erosion. The annual crops are sown mainly after the rainy season begins, allowing early rains to directly impact and erode the soil unlike soil under forest.

The area of intensively cultivated land in the Ethiopian CRV increased in the period 1973–2006 mainly at the expense of woodland and mixed cultivation land that exposes the soil and becomes more vulnerable to erosion; thus, the area of degraded land (DL) has expanded at the expense of intensively cultivated land (CL) much faster than any other Land use and cover type. There is also a similar trend in the CRV for land use to transition from forest/woodland to mixed cultivated land, then to intensively CL and finally to DL (Derege *et al.*, 2012).

Land tenure system

Ethiopia has implemented several changes in its land ownership system since 1975, and these changes are a source of uncertainty among farmers and rural communities. The reform act of 1975 proclaimed a radical land reform, which nationalized all rural lands and eliminated private land ownership. The current Ethiopian government adopted a policy of public ownership of rural and urban land, but there is still confusion about security of tenure and land rights. Most farmers feel uncertain and hesitant about land ownership, so reduced motivation have to take care of their land and practice resource conservation methods (Tadesse, 2001; Ayenew, 2004).

Poverty

As noted earlier, poor farmers (farm size < 0.5ha and no other income) in the CRV practice mixed rain-fed agriculture. Crop yields are very low. Many farmers do not achieve food security and depend on food relief. To supplement their livelihoods, farmers clear vegetation and trees from their farms or nearby forest to sell as firewood or charcoal to urban people, thus energy use is a critical factor in LULC change. As the rural population of Ethiopia grows, clearing of vegetation for fuel increases and contributes to land degradation (Derege *et al.*, 2012).

Cimate and slope

Climate and slope are natural but only minor causes of LULC change and land degradation. The maximum daily temperature increased, whereas annual rainfall showed a generally decreasing trend. Hence, natural factors associated with climate change partly contribute to the land use change in the area, especially driving the decrease in size of lakes (Jansen *et al.,* 2007).

As the largest part of the valley (80%) is found in relatively gentle to flat topography (excluding the surrounding escarpment), most of the degraded areas are found in gentle to moderate slope area. Thus, slope is less associated with LULC change and land degradation in the CRV than are anthropogenic factors. However, it is generally understood that soil lose amount would be higher in the smaller areas that are steep and certainly adjacent sloping lands upslope from the CRV (Derege *et al.,* 2012).

2.9. Potential impacts of LULC change

Lake size reduction

Decline in the size of lakes is the other major phenomenon resulting from LULC change in the CRV. Lake Abiyata is shrinking drastically and the average level of Lake Ziway decreased by approximately 0.5m in 2000 and 2006 (Derege *et al.,* 2012; Scholten, 2007) and the decrease in Lake Ziway's water level reduced the discharge of the Bulbula River from 200 million m^3 y^{-1} before 2000 to less than 50 million m^3 y^{-1} in 2003 (Derege *et al.,* 2012; Ayenew, 2004) that causes shrinkage of Lake Abiyata to 40% and a soda-ash factory partly contributes to the decline of the lake (extraction of 0.9 million m^3 y^{-1}) (Derege *et al.,* 2012; Jansen *et al.,* 2007).

The development of 7500–10000 ha of newly irrigated lands (Derege *et al.,* 2012; Scholten, 2007) coupled with increasing mean temperature and decrease in annual rainfall (Derege *et al.,* 2012; Abraham, 2006), will eventually reduce Lake Ziway's water level and it will become saline; if this occurs, it will negatively affect all water users - fisheries, domestic water users, livestock, irrigated farms, and ecosystems. Moreover, if this condition continues and Lake Abiyata dries up, Abiyata-Shalla National Park will be severely affected (Derege *et al.,* 2012).

Physical and socio-economic impacts

Land degradation is the major negative impact of LULCC in the CRV; the most widely available form of degradation is produced by sheet erosion. The area of degraded land in the CRV increased by about 200 per cent between 1973 and 2006. As a result, grain production per head decreased from about 245 kg capita $^{-1}$ y $^{-1}$ in 1965 to 200 kg capita $^{-1}$ y $^{-1}$ in 1975, 156 kg capita $^{-1}$ y $^{-1}$ in 1985 and below 100 kg capita $^{-1}$ y $^{-1}$ in 2008 (Derege *et al.*, 2012; NACID, 2006). Due to lower production per capital and per hectare coupled with increased human population, food shortages have become common i Ethiopian CRV and dependence on food aid is growing, and as counteracting the problem the government designed a policy of resettlement programme to the western Ethiopia (Derege *et al.*, 2012; Rahmato, 1989; Mberu, 2006).

Salinity

Farmers believed that declining of crop productivity and food scarcity is caused by soil degradation due to the destruction of woodlands (Derege *et al.*, 2012; Garedew *et al.*, 2009) and soil salinity-sodicity (Engidasew, *et al.*, 2020). Soil salinity-sodicity adversely affected growth of vegetables, land productivity and household economy. The social survey also indicated that farmers lack knowledge, skills and capital to apply various ameliorative measures of soil salinity and sodicity. This requires monitoring of irrigation water, planting salt tolerant crops, designing environmentally friendly irrigation practices and empowering farmers on farming practices in order to mitigate and ameliorate soil salinity-sodicity problems, and to enhance sustainability of irrigation farming in the study areas (Engidasew, *et al.*, 2020).

2.10. Curve number of different land use land covers and soil types

Soil Conservation Curve Number (SCS-CN) is an empirically derived relationship between location, land use, antecedent moisture conditions and runoff and it was used in many event-based models to establish the infiltration characteristics (Iliasse & Adil, 2014) and it has inverse relationship with runoff generation capacity (Vaezi, et al., 2010; Zehetner & Miller, 2006; Zeiger & Fohrer, 2009) and studies showed that organic matter (OM) influences CN and results in low surface runoff (Vaezi, et al., 2010; Zehetner & Miller, 2006; Zeiger & Fohrer, 2009).

OM improved and accelerated both the infiltration rate and water holding capacity of the soil (Mesfin, et al, 2017; Barbora and Jaroslava, 2014) which in turn influenced the CN of the watershed and EBLUS exhibited a good carbon stock, which was equivalent to high-vegetation areas (Mesfin et al., 2017; Deng et al., 2016).

Curve number (CN) matrix was developed for major land use systems except Enset-Based land use system (EBLUS) as shown in Table 2.2 that was used to develop a relationship among different lad use systems to model the CN matrix for EBLUS relative to other land use systems with predetermined CN.

Table 2.2: Curve number lookup table (ERA, 2013; Chow, 1988)

	Hydrologic Soil Group (HSG)			
Land Cover/Land Use	**A**	**B**	**C**	**D**
Open Water	100	100	100	100
Developed, Low Intensity	57	72	81	86
Developed, Medium Intensity	77	85	90	92
Developed, High Intensity	98	98	98	98
Barren Land, Rock, Sand, Clay	63	77	85	88
Mixed Forest	36	60	73	79
Scrub/Shrub	35	56	70	77
Grasslands, Herbaceous	39	61	74	80
Pasture, Hay	49	69	79	84
Cultivated Crops	67	78	85	89
Woody Wetlands	100	100	100	100

The CN matrix of the dominant land use land covers are used in modeling the CN matrix of EBLUS in Meki river watershed. Accordding to ERA 2013 and Oliver *et al*., 2006, Hydrologic soil group of different soil types was derived from USDA and presented in Table 2.3 and it was used in the modeling of curve number of enset based land use system studies in Meki river watershed. Meki river watershed soil type was identified from MOWIE GIS data and HSG was assigned to each of the soil types accordingly.

Table 2.3: Hydrologic soil group of different soil types (ERA, 2013; Oliver et al., 2006)

Soil Types	**Description**	**Hydrologic Soil Group (HSG)**	**Soil Types**	**Description**	**Hydrologic Soil Group (HSG)**
Ao	OrthicAcrisols	B	Ne	EutricNitosols	B
Bc	Chromic Cambisols	B	Od	DystricHistosols	D
Bd	DystricCambisols	B	Oe	EutricHistosols	D
Be	EutricCambisols	B	Qc	Cambric Arenosols	A
Bh	HumicCambisols	C	Rc	CalcaricRegosols	A
Bk	Calcic Cambisols	B	Re	EutricRegosols	A
Bv	VerticCambisols	B	Th	HumicAndosols	B
Ck	Calcic Chernozems	B	Zo	OrthicSolonchaks	B
E	Rendzinas	D	Tv	Vitric Andosols	B
Vc	Chromic Vertisols	D	Je	EutricFluvisols	B
Vp	PellicVertisols	D	Lc	Chromic Luvisols	B
I	Lithosols	D	Lv	VerticLuvisols	C

2.11. Impact of land use/land cover change on curve number and stream flow

Much research is currently being conducted about the impacts of land cover changes on the hydrological behavior of watersheds. These studies make this relationship using techniques such as remote sensing, geoprocessing, hydrosedimentological, and, in some cases, meteorological modeling, besides statistical analysis. However, despite the techniques and methods available, the relationship between land cover and hydrological processes is complex, because changes in land cover affect several natural processes, such as evapotranspiration, surface runoff, infiltration, and precipitation (Thalita Costa de Moraes, *et al.*, 2017) and all of these processes depend not only on land cover, but also on other factors such as the size, topography, types of soils and rocks, and other physical and natural aspects of watersheds (Thalita Costa de Moraes, *et al*., 2017).

2.12. Hydrologic response to land cover change

Gebrejewergs (2020) found that there was a strong correlation between seasonal rainfall and runoff depths. Nyssen *et al*. (2010) & Gebrejewergs (2020) studied the impact of soil and water conservation measures on hydrological responses by calculating the runoff curve number (CN) for various land uses and land management techniques and found a reduction in runoff and a rise of ground water after catchment management.

Land use and Soil organic carbon are the critical factors to influence the infiltration rate of the soil (Yimer, 2008; Ibeje, 2018). The mean steady state infiltration rates of farmlands, bamboo fields and forestland are 1.98 cm/h, 2.44cm/h and 2.43cm/h respectively (Ibeje, 2018).

Table 2.4: Infiltration Rate (mm/Hour) influenced by slope and soil texture (Oliver *et al.*, 2006)

Soil Texture, Type	Percent of Slope					Basic infiltration rate
	0-4%	5-8%	8-12%	12-16%	Over 16%	
Coarse Sand	31.75	25.4	19.05	12.7	7.874	More than 30
Medium Sand	26.924	21.59	16.256	10.668	6.858	
Fine Sand	23.876	19.05	14.224	9.652	6.096	
Loamy Sand	22.352	17.78	13.462	8.89	5.588	
Sandy Loam	19.05	15.24	11.43	7.62	4.826	20 – 30
Fine Sandy Loam	16.002	12.7	9.652	6.35	4.064	
V. Fine Sandy Loam	14.986	11.938	8.89	6.096	3.81	
Loam	13.716	10.922	8.382	5.588	3.556	10 – 20
Silt Loam	12.7	10.16	7.62	5.08	3.302	
Silt	11.176	8.89	6.604	4.572	2.794	
Sandy Clay	7.874	6.35	4.826	3.048	2.032	
Clay Loam	6.35	5.08	3.81	2.54	1.524	5 – 10
Silty Clay	4.826	3.81	2.794	2.032	1.27	
Clay	3.302	2.54	2.032	1.27	0.762	1 – 5

Note: Rates based on full cover. These figures decrease with time and percent of cover.

Oliver *et al.,* (2006), reported that Infiltration rate ranges are affected by slope and soil textural classes of the soil as shown in Table 2.4. This shows that land use change can affect the infiltration rate of the soil (Ibeje, 2018) in addition to the topography of the watershed.

Many hydrological studies have shown that LULC changes have affected the hydrology of various watersheds of the World (Ambika 2012). The LULC change can alter both the infiltration and runoff amount by following the falling of precipitation (Hougton 1995). Land-use change is one of the main driving forces that affect watershed hydrological processes. Separately assessing their impacts on hydrology is important for land-use planning and management of water resources. It is one of the main factors that influence surface runoff (Petroviˇc, 2021).

To prevent the ecosystem degradation and maintain the inherent ecological functions of rivers, quantitative assessment of the influence of land-use change on hydrology is of great importance. Such evaluations can provide insight into the extent of land use/cover change on regional water balance and help to develop appropriate watershed management strategies (Petroviˇc, 2021).

Land use and land cover (LULC) changes affect the processes that provide redistribution of soil material and soil properties (Jerzy, *et al.,* 2014) and it leads to change in soil organic carbon (SOC) and soil quality (Nyssen, *et al.,* 2008) that affects the hydrology of the watershed by affecting the infiltration rate of the soil, by shifting the surface and subsurface flow regimes including base flow contributions to streams and recharge (Nejadhashem, *et al.,* 2011; Tu, 2009), by changing the roughness of the surface (Nejadhashem, et al., 2011; Feddema, *et al.,* 2005), by influencing runoff generated (Nejadhashem, *et al.,* 2011; Burch, *et al,* 1987) and by changing flood frequency and magnitude (Nejadhashem, *et al.,* 2011; Ward, *et al.,* 2008; Remo, *et al.,* 2010; Qiu, *et al.,* 2010).

The change in Soil organic carbon may alter the hydrological processes (Elfert and Bormann, 2010) such as infiltration, groundwater recharge, base flow and runoff (Ermias *et al.,* 2013; Uhlenbrook, 2007; DeFries and Eshleman, 2004) for which published articles are reviewed to get the carbon stock of different land use systems which accounts EBLUS. According to Mesfin *et al.,* 2017, carbon stoke of land uses are measured and reported as shown in Table 2.5 and considered to develop the CN of EBLUS.

Table 2.5: Carbon stock of different land use systems (Source: Mesfin *et al.*, 2017)

Land Cover/Land Use	Carbon stock (ton/yr)
Open Water	0
Built-up, Medium Intensity LUS	132
Natural Forest LUS	45,714
Grasslands (Pasture) & plantations LUS	8350
Cultivated LUS	19,950
Enset-Based LUS	77,286

Therefore the change in Soil organic carbon and Land use land cover change may alter the hydrological processes (Elfert and Bormann, 2010) such as infiltration, groundwater recharge, base flow, runoff (Ermias *et al.*, 2013; Uhlenbrook, 2007; DeFries and Eshleman, 2004) and influence soil erosion and sediment yield (A.Kavian, *et al.*, 2017; Shigeta 1990).

Soil erosion by water is the most pressing environmental problem in the Highlands of Ethiopia, where the topography is highly rugged, population pressure is high, steep lands are cultivated and rainfall is erosive (Ermias *et al.*, 2013; Bewket and Teferi, 2009).

Yueqing *et al*. (2011), Shi *et al*. (2004), Ouyang and Bartholic (2001) and Mallick *et al.* (2014) investigated land use based soil erosion risk using RUSLE and GIS and displayed the results as erosion risk maps and they confirmed that the model is practical for soil conservation plans and natural resources management (N.Kayet, 2018; A.Kavian *et al*. 2016; Shi *et al*. 2004; Angima *et al*. 2003; Merrit *et al*., 2003; Liu *et al*. 2000; Andrew *et al*. 1999).

2.13. Hydrologic Model Selection

2.13.1. Types of Hydrologic Models

According to (Singh and Woolhiser, 2002), the model structure and architecture are determined by the objective for which the model is built. Watershed hydrologic models have been developed for many different reasons and therefore have many different forms. However, they are in general designed to meet one of the two primary objectives.

One objective of watershed modelling is to gain a better understanding of the hydrologic processes in a watershed and of how changes in the watershed may affect these phenomena. Another objective of watershed modelling is the generation of synthetic sequences of hydrologic data for facility design or for use in forecasting. They are also providing valuable information for studying the potential impacts of changes in land use or climate. The variety of uses and the rapid increase both in scientific understanding and in technical support, from data collection systems and computer technology, have produced an enormous range in levels of sophistication.

Every hydrological model requires two essential components: the runoff production component and the runoff routing component (Beven, 2001). Practical experiences suggest that the complexities and nonlinearities of modelling in the flow generation process are much greater than the routing processes. Singh and Woolhiser (2002) state that watershed models can be classified according to different criteria that may encompass process description, time scale, space scale and technique of solution.

Singh (1995) classified hydrologic models based on process description; timescale; space scale; techniques of solution; land use; and model use. Depending upon the way the hydrological processes are described, the models can be also classified as deterministic, stochastic, or mixed. In a deterministic model outcomes are precisely determined through known relationships among states and events, without any room for random variation while if a model has only implicit or hidden input called stochastic model. If the model components are described by a mix of deterministic and stochastic components called stochastic-deterministic or hybrid model.

On the basis of process description, the hydrological models can be classified into three main categories: lumped models, semi-distributed models and distributed models (Figure 2-1).

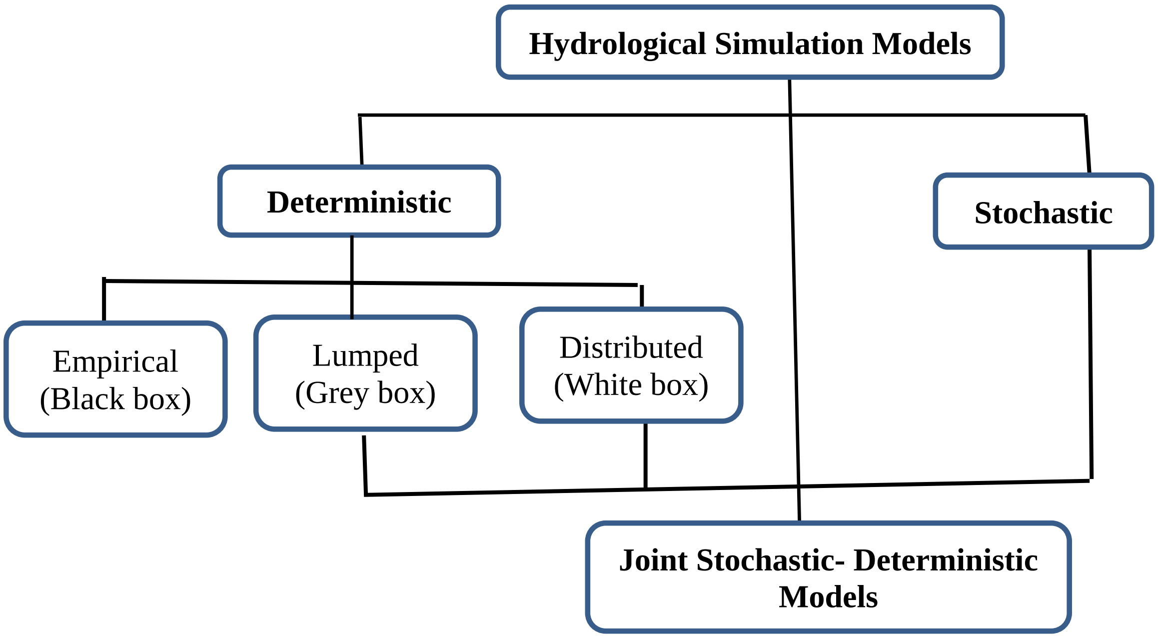

Figure 2-1: Classification of models based on process (Refsgaard, 1996)

Parameters of lumped hydrologic models do not vary spatially within the basin and thus, basin response is evaluated only at the outlet, without explicitly accounting for the response of individual sub-basins. The impact of spatial variability of model parameters is evaluated by using certain procedures for calculating effective values for the entire basin. The most commonly employed procedure is an areaweighted average. These models are not usually applicable to event-scale processes while for discharge prediction they can provide just as good simulations as complex physically based models (Beven, 2001). Most of such models are not capable of representing all hydrologic processes for investigating the impacts of land use and climate change on the hydrological regime.

Distributed models on the other hand fully allow parameters to vary in space at a resolution usually chosen by the user. Distributed modeling approach attempts to incorporate data concerning the spatial distribution of parameter variations together with computational algorithms to evaluate the influence of this distribution on simulated precipitation-runoff behavior. These models generally require large amounts of (often unavailable) data for parameterization in each grid cell (MIKE SHE (Refsgaard and Storm, 1995) and CASC2D (Ogden, 1998)).

Semi-distributed (simplified distributed) models partially allow parameters to vary in space by dividing the basin into a number of smaller sub-basins. The main advantage of these models is that their structure is more physically-based than the structure of lumped models, and that they are less demanding on input data than fully distributed models. SWAT (Arnold, 1993), HEC-HMS (US-ACE, 2001), HSPF (Bicknel et al., 2001), PRMS (Leavesley et al., 1983), DWSM (Borah et al., 2001), TOPMODEL (Beven et al., 1993), HBV (Bergström, 1995), are considered as semi-distributed models.

Furthermore, hydrologic models can be divided into event-driven models, continuous-process models, or models capable of simulating both short-term and continuous events. Event-driven models are designed to simulate individual precipitation-runoff events, are capable of simulating short-term events. Their emphasis is placed on infiltration and surface runoff, their objective is the evaluation of direct runoff. Typically, event models have no provision for moisture recovery between storm events and, therefore, are not suited for the simulation of dry weather flows. On the other hand, a continuous model simulates instead a longer period, predicting watershed response both during and between precipitation events. These models take explicit account of all runoff components, including direct and indirect runoff. They focus on long-term hydrologic abstractions responsible for the rate of moisture recovery during the periods of no precipitation. They are suited for simulation of daily, monthly or seasonal streamflow, usually for long-term runoff-volume forecasting and for estimates of water yield (Singh, 1995).

2.13.2. Model selection for Meki river watershed

The selection of a particular model is a key issue to get satisfactory answers to a given problem. Currently, there are numerous hydrological models simulating the hydrological process at different spatial and temporal scales.

Although there are no clear rules for making a choice between models, some simple guidelines can be stated. Starting from the studied physical system, the first step is to define the problem and determine what information is needed and what questions need to be answered. This means that it is necessary to evaluate the required output, the hydrologic processes that need to be modelled, availability of input data.

Subsequently the simplest method that can provide the answer to the questions has to be chosen. In particular it‘s necessary to identify the simplest model that will yield adequate accuracy, bearing in mind that model complexity is not synonymous with the accuracy of the results, that the model has to be characterized by flexibility, by the possibility of making it applicable under various spatial and temporal conditions and that increased accuracy has to be worth the increased effort.

Different models are being used to forecast effects of land use change on hydrological process (Legesse et al., 2003). Recently, hydrological simulation models including: SWAT, MIKE-SHE, HSPF, WASIM-ETH, DWSM, HEC-HMS and others have been developed partly to quantify the influence of change in land use, land cover and management practices on the hydrologic processes. Hence, the ability of a hydrological model to integrate GIS for hydrologic data development, spatial model layers and interface may be considered as model selection criteria.

Model selection criterias are always project-dependent, since every project has its own specific requirements and needs. Some models are data intensive that often does not exist or are not available in full (Kassa, 2009). Therefore to select a model to accomplish the objectives of this research in the MRWS, the following selection criteria were formulated:

- The model must be able to simulate agricultural/rural/urban areas because the Meki river watershed can be classified as mixed watershed
- It should be able to simulate different components of the streamflow (surface runoff, lateral flow and base flow) in MRWS.
- It should incorporate tools that would allow land use and land cover changes to enable assessment of the impacts of land use and land cover change on water resources.
- The minimum input data requirements for the model must be available or can be met with some efforts through gathering data from a data-poor watershed such as the MRWS
- Its temporal scale should be long term, continuous and able to simulate on daily bases
- The model must be readily and freely available, both for research and for future use
- The model should be one that can be applied over a range of watershed sizes from small to large catchments/basins so that the Meki river watershed and other similar watersheds could be modelled

A two-level selection approach was used to objectively determine the most suitable models for this research: a large number of existing hydrologic models were reviewed and Empirical and Lumped models were considered inappropriate and six selected models were then reviewed in detail according to the above evaluation criteria (Table 2.6). Temporal and spatial scales, processes modeled, technical support, set-up time, expertise required, and etc were considered.

Table 2.6: Description of six screened semi-distributed hydrological models

Description	**HEC-HMS**	**SWAT**	**HSPF**	**WaSiM-ETH**	**DWSM**	**HBV**
Model type	Semi-distributed Physically-based	Semi-distributed Physically-based long-term	Semi-distributed conceptual model	Semi-distributed Physically-based modular	Semi-distributed Physically-based	Semi-distributed conceptual model
Model objective	Simulate the rainfall-runoff process of dendritic watersheds	predict the impact of land management practices on water and sediment	Simulates watershed hydrology, and sediment-chemical interactions	Simulate watershed water balance	Simulations of surface and subsurface storm water runoff , flood, sediment transport	Simulate rainfall-runoff process and floods
Temporal scale	Day	Day	Flexible	Day	Day+	Day
Watershed representation	Uses sub-basins as primary hydrological units	Sub-watersheds grouped based on climate, HRU, ponds, groundwater, and main Channel	Uses sub-basins as primary hydrological units	Grid based	Sub-watersheds (1-D overland elements, channel, and reservoir units.	Uses sub-basins as primary hydrological units
Process modelled	Continuous & event	Continuous	Continuous & event	Continuous	Single event	Continuous & event
Runoff on overland	Clark‘s, Snyder‘s, SCS UHs, ModClark Kinematic wave	Runoff volume using CN and flow peak using Rational formula.	Chezy-Manning equation	Using saturation time	Kinematic wave equations	Uses response function to transform excess rainfall to runoff
Water routing	Kinematic wave, Lag, Muskingum, Muskingum -Cunge	Variable storage coefficient method Or Muskingum method	Inflows enter upstream point, and outflow is a function of reach volume	Translation-retention approach using hydraulic parameters	Kinematic wave equations	Muskingum method or simple time lag
References	US-ACE (2001)	Neitsch et al. (2005)	Bicknell et al. (2001)	Schulla, 2000	Borah and Bera (2004)	Shyam (1994)

From the preceding sections and considering the criteria developed, HEC-HMS model has been selected for this research since HEC-HMS predicts a comparatively effective result than SWAT model (Pak et al., 2015). The basic reason, amongst others, is in an economically poor region like Ethiopia, the data requirements of these models can be acquired from second sources and some efforts from the field and the models will have potentially important pragmatic advantages for their wider future use in the region.

2.14. HEC-HMS Model runoff generation mechanism

Runoff is one of the most important hydrologic variables influenced by land use systems. Hence, knowing the quantity and rate of runoff from land surface into streams and rivers is vital for policy makers for informed decision making (Jeevika and Jagritee, 2018; Vaze, 2012). There are ranges of methods available to estimate stream flow from catchments, using observed data known as rainfall-runoff models. However, modeling surface runoff is challenging as the calculation involves complexities with many interconnected variables and general model components including inputs, governing equations, boundary conditions or parameters, model processes and outputs (Jeevika and Jagritee, 2018).

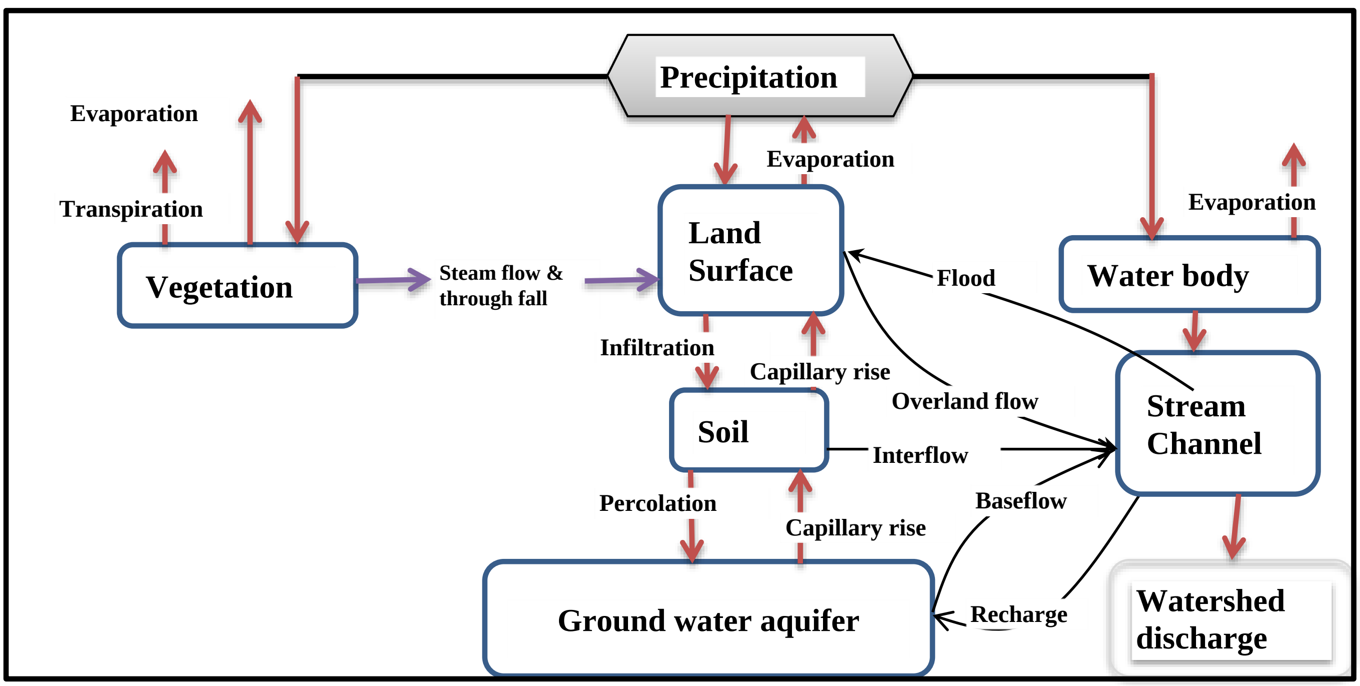

Figure 2-2: Runoff processes in HEC-HMS (Bill, 2018 & Feldman, 2000)

HEC-HMS model depends on hydrologic parameters that cannot be extracted from readily available spatial data. Therefore, HECGeo-HMS technique was used to generate and analyze watershed characteristic and to create HEC-HMS project to make the spatial data readily available to HEC-HMS model while the basic function of the model was to receive precipitation as an input, determine what volume of this precipitation infiltrates into the ground versus what volume becomes overland runoff and to route this overland runoff as shown in Figure 2-2.

2.15. Optimization processes in HEC-HMS

HEC-HMS model is capable of simulating rain fall runoff relation for dendritic watershed in space and time and it has been used successfully in different parts of the world river basins for catchment modeling (Sintayehu, 2013). Surface runoff simulation results may not fit to the recorded values of the streams due to several inputs and processing faults which causes disparity of the simulation result with the observed one. Hence, optimization can be done following the procedures mentioned as follows: The automated calibration can be used to adjust initial losses, CN and lag time to minimize the objective function value and to find optimal parameters. When the manual calibration of the observed and simulated hydrograph not acceptable, initial parameters will be adjusted to provide a better optimization target value for the optimization process (USACE, 2000) as shown in Figure 2-3.

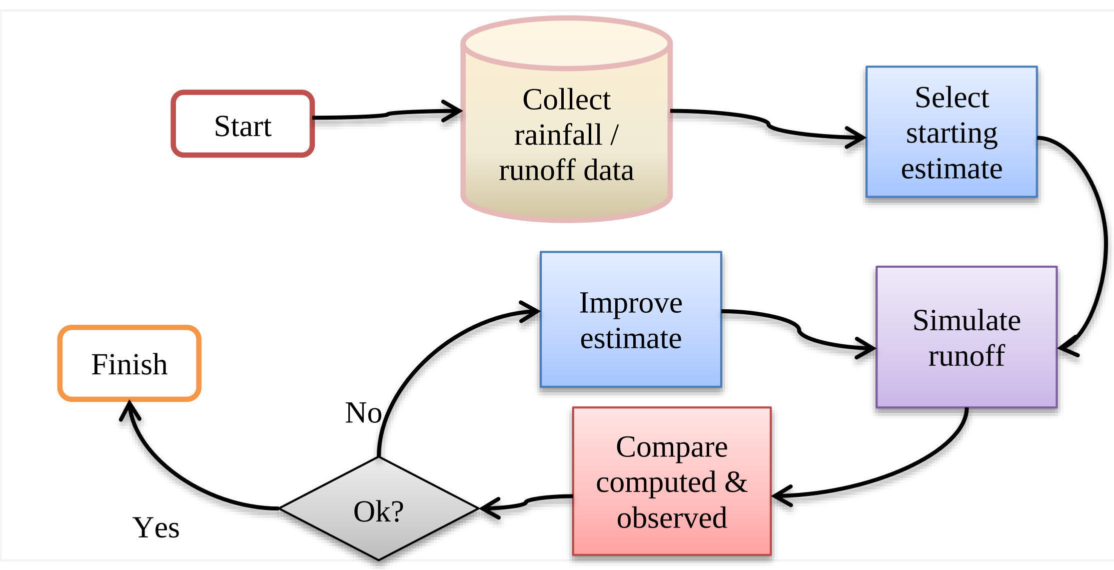

Figure 2-3: Calibration and optimization processes

The peak weighted root mean square error (PWRMSE) with a simplex method for search method could be the objective function. These methods evaluate and adjust one parameter at a time while holding all other parameters constant (Kathol et al., 2003). Besides evaluating the objective function for determining if the process produced an accurate calibration, graphical comparisons can be made between the fit of the model and the actual measured data (Kathol *et al.,* 2003).

The automated calibration was used to adjust initial losses, curve number, lag time, initial discharge, recession constant, muskingham K and muskingham x to minimize the objective function value and to find optimal parameters. When manual validation of the observed and simulated hydrograph was not acceptable, initial parameters were adjusted to provide a better optimization target value for the optimization process (USACE, 2000).

The optimization procedure used a search method of simplex for minimizing an objective function and finding optimal parameters. The simplex method estimates the optimal parameters but do not indicates which parameters had the greatest impact on the solution (Kathol *et al.*, 2003). This method evaluated and adjusted one parameter at a time while holding all other parameters constant. Besides evaluating the objective function for determining if the process produced an accurate calibration, graphical comparisons were made between the fit of the model and the actual measured data. Graphical comparisons of scatter plots and time series plots of residuals between computed and observed flow were used to visually inspect the results of the calibration (Kathol *et al.*, 2003).

2.16. Effects of surface runoff

McGraw-Hill (2003) reported that surface runoff has several effects such as erosion and deposition, flooding and agricultural as it has been discussed as follows:-

Surface runoff causes four principal types of erosion: splash erosion, gully erosion, sheet erosion and stream bed erosion. In the case of gully erosion, large amounts of material can be transported in a small time period. Stream bed erosion is the attrition of stream banks or bottoms by rapidly flowing rivers or creeks.

Flooding is a natural process, which maintains ecosystem composition and processes, but it can also be altered by land use changes such as river engineering. Floods can be both beneficial to societies or cause damage like loss of life, property damage, and contamination of water supplies, loss of crops, and social dislocation and temporary homelessness. Floods are among the most devastating of natural disasters.

A common context of run-off deals with agriculture. When farmland is tilled and bare soil is revealed, rainwater carries billions of tons of topsoil into waterways each year, causing loss of valuable topsoil and transport of agricultural chemicals (nitrates, phosphates, pesticides, herbicides etc) via surface runoff. This result occurs when chemical use is excessive or poorly timed with respect to high precipitation. The resulting contaminated runoff represents not only a waste of agricultural chemicals, but also an environmental threat to downstream ecosystems.

2.17. Soil surface erosion and types of erosion

Soil erosion is extensive and the main environmental issue to the world's terrestrial ecosystems that destroyed around 33 % of the agricultural land for the last forty years (Pimentel *et al.*, 1995; Sun et al. 2014; Yang, D et al. 2003) and also it can destroy physical infrastructures, and reduce the water quality and agricultural productivity (Nearing et al. 2005; Sun et al. 2014).

According to Blanco & Lal 2008 and Morgan 2009, there are different types of soil erosion due to precipitation namely: splash erosion, inter-rill erosion, rill erosion, and gully erosion. The first phase of erosion is splash erosion; raindrops hit the soil on the top of the ground then the splash of the soil particles starts. Splash erosion is caused by the momentum during raindrop striking the soil surface. Inter-rill erosion is mostly due to a thin sheet of water flows over the soil surface; this type of erosion is a function of precipitation amount and basin slope; erosion starts when rainfall intensity exceeds the infiltration capacity of the soil. 70% of the total erosion is produced by splash and inter-rill erosion (Blanco & Lal 2008). Rill erosion appears due to the intensity of flow in small channels or rills. The transportation of soil particles in rill erosion is faster than in inter-rill due to the concentrated flow. Gully erosion is advanced form of rill erosion; it creates V-shaped or U-shaped channels. Gully erosion can remove the entire soil profile from the field. Gully erosion is divided in two types: ephemeral and permanent.

2.18. Erosion process and Sediment yield by surface runoff

According to Merritt, Letcher & Jakeman 2003, surface runoff occurs due to precipitation exceeds losses, which exists of a thin layer of water. Shear stress of soil surface due to the surface runoff exceeds the cohesive strength of soil, results in soil particles detachment. The detached and transported amount of sediment is controlled by the capacity of rainfall, runoff water, and downslope of the watershed. Therefore, the sediment yield is depending on terrain slope and transport capacity of runoff. The concepts of detachment capacity and transport capacity are generally used to explain the quantity of sediment deposition (Bennett 1974; Nearing, Lane & Lopes 1994).

Based on Julien 2010; Yang, CT 1996, the sediment yield (Sediment deposition) at the basin outlet is generally estimated by multiplying total upstream erosion with sediment delivery ratio. The mathematical forms are shown in Equation 2-1.

$SDR = Y/A_T$ (Equation 2.1.)

Where, SDR is sediment delivery ratio (dimensionless), Y is the average annual sediment yield per unit area and A_T is total soil erosion at measuring point from the basin upstream throughout inter-rill, rill, gully, and stream bank erosion process.

2.19. Factors controlling surface erosion

The main components, which control the erosion process are precipitation that soil erosion is directly linked through detaching the soil particle; the topography of the land that can be estimated by using the Universal Soil Loss Equation (USLE), Revised Universal Soil Loss Equation (RUSLE), and Modified Universal soil Loss equation (MUSLE) (Hickey, 2000; Zhang, X et al., 2018); Land cover that is considered as the significant factor affecting runoff and erosion (García-Ruiz, 2010; Nunes, De Almeida & Coelho, 2011), and (Blanco & Lal, 2008; Morgan 2009) and soil type that include soil structure, soil texture, and organic matter which affects the soil erosion and sediment transport process (Blanco & Lal 2008; Wuest, Williams & Gollany 2006).

3. Materials and Methods

3.1. Location and watershed descriptions

3.1.1. Location

Meki river watershed is found in the western part of lake Ziway as shown in Figure 3-1 between 7045'N to $8^0$30'N and $38^0$10'E to $39^0$00'E in the Central Rift Valley (CRV) of Ethiopia and based on digital elevation model (DEM) analysis, the Elevation in the watershed varies from 1612m.a.s.l (at the inlet to lake Ziway) to 3612m.a.s.l (at Zebidar Mountain). Oliver *et al.*, (2007) and Ethiopian meteorological agency data analysis shows the annual rainfall of 824mm to 1292 mm, the mean monthly minimum and maximum temperature are 15^oC and 29^oC respectively, the mean relative humidity of 60%, average wind speed of 1.66m/s and average sunshine of 7.3 hours.

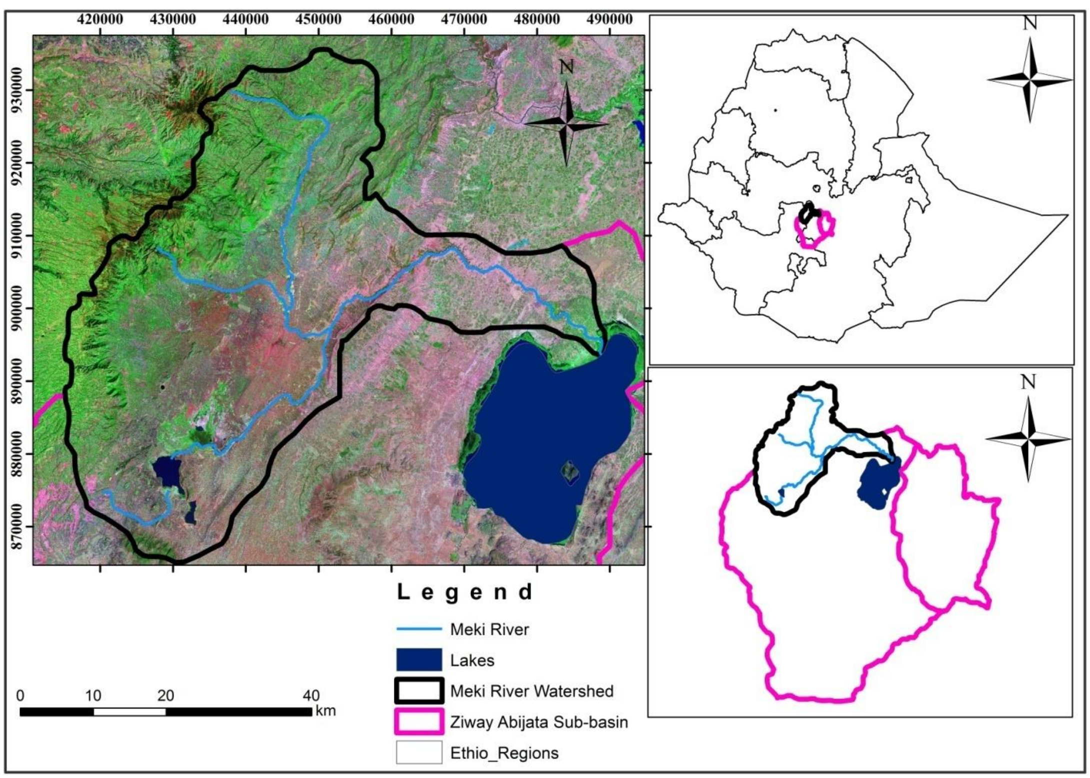

Figure 3-1: Meki River watershed (left panel) in CRV of Ethiopia

3.1.2. Topography and slope

Elevation in the watershed varies from 1612 meters above sea level (m.a.s.l) (at the joining point to Ziway Lake) to 3612m.a.s.l at Zebidar Mountain with a mean elevation of 2169m.a.s.l. The upper tip of the watershed is characterized by steep slopes as shown in Figure 3-2.

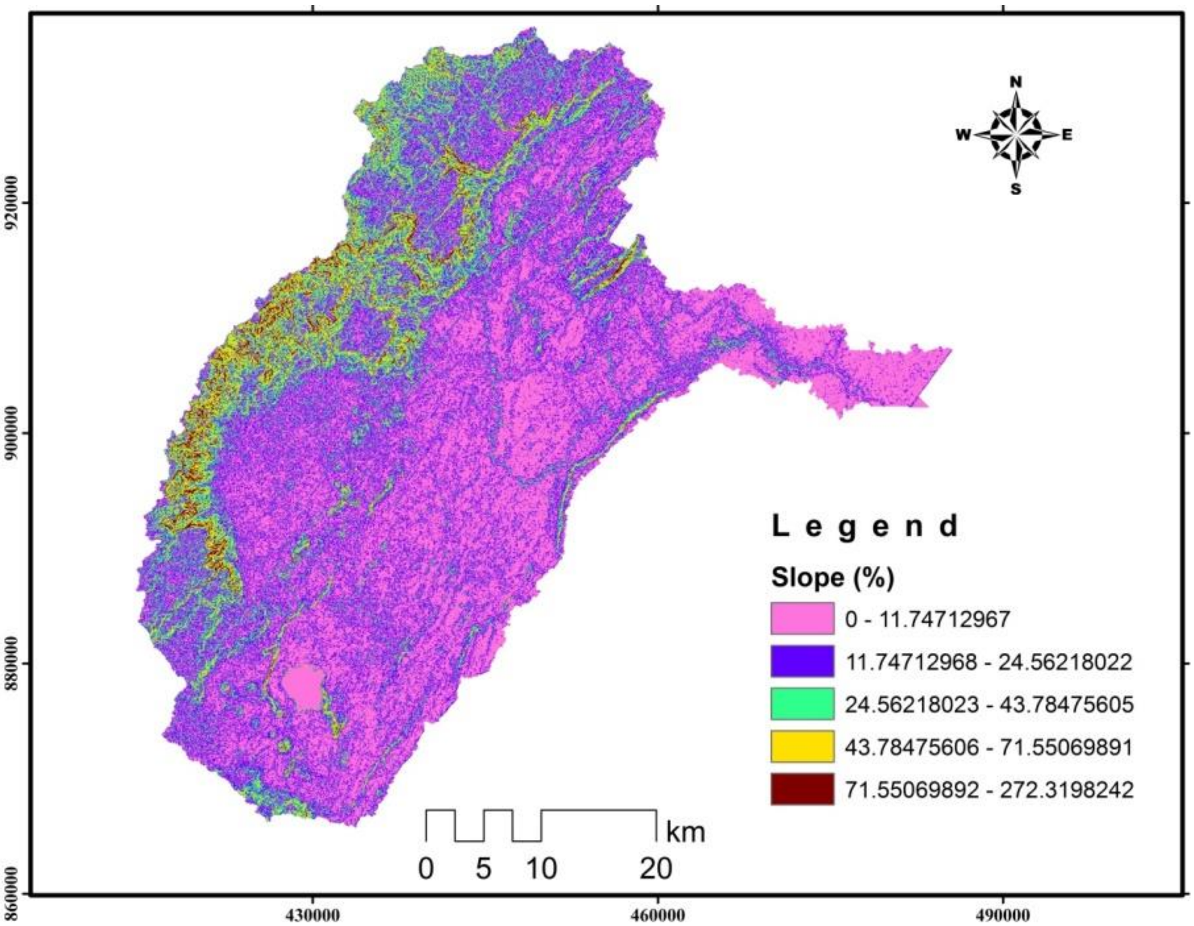

Figure 3-2: Slope map of the watershed

Farmers are cultivating the mountain (slope more than 30 degree) due to high population pressure, which is noticeably susceptible if the natural setting is not treated well. 7% of the area is with slope between 8 to 30degrees and most parts of the watershed are cultivated to non-suitable agricultural activities. Considerable portion of the watershed (92.5%) has a slope between 0 to 8 degrees as shown in Table 3.1, which are relatively gentle to flat slopes and mainly it can be used for agricultural activities.

Table 3.1: Percent of slope range

Grid Code	Range of slope (Degree)	Area (ha)	Percent
1	0 to 3	183548.1264	79.14965
2	3 to 8	31211.51665	13.45904
3	8 to 15	14100.29553	6.080332
4	15 to 30	2409.423512	1.038992
5	30 & more	630.738452	0.271987

3.1.3. Climate

The annual rainfall ranges from 824 – 1292 mm, as per the records from ten meteorological stations, which are located in Agena, Bui, Butajira, Hassan Usman, Imdibir, Koshe, Lemen, Meki, Werabe and Ziway. The isohytal map of the precipitation of the area is interpolated using kriging method and presented as shown in Figure 3-3.

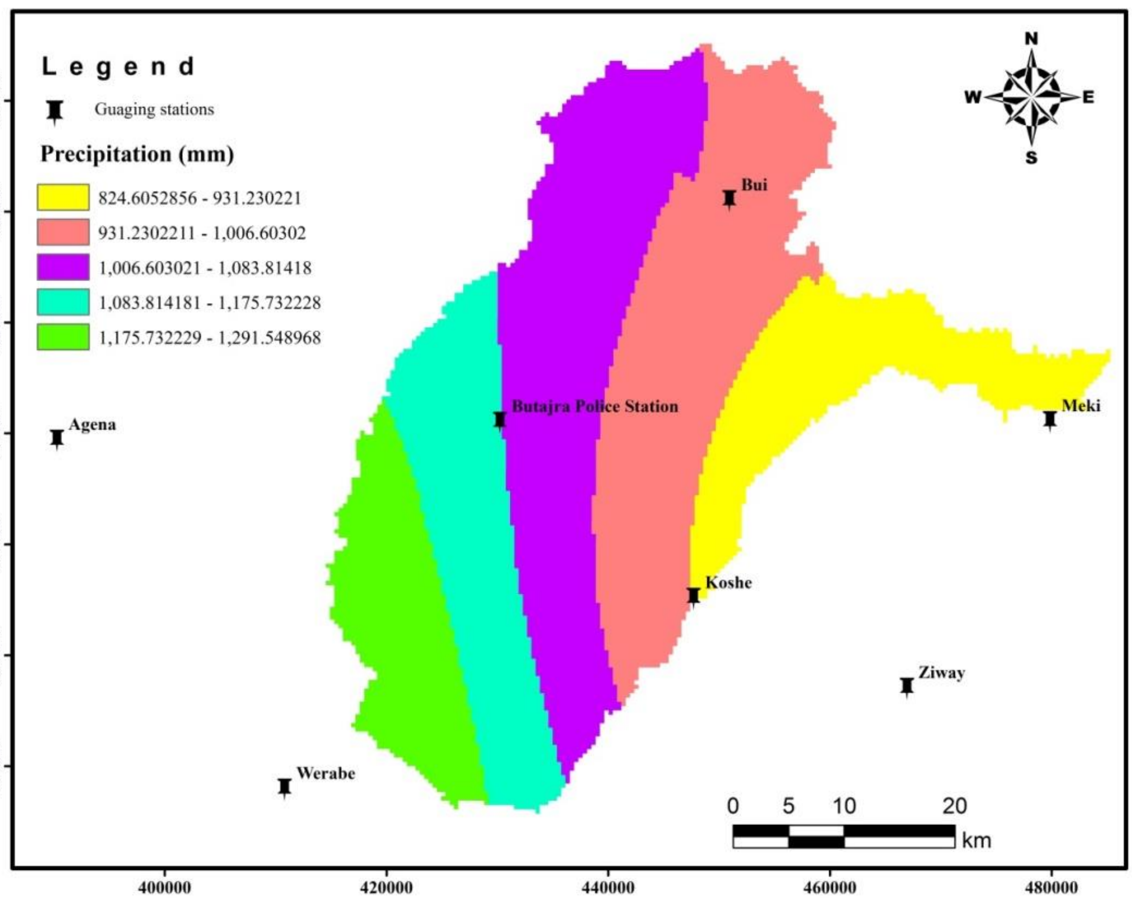

Figure 3-3: Spacial distribution of annual Precipitation (mm) of Meki river watershed

The thirty years of rainfall data collected from Ethiopian National Meteorology Agency (ENMA) for the stations estimated mean annual rainfall of 1067.7mm for the study area which shows a decreasing trend in most part of Meki river watershed based on the analysis result of the data (Figure 3-4).

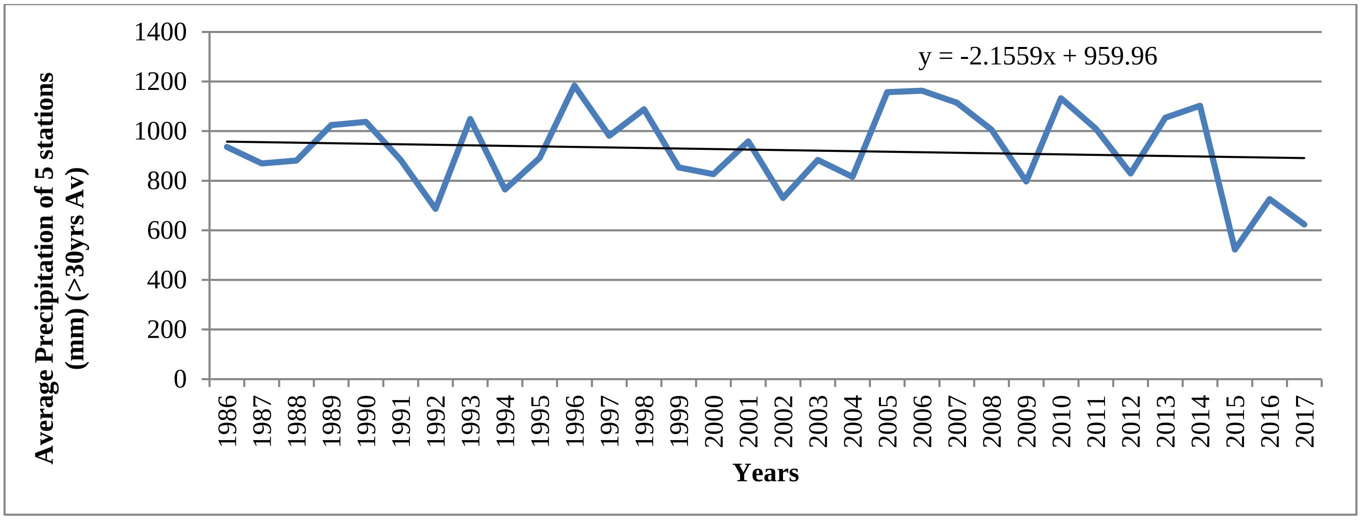

Figure 3-4: Mean annual rainfall of Meki river watershed

The rainfall pattern is bimodal with two distinct rainy seasons in upper part of Meki river watershed, long rains from June to August and short rains from February to April. The long rains contribute 75% while the short rains contribute 25% of the total annual rainfall amount.

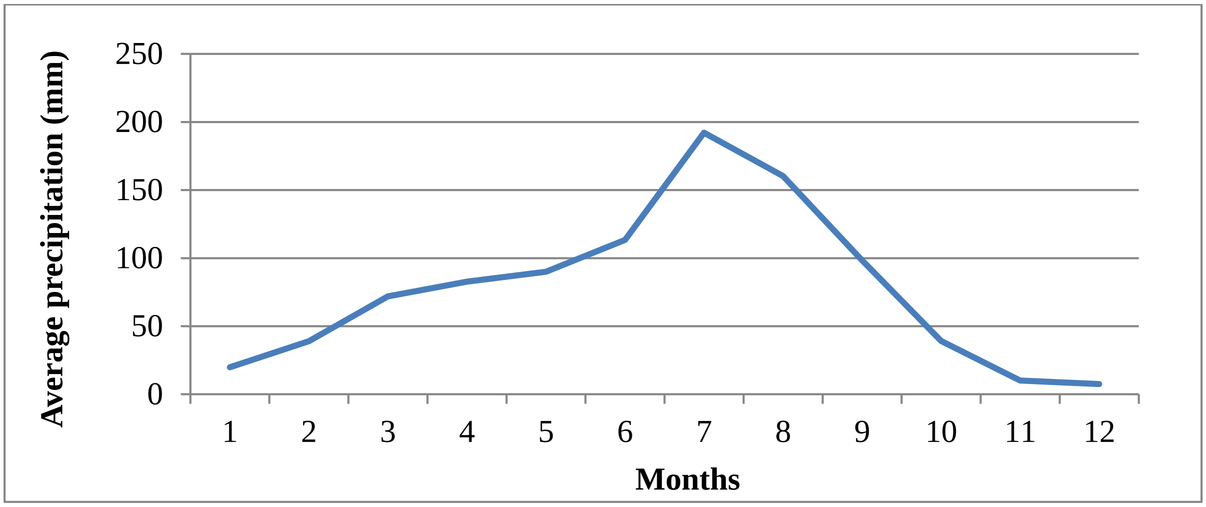

Figure 3-5: Mean monthly rainfall of Meki river watershed

The mean monthly temperature varies between 15°C and 29°C throughout the year. The hottest season extends from December to late in May (Oliver *et al.*, 2006). The meteorological data collected from EMA (2017) (Table 3.2) averages the values of precipitation (ppt), maximum temperature (Tmax) and minimum temperature (Tmin) of all stations in and around MRWS.

Table 3.2: Meteorological stations & components considered for modeling processes in the study

Station	**Data years**	**Daily Av. ppt**	**Annual Av. ppt**	**Tmax**	**Tmin**
Agena	2009-2017	3.939265	1438.816619	23.5943	11.3584
Bui	1986-2017	2.854736	1042.692489	26.0537	9.67935
Butajra Police Station	1986-2017	3.065233	1119.576344	26.3462	11.989
Hasen Usuman	2010-2017	2.871949	1048.979306	26.9334	13.42
Imdibir	1986-2017	3.365248	1229.156815	25.7102	12.2718
Koshe	1986-2017	2.261704	826.087214	26.9334	13.42
Lemen	2007-2016	2.512997	917.872281	26.5668	12.2072
Meki	1986-2017	2.102041	767.770408	27.6119	14.1493
Werabe	2006-2017	4.180731	1527.012131	25.0382	12.1344
Ziway	1986-2017	2.078043	759.005351	27.6119	14.1493
Average		**2.923195**	**1067.696896**	**26.24**	**12.47788**

3.1.4. Land use land cover and farming system

The land use land cover map of the study area was obtained from the Ministry of Water and Energy of Ethiopia (MOWE, 2010) and the land use land cover (LULC) of the study area includes the forest land use system, Enset based land use system, cultivated land use system, water body, Bush and khat land use system, Grass land use system, Eucalyptus land use system and bare soil/built-up land use system.

Central statistics agency of Ethiopia has reported that, 302,000 ha of land are covered by enset plant in Ethiopia. Out of the total enset plant production, 211,000 ha of land covered by enset found in South Nations and Nationalities of People Regional State (SNNPR). In general, around 75% of enset production is located in southern part of the country (Ambachew, et al, 2018).

Most of the upper tip of the watershed is dominated by Erica bush land use system with natural vegetation and bush land use system there are several patches of Enset plantation with dense agro forestry trees and also there are some patches of cultivated land use system surrounded by agro forestry trees.

In the middle of the watershed natural vegetation with dense grass and natural vegetation with eucalyptus and cupressus plantation are the dominant ones while there are also several patches of cultivated land with agro forestry trees and Enset plantation with dense agro forestry trees.

Cultivated land use system is the dominant LULC type that covers the middle and downstream parts of the watershed and also intruding to the forest and grass lands. In the upper and middle part of the watershed the crops grown are; Enset, beans, peas, teff, maize, sorghum, barley, Potato, Coffee and wheat. Cattle raring are practiced at the side of cultivation (MOA, 2002).

The major crops growing in the area are teff, maize, pepper, barley, wheat, etc in the lower portion of the watershed. Moreover in the lower part of the watershed irrigation enabled to extend the growing of crops like, sugar cane, and vegetables as shown in Figure 3-6. In those areas, irrigation is rarely practiced but fruits and coffee are grown by rain-fed on the upstream part of the watershed while it is practiced on the downstream part of it especially around and below Meki town.

Figure 3-6: Vegitables from irrigation field in Meki river watershed

3.1.5. Geology

The Main Ethiopian Rift (MER) is a NNE–SSW to N–S- trending trough 80 km wide in its central portion and 1,000 km long. It separates the southern Ethiopian plateau to the west from the Somali plateau to the east (Ernesto, *et al.*, 2015). Northward, it progressively widens out into the complex Afar triple junction, while at its southern end, a 200– 300km tectonically disturbed area (Baker *et al.*, 1972) marks the transition to the Kenyan Gregory Rift in the Turkana depression.

Most of the ignimbrite layers are believed to have formed by catastrophic eruptions related to the collapse of large calderas, such as the 3.5-Ma old Munesa caldera now buried beneath the Ziway–Shala lakes. These two units, common to the whole MER, are followed by Late Pliocene basalts with pyroclastic fed by calderas which are limited to the northern and central sectors (Grove *et al.*, 1975) and the subsequent Quaternary volcanic unit, which outcrops throughout the MER (Mohr, 1962) with basalt flows and scoria cones as shown in Figure 3-7.

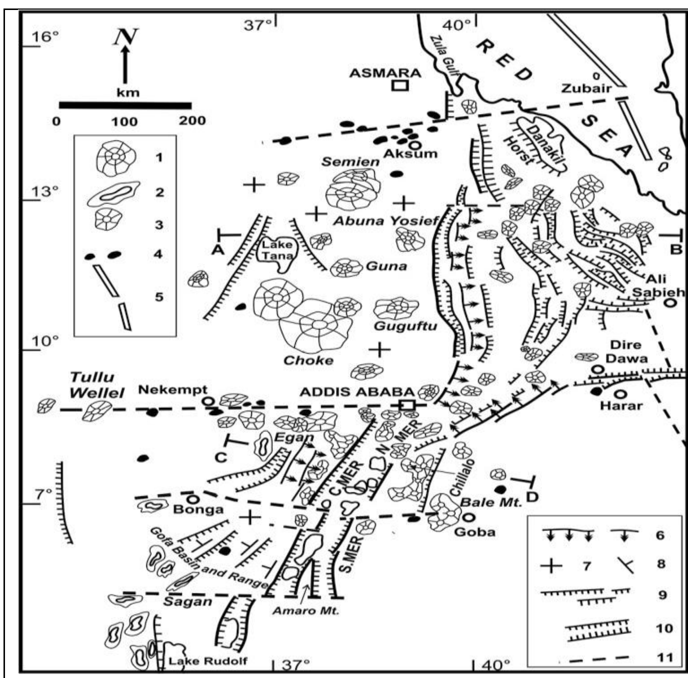

Legend:

1 Miocene volcanic centers of Tarmaber unit in the northern Ethiopian plateau;
2 Pliocene acidic domes and plugs;
3 Plio-Quaternary volcanic centers;
4 Per-alkaline plugs;
5 Red Sea axis;
6 Flexures;
7 Horizontal lava flows and sedimentary sequences;
8 Tilted lava flows and sedimentary sequences;
9 Block faulting;
10 Major graben;
11 Transversal tectonic lines. C–D cross sections shown in Figure 3-7 Modified from Abbate and Sagri (1980)

Figure 3-7: Structural sketch map of the Ethiopian and Somali plateaus, Afar depression, and Main Ethiopian Rift (Northern, Central, and Southern MER) with the main transversal tectonic line and major volcanic edifices (Ernesto *et al.*, 2015).

Lake Ziway is in the Ethiopian Rift valley System, which consists of three major rift zones with distinct volcanic and tectonic characteristics that are at different stages of rifting: the broadly rifted zone of south western Ethiopia, the Main Ethiopian Rift (MER) of central Ethiopia, and the Afar Rift System (Ernesto *et al.*, 2015).

Figure 3-8: The Jima Volcanites at the top of the Guraghe escarpment. Gently inclined rhyolite ignimbrites incised by a channel in turn filled by horizontally laminated ignimbrite flows. New road on the western flank of the MER between Butajira and Welkite shows the existing geological features (Ernesto *et al.*, 2015).

3.1.6. Hydrology

Lake Ziway has two main tributaries continuously providing water which are under influence of population pressure in the form of abstraction of water for irrigation and domestic water supply of Ziway town. Precipitation is also one of the sources of water for the lake. The Western portion of the lake watershed is drained to Meki River while the Eastern portion of the lake is fed through Katar River. There is no surface outflow identified except overflow of the lakes to the nearby rivers while water level is beyond its capacity (Awulachew, 2001). The frequency of the flow of the western portion of the lake (Meki river watershed) with its coresonding return period was presented as shown in Figure 3-9.

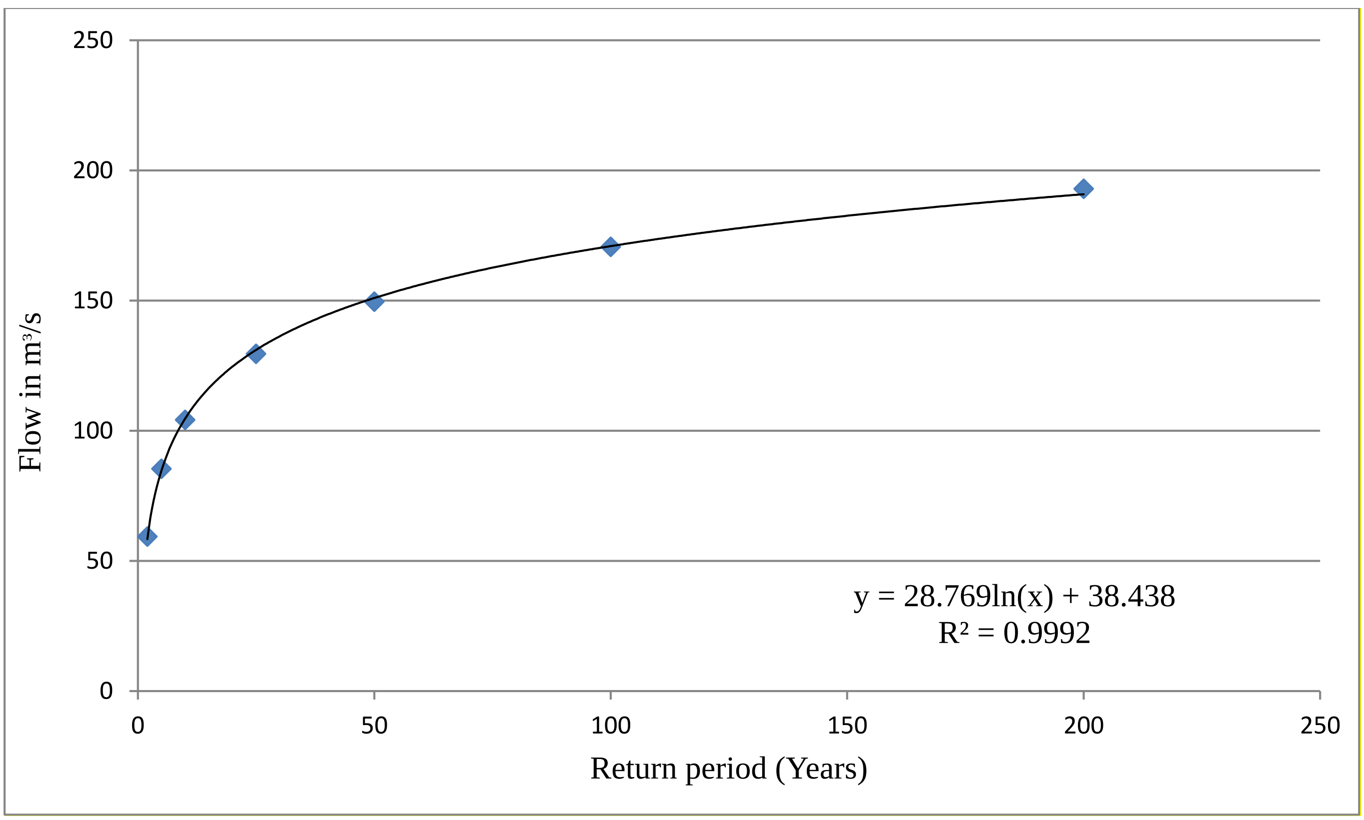

Figure 3-9: Peak Flow of the watershed at Meki station for their respective return period (Generated: Log Pearson type III from MOWIE data) (MOWE, 2013)

3.1.7. GIS based population distribution in Meki river watershed

The geometrically projected population at a national level taken from CSA and kebele based population projection was done in Microsoft excel and database was developed in Arc GIS. Kebele shape file from CSA was combined and clipped for Meki river watershed and the number of projected human population was determined and transfered.

Base year population was recoded in ArcGIS for mapping and multiplication purposes with area of kebele included in Meki river watershed was computed and the population of portion of the kebele was calculated on the basis of the area ratio as shown in Figure 3-10.

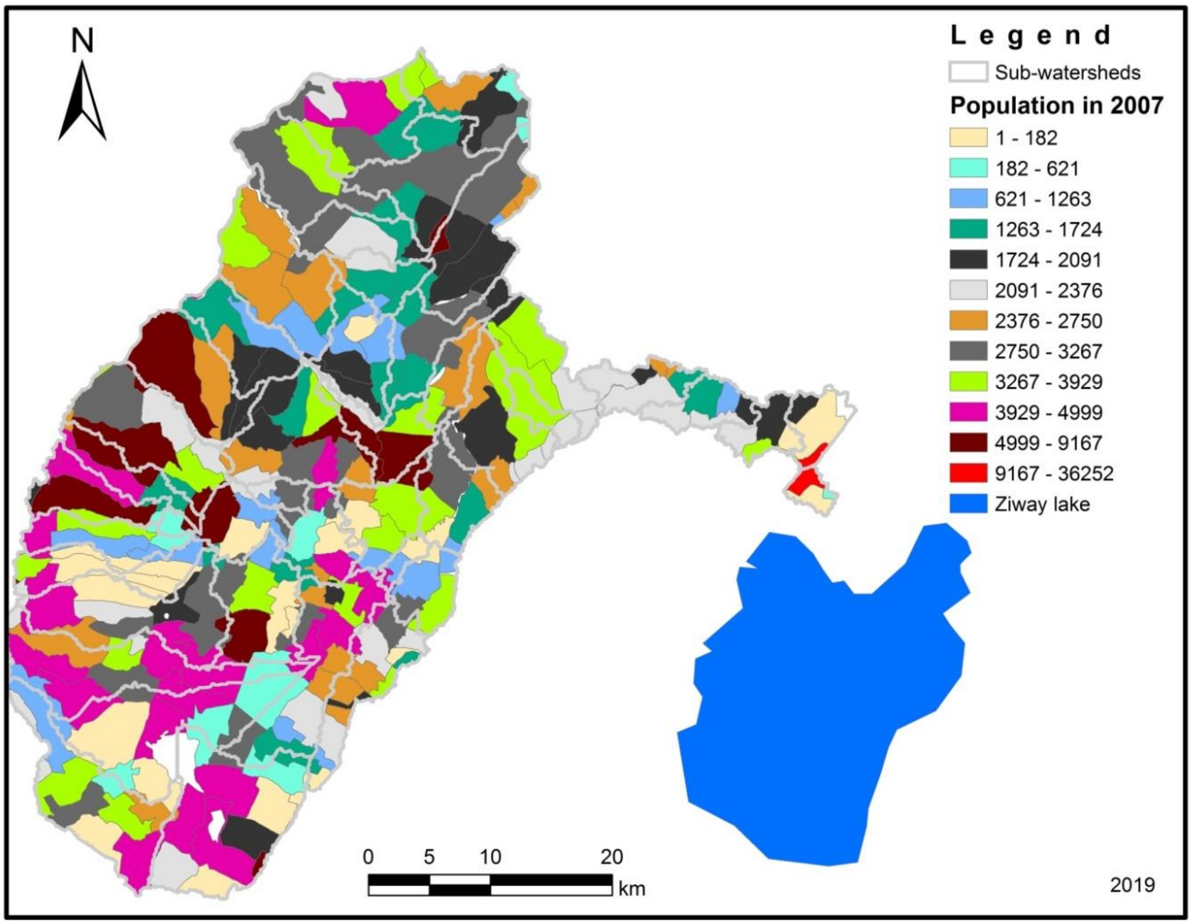

Figure 3-10: Kebele based base year population of Meki river watershed (CSA, 2007)

3.2. Study design

3.2.1. General Research Framework

Due to consideration of EBLUS in the land cover classification process, cover factor and management factor of Meki river watershed will vary and hence, there may be a change in the soil loss rate, infiltration rate of the soil, CN of the soil and runoff flow volume. Therefore, this study articulates the contribution of EBLUS to change in soil loss rates, infiltration rate change, CN change, runoff flow change and for water resources and watershed management as presented in the Flow diagram of hydrological modeling processes shown in Figure 3-11 in Meki river watershed.

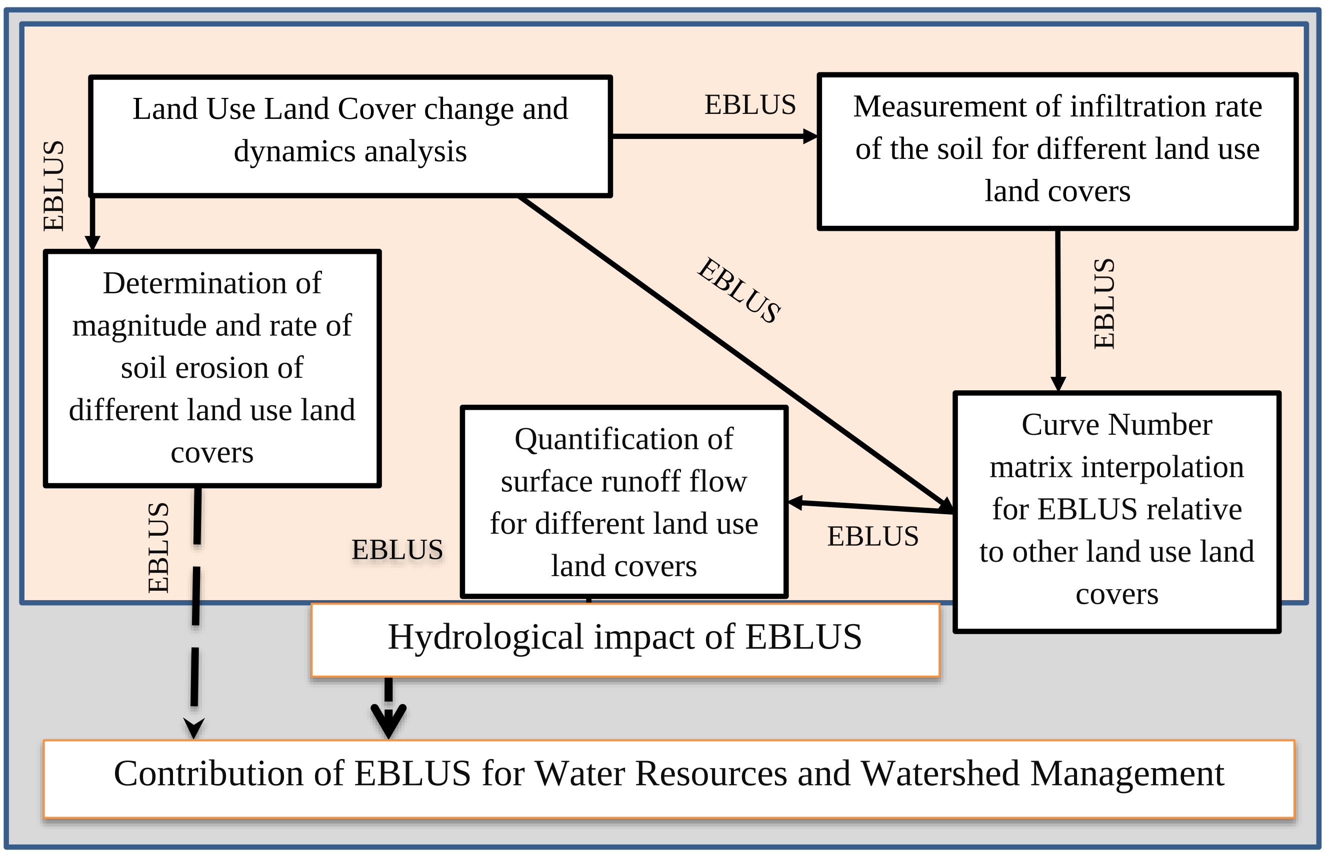

Figure 3-11: Flow diagram for Hydrological impact of Enset-Based land use system

3.2.2. Data quality assessment and rainfall evaluation for a better simulation

In hydrologic studies, the cumulations of one of the variables can be plotted against the cumulations of a pattern composed of all similar records in a given area that the pattern is composed of the average of many records, is less affected by an inconsistency in the record of any one station. If a pattern is used, as in checking the consistency of precipitation records, enough stations should be included to insure that the average is not seriously affected by an inconsistency in the record for one of the stations. The number of stations that can be included in a pattern is sometimes limited by the criterion that the area in which the stations are located should be small enough to be influenced by the same general weather conditions. If less than 10 stations are used in the pattern, each record should be tested for consistency by plotting it against the pattern, and those records that are inconsistent should be eliminated from the pattern as shown in Figure D-2 (Merriam, 1937; James and Clayton, 1960).

The recorded Meki river flow value from 1985 to 2010 (Missing >25%) (Filled with the Series mean method of SPSS) was compared with all five rainguage station precipitation values in MRWS (Ziway, Meki, Koshe, Butajira and Bui) and there was a gap in the readings of the precipitation with missing more than 20% (filled with the Series mean method). The observed flow was illogical to have flow value while there was no precipitation in all rainguages found in the catchment in the dry time of the watershed. An abrupt increase in an observed flow with out the presence of precipitation in all guages for consecutive days in the watershed as shown in Table D.6 of appendix 4 that shows the presence of precipitation data quality problem.

Hence, the choice of precipitation was mandatory for a better performance of HEC-HMS model (Bitew et al., 2019; Chu and Steinman, 2009). To achieve comparison of rainfall: the average Climate forcasting system reanalysis (CFSR) precipitation, average precipitation of five gauging stations, maximum precipitation of five gauging stations, minimum precipitation of five gauging stations, EBLUS modified precipitation (modification of five gauging station values using

Thiesson polygon area factor) were considered for further performance evaluation as shown in Table 3.3. Accordingly, the maximum and EBLUS modified ones overestimates, the minimum under estimates from the beginning of flow calibration at nominal parameter values (Table 3.3) while CFSR precipitation underestimated the observed rainfall recordes (Figure D-2) that forces us to decide not to use maximum, EBLUS modified, minimum and CFSR for further modeling of the watershed. Therefore, the average precipitation values are used for further modelling of the watershed hydrological and watershed components.

Table 3.3: HEC-HMS based rainfall evaluation

	Max	**Min**	**Average**	**EBLUS Modified**	**CFSR**	**Remark**
Peak flow simulated (m3/s)	817.5	110.8	370.5	1097.2	293.2	
Volume simulated (Million m3)	134,613.7	4,695.6	49,249.5	68,411.9	19,824	
Peak flow observed (m3/s)	139.6	139.6	139.6	139.6	139.6	
Volume observed (Million m3)	6908	6908	6908	6908	6908	
Rank	5	1	3	4	2	

As shown in the double mass curve, break in the slope is observed for all stations except for average precipitation of the CFSR in Meki River watershed. Relatively, the straight line slope is observed for CFSR than others but it underestimates the values of the rainfall so that CFSR data is not better represents the watershed than other stations in the watershed.

After choosing the average precipitation for calibration and validation of HEC-HMS model for further modeling of the impact of EBLUS on surface runoff, the consecutive years were selected based on the performance as shown in Table D**.1** of Appendix 4 hence, calibration (1985-1989) and validation (1990-1994) years were considered for modeling.

3.2.3. Land use land cover change and dynamics analysis

Enset-Based land use system (EBLUS) was not considered in all former LULC studies (Alemu *et al.*, 2020; Anita, *et al.*, 1996; Uloro & Mengel, 2014) that urges us to give emphasis EBLUS classification, change detection and dynamics analysis while giving consistent attention to all other land use land covers analysis by collecting images from different sources and following the technical procedures and scientific methods as follows:

3.2.3.1. Data collection, pre-processing and Digital Image processing

United States Geological Survey (USGS) landsat images were downloaded from USGS portal of earth explorer database as shown in Table 3.4. Image registration, extracting images, band correlation & tasseled cap analysis has been done to improve the differentiability of features such as soil, green features, moisture availability of the land and canopy (Anderson et al., 1976).

Different bands of the imageries with similar spatial resolution have been stacked, radio-metrically calibrated, resolution merge have been done for different spatial resolution imageries such as merging 30m with 15m spatial resolution imagery (PAN) to sharpen the area & topographically normalized with DEM (Alemu *et al.*, 2020; Anderson et al., 1976).

Mosaics four different scenes to get full area of interest (AOI) and it was delineated using HEC-GEOHMS software from DEM & the image subset was prepared for the imageries based on the AOI. All images and maps were geo-referenced or Projected to: Datum: UTM/WGS 84, 37 N and it was classified with unsupervised classification for further field survey sampling and to assist the supervised classification (Alemu *et al.*, 2020; Anita, *et al.*, 1996).

Table 3.4: Satellite image data collected from different sources

Year	Sensor	No. of bands	Date of acquisition	Paths	Row	Mission	Image Source
1987	TM	7	01-01-87	168 & 169	054 & 055	LS 5	USGS
2017	ETM+	12	01-01-17	168 & 169	054 & 055	LS 7	USGS
DEM			10-01-17	168 & 169	054 & 055	SRTM	USGS

3.2.3.2. Field work and Image classification processes

Evidence was collected from local elders and experts of Woreda Agriculture offices and NGOs in Meki river watershed through key informant interview with the idea extending to 30 years regarding the retrospective and prospective cover and erosion conditions of the watershed.

The ground truth data collected in the field using geographical positioning system (GPS) at an accuracy of 2m with its corresponding photographs at the point of data gathering and descriptions of the data was prepared based on vegetation zones of the area. Ground truth information was collected using the primary unsupervised classification image, land form types, and visual interpretation of multi-temporal imagery of Google earth images. Infiltration rate measuring sites were also used as a source of database for supervised classification (Alemu *et al.,* 2020; Anita, *et al.,* 1996).

Field surveying was carried out as a transect walk and data was collected to train the algorithm or the interpreter and data collected to evaluate the land cover map and for supervised classification based on the ground control points (GCP) on the upper zone, middle zone and lower zone of the watershed (Alemu *et al.,* 2020; Anita, *et al.,* 1996).

The classification of the satellite images was performed using ERDAS Imagine 2014 after a careful signature creation from the collected sets of points of the land covers and the per-pixel classifier was trained on a representative sample of each of the land cover classes by using a supervised maximum likelihood classification (MLH) algorithm with equal prior probabilities for each class (Alemu *et al.,* 2020; Anita, et al., 1996; Pal M, Mather PM, 2003). The LULC classes were categorized into eight types, including water bodies, EBLUS, Grass, Bush and Khat, plantation (Eucalyptus), cultivated and degraded, Forest and natural vegetation and builtup.

According to Ermias *et al* (2013), image differencing appeared to perform generally better than other methods of change detection. It involved subtracting one date of imagery from a second date that was precisely registered to the first with ENVI 4.3 software and also ArcGIS extension of image differencing and discussed in the result part of the paper which shows a significant increase in cultivated land cover and a significant decrease in forest cover while a considerable increase in enset land cover proportional to the population number.

3.2.2.4 Post classification processes

Majority/Minority analysis

The existing enset plantation with dense natural and planted tree cover is well mixed with the cultivated land with agro forestry trees and at the same time there are small patches of grazing land with dispersed trees that made classification process difficult. Therefore, the majority / minority analysis was applied to filter out confusing pixels and to homogenize the dominant and the major land use land cover types using ENVI 3.4. This process removes confusion of the land cover overlap and the area has been classified to the major land use category based on collected ground control points or GPS points (Appendix 4).

Change detection analysis

An image differencing technique has been employed to detect the change in LULC. Image differencing appears to perform generally better than other methods of change detection (Campbell, 1987). It involves subtracting one date of imagery from a second date that has been precisely registered to the first with ENVI 4.3 software. Change detection matrix is prepared and discussed and the resulting matrix is shown in Appendix 4.

Confusion matrix for accuracy assessment

The statistics report does include a class-for-class image difference that was performed using ENVI 3.4 which report changes as percentages/hectar (ITT Industries, Inc., 2006) and the accuracy of the classification was evaluated using the overall accuracy (OA) (Table 3.5) (Lu D, Weng Q, 2007; Congalton RG and Green K, 1999) (the total number of correctly classified pixels to the total number of sample data) (Congalton RG, Green K, 1999) (Appendix 4)

Table 3.5: Accuracy assessment result

Year	1987	2017
Overall Accuracy	95.12	94.17
Kappa Coefficient	0.9676	0.9512

3.2.4. Soil loss modeling methods to EBLUS

Soil erosion by water is the most pressing environmental problem in the Highlands of Ethiopia, where the topography is highly rugged, population pressure is high, steep lands are cultivated and rainfall is erosive (Ermias *et al.*, 2013; Bewket and Teferi, 2009). Similarly Meki river watershed shows considerable erosion sign posts evident from the numerous gullies in cultivated and grazing lands.

Land use change effects on soil loss risks were estimated using revised universal soil loss equation (RUSLE) and GIS models. Yueqing *et al.* (2011), Shi *et al.* (2004), Ouyang and Bartholic (2001) and Mallick *et al.* (2014) investigated soil erosion risk using RUSLE and GIS and displayed the results as erosion risk maps and they confirmed that the model is practical for soil conservation plans and natural resources management.

The soil loss of Meki river watershed to compute the relative influence of EBLUS on sediment load for the sustainability of lake Ziway was done using ArcGIS based RUSLE model (N.Kayet, 2018; Jetten *et al.*, 1988; Bork and Hensel, 1988; Saha, 1996 and Gupta, 2001) and pair wise comparison was done for Enset growing zones and Non-Enset growing zones of the watershed to evaluate the contribution of EBLUS to soil erosion control for sustainability of downstream water bodies including lake Ziway.

Therefore, the average annual soil loss can be estimated from eqn. 9 based on Asnake & Amare (2019); Mengesha *et al.* (2018); N.Kayet (2018); Renard *et al.*, (1997); Yoder and Lown, (1995); Renard and Freimund (1994); Wischmeier and Smith, (1978) (Equn 3-1):

$$\mathrm{A} = \mathrm{RKLSCP} \tag{3-1}$$

Where A is the amount of soil erosion (t ha-1yr-1) that is eroded within unit area during the corresponding period of rainfall-runoff; R is a rainfall-runoff erosivity factor; K is a soil erodibility factor; LS is a surface characteristic factor (slope-length and steepness factors; C is a cover management factor; P is support practice factor.

3.2.4.1. Determination of Rainfall - Runoff erosivity factor (R)

Rainfall data have been collected from Ethiopian National Meteorology Agency (ENMA) for Meki river watershed for the last 30 years and rainfall records of 10 surrounding representative stations have been analyzed in excel and converted to shape file to determine R factor.

The rainfall erosivity (R) factor expresses the energy of rainfall to erode the soil which is influenced by the intensity and amount of rainfall and canopy cover of the soil surface. The value of R was interpolated based on the values Modified (Mekuria, 2005; Hurni, 1993) for Ethiopian condition which was developed by Hurni (1985) and adopted by different researchers (Mengesha *et al.*, 2018; Asnake & Amare, 2019; Bewket and Teferi, 2009) and presented as shown in Table 3.6 and Equation 3-2 and the average R values derived between 478.3 and 700 for Meki river watershed as shown in Figure 3-12.

$$\mathbf{R = 0.562P - 8.12} \tag{3-2}$$

Table 3.6: Rainfall Erosivity interpolation

Station	**Annual Average rainfall (mm)**	**Erosivity (R) (Mekuria, 2005; Hurni, 1985)**	**R = (0.562P-8.12)**	**Average R ($MJmmha^{-1}h^{-1}year^{-1}$)**
Agena	1438.82	799.334	801.94	800.63
Bui	1042.69	576.908	578.91	577.91
Butajra Police Station	1119.58	619.963	622.2	621.08
Hasen Usuman	1048.98	580.428	582.46	581.44
Imdibir	1229.16	681.401	683.9	682.65
Koshe	826.087	455.609	456.97	456.29
Lemen	917.872	507.008	508.64	507.82
Meki	767.77	422.951	424.13	423.54
Werabe	1527.01	848.944	851.59	850.27
Ziway	759.005	418.043	419.2	418.62
Average	1067.7	591.059	593	592.03

Based on Webster & Oliver (2007) & Bewket and Teferi (2009), the Geo-statistical extension of ArcGIS is used to interpolate the spatial value of R with the geo-statistical method of kriging/cokriging and the kriging type is simple normal score with the prediction output surface types because it is easy to generate relatively accurate rainfall erosivity information from known sample points to the points of unknown values at a closer distance than those located far.

Transformation of annual average R is performed at a five number of bins and one number of kernels (μ=591.059, σ= 142.4 and π=1). It is a general optimize model at a false examine bivariate distribution of the covariance variable with a model nugget of 0.5 true enabled at a measurement error of 100.

The model number is one with stable type at a parameter of 1.83 and major range of 0.735 with a false anisotropy. Partial sill is calculated as a true with a partial sill of 0.5 at a lag size of 0.103 and number of lags 12 and the standard neighborhood type at a maximum neighbors of five and at a minimum neighbors of two with four sectors of 45° offset and true variogram at zero angle with major semi-axis of 0.735, minor semi-axis of 0.735, anisotropy factor of 1, predicted Value (x=38.3765 & y=8.17) of 606.2 and weights (10 neighbors) (Webster & Oliver, 2007).

The export result table shows that regression function is given as 0.286X + 406.65, mean of -4, root-mean-square of 103.55, mean standardized at -0.0262, root-mean-square standardized at 0.811, average standard error of 126.56. The value of R is reclassified to suitably compute the average annual soil loss (A) and the R value ranged from 478.3 to 700 MJ mm ha^{-1} h^{-1} $year^{-1}$ for Meki river watershed and mapped as shown in Figure 3-12. A similar approach was adopted to compute the R factor in Ethiopia by Bewket and Teferi, 2009; Abate, 2011; Mengesha *et al.*, 2018; Asnake & Amare, 2019.

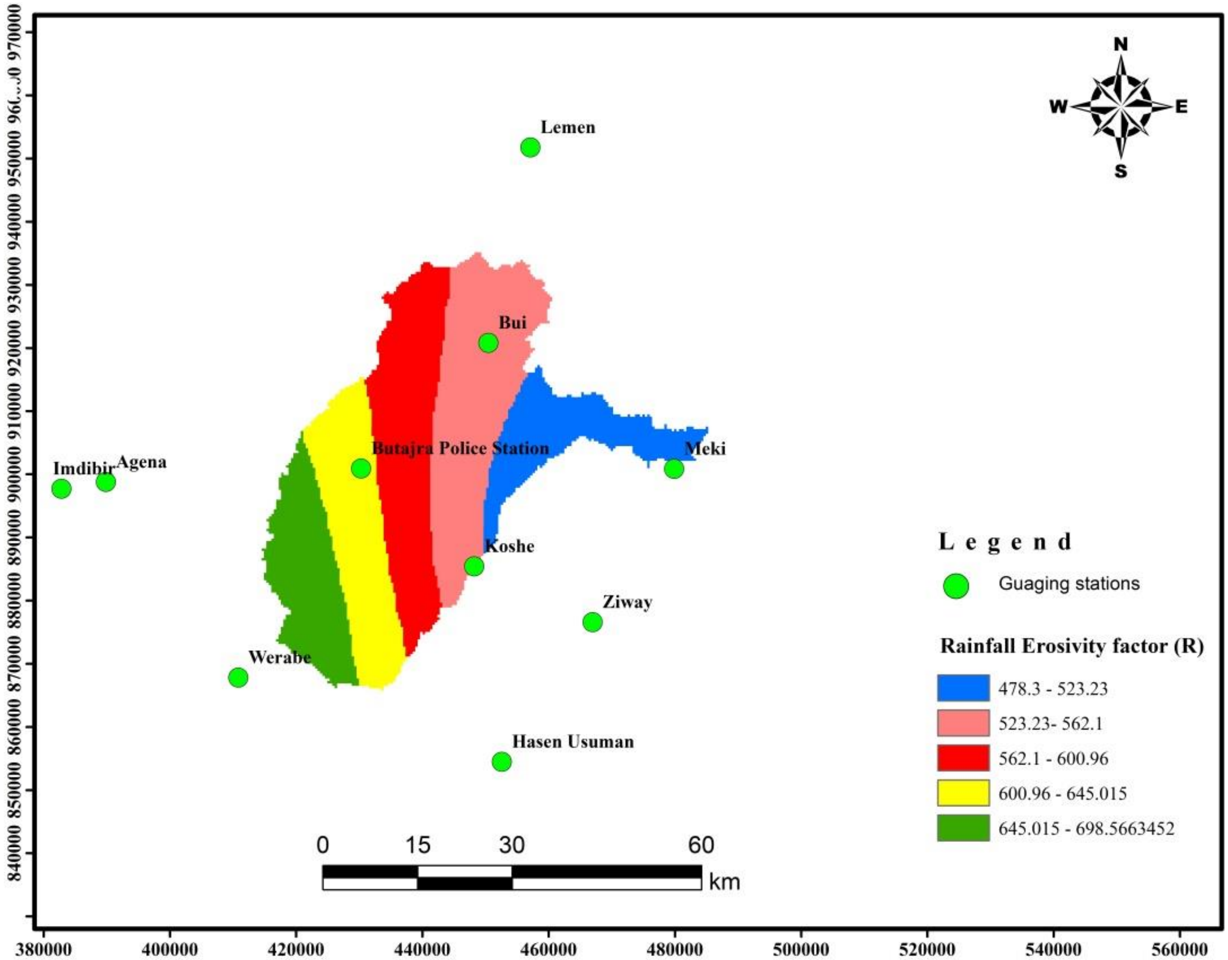

Figure 3-12: Rainfall Erosivity factor (R) map of the watershed

3.2.4.2. Determination of soil erodibility factor (K)

Erodibility factor (K) is a measure of soil susceptibility to detachment as well as transport, and ranges from 0.05 for low erodibility to 0.4 for high erodibility. Clays have low K values because they are not as easily detached, sandy soils also have low K values because they are difficult to transport via runoff. Silt loam soils have medium K values and soils high in silt have high K values.

The Soil property (soil texture, soil structure, organic matter, water content, density and chemical and biophysical characteristics of the soil) affects infiltration rate and the extent to which the soil particles can be detached and transported (El-Swaify and Dangler, 1976).

Hurni (1985) has developed the factor table from the USLE monograph (A. Kavian *et al.*, 2017; Yang *et al.*, 2005; Wischmeier & Smith, 1978) & adopted by Bewket and Teferi (2009); Mekuria (2005) relating the color of soil used to assign K value of the soil for Ethiopian condition. The color of the soil is determined through an intensive literature review of the relationship of soil type to its color supported by a field observation. Harmonized World Soil Database (HWSD) is used to determine the soil type and soil color is assessed and K value is assigned for each soil type as shown in Table 3.7 as black, brown, red and yellow, and their corresponding K factor values are 0.15, 0.2, 0.25 and 0.3 respectively.

A similar method of determining K factor values from colour of soils has also been suggested by the Soil Conservation Research Project (SCRP, 1996) and adopted by Bewket and Teferi, 2009; Mekuria, 2005. According to Asnake and Amare (2019), due to scantiness of data, only soil colors and stone covers were selected to determine K factor. Those different color polygons are reclassified to assign K values and finally K map is prepared.

Table 3.7: Erodibility (K) value of soils of Meki river watershed

Soil type	Soil Code	Color of soils	K	Adopted by researchers
Vertisol	16851	Black	0.15	Asnake and Amare, 2019; Bewket and Teferi, 2009; Mekuria, 2005; Hurni, 1985
Luvisol	16739	Brown	0.2	
Cambisol	16932	Red	0.25	
Leptosol	16808	Yellow	0.3	
Fluvisol	16903	Brown	0.2	
Water	16994		0.4	Hurni, 1985

The K factor is rasterized after assignment of those values to each soil types based on their inherent characteristics and reclassified as shown in Figure 3-13.

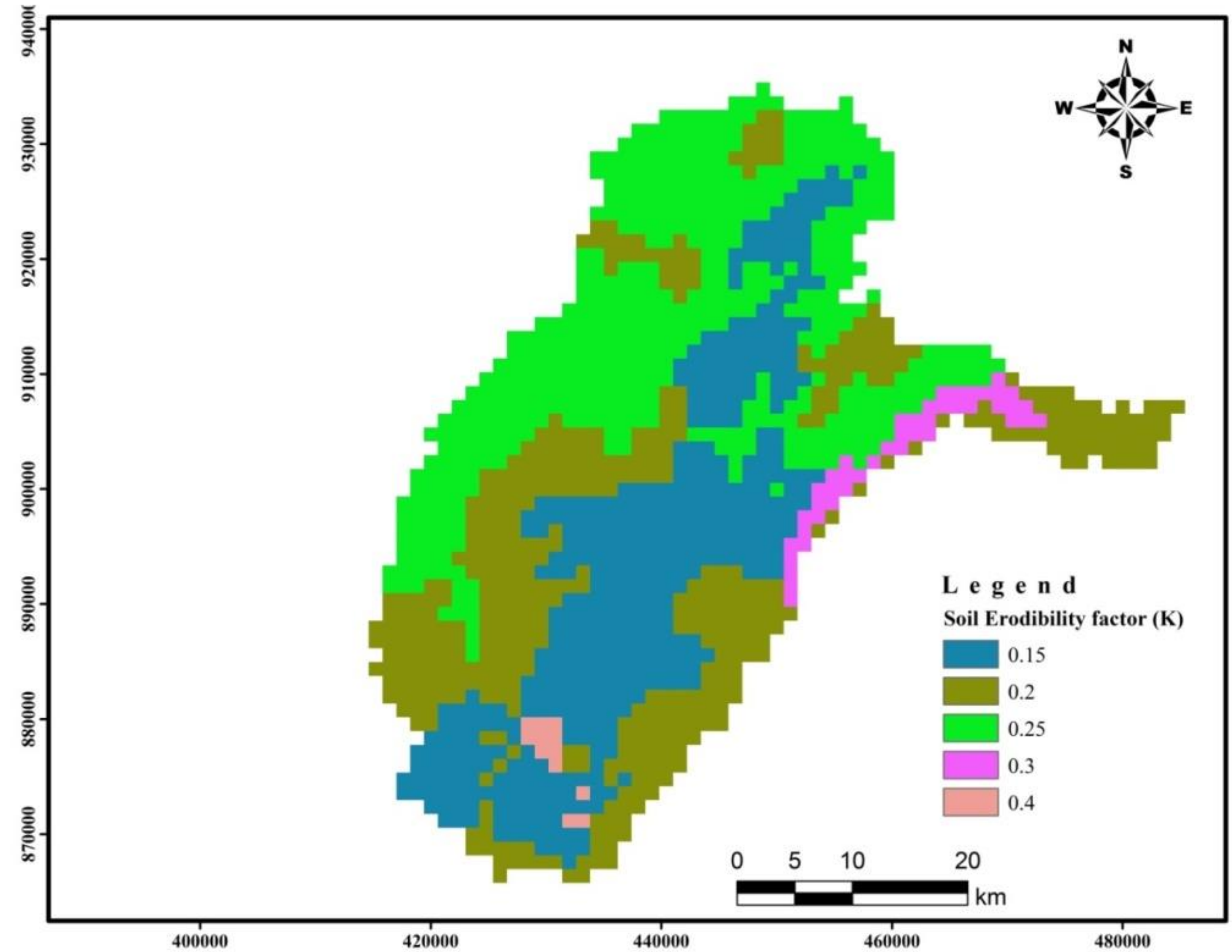

Figure 3-13: Soil erodibility (K) value map of Meki river watershed

3.2.4.3. Determination of topographic factor (LS)

The LS factor expresses the effect of topography (hill slope length and steepness) on soil erosion. The increase in L and S results in an increase in the LS factor and soil erosion (Asnake and Amare, 2019; Kavian *et al.,* 2017) for which various approaches have been used to estimate the LS factor. DEM (30 m resolution) with ArcGIS techniques devised to obtain slope gradient (S) and slope length (L) (Kebede *et al.,* 2015; Bewket and Teferi, 2009; Nekhay *et al.,* 2009).

Several researchers followed different methods of computing LS factor using Arc-GIS as shown in Table 3.8.

Table 3.8: Table of topographic factors formula for different studies

Equation	**Description**	**Source**	**Av. LS**	**Area**
$\mathbf{LS = 1.4[\frac{\mathit{As}}{22.13}]^{0.4} * \left(\frac{\sin(\beta)}{0.0896}\right)^{1.3}}$	As = the specific area defined as the upslope contributing area for overland grid per unit width normal to flow direction, and β is the slope gradient in degrees	Kavian *et al.*, 2017	2.83	Iran
$\mathbf{LS = [\frac{\beta\chi}{22.13}]^{0.5} * (\frac{\sin(0.01745\mathit{s})}{0.0896})^{1.3}}$	β is flow accumulation, χ is grid cell size (30m), 22.13 is the RUSLE standard plot length; 0.5 is the exponent of slope length; s is Slope of DEM in degrees	Asnake and Amare, 2019; Fenta *et al.*, 2016	7.3	Blue Nile Basin
$\mathbf{LS = [\frac{fac*DEM\ resolution}{22.13}]^{0.4} * (\frac{\sin(\mathit{s})}{0.0896})^{1.3}}$	fac is flow accumulation, s is slope in degree	Habtamu *et al.*, 2020	33	West Shoa Ethiopia
$\mathbf{LS = \left(\frac{\lambda^{0.3}}{22.1}\right) * (\frac{S}{9})^{1.3}}$	λ is Flow length and S is Slope in percent	Kebede *et al.*, 2015	3.5	CRV of Ethiopia
$\mathbf{LS = \left(\frac{\lambda}{22.1}\right)^{\mathit{m}} * (0.065 + 0.045x + 0.0065(x)^2}$	λ is flow length, m is an exponent that depends on slope steepness	Bewket and Teferi, 2009	2	Blue Nile Basin

From those equations listed in Table 3.8, the following equation was selected as it has been widely used and tested in several studies in Ethiopia context and specifically applied in central rift valley of Ethiopia and the flow chart for LS value determination is shown in Eqn. 3-3 and Figure 3-14.

$$\mathbf{LS = \left(\frac{\lambda^{0.3}}{22.1}\right) * (\frac{S}{9})^{1.3}} \tag{3-3}$$

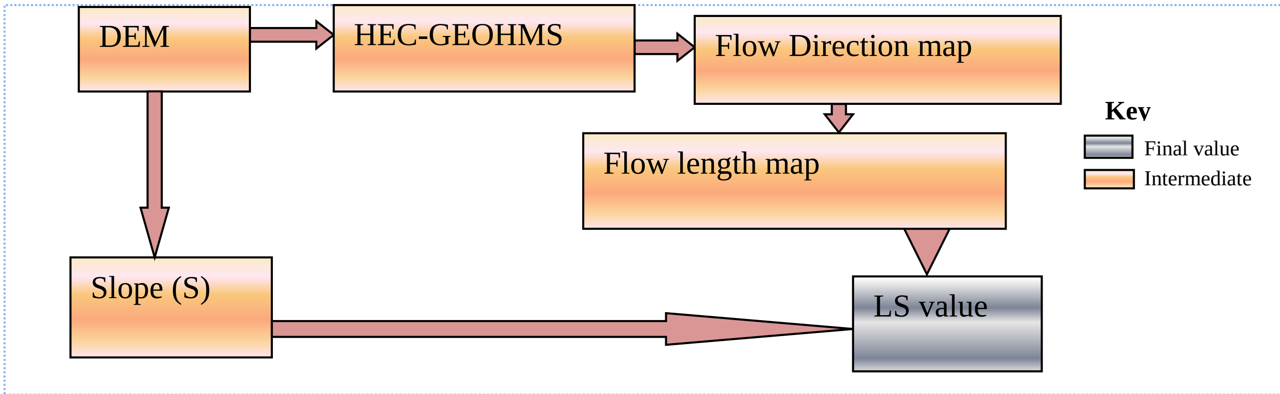

Figure 3-14: Flow chart for LS value determination

Based on the flow chart shown in Figure 3-14 for LS determination, the flow direction map and slope maps were converted to LS value using raster calculator and mapped in Figure 3-15.

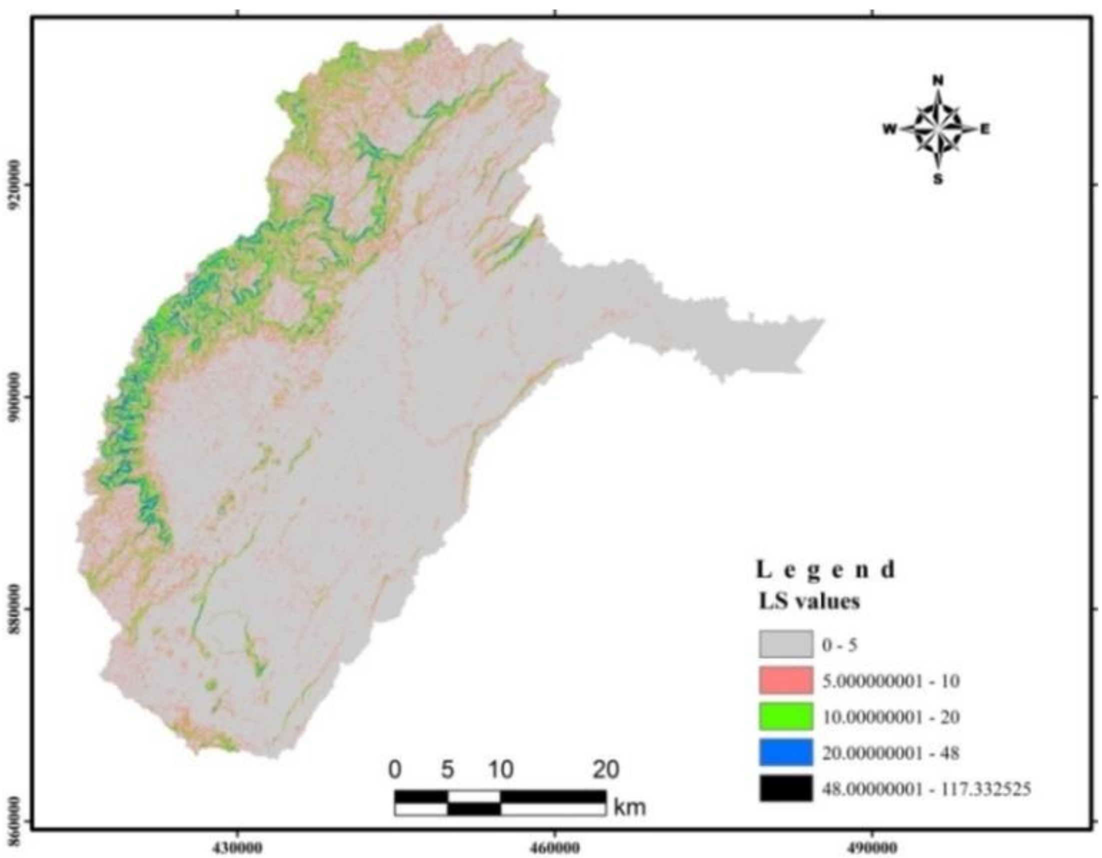

Figure 3-15: Topographic (LS) map of Meki river watershed

3.2.4.4. Determination of land cover factor (C)

The cover-management factor (C) and support practice (P) are dynamic factors through time (Kavian *et al.*, 2017) and C factor expresses the effect of plants and soil cover to reduce the runoff velocity and to protect surface pores and that is most readily changed by human activities.

C factor is assigned to the classified satellite images supported by interviews of local farmers for land use land cover condition of the area. C-value was assigned to each land use classes using reclassify method in Arc GIS 10.1 as reviewed in literatures as shown in Table 3.9. Wheat, Enset, maize and teff are the dominant crops growing surrounded by woody agro forestry trees in the watershed.

Table 3.9: Land cover factor assigned

<table>
<tr><th>Land cover</th><th>C value</th><th>Source</th></tr>
<tr><td>Cultivated & Degraded</td><td>0.15</td><td rowspan="6">Asnake and Amare (2019); Bewket and Teferi, (2009); Mekuria (2005); Hurni, (1985b);</td></tr>
<tr><td>Forest & other natural vegetation</td><td>0.001</td></tr>
<tr><td>EBLUS</td><td>0.02</td></tr>
<tr><td>Grass</td><td>0.05</td></tr>
<tr><td>Eucalyptus</td><td>0.05</td></tr>
<tr><td>Bare land</td><td>0.6</td></tr>
<tr><td>Bush & khat</td><td>0.1</td><td>Tamene et al. (2014); Haregeweyn et al. (2013); Bewket and Teferi, (2009); Mekuria (2005); Hurni, (1985b);</td></tr>
</table>

Hence, the land cover factor map of the watershed was prepared for the 1987 & 2017 land sat image classified land covers and mapped as shown in Figure 3-16.

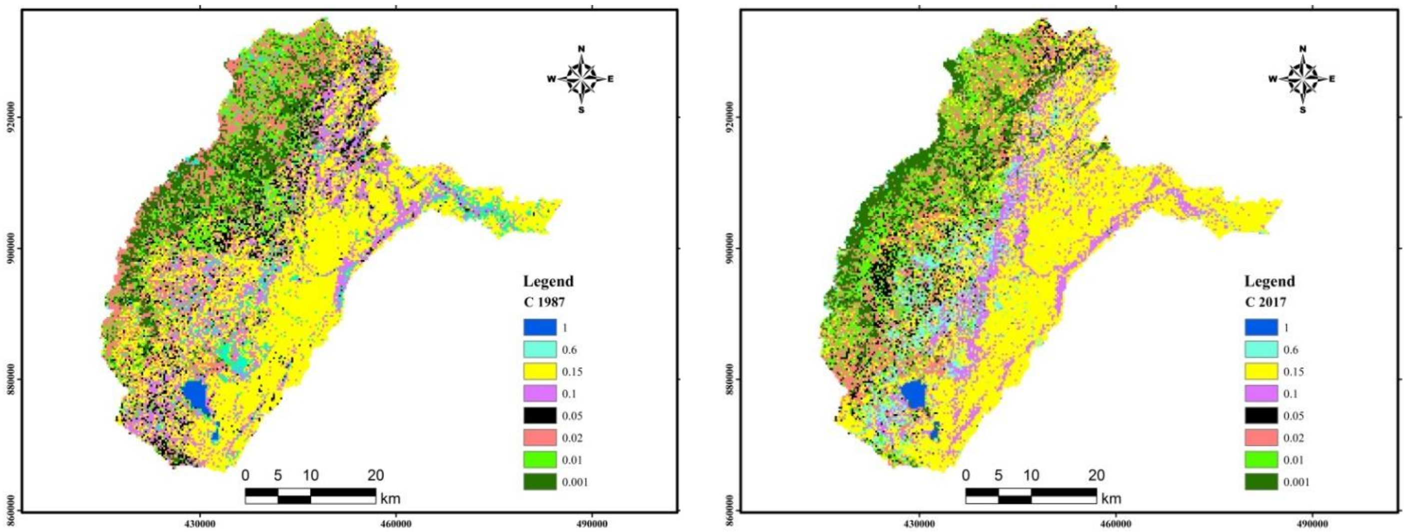

Figure 3-16: Land cover factor map of Meki river watershed in 1987 & 2017

3.2.4.5. Determination of land management factor (P)

The P factor expresses the effects of supporting conservation practices, such as contouring, buffer strips of close-growing vegetation and terracing at a particular site. A good conservation practice will result in reduced runoff volume, velocity and less soil erosion.

The present management practices have been collected through observation of the site and secondary information collected from different governmental and non-governmental organizations working on conservation practices in the watershed and also an interview of local farmers who lived at least for the last 30 years for its change on management practices done using structured questionnaire with GPS based site specific checkup of the reported cases of conservation structures. The key informant interview, field observation and secondary information collected from different governmental and non-governmental organizations shows that almost all land covers are without conservation measures although some watershed management trials by the government.

Therefore, a unity was assigned to all land covers as a management factor except for forest and EBLUS for which 0.5 & 0.6 is assigned respectively because enset is planted in rows serving as a contour with mulching practices and mapped as shown in Figure 3-17.

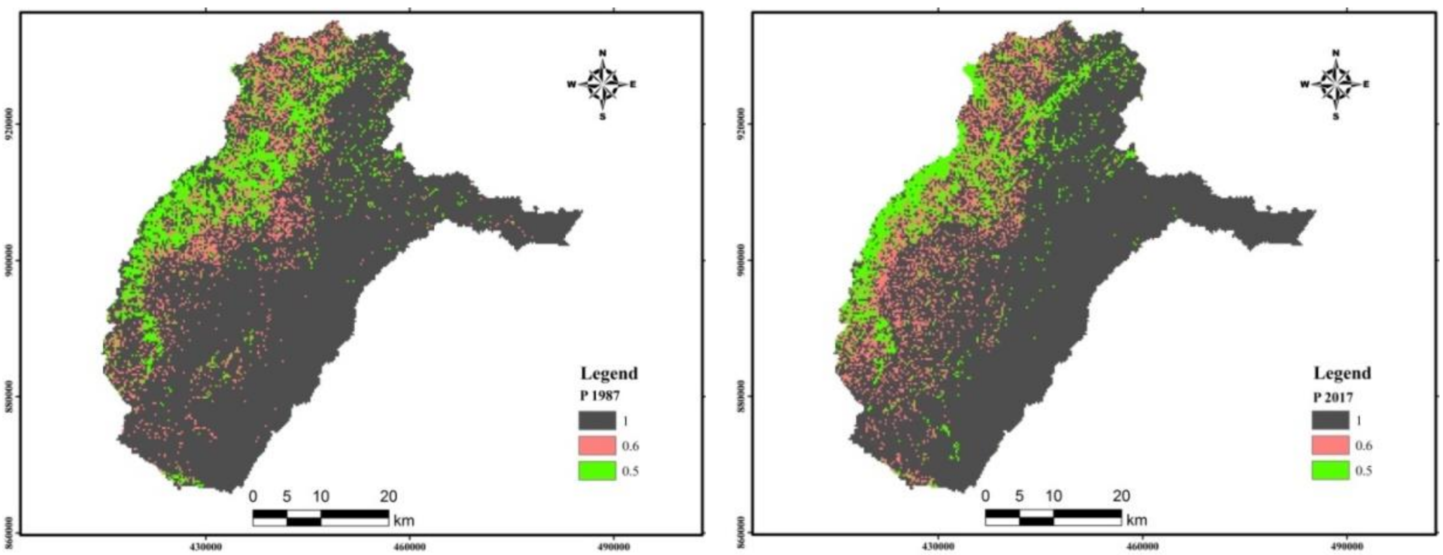

Figure 3-17: Management factor map of Meki river watershed in 1987 & 2017

3.2.4.6. Determination of mean annual soil loss

All the factors of the RUSLE model were transformed into raster format and same coordinate system (UTM WGS 1984 37^0 North) with a pixel size of 30×30m. Then, all layers were multiplied together using raster calculator in Spatial Analyst tool in ArcGIS 10.1. The mean annual soil loss was therefore determined for each pixel for 1987 and 2017 and the soil loss of Meki river watershed was calculated from all the inputs and the difference in soil loss for the 1987 and 2017 was computed.

The result was extracted and reported for the classified land use land covers of Meki river watershed and also it was extracted to 34 sub-watersheds and two major growing zones (Enset growing and non-Enset growing zones) of Meki river watershed as shown in Figure 3-18.

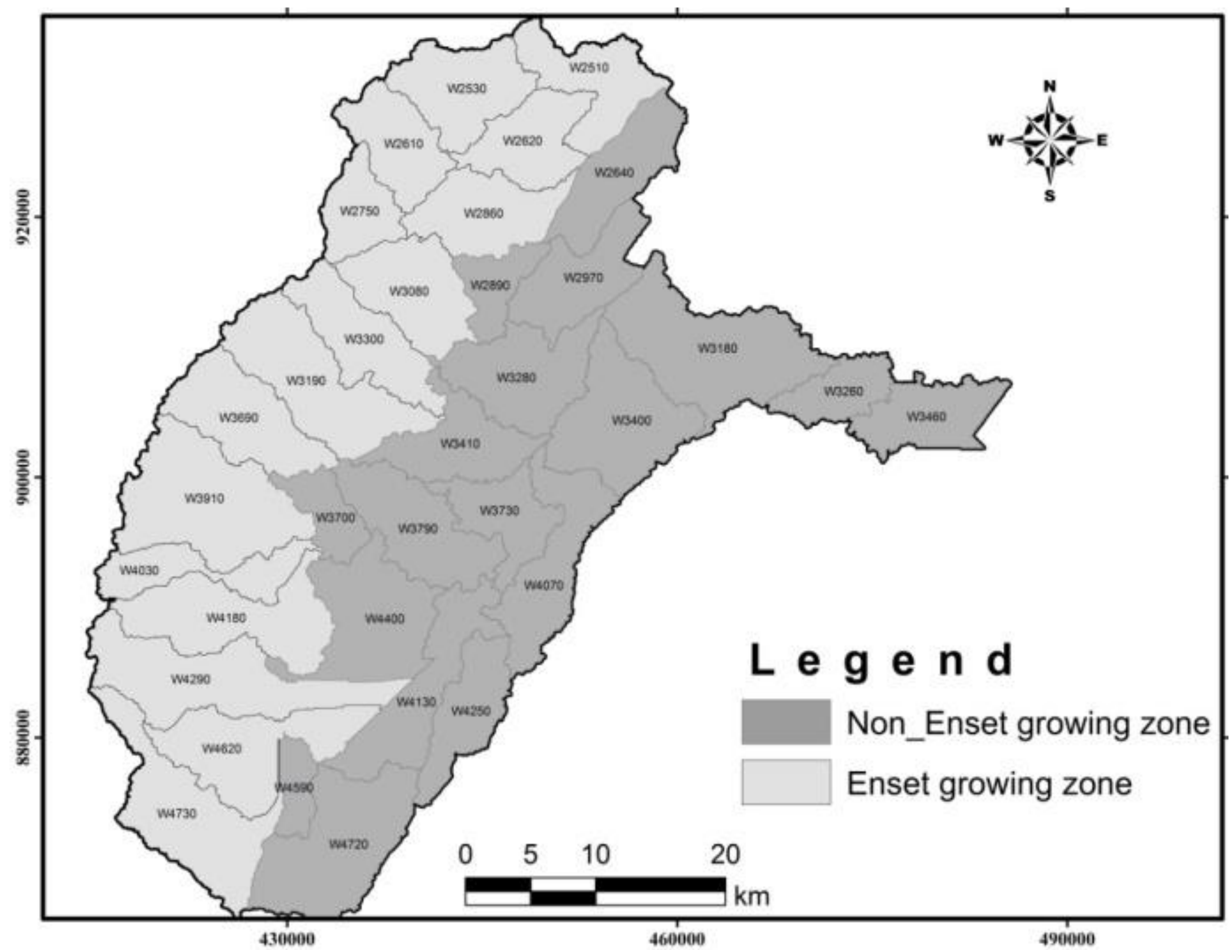

Figure 3-18: Sub-watersheds and major zones in Meki river watershed

The enset growing zone is known for its medium altitude but the non-enset growing zone of Meki river watershed is known for its lower altitudes although enset plant has the capacity to resist droughts.

3.2.5. Modeling and Evaluation of impact of EBLUS on sediment load

i. Model selection for sediment load modeling

According to Hajigholizadeh, Melesse & Fuentes (2018), erosion models delivered the concepts of reality used to simulate and the selection of erosion model depends on several factors such as input data requirements, the objective and scale output of the model, and basin characteristics.

The Modified Universal Soil Loss Equation (MUSLE) is an advanced form of USLE and RUSLE and it is developed by using runoff energy factor instead of the rainfall erosivity used in previous models (Renard, 1997). MUSLE model estimates the sediment yield based on the runoff energy factor and it is used in HEC-HMS or SWAT models but based on Pak et al., 2015; HEC-HMS predicts a comparatively effective result than SWAT model.

According to Halwatura & Najim 2013; Pak et al., 2015, HEC-HMS models have been tested for different watersheds throughout the world. It can simulate a single event or long-term continuous models and can be used for scale watershed to large watershed, Urban as well as a natural basin. Researchers who used the HEC-HMS model in different watersheds with different methods obtained satisfactory results that were consistent with the previous studies. The HEC-HMS model comprises six different methods to represent the runoff process, erosion, and sediment yield. In this study for the hydrological and meteorological model, the selected methods are presented in Table 3.10 and Table 3.11 respectively (Pak et al., 2015).

Table 3.10: Selected methods in the HEC-HMS

Model Type	Surface Method	Loss Method	Transform Method	Erosion Method	Sediment Transport Method
Continous	Simple surface	SCS-CN	SCS Unit Hydrograph	MUSLE	Laursen-Copeland

Table 3.11: Selected method in a meteorological model

Model Type	Precipitation	Evapotranspiration	Snowmelt
Continous	Specified Hytograph	None	None

i. Types of Sediment load and erosion method in HEC-HMS

Five surface erosion methods have been included in HEC-HMS version 4.3 (USACE, 2020). These are: Build up wash-up, LA Debris Method EQ1, Modified USLE, Multi-Sequence Debris Prediction Method and USGS Long-Term Debris Model. Method selection depends on soil type, land use, and terrain data. According to Pak et al., 2008; Pak et al., 2009; USACE, 2016; USACE, 2020; Gartner, Cannon & Santi, 2014; Build-up -wash-up method can simulate the erosion from an urban or impervious area, LA Debris Method EQ1 was applied to a small area watershed varies from 0.1 to 7.7Km2 and MUSLE is more suitable in agricultural land but many users have used it in construction and urban areas and hence in this study, MUSLE has been selected to simulate the erosion model. Multi-Sequence Debris Prediction Method (Pak et al., 2008) applies to the small watershed area (0.1 to 7.7 km2) with no peak flow data available (USACE, 2020) and USGS Long-Term Debris Model was established by using the hundreds of datasets from debris flow (USACE, 2020).

According to Banasik & Walling, 1996; Sadeghi & Mizuyama, 2007, MUSLE is commonly used in the world and its' mathematical equation to estimate the sediment yield is as in Eqn. 3-4.

Sed= 11.8 $(Qsurface * qpeak)$ 0.56 $* K * LS * C * P$ .... (3-4)

Where, Sed is sediment load in Tons, Qsurface is the volume of surface runoff in m3, qpeak is Peak discharge in (m3/s), K is Erodibility Factor, the unit is (ton/ha, R), LS is Topographic factor, C is cover management factor, and P is Practice factor. The LS, C, and P are unitless.

- **Erodibility factor (K)**: According to Addis & Klik, 2015; Duiker, Flanagan & Lal, 2001; Morgan, 2009, K factor describes the resistance to soil erosion and is depends on soil properties, organic matter content (OM), bulk density, particle size, and shape and it ranges from 0 to 1 (Gwapedza et al., 2018; Schulze et al., 2007) and it can be calculated based on observed soil parameters such as organic matter content (OM), texture, coarse fragments, structural class, and permeability (Addis & Klik, 2015; Parwada & Van Tol, 2017; Wischmeier & Smith, 1978; Wischmeier, 1971) that based on Eqns (3-5 & 3-6).

$K = 2.77 * 10{-}7(12 - OM)M1.14 + 4.28 * 10{-}3(s - 2) + 3.29 * 10{-}3(p - 3)$ .... (3-5)

$M = [(100 - C)(L + Armf)$ .... (3-6)

Where, C is the percentage of clay (<0.002 mm), L is the percentage of silt (0.002 mm to 0.05 mm), Armf denotes the percentage of very fine sand (0.05mm to 0.1mm), OM is the percentage of organic matter content, S is code of the structure size, type, and grade based on field observation and P is code of the permeability. Source: (Addis & Klik, 2015; Pérez-Rodríguez, Marques & Bienes, 2007).

• **Topographic factor (LS)**: The LS is defined as vulnerability to erosion that depends on the length and slope of the terrain. Generally, the value of (LS) ranges from 0.1 (flat slope) to 10 (steep-slope) (Van Remortel, Maichle & Hickey, 2004; Zhang, H et al. 2017) and it is computed indetail in RUSLE part of soil loss computation.

• **Cover factor (C):** it defines the impact of vegetation on soil erosion. A higher value of cover factor indicates to the most vulnerable of soil erosion and vice-versa and the value ranges from 1 to 0.1 and it is presented in the soil loss part of the paper (Scharffenberg, 2016).

• **Practice factor (P):** The Practice factor (P) shows the ratio of soil loss based on conservation practice to the soil loss based on certain cultivation. The P-value range from 0 to 1. The lower value 0 indicates higher erosion resistance capacity whereas higher value 1 represents lower erosion resistance capacity (Parveen & Kumar, 2012) and it is presented in the soil loss part of the paper.

• **Exponent:** The exponent in erosion is used to distribute the sediment concentration in time-series sedigraph. The sediment concentration can be calculated by using a power function (Haan, Barfield & Hayes 1994; Pak et al., 2015) is shown in equation (3-7). The value of exponent is generally range from 0.5 to 1(Pak et al., 2015).

$Ct = KiQtb$ .... (3-7)

Where, Ct = Sediment concentration at time t, Ki is constant calculated from runoff, Qt is discharge from the sub-basin.b= exponent entered to HEC-HMS platform.

A total of seven parameters estimated based on terrain, land use, and soil type of the catchment are required to input for the erosion model. These are: K, LS, C, P, Threshold (1m3/s = no sediment transport if flow is >1 m3/s), Exponent and Gradation curve.

Erosion model parameters were extracted from the values computed for RUSLE model and feed to the erosion part of each of the 34 sub-watersheds (Alemu et al., 2020; Arvad, 1993). In this case Erosion method of Modified USLE was chosen and the erosion icon displayed so that K, LS, C, P factors were coded to each of the sub-watersheds for modeling sediment (Table 3.12).

Table 3.12: Erosion model parameters assigned to each sub-watershed

SWS	Erodablility factor	Topographic factor	Cover factor	Practice factor	Threshold (m3/s)	Exponent
W2530	0.24441	5.924	0.038	0.795	1	0.75
W2510	0.231	3.7	0.10042	0.918	1	0.75
W2620	0.2105	5.267	0.091	0.832	1	0.75
W2610	0.224	4.58	0.074	0.8582	1	0.75
W2860	0.25	7	0.0374	0.728	1	0.75
W2750	0.23	6.5	0.03221	0.7363	1	0.75
W3080	0.21	3.704	0.149	0.9124	1	0.75
W2890	0.218	2.99	0.159	0.966	1	0.75
W2640	0.2041	2.852	0.1555	0.974	1	0.75
W2970	0.234	6.923	0.049	0.761	1	0.75
W3280	0.186	1.78	0.159	0.9834	1	0.75
W3190	0.2363	7.15	0.0511	0.7512	1	0.75
W3300	0.245	7.2	0.033	0.72	1	0.75
W3410	0.1834	1.67	0.18	0.97	1	0.75
W3910	0.22	6	0.075	0.781	1	0.75
W4030	0.22	5.6	0.121	0.793	1	0.75
W3690	0.232	7.42	0.039	0.74	1	0.75
W3700	0.16143	2.63	0.1765	0.925	1	0.75
W3790	0.16	1.784	0.2	0.97	1	0.75
W4720	0.15223	1.351	0.17	0.996	1	0.75
W4730	0.181	2.425	0.16	0.99	1	0.75
W4590	0.165	3.26	0.17	0.95	1	0.75
W4620	0.197	2.644	0.39	0.96	1	0.75
W4290	0.16331	2.5	0.24	0.96	1	0.75
W4180	0.19	3.53	0.094	0.885	1	0.75
W4400	0.19622	4.544	0.121	0.855	1	0.75
W4130	0.153	2	0.19	0.97	1	0.75
W4250	0.18	1.77	0.1601	1	1	0.75
W3730	0.196	1.7	0.144	1	1	0.75
W4070	0.199	1.64	0.15	1	1	0.75
W3400	0.2324	1.751	0.145	0.99	1	0.75
W3180	0.232	1.71	0.1442	0.998	1	0.75
W3260	0.2132	1	0.1461	1	1	0.75
W3460	0.2	0.513	0.1653	1	1	0.75

Gradation curve: The gradation curve in HEC-HMS describes the distribution of total sediment load into different grain size classes at the outlet of the sub-basin. The gradation curve is the particle size distribution curve, and it is input as a diameter-percentage function from the Paired Data Manager in HEC-HMS (Table D.4 of appendix 4). In non-cohesive sediments the particle or grain size and weight were the dominant parameters for sediment movement and transport. In most soils clay assumed control of soil properties at less than 10% clay content (Arvad, 1993).

Figure 3-19: Texture class assessment in the field

Gradation curve tells us the proportion of clay, silt and sand components of the soil and also it tells us the probability of the sediment to be carried by runoff. Gradation curve was prepared by collecting the data from Harmonized World Soil Database (HWSD) table and verified by field based finger analysis method to determine the textural class of the major soils in the watershed as shown in Figure 3-19 that helps to determine the particle size distribution of the soil. Hence eight category of textural gradation was done which were T1, T2, T3, T4, T5, M1, L1 and L2 to express the textural class found at the top watershed (T), middle watershed (M) and lower watersheds (L) got different textural proportions as shown in Table D.4 of appendix 4.

Each of the gradation proportions were fed to the paired data created through component portion of well calibrated and validated HEC-HMS model. Finally, sediment load was presented for all the sub-watersheds and for calibration and validation years as well as a time series daily based sediment load were prepared and presented in the result part of this thesis.

ii. Evaluation of impact of EBLUS on sediment load

Precipitation variation is the prominent and the only climate factor to significantly affect runoff and all other elements of water balance (Mewded et al., 2021; Koneti et al., 2018) but to avoid its effect the same year precipitation was used. Therefore, 4 scenarios were developed by combining different LULC and EBLUS (EBLUS as a Cultivated LUS and EBLUS as a separate LUS) data keeping precipitation constant (Koneti et al., 2018) to compute the contribution rate of EBLUS change as shown in Table 3.24.

Table 3.13: Scenarios used for quantitative impact analysis of EBLUS

Scenario	LULC	Precipitation	EBLUS considered	Simulated Sediment (Si)
1	1987	Average	Yes	S1
2	1987	Average	No	S2
3	2017	Average	Yes	S3
4	2017	Average	No	S4

The scenarios created were used to determine the rate of impact of EBLUS change (L) on the generation of sediment (Koneti et al., 2018; Mewded *et al.*, 2021) relative to cultivated LUS in Meki river watershed (Eqn.3-8). Therefore, calculating the contribution rate between 1987 and 2017 based on the 1987 reference period is given as:-

$$\boldsymbol{L_{1987-2017}}(\%) = \left(\frac{\mathbf{(S4-S2)-(S3-S1)}}{\mathbf{S4-S2}}\right)\mathbf{x100}\% \tag{3-8}$$

The sediment load routing through the rivers were computed using HEC-HMS based MUSLE model. MUSLE performs in a similar way with USLE or RUSLE but it uses volume of runoff to quantify the amount of sediment carried and routed in the route in Meki river watershed. The impact of EBLUS on magnitude of sediment load was determined and the result was presented in a table and graphically.

3.2.6. Infiltration rate measurement and analysis

3.2.6.1. Sample site selection criteria

Measurement of vegetation zone based infiltration rate of the soil under different land use land covers to evaluate their relative hydrological influence were achieved using Amozi-meter (Hood infiltrometer) in the labor intensive field work and mapping was done using Arc-GIS 10.1. The soil type (soil texture) was one of the bases for sample site selection next to vegetation zone.

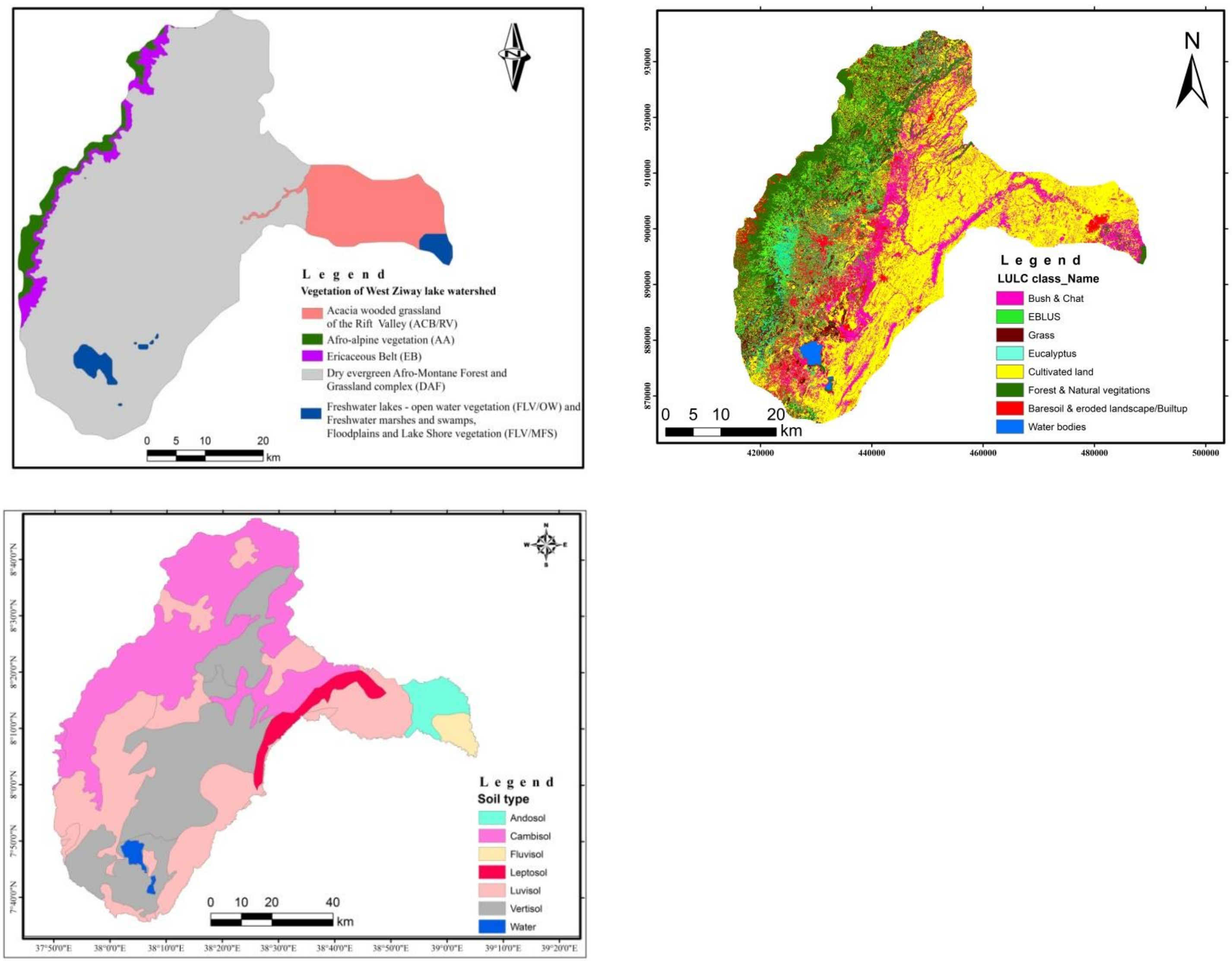

Figure 3-20: Vegetation zone, Land use land cover & soil type maps of the study area

3.2.6.2. Sampling and Measurement techniques

According to Azene *et al.*, 1993, like the common banana, Enset is a giant herb. It grows in wet upland valleys and ravines and along streams in the forests of lower mountain slopes, 1,600-2,400 m with a leaf length of 6-12meters and grows in spirals. In south-central Ethiopia enset is extensively cultivated for food up to 3,000m in Moist, Wet Weyna Dega and Dega agroclimate.

Therefore, in the process of site selection; Vegetation zone was considered together with land use land cover and Dominant soil types as shown in Figure 3-20 that were considered as the main factors influencing the infiltration rate of the soil and the sampling matrix was prepared and field measurement performed after the overlay analysis of those maps using ArcGIS 10.1.

GPS based site assessment was carried out starting from the highest point of the watershed to Lake Ziway which was characterized by high elevation differences from 1633m.a.s.l at the gauging station of Meki river flow to 3612m.a.s.l at Zebidar Mountain.

Forest and natural vegetation, EBLUS, bush and chat, grass/grazing, eucalyptus, cultivated, bare soil and eroded landscape/ built-up, and water bodies were LULCs classified from landsat image (Alemu *et al.*, 2020) and based on USGS criteria, the LULCs are aggregated in to five classes as EBLUS, Cultivated, Bare soil & eroded landscape/ built-up, Grass & Plantation and Natural Forest for the sampling purposes.

The soil type data was collected from MOWIE and verified by harmonized world soil database (HWSD) and four dominant soil types found in the watershed are Vertisol, Cambisol, Luvisol and Leptosol which were named as soil type 1, soil type 2, soil type 3 and soil type 4 respectively.

Vegetation zones were expressed as Afro-alpine, Dry Afro-montane and Acacia wooded grass land of rift valley as vegetation zone 1, 2 and 3 respectively and verified in the field as shown in Figure 3-21 (Azene *et al.*, 1993).

Figure 3-21: Vegetation zone verification assessment (Source: Field assessment)

Where: A refers to divide line (western end of the watershed) where more than half part of the watershed is visible; B & F refers to western upper part of Meskan woreda (Yewutin & Yetebon respectively; C refers Found around Eastern Meskan woreda and Western Sodo woreda D refers Scene at Chohamba Meskan woreda and E refers Conversion from lake to wetland (Lake Ziway).

To measure and compare the hydrological characteristics (infiltration rate) of EBLUS, experimental sampling matrix was prepared with replication as shown in Table 3.14.

Table 3.14: Sampling points based on vegetation zone, Dominant soil type and Dominant LULC

		Cultivated LULC	Bare soil & eroded land scape / Built-up	Grass & Planted Forest LULC	EBLUS	Natural Forest LULC
Combined Vegetation & Dominant Soil type [1]	Z11	CZ11	BZ11	GZ11	EZ11	NZ11
	Z12	CZ12	BZ12	GZ12	EZ12	NZ12
	Z13	CZ13	BZ13	GZ13	EZ13	NZ13
	Z14	CZ14	BZ14	GZ14	EZ14	NZ14
	Z21	CZ21	BZ21	GZ21	EZ21	NZ21
	Z22	CZ22	BZ22	GZ22	EZ22	NZ22
	Z23	CZ23	BZ23	GZ23	EZ23	NZ23
	Z24	CZ24	BZ24	GZ24	EZ24	NZ24
	Z31	CZ31	BZ31	GZ31	EZ31	NZ31
	Z32	CZ32	BZ32	GZ32	EZ32	NZ32
	Z33	CZ33	BZ33	GZ33	EZ33	NZ33
	Z34	CZ34	BZ34	GZ34	EZ34	NZ34

There were about 60 sampling possibilities, but EBLUS is not common in acacia wooded part of the watershed for which zones Z31 to Z34 to all land use land covers were not applicable for experimental sampling in this research and the resulting sampling points has been Z11 up to Z24 (8 combined zones) for five LULCs which results in 40 sampling points replicated to four fold (Figure 3-23) based on the presence of different soil textural classes to make it representative and to reduce human and instrumental errors. The infiltration rate data collected from those sampling points using Amozi-meter (Hood infiltrometer) as shown in Figure 3-22.

[1] CZ23 refers to Cultivated LULC in vegetation zone two (Dry afro-montane) and soil type three (Luvisol)

Figure 3-22: Amozi-meter (Hood infiltrometer) infiltration rate measurement of EBLUS

Hence, 116 samples were collected as shown in Table C.2 of appendix 3 excluding the lower zone of the watershed since it has no sufficient EBLUS to be considered and the upper zone of the watershed misses some of soil textural classes and the result was analyzed for their hydrological characteristics of different LULCs compared with EBLUS Using Microsoft excel and mapped using ArcGIS 10.1 (Figure 3-23).

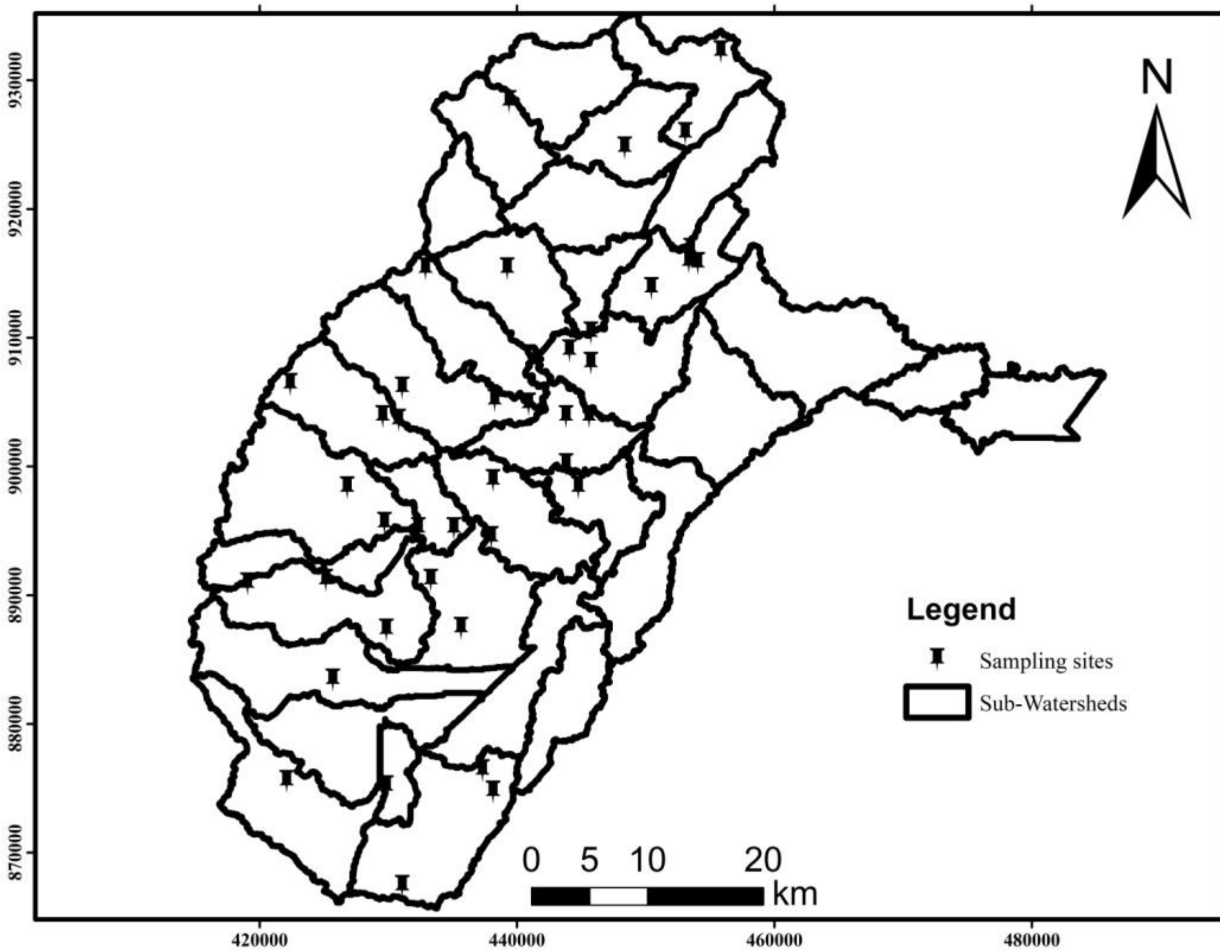

Figure 3-23: Sampling site mapping

Enset-Based land use system (EBLUS) was not included in all former land use studies (Alemu *et al.*, 2020; Anita, *et al.*, 1996; Uloro & Mengel, 2014) and now in this portion more focus deputed to the infiltration rate of EBLUS relative to all other LULCs in Meki river watershed. Amozi-meter (Hood infiltrometer) was used to measure the infiltration rate of the soil under each LULC, including EBLUS as shown in Figure 3-22 and considered to interpolate CN matrix of EBLUS.

3.2.6.3. Working principles and procedures of Hood infiltrometer

A. Underlying theoretical principles of Hood infiltrometer

Hood infiltrometer works in the principles of Hydraulic conductivity (Ku) as a function of water tension *h* in soils or other open-pored materials near saturation can be described according to Gardner, 1958 Eqn.3-9:

$$\mathbf{K_u = K_f . e^{(\alpha . h)}} \qquad (3\text{-}9)$$

kf - saturated hydraulic conductivity, h - Hydraulic pressure head and α - Gardner-Koeffizient.

Such approach allows an analytical solution for a large number of two - and three - dimensional flow processes. It is the regular basis for the interpretation of test results with the infiltrometer systems common so far.

Wooding (1968) found the steady state flow Q from a circular infiltration area (radius a) into the infinite soil and he developed a model and constants as Eqn.3-10:

$$\mathbf{\frac{Q}{\pi a^2} = K_u . C} \qquad (3\text{-}10)$$

Where,

Q = steady infiltration rate, a = radius of hood, Ku = Hydraulic conductivity of the soil and C = constant dependent on parameter (α) of the material by which the hood is madeof as shown in Table 3.15 (Schwärzel, K. & J. Punzel, 2007).

Table 3.15: Material parameter vs constant

Material parameter, α (m^{-1})	**Constant, C**	**α (m^{-1})**	**C**	**α (m^{-1})**	**C**	**α (m^{-1})**	**C**
14.5	2	3.6	5	5.9	3.5	2.7	6.4
12.4	2.2	1.6	10	1.9	8.6	0.5	30
7.5	2.9	2	8.2	1	15.5	0.8	19.1

B. Technical Parameters, Set Up and Operation of the Hood Infiltrometer

Assembly and operation of the Hood Infiltrometer

A hood (2) with circular base is standing directly on the soil surface. The space under the hood is filled with water, hydraulic pressure head getting controlled through a MARIOTTE water supply system (5, 6, and 7). Water-saturated fine sand is used to seal the edge of the hood against the soil up to an outer ring (1). Such sealing will be effective only if the pressure in the water volume under the hood is negative. The negative pressure can be adjusted freely from zero up to the bubble point (air permeation point). The soil pore system on the measuring surface will remain absolutely undisturbed (Schwärzel, K. & J. Punzel, 2007).

When setting up the test system, first the overflow chamber (3) under the hood has to be filled – well controlled - with water. Upon overflow of that chamber begins the volume under the hood gets filled with water and the infiltration into the soil starts. The enclosed air is piped into the air volume of the infiltration reservoir (5) through the vent pipe (10) as shown in Figure 3-24.

After the air escape hose has been closed (V2, V3), the water volume under the hood remains in steady-state. Now the infiltration flow is delivered directly from the infiltration reservoir of the MARIOTTE water supply system from where the reading can be taken of a scale (filling height).

Preparation of the Hood Infiltrometer

Putting up the Hood Infiltrometer please mind that it only works properly on level measuring sites. First screw the tripod [12] into the base plate of the infiltration reservoir and align it vertically. Fill the bubble tower [6] with water up to the marking “B”. Therefore draw the air intake pipe [7] and insert the funnel. Close Valve “V1” and fill the infiltration reservoir with water up to the marking “I” following close it with the plug. Therefore filling the infiltration reservoir should be carried out as last step and the calibration process at the handheld device needs to be started before filling the infiltration reservoir. Connect the hood to the infiltration reservoir with the hose connection [11] and the vent pipe [10] and make sure the valves “V2” and “V3” are closed. Connect the U-tube manometer to the upper end of the standpipe with the hose connection [9] and fill the U-tube manometer up to the zero marking as shown in Figure 3-24.

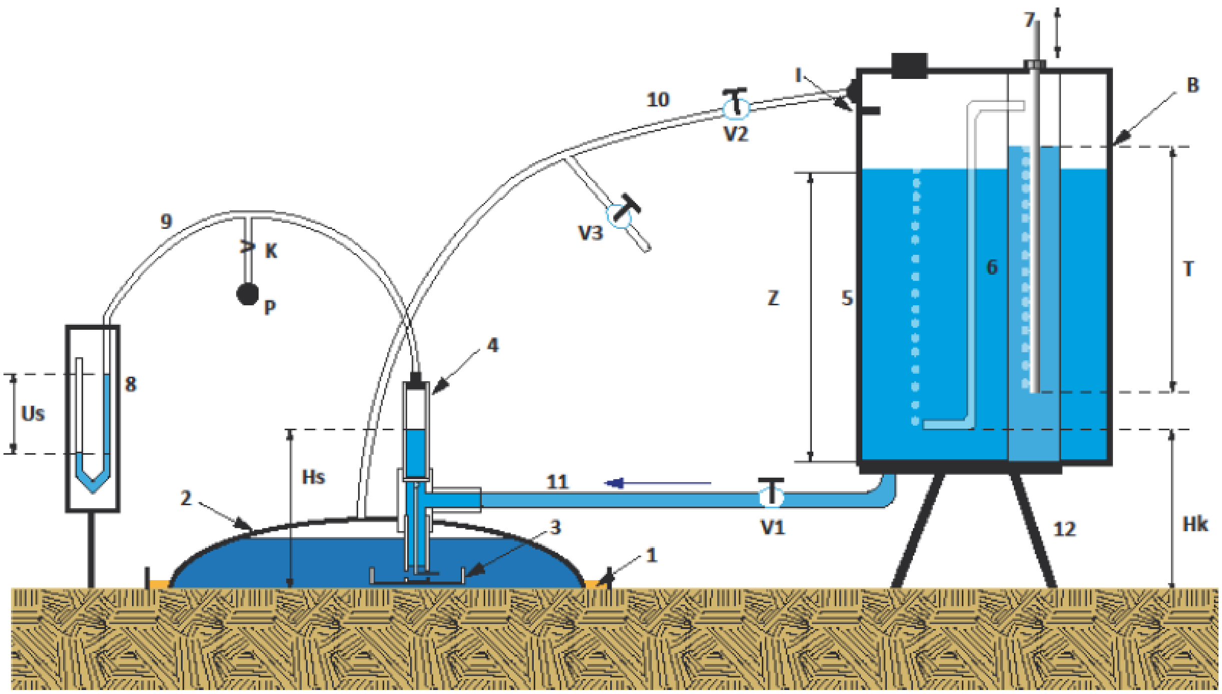

Figure 3-24: Schematic setup of the Hood Infiltrometer (Schwärzel, K. & J. Punzel, 2007)

1 Fine sand sealing
2 Plastic hood
3 Buffer vessel
4 Standpipe
5 Infiltration reservoir
6 Bubble Tower
7 Air intake pipe
8 U-tube manometer
9 Hose connection 1
10 Vent pipe
11 Hose connection 2

12 Stand
B Filling level of the bubble tower
Hk Distance between soil surface and air outlet
Hs Water level in the standpipe
I Maximum filling level of the infiltration reservoir
K Valve for cutting off the pipette ball
P Pipette ball

T Immersion depth of the air intake pipe
Us height difference at the U-tube manometer
V1 Valve for separating the water volumes
V2 Valve for separating the air volumes
V3 Valve for pressure adjustment
Z Filling height of the infiltration reservoir

Setting up the Hood Infiltrometer

The site for the hood should be levelled and put the outer ring onto the ground and push it in evenly a few millimetres and place the hood centrically in the outer ring. Place the infiltration reservoir in its designed position and align it vertically using the screws. The hose connection [11] should decline in a bow. Fill the gap between the hood and the outer ring [1] with fine sand and moisten the sand as shown in Figure 3-24.

Filling the hood

The immersion depth "T" of the air intake pipe should be about 2 cm more than the distance between soil surface and air outlet "Hk". Thus the hydraulic pressure "zero" appears narrow under the soil surface.

Open [V1] slowly and the overflow chamber [3] gets filled with water. In doing so the hose connection 2 should be completely deaerated. Remaining air bubbles may be removed by moving the hose connection and lifting or tipping the infiltration reservoir by assuring that the hood isn`t moved.

The Water in the infiltration reservoir is set to a negative pressure. As long as the system is airtight the overflow chamber won`t overflow. If the overflow chamber overflows please check that all Valves are closed and none of the 2 gaskets at the connection faces of the hose connection or the gasket of the socket for the air intake pipe is missing or damaged.

Open Valve "K" and suck air off the hose connection 1 [9] (pipette bulb) till the water level in the standpipe [4] reaches center scale. Following close valve "K" and keep it closed. Slowly open the aeration valve "V2". Thereby the space under the hood is set to a negative pressure and the water flows over the overflow chamber. Now the filling of the hood started (Figure 3-24).

Shut [V2] as soon as the water table has reached the mark on the hood. Thus the infiltration flow raises the underpressure until the aeration of the Mariotte water supply system starts. Once the aeration started the the underpressure under the hood remains at a steady state. It is determined and controlled by the immersion depth "T" of the air intake pipe (Figure 3-24).

On sites with poor infiltration the underpressure under the hood might not be enough to start the aeration. In this case evacuate additional air through the valve [V3] to keep the negative pressure under the hood at the desired value. The negative pressure Us at the U-tube manometer should always be higher than the water table Hs on the scale of the standpipe.

Choosing the effective water tension

The effective water tension "h" on the soil surface is calculated irrespective to the regulation directly out of the water level "Hs" in the standpipe and the negative pressure "Us" at the U-tube manometer Eqn.3-11.

$$\mathbf{h = H_s - U_s \ \ (h < 0)} \qquad (3\text{-}11)$$

It is advisable to start the test with water tension "Zero"to record the saturated hydraulic conductivity

The scale values at the hood (Hs) and at both brackets of the U-tube manometer "Us" should be recorded.

Measuring the infiltration rate

After choosing the water tension, the leakage rate "ΔZ/Δt"(cm/s) is measured on the infiltration reservoir. Therefore the filling height Z is recorded as a function of time (if possible, ΔZ > 1cm).

For the data recording it is convenient to use a log as shown in Table 3.16.

Table 3.16: Heading for data recording

Infiltrations reservoir			U – Tube1)		Hood	
Time	Z (Scala)	ΔZ / Δt	Us(le)	Us(ri)	Hs	h
min:s	cm	cm/s	cm	cm	cm	cm

Us = Us(le) + Us(ri) (left/right limb of the U-tube manometer)

Each test has to be run up to a steady-state infiltration rate. Depending on the type of soil involved, infiltration to mid-column will be required. Following each test run increase the water tension step by step (Δh = 1 - 2 cm) up to the soil bubble point. Determine the steady-state infiltration rate for each step. This being calculated from the steady-state leakage rate A divided by the ratio of the sectional areas of infiltration reservoir to hood.

Bubble point (BP) of the soil

To determine the bubble point of the soil Shut [V1] and watch the pressure rise on the U-tube manometer.

Determine the maximum of Us Eqn.3-12.

$$\mathbf{BP = H_s - U_{s\,max}} \qquad (\mathbf{BP < 0}) \qquad (3\text{-}12)$$

Calculation of hydraulic conductivity

In the test run the final steady-state value of the infiltration rate "ΔZ/Δt" on the infiltration reservoir at the chosen water tension h is determined. Insert the infiltration rate of the soil vB in equation (3-13 and 3-14). The following applies (with rs = radius of infiltration reservoir).

$$\mathbf{Q = \pi.a^2.v_B = \pi.r_s{}^2.\frac{\Delta Z}{\Delta t}} \qquad (3\text{-}13)$$

$$\mathbf{\frac{Q}{\pi.a^2} = v_B = \frac{r_s{}^2}{a^2}.\frac{\Delta Z}{\Delta t} = q.\frac{\Delta Z}{\Delta t}} \qquad (3\text{-}14)$$

Factor q is the ratio of the cross-sectional area of the infiltration reservoir and the respective infiltration areas that are effective on the soil surface.

In equation (16) applies for the ratio of the infiltration rates at different water tensions:

$$\mathbf{\frac{Q_1}{Q_2} = \frac{\frac{\Delta Z1}{\Delta t}}{\frac{\Delta Z2}{\Delta t}}} \qquad (3\text{-}15)$$

3.2.7. Interpolation of Curve Number Matrix of EBLUS

3.2.7.1. EBLUS CN matrix interpolation processes

Organic matter improved and accelerated both the infiltration rate (Yimer, et al., 2009) and water holding capacity of the soil (Mesfin, et al, 2017; Barbora and Jaroslava, 2014) and it influences CN and resulted in low surface runoff (Vaezi, et al., 2010; Zehetner & Miller, 2006; Zeiger & Fohrer, 2009). EBLUS exhibited a good carbon stock, which was equivalent to high-vegetation areas (Mesfin et al., 2017; Deng et al., 2016) that is an indicator that EBLUS influences infiltration rate, CN and surface runoff. Hence, Carbon stock considered as criteria to interpolate the CN matrix of EBLUS next to infiltration rate of the soil.

The CN matrix was not developed for EBLUS (Table 3.17). Hence, the field measured infiltration rate and Carbon stock (Mesfin et al., 2017) of the soil was considered as a criteria to interpolate the CN of EBLUS through the inter-relationship between infiltration characteristics of the soil (Iliasse & Adil, 2014) and soil carbon stocks (Mesfin et al., 2017).

Table 3.17: State of Curve Number for different land use systems

Land Cover/Land Use	**Hydrologic Soil Group** (Iliasse and Adil, 2014; ERA, 2013)				**Parameters considered in interpolation of CN matrix of EBLUS**	
	A	**B**	**C**	**D**	**Carbon stock (tonyr^{-1})** (Mesfin *et al.*, 2017)	**Average Infiltration rate (mmhr^{-1})**
Open Water	100	100	100	100	0	0
Bare soil and eroded landscape/built-up LUS	77	85	90	92	132	7.0625
Natural Forest LUS	36	60	73	79	45,714	12.9675
Grasslands & plantations LUS	49	69	79	84	8350	11.1875
Cultivated LUS	67	78	85	89	19,950	10.375
EBLUS	EA	EB	EC	ED	77,286	12.8125

Infiltration rate of the soil under all LUSs was measured in the field and carbon stock of the soil under all LUSs including EBLUS as shown in Table 2.5 were used to develop a CN matrix of EBLUS relative to other LUSs with predetermined CN using simple linear regression method (Stewart, et al., 2002 and Mitchell, 2005) and a mathematical formulation of EBLUS was done from the existing CN matrixes after ANOVA analysis for the significance of EBLUS.

Therefore, CN for EBLUS (EA, EB, EC and ED) at hydrologic soil group (A, B, C and D) respectively was computed after developing the following formula (Eqns. 3-16 to 3-19) that was derived using simple (multiple linear regressions) model (Mohammed Reza Pahlavan-Rad, *et al.*, 2020) to compute the CN matrix for EBLUS relative to the other land use systems dominantly practiced in the study area.

$$\mathbf{EA} = \frac{Ci(FA*IF+GA*IG+CA*IC+BA*IB)}{IE} + \frac{CSq(FA*SqF+GA*SqG+CA*SqC+BA*SqB)}{SqE} \tag{3-16}$$

$$\mathbf{EB} = \frac{Ci(FB*IF+GB*IG+CB*IC+BB*IB)}{IE} + \frac{CSq(FB*SqF+GB*SqG+CB*SqC+BB*SqB)}{SqE} \tag{3-17}$$

$$\mathbf{EC} = \frac{Ci(FC*IF+GC*IG+CC*IC+BC*IB)}{IE} + \frac{CSq(FC*SqF+GC*SqG+CC*SqC+BC*SqB)}{SqE} \tag{3-18}$$

$$\mathbf{ED} = \frac{Ci(FD*IF+GD*IG+CD*IC+BD*IB)}{IE} + \frac{CSq(FD*SqF+GD*SqG+CD*SqC+BD*SqB)}{SqE} \tag{3-19}$$

Where:

- EA, EB, EC and ED are CN of EBLUS for HSG of A, B, C and D respectively
- FA, FB, FC and FD are CN of Forest LUS for HSG of A, B, C and D respectively
- GA, GB, GC and GD are CN of Grass LUS for HSG of A, B, C and D respectively
- CA, CB, CC and CD are CN of Cultivated LUS for HSG of A, B, C and D respectively
- BA, BB, BC and BD are CN of Bare soil and eroded landscape/built-up LUS for HSG of A, B, C and D respectively
- IE, IF, IG, IC and IB are infiltration rate of EBLUS, Forest, Grass, Cultivated and Bare soil and eroded landscape/built-up LUSs respectively.
- SqE, SqF, SqG, SqC and SqB are Carbon stock of EBLUS, Forest, Grass, Cultivated and Bare soil and eroded landscape/built-up land use systems respectively.
- Ci and CSq are coefficients for the relative influence of infiltration rate and Carbon stock on curve number of land use systems.

Finally, a formula was developed and presented in Equation 8 that will contribute to the scientific community as a new hydrological model to be used by future scientists working in those enset growing areas with similar watershed features.

3.2.8. Determination of CN Grid of EBLUS

Based on the developed formula, CN matrix was determined for EBLUS and incorporated to the existing CN matrix system of USGS so that it was used by HEC-GeoHMS model to extract the CN for the watershed (Fleming & Brauer, 2018; Merwade, 2012) for runoff modeling. To produce the CN grid several activities were performed that include watershed delineation, land use land cover grid preparation, HSG grid preparation, merge the land use land cover and soil data, create CN lookup table and finally creating the CN grid for Meki river watershed.

3.2.8.1. Delineation and preprocessing of the watershed from DEM

Meki river watershed and sub-watersheds were automatically extracted from Digital Elevation Model (DEM) and the DEM was preprocessed to produce the watershed fill, flow direction, flow accumulation, stream definition, stream segmentation, combined stream link, sink link, catchment grid delineation, catchment polygon processing, flow length, slope, Elevation, aspect, contour line, drainage line processing and adjoinment catchment processing, etc were derived using HEC-GeoHMS model of Arc GIS 10.1 (Iliasse & Adil, 2014) (Figure D-1 of Appendix 3).

3.2.8.2. LULC and hydrologic soil groups (HSG) data preparation

According to Fleming and Brauer (2018) and Merwade (2012) in order to perform CN modeling, various types of information were required that includes DEM based watershed parameters, HSG and LULC. Land cover map was generated using Land sat image data (30m) supported by Google earth. GPS based field visit was performed to collect data to train ERDAS imagine 2014 to classify the images with maximum likelihood clustering algorithm of supervised classification method (Iliasse and Adil, 2014; Fleming and Brauer, 2018).

Eight Land use systems were identified and reclassified into five classes on the basis of USGS land cover institute (LCI2) (Table 3.18) and modified to include the recently recognized EBLUS as a separate land use system in the watershed (Fleming and Brauer, 2018; Okirya, et al., 2012;

[2] http://landcover.usgs.gov/classes.php

Merwade, 2012). According to Fleming and Brauer (2018) and Merwade (2012), the Spatial Analyst Tools in Arc Toolbox was used to re-classify the LULC based on USGS LCI table.

Table 3.18: Land use reclassification based on USGS LCI with modification

No.	**Description**	**New No.**	**Description**	**No.**	**Description**	**New No.**	**Description**
11	Water bodies	1	Water	**43**	Mixed forest	3	Forest& Natural vegetation
95	Wetlands with herbaceous plants			**42**	Natural forest		
21	Developed, Open space	2	Built ups	**41**	Plantation		
22	Developed, Low and medium intensity			**31**	Bare land	4or 5	Agricultural
23	Developed, High intensity			**82**	Cultivated land		
	EBLUS	**6**	**EBLUS**	**52**	Grass land		

The new numbers were manually assigned from Table 3.18 and the output raster was saved as shown in Figure C-2 of Appendix 3. The final steps in processing land use data were converting the reclassified land use grid (raster) into a polygon feature class following the procedure in Conversion Tools of the Arc Toolbox and assign the new value.

The hydrological soil data were collected from Ministry of Water, Irrigation and Energy (MOWE, 2013) of Ethiopia and verified by Harmonized World Soil Database (HWSD). The soil categories such as Cambisol, Andosol, Fluvisol, Leptosol, Vertisol and Luvisol were identified and hydrologic soil group was assigned to each category based on US Natural Resource Conservation Service (NRCS) that may fall into four hydrologic soil groups (HSG) (A, B, C and D): high, moderate, slow and very slow infiltration rates respectively (Merwade, 2012; USDA-NRCS, 1986).

Add Soil_WZ_2018_1 feature class from spatial dataset and in its attribute table create an empty field for storing soil group data as shown in Table 3.19. Hence the hydrologic soil group data was populated to Soil_WZ_2018_1 after identifying the type of soil with its corresponding description.

USDA-NRCS (1986) and ERA (2013) manual were used to generate the relationship of soil type and hydrologic soil group of Meki river watershed and also verified by HWSD viewer and also shape file data acquired from MOWIE as shown in Table 3.19.

Table 3.19: Hydrologic soil group (HSG) assignment (ERA, 2013; USDA-NRCS, 1986)

Soil Types	HSG	Soil Types	HSG	Soil Types	HSG
Chromic Cambisols	B	Orthic Luvisols	B	Dystric Histosols	D
Eutric Cambisols	B	Vertic Luvisols	C	Eutric Histosols	D
Humic Cambisols	C	Dystric Nitosols	B	Cambric Arenosols	A
Luvic Phaeozems	C	Gypsic Yermosols	B	Humic Andosols	B
Lithosols	D	Gleyic Solonchaks	D	Mollic Andosols	B
Calcaric Fluvisols	B	Orthic Solonchaks	B	Vitric Andosols	B
Eutric Fluvisols	B	Pellic Vertisols	D	Chromic Vertisols	D
Chromic Luvisols	B	Eutric Nitosols	B	Haplic Xerosols	B

Accordingly, the HSG was assigned to each of the six soil types identified in the watershed as shown in Table 3.20 and during the assignment the HSG of Leptosol was assigned after referring the field characteristics of the soil and it had more similarity to Luvisol with its insignificant areal coverage to influence the value of the curve number and hence HSG of C was assigned to it.

Table 3.20: Hydrologic soil group (HSG) assignment to the corresponding soil type

Name	**Soil mapping unit**	**MU_GLOBAL**	**HSG**	**PctA**	**PctB**	**PctC**	**PctD**
Luvisol	LVh 1/2 cd	16739	C	0	0	100	0
Cambisol	CMe 3 de	16932	B	0	100	0	0
Leptosol	LP 3 cd	16808	C	0	0	100	0
Vertisol	VRe 1 a	16851	D	0	0	0	100
Andosol	ANz 2/3 ab	16903	B	0	100	0	0
Fluvisol	FLc 1/2 ab	16982	B	0	100	0	0

Based on Merwade (2012), after editing the Soil_WZ_2018_1 and transferring HSG to its database, now we have a Soil Code (soil group) assigned to each polygon in Soil_WZ_2018_1. Following soil group assignment, four more fields were created named PctA, PctB, PctC, and PctD all of type short integer in Soil_WZ_2018_1 feature class.

For each feature (polygon) in Soil_WZ_2018_1 PctA defined as what percentage of area within the polygon had a soil group A, PctB defined as what percentage of area within the polygon had soil group B and so on (USDA-NRCS, 1986).

For Meki river watershed, we had only one soil group assigned to each polygon so a polygon with soil group "A" had PctA = 100, PctB = 0, PctC = 0, and PctD = 0. Similarly for a polygon with soil group D, only PctD = 100, and other three Pcts were assigned 0 (Merwade, 2012) and populated as PctA, PctB, PctC and PctD based on Soil Code for each polygon. Features selected based on Soil Code and then field calculator used to assign numbers to polygons and the attribute table looks as shown in Table C.6.

3.2.8.3. Merging of Soil and Landuse Data

The next step was to merge/union both soil data and land use data to create polygons that have both soil and land use information (Merwade, 2012). Accordingly, to merge/union soil and land use data, the Union tool in Arc Tool box available under Analysis Tools was used. Browsing Soil_WZ_2018_1 and LULC_2017_March2019Pol as input features, name the output feature class as "Meki_Soil_LU".

The result of union/merge features inherit attributes from both feature classes and if the outer boundaries of input feature classes do not match exactly, the resulting merged feature class (Meki_Soil_LU) usually will have features that will have attributes from only one feature class called "slivers" and if we open the attribute table for Meki_Soil_LU, sliver polygons in this feature class have attributes only from LULC_2017_March2019Pol and the soil attributes are empty, and vice versa as shown in Table 3.21. One way to deal with sliver polygons was to just delete them (Merwade, 2012). Accordingly, the sliver polygons were selected in the selection attribute of Arc-GIS and deleted.

Table 3.21: Avoiding sliver (-1) of the soil land use union of the watershed

FID_landus	FID_Soil_W	Soil mapping unit	Name	MU_GLOBAL	Class_Name
-1	0	LVh 1/2 cd	Luvisol	16739	Cultivated & degraded
-1	2	LP 3 cd	Leptosol	16808	Cultivated & degraded
-1	5	CMx 2/3 bc	Cambisol	16932	Grass
-1	6	ANz 2/3 ab	Andosol	16903	Cultivated & degraded
-1	10	VRe 1 bc	Vertisol	16855	Grass
-1	14	FLc 1/2 ab	Fluvisol	16982	Grass
-1	16	LVh 1/2 de	Luvisol	16739	Cultivated & degraded
-1	20	VRe 1 bc	Vertisol	16839	Cultivated & degraded

3.2.8.4. Creating CN Look-up table and CN Grid

The next step was to prepare a look-up table with curve numbers for different combinations of land uses and soil groups. The spatial features in conjunction with the lookup table then used to create curve number grid (Merwade, 2012). Create a table named "CNLookUp". In Arc tool box, select Data Management Tools…Table…Create Table. Now start the Editor to edit the newly created CNLookUp table and populate it (Table 3.22).

Table 3.22: Lookup table considering EBLUS

Class Name	Hydrologic Soil Group (HSG)			
	A	B	C	D
Water bodies	100	100	100	100
Bare/Builtup	77	85	90	92
Eucalyptus/Forest	36	60	73	79
Bush & Chat/Grass	49	69	79	84
Cultivated & degraded	67	78	85	89
EBLUS	EA	EB	EC	ED

Columns A/B/C/D store curve numbers for corresponding soil groups for each land use system (LUValue) incuding EBLUS that were obtained from ERA (2013) and USDA-NRCS (1986).

HEC-GeoHMS uses the merged feature class (Meki_Soil_LU) and the lookup table (CNLookUp) to create the curve number grid. A field created in the merged feature class named “LandUse” that will have land use category information to link it to CNLookUp table. Create a field named LandUse and populate it by equating it to GRIDCODE.

On the HEC-GeoHMS Project View toolbar, click on Utility … Create Parameter Grids... Choose the lookup parameter as Curve Number (which is the default), Click OK, and then select the inputs. Select Hydro DEM, merged soil and land use, CNLookUp table and leave the default CNGrid name for the Curve Number Grid and processing generated the CN matrix of the watershed.

3.2.9. Impact assessment of EBLUS on magnitude of surface runoff, water resources and watershed management in MRWS

3.2.9.1. Data used, processes and Conceptual framework of the research

The datasets required for this study were time series data (30 years precipitation data from Ethiopian National Meteorology Agency (ENMA) and 20 years Meki river discharge from Ministry of Water Irrigation and Energy (MOWIE)); Landsat images for the years 1987 and 2017 and Digital elevation model (DEM) from United States Geological Survey (USGS) earth explorer portal (Reza Kabiri, 2014) and soil data from MOWIE. Five rainfall station data (Butajira, Bui, Koshe, Meki and Ziway) were used for this research.

Digital elevation model (DEM) was one of the main inputs of HEC-GeoHMS model with 30mx30m resolution was used to delineate the boundary of the watershed and the drainage patterns and terrain parameters such as slope gradient and length and stream network characteristics such as channel slope, length and width have been analyzed (Matthew, *et al.*, 2013). During the CN generation, the slope was classified to five ranges using ArcGIS 10.1 (Merwade, 2012).

The soil textural and physicochemical properties required by the HEC-HMS model (Fleming & Brauer, 2016) in Meki river watershed was classified on the basis of the revised FAO/UNESCO-ISWC legend to soil map of the world (1995; 1998; 2002) that was verified by HWSD (FAO, *et al.*, 2003). Accordingly, the six major soil types identified in the Meki river watershed were: Andosols, Cambisols, Fluvisol, Leptosols, Luvisols, and Vertisols. Out of the six soil types identified, Cambisols and Vertisols jointly covered more than half of the watershed area (Jackson, *et al.*, 2007).

The land use of an area was one of the most important factors that affect erosion and runoff in the watershed during simulation (Neitsch *et al.*, 2005). The 1987 and 2017 land use map of the study area were classified using ERDAS imagine 2014 with maximum likelihood algorithm and used in CN grid generation. Enset-Based land use system (EBLUS) considered in the land cover classification process and used to model its impact on magnitude of surface runoff in Meki river watershed.

According to Bill, 2018, the first step in hydrologic modeling involved pre-processing, project setup, basin processing, characteristics, parameter selection, HMS create and import and utilities (Figure D-1 of Appendix 4) using HEC-GeoHMS tools that can derive several data sets.

The project setup was done in HEC-GeoHMS by defining the outlet of the project at Meki gauging station from the flow accumulation of the watershed and raster and shape files that were derived during the terrain processing were transferred to the new workspace including creation of a project outlet location, river reaches, sub-watersheds and other hydrologic parameters including CN generation (Bill, 2018) and the methodology is summarized in Figure 3-25 as:-

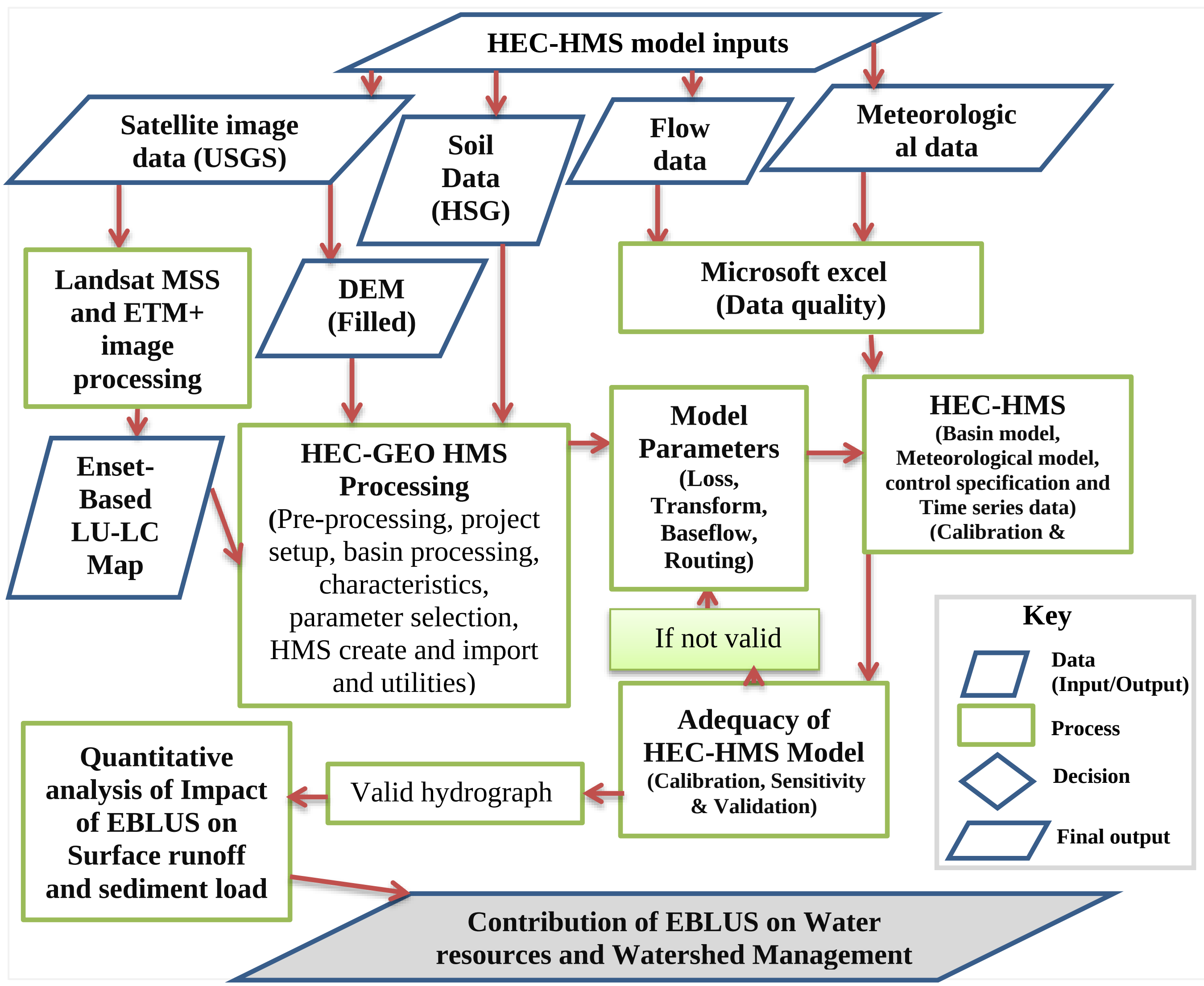

Figure 3-25: Flow of activities diagram to evaluate the impact of EBLUS on surface runoff

3.2.9.2. HEC-HMS Model parameter estimation and processes

The physical characteristics of subwatersheds (basin slope, longest flow path, basin centroid, centroid elevation, and centroidal longest flow path) and streams (river length, upstream and downstream elevations, and river slope) were extracted from terrain data using HEC-GeoHMS. HEC-GeoHMS used these data with LULC and soil data to generate the model parameters (CN, lag time, initial abstraction, initial discharge and recession constant) in each subwatershed (Mewded et al., 2021) and also Muskingham K and x from each reache.

The model parameters, daily precipitation, and daily observed surface runoff were used to calibrate and validate the HEC-HMS model and the adequate model was used to simulate surface runoff and quantitatively assess the impact of EBLUS on surface runoff from 1987 to 2017.

Basin model was imported from the HEC-GeoHMS portal to HEC-HMS 4.3 and the values of CN, initial abstruction, lagtime, initial discharge and recession constant were recoded to each sub-watershed while muskingham K and muskingham x were recoded to each reach. Continuous simulation was carried out to determine the amount of surface runoff to Meki gauging station (Scharffenberg, 2010; Coleman, 2014; Putra, 2013) which have different components including Basin Models (sub-basins, junctions, reach and drainage network of the catchment), Meteorological Models (precipitation), Control Specification (Starting date and time, ending date and time and computational time step for the simulation) and Time series Data (meteorological elements and discharge data which was supplied to the software) (Scharffenberg, 2010).

For the basin model, metric unit system was adopted and the downstream for each of the sub-watershed, route and junction was assigned automatically. The hydrological procedure of changing rainfall into runoff has been represented by four processes in HEC-HMS: loss, transform, base flow and routing (Jeevika and Jagritee, 2018) as described below:

i. Precipitation Loss Method

In this research, the Soil Conservation Service-Curve Number (SCS-CN) model (Fleming & Brauer, 2016; Ramakrishnan, 2009) was selected as given by Eqns. (3-20) to perform the hydrologic modeling of Meki river watershed that determined what percentage of precipitation infiltrates through the ground and becomes runoff contributing to the River flow.

$\mathrm{Q} = \frac{(\mathrm{P}-\mathrm{I_a})^2}{\mathrm{P}-\mathrm{I_a}-\mathrm{S}}$) for $\mathrm{I_a} \leq \mathrm{P}$ other wise $\mathrm{Q} = 0$ and $\mathrm{S} = \frac{25400}{\mathrm{CN}} - 254$ (Chow et al, 1988)

$\mathbf{I_a} = \boldsymbol{\lambda S}$ **where** $\mathbf{P} \geq \mathbf{0.2S}$ Hence, $\mathbf{Q} = \frac{(\mathbf{P}-\mathbf{0.2S})^2}{(\mathbf{P}+\mathbf{0.8S})}$ (3-20)

Where: P is total rainfall (mm), $\mathrm{I_a}$ is initial abstraction (mm), Q is direct runoff (mm), S is potential maximum retention (Sorpitivty) (mm) (0, ∞) and λ is the initial abstraction coefficient or ratio (SCS has adopted a standard value of 0.2) (unit less).

CN is a dimensionless parameter that is dependent on the LULC, HSGs, and the antecedent soil moisture condition (AMC) and the AMC is the wetness condition of the soil based on total precipitation 5 days antecedent to the storm (Mewded et al., 2021; McCuen RH, 1982). In practice, CN values range from 100 for water bodies to about 30 for permeable soils with high infiltration rates (Mewded et al., 2021; Wang, Woonsup, Brian, 2005). The weighted average CN (CNw) value of the subwatershed (SWS) can be calculated using Eq. (3-21).

$\boldsymbol{CN_W} = (\sum_{i=1}^{n} \boldsymbol{CN_i A_i})/\boldsymbol{A}$ (3-21)

Where i is an index of the subwatershed (SWS) of uniform LULC and soil type; CNi is the CN for SWS i; and Ai is the area of SWS i.

Accordingly, using the sub-watershed based CN automatically assigned by HEC-GeoHMS, the sorpitivity and initial abstraction (Ia) were computed using Microsoft excel and re-assigned to each sub-watershed in HEC-HMS.

ii. Transform Method

According to Jeevika and Jagritee (2018) and Subramanya (2008), transform methods was an approach for computing direct runoff at each junctions of the reaches on the upstream of Meki river watershed and also at the Meki river gauging station (outlet) of the watershed from the excess precipitation falling over it and this was done based on principles of unit hydrograph.

Computation of sheet flow, shallow concentrated flow and Channel Flow Characteristics were performed in HEC-GeoHMS and exported to excel (Chow *et al.*, 1988). The SCS UH then transforms the precipitation excess to produce direct runoff hydrograph in which the hydrograph is scaled by called lag time to produce unit hydrograph (Mewded et al., 2021; Crowe and Schwartz, 1985).

The lag time (T_{lag}) of each subwatershed in Meki river watershed is highly related to the characteristics of the main stream (length, slope, and roughness) as shown in Eqn.(3-22) (USDA S, 1972) and Lag time can be related to time of concentration (Tc) as follows (Chow, et al., 1988) in Eqn.(3-23):

$$\mathbf{Tc = \frac{1}{60}\sum\frac{L}{V}} \quad (3\text{-}22)$$

$$\boldsymbol{T_{lag}} = \mathbf{\frac{Tt}{2} + 0.6Tc} \quad (3\text{-}23)$$

Where: Tc = Time of concentration (Min), L = Longest flow path (Length of flow path) (ft), V = Average velocity in sheet flow and channel in the TR55 of HEC-GeoHMS (ft/s), Tt = Time of travel (Min), T_{lag} = Lag time (Min), L = Longest flow path (Length of flow path) (ft).

The value of the lag time was assigned to HEC-HMS 4.3 through parameter, transform and SCS unit hydrograph and copy and paste from Microsoft excel on similar ways to CN.

iii. Routing Model

The reach routing process converts a hydrograph at the upstream boundary of the sub-watershed to a resultant hydrograph at the downstream boundary of the sub-watershed for each reach, accounting for gains and losses (energy and mass) experienced as the river travels through that particular sub-watershed (Fleming & Brauer, 2016; Feldman, 2000 and Elizabeth, 1994). As the flood runoff travels through the channel reach, it becomes attenuated due to channel storage effects. The routing models available in HEC-HMS account for this attenuation (Bitew et al., 2019). The Muskingum method, which was developed by McCarthy (1938), is a popular lumped flow routing technique which was selected for this study.

The Muskingum routing method is a simple approximate method to calculate the outflow hydrograph at the downstream end of the channel reach from the inflow hydrograph at the upstream end (Bitew et al., 2019). Among many models used for flood routing in rivers, it is a straightforward hydrological flood routing technique used in natural channels (Bitew et al., 2019 and Elizabeth, 1994), In this model calibration, two parameters are needed; travel time (K) of the flood wave through routing reach; and dimensionless weight (X) which corresponds to the attenuation of the flood wave as it moves through the reach.

The routing parameters in the models are usually derived through calibration using measured discharge hydrographs (Birkhead and James, 2002) as shown in Eqn. 3-24.

$$\mathbf{S} = \mathbf{K}[\mathbf{XI} + (\mathbf{1} - \mathbf{X})\mathbf{Q}] \qquad (3\text{-}24)$$

The parameter K and x are proportionality factor with the dimension of time or the travel time of a flood wave through the reach and a dimensionless weighting factor with $0 \leq x \leq 0.5$. In natural streams, X is between 0 and 0.3 with a mean value near 0.2 (Tewolde *et al.,* 2006, Birkhead and James, 2002; Elizabeth, 1994). Great accuracy in determining x may not be necessary because the results of the method are relatively insensitive to x (Chow, et al., 1988). Both Muskingham K and x was assigned to HEC-HMS model to parameters in the main menu of the software.

iv. Base-flow Method

Sub-surface flow in the catchment was illustrated by base flow in HEC-HMS. There was insignificant contribution of base flow in case of short rainfall event, so it has been ignored. While in case of long rainfall event, the base-flow contributed to the recession limb of hydrograph and had a significant contribution in flood volume (Jeevika and Jagritee, 2018; Cunderlik and Simonovik, 2004). Hence, in this research, recession model was used for base flow computation which involved initial discharge and recession constant with a ratio to peak of 0.1 entered to the model using component editor to each sub-watershed.

3.2.9.3. Sensitivity analysis in HEC-HMS Model

A sensitivity analysis is usually undertaken in most modelling studies (Bitew et al, 2019; Kim and Maeng, 2017) to explain how the variation in model output can be attributed to different sources of variation in the model input and it helps in identifying a series of parameters for the HEC-HMS model calibration (Nejadhashemi, et al., 2011; Yakir and Morin, 2011). It is a necessary process to identify the key parameters for calibration (Bitew et al, 2019). The simplest sensitivity analysis technique involves perturbing parameter values one at a time (Hamby, D., 1994). Similarly in this study, the sensitivity analysis was performed by changing the parameter values in the range of ±50% with 10 % intervals.

Zelelew and Melesse (2018) and Mewded *et al* (2021) conducted a sensitivity analysis by changing the parameter values in the range of ±30% with 5% intervals and ±20% with 5% intervals respectively until the best fit between the observed and simulated parameters in the given hydrograph was obtained. The sensitive parameters were then selected based on their effect on peak discharge and total volume.

The model was run repeatedly with the baseline value for each parameter multiplied, in turn, by 0.9 and 1.1, while keeping all other parameters constant at their nominal starting values (Juraj and Slobodan, 2004). The sensitivity of six model parameters (CN2, LT, MK, Mx, ID, RC and IA) on the runoff volume, peak discharge, and time to peak runoff characteristics were analyzed using HEC-HMS. The initial parameter values were used as base values (nominal) for the evaluation and one parameter at a time was analyzed accordingly.

The initially calculated and assumed values of the parameters (SCS CN, lag time, Muskingham K, Muskingham x, base flow initial discharge and base flow recession constant and initial abstraction) as shown in Table D.2 of Appendix 4 were kept as base value for the evaluation and one parameter at a time was analyzed depending on the shape of the percentage volume change graph of each parameter and plotted separately (Cunderlik and Simonovik, 2004). The parameters that showed greater variation in simulated volume of flow were considered as most sensitive for each case and ranking was done based on the slope of the graph.

3.2.9.4. Calibration and validation processes in HEC-HMS

The model calibration was done with the Simple optimization package and Peak-Weighted Root Mean Square Error (PWRMS) objective function because of their simplicity and performance (Bitew 2019 et al., and Deng et al., 2010, as cited by Jin et al., 2021). The selection of simulation time step is a critical step for hydrologic modelling and model calibration and validation.

The choice of calibration (1985-1989) and validation (1990-1994) years were done based on availability and completeness of rainfall and stream monitoring data (Bitew et al., 2019; Chu and Steinman, 2009) in Meki river watershed. Calibration of the models was performed to obtain the outflow volume, peak flow, Percent bias, RMSE, and time of peak as closely as possible to the observed flow (Chu and Steinman, 2009) at Meki river gauging station and calibration involved combination of automated and manual calibration.

The model was validated using the same input parameters as determined by the calibration process but with different simulation time and the Model was calibrated for five years and validated for five years at a calibration and validation time step of one day as shown in Table 3.23.

Table 3.23: Control Specification for calibration and validation of the model

Control Specification	Meki river	Control Specification	Meki river
Calibration period	Jan 01, 1985 - Dec 31, 1989	Validation period	Jan 01, 1990 - Dec 31, 1994
Calibration time step	1day	Validation time step	1day

The process was completed manually by repeatedly adjusting the parameters, computing, and inspecting the goodness of fit between the computed and observed hydrographs.

The peak weighted root mean square error (PWRMSE) with a simplex method for search method was the objective function (Eqns. 3-25 & 3-26). The automated calibration was used to adjust initial losses, curve number, lag time, initial discharge, recession constant, muskingham K and x to minimize the objective function value and to find optimal parameters.

When validation of the observed and simulated hydrograph was not acceptable, initial parameters were adjusted to provide a better optimization target value for the optimization process (USACE, 2000). Through the process, more than 100 runs performed due to mismatch and poor recorded values of precipitation as shown in Table D.6 of Appendix 4.

$$\mathbf{PWRMSE} = \sqrt{\sum_{\mathbf{t=1}}^{\mathbf{N}} \frac{(\mathbf{Qo(t)}-\mathbf{Qs(t)})^{2\frac{\mathbf{Qo(t)+Qa}}{\mathbf{2Qa}}}}{\mathbf{N}}} \quad (3\text{-}25)$$

$$\mathbf{Qa} = \frac{\mathbf{1}}{\mathbf{N}}\sum_{\mathbf{t=1}}^{\mathbf{N}} \mathbf{Qo(t)} \quad (3\text{-}26)$$

Where: Qo(t), Qs(t), Qa and N are observed flow at time t, Simulated flow at time t, Average of observed flow and Number of data counts respectively.

Statistical evaluation techniques like Nash–Sutcliffe Efficiency (NSE) by Nash and Sutcliffe (1970) (Eqn. 3-27) and coefficient of determination (R2) as described in Neter et al. (1990) were applied to evaluate the performance of the model.

$$\mathbf{NSE = 1 -} \left(\frac{\sum_{i=1}^{N}(Oi - QSi)^2}{\sum_{i=1}^{N}(Oi - \bar{O})^2}\right) \quad (3\text{-}27)$$

Where: Qoi, Qsi, $\bar{O}$ and N are observed flow, simulated flow, Average of observed flow and Number of data counts respectively.

3.2.9.5. Evaluation of impact of EBLUS on magnitude of surface runoff

Precipitation variation is the prominent and the only climate factor to significantly affect runoff and all other elements of water balance (Mewded et al., 2021; Koneti et al., 2018) but to avoid its effect the same year precipitation was used. Therefore, 4 scenarios were developed by combining different LULC and EBLUS data keeping precipitation constant to compute the contribution rate of EBLUS change as shown in Table 3.24.

Table 3.24: Scenarios used for quantitative impact analysis of EBLUS

Scenario	LULC	Precipitation	EBLUS considered	Simulated annual runoff (Qi)
1	1987	Average	Yes	Q1
2	1987	Average	No	Q2
3	2017	Average	Yes	Q3
4	2017	Average	No	Q4

The scenarios created were used to determine the rate of impact of EBLUS change (L) on the generation of surface runoff (Mewded *et al.*, 2021) in Meki river watershed (Eqn.3-28). Therefore, Calculating the contribution rate between 1987 and 2017 based on the 1987 reference period is:-

$$\boldsymbol{L}_{\mathbf{1987-2017}}(\%) = \left(\frac{\mathbf{(Q4-Q2)-(Q3-Q1)}}{\mathbf{Q4-Q2}}\right)\mathbf{x100}\% \qquad (3\text{-}28)$$

The sediment load routing through the rivers were computed using HEC-HMS based MUSLE model. MUSLE performs in a similar way with USLE or RUSLE but it uses volume of runoff to quantify the amount of sediment carried and routed in the route in Meki river watershed. The impact of EBLUS on magnitude of sediment load was determined in similar methods to surface runoff and the result was presented in a table and graphically.

3.2.9.6. Evaluation of impact of EBLUS on WR and WS management

All portions of the research are cummulated to evaluate the impact of EBLUS on water resources and watershed management and descriptive discussion was done and reported in the result part.

4. Results and Discussion

4.1. State of Land use Land Cover change and dynamics in MRWS

Accurate and timely change detection of earth's surface features is extremely important for the understanding of the relationships and interactions between human and natural phenomena in order to promote better decision making (Lu *et al.*, 2003). The LULC analysis shows that about 40.16% and 14.46% of the watershed is covered by cultivated land and Bush and Khat land respectively. The watersheds' vegetation cover except bush and khat land are composed of Grass land, Forest and Natural vegetation, Eucalyptus plantations and EBLUS that composed of 11.9%, 10.07%, 4.2% and 10.8% respectively as shown in Table 4.1.

Table 4.1: Percent of Land use land cover and change

Class name	Area (ha) 1987	Area (ha) 2017	Change 2017-1987	Land cover (%) in 2017
Bare land	9865.01	15911.22	6046.21	7.85
Grass land	29716.45	25533	-4183.5	11.9
Forest and Natural vegetation	21768.76	20967.58	-801.18	10.07
EBLUS	20534.87	22733.9	2199.03	10.8
Eucalyptus plantation	12499.19	9111.22	-3388	4.2
Cultivated land	85816.29	86677.53	861.24	40.16
Bush and Khat land	29455.42	28896.83	-558.59	14.46
Water bodies	1383.07	1207.76	-175.31	0.58

According to Mesfin, Osamu and Sebsebe 2021, Enset-based agroforestry covered ~ 10.2% of the land-scape. Borrell, *et al.*, (2020) found that the area of land under enset production has increased approximately 46% over the past twenty years, which was the evidence for the increase in area coverage of EBLUS in Meki river watershed over the last 30 years as shown in Figure 4-1. Even though the LULC analysis presented that currently there is high vegetation cover in the watershed, the ground cover status of the area have been highly exposed to rain fall erosive forces due to free grazing (Charles *et al.*, 2016), presence of patches of cultivated land in between the vegetations and the wasteful nature of the former fuel wood consumption pattern of the local farmers (Bewket and Teferi, 2009) who are using biomass only for energy sources.

Charles et al., (2016) and Bewket and Teferi (2009) expressed that expansions of subsistence crop production into ecologically marginal areas and deforestation have been the common forms of transitions. Similar trends of transitions have been taken place in Meki river watershed, which is manifested by a high increase in bareland and cultivated land while a fast and sharp decrease in grass land and plantation forests with considerable decrease in natural forest cover and bush land cover as shown in Figure 4-1.

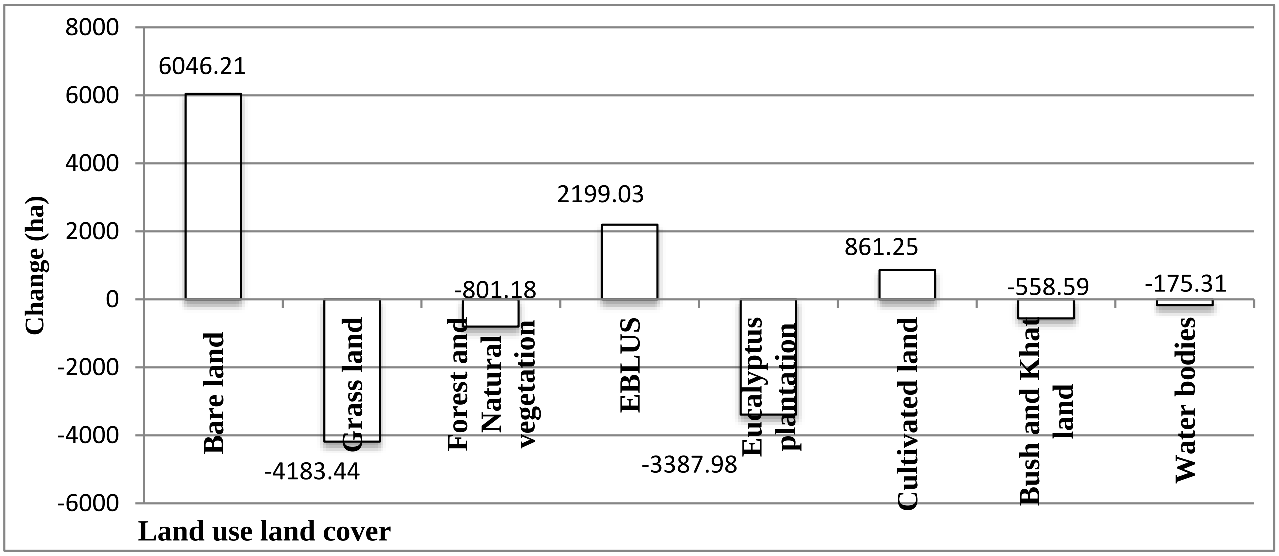

Figure 4-1: Land use land cover change in Meki river watershed

The increase in EBLUS has a positive implication to increase the ground cover of the area from rain drop impact and it can improve the infiltration rate of the soils irrespective of their type which was evidenced by Tesfaye and Bongers (2012); Holden and Linnerud (2007); Neher (1992); Ojiem et al., (2006); Peyre et al., (2006) and Pretty et al., (2003) that enset agroforestry would contribute to ecological sustainability.

Although the change in EBLUS has several ecological sustainability implications (Tesfaye and Bongers, 2012; Holden and Linnerud, 2007; Neher, 1992; Ojiem et al., 2006; Peyre et al., 2006 and Pretty et al., 2003), the cumulative land use land cover change trend shows the watershed is suffering from degradation of resources (Charles et al., 2016) since the change in EBLUS (2199.03ha) is not comparable with the change in bare or degraded land use land cover type (6064.21ha).

The field assessment supported by James S Borrell, et al, (2020) shows that three vegetation zones found in the watershed namely: upper zone (Afro-alpine vegetation zone), middle zone (Afro-montane vegetation zone) and lower zone (Acacia wooded vegetation zone).

The upper zone of Meki river watershed composed of Erica dominated natural forest lands with patches of grazing lands; eucalyptus plantations and EBLUS with highly sensitive ecological setups (Figure 4-2). The high slopes (including slopes greater than 50%) of the watershed have been sparsely populated but encroachment of the existing dense natural vegetation by cultivation of seasonal crops manifested as a prominent problem of the upper zone of the watershed which will pose a degradation threat to the water bodies found in the downstream.

Figure 4-2: Land cover in the resourceful upper zone of Meki river watershed

The middle zone (Afro-montane vegetation zone) of Meki river watershed was dominated by EBLUS with dense natural and eucalyptus tree cover. The presence of eucalyptus tree cover well mixed with the cultivated land with agro-forestry trees and small patches of grazing land as shown in Figure 4-3 found as the common LULC types in the middle zone of the watershed. The rain-fed agricultural practice is the dominating one as compared to irrigation practices that is sparsely observed.

Most of degraded areas were detected in the middle zone of the watershed because of the population pressure and high numbers of cattle per head based on the observation during transact walking and interviews.

Figure 4-3: Land cover in the middle zone of Meki river watershed

The lower zone (Acacia wooded vegetation zone) of Meki river watershed was dominantly covered by cultivated land with acacia dominated bushes as shown in Figure 4-4 with expansion of irrigation practices which were under the threat of sodicity development due to a long term accumulation of salts of irrigation water from boreholes (Engidasew et al., 2020).

Figure 4-4: Land cover in the lower zone of Meki river watershed

Enset-Based land use system (EBLUS) was not considered as a separate land use system in former researches that classified land use systems in Meki river watershed as cultivated land, afro-alpine and sub afro-alpine, forest, woodland, riparian vegetation, shrub land, grassland, swamp and marshland, exposed surface & water bodies as a land cover (MoWR, 2008). Therefore, land cover classification devised for 2017 satellite image to treat EBLUS as a separate unit which resulted in eight categories as: EBLUS, bare/built-up, water bodies, bush and khatland, cultivated land, grass land, eucalyptus plantations and forest and natural vegetation.

The land cover change detection performed among 1987 and 2017 satellite images to fit with modeling objective of the study and consequently, more than 40% of the watershed was covered by cultivated land. More than ten percent of the watershed was covered by EBLUS that increased in area coverage which may have a significant implication to hydrology of the watershed (Ermias et al., 2013; DeFries and Eshleman, 2004; Uhlenbrook, 2007), ecology (Kavian, 2017) and sustainability of water resources (Kebede et al., 2015) in the watershed.

Evidence from elders and experts interviewed, data from Woreda Agriculture offices and NGOs in the watershed showed that the EBLUS, cultivated land and bare soil and eroded landscape/built-up area coverage was increasing over the last 30 years while the forest cover and grass land coverage were decreasing which was evidenced by a significant positive change in cultivated land (Kebede et al., 2015), EBLUS and bare/built up LUS's from 1987 to 2017. Grass land, eucalyptus plantation, forest and natural vegetation, bush and khatland and water bodies decrease in their area coverage over the last 30 years in their order of decreasing change as shown in Table 4.2.

The land use dynamics analysis shows that most of the land use land covers were dwindled to bare or degraded land use land cover type as shown in Table 4.2 and Table A.2 of Appendix 1 as supported by Charles et al., (2016) and Bewket and Teferi (2009) that expressed expansions of subsistence crop deforestation have been one of the common forms of transitions which posed threat of degradation.

Table 4.2: Land use land cover dynamics in Meki river watershed (1987-2017)

Bush and Khat land (B&KLUS)	**BLUS**	**CLUS**	**EBLUS**	**GLUS**	**Euca. LUS**	**FLUS**	**Water bodies**	**Net Total**
Gain (ha)	15	14	0	122.3	227.24	148.48	1.02	**-558.59**
Loss (ha)	-316	-280.9	-342	-22.3	-29	-13.2	-83.23	
Sub Net (ha)	-301	-266.9	-342	100	198.24	135.28	-82.21	
Cultivated land (CLUS)	**BLUS**	**B&KLUS**	**EBLUS**	**GLUS**	**Euca. LUS**	**FLUS**	**WB**	
Gain (ha)	73	280.9	4	133.03	10.1	780.4	0	**861.24**
Loss (ha)	-195	-14	-29	-0.5	-177.69	-4	0	
Sub Net (ha)	-122	266.9	-25	132.53	-167.59	776.4	0	
Eucalyptus plantation (Euca.LUS)	**BLUS**	**B&KLUS**	**EBLUS**	**GLUS**	**CLUS**	**FLUS**	**WB**	
Gain (ha)	3.5	29	5.03	754.23	177.69	2	0	**-3387.97**
Loss (ha)	-3106.52	-227.24	-466.23	-112.1	-10.1	-437.23	0	
Sub Net (ha)	-3103.02	-198.24	-461.2	642.13	167.59	-435.23	0	
EBLUS	**BLUS**	**B&KLUS**	**Euca.LUS**	**GLUS**	**CLUS**	**FLUS**	**WB**	
Gain (ha)	3.85	342	466.23	1135.2	29	233.8	0	**2199.03**
Loss (ha)	-0.82	0	-5.03	-1.2	-4	-1	0	
Sub Net (ha)	3.03	342	461.2	1134	25	233.8	0	
Forest and Natural vegetation (FLUS)	**BLUS**	**B&KLUS**	**Euca.LUS**	**GLUS**	**CLUS**	**EBLUS**	**WB**	
Gain (ha)	141	13.2	437.23	158.28	4	1	0	**-801.18**
Loss (ha)	-208.21	-148.48	-2	-183	-780.4	-233.8	0	
Sub Net (ha)	-67.21	-135.28	435.23	-24.72	-776.4	-232.8	0	
Grass land (GLUS)	**BLUS**	**B&KLUS**	**Euca.LUS**	**FLUS**	**CLUS**	**EBLUS**	**WB**	
Gain	0.28	22.3	112.1	183	0.5	1.2	142.21	**-4183.5**
Loss	-2321	-122.3	-754.23	-158.28	-133.03	-1135.2	-21	
Sub Net	-2320.72	-100	-642.13	24.72	-132.53	-1134	121.21	
Bare land (BLUS)	**CLUS**	**B&KLUS**	**Euca.LUS**	**FLUS**	**GLUS**	**EBLUS**	**WB**	
Gain (ha)	195	316	3106.52	208.21	2321	0.82	135.29	**6046.21**
Loss (ha)	-73	-15	-3.5	-141	-0.28	-3.85	0	
Sub Net (ha)	122	301	3103.02	67.21	2320.72	-3.03	135.29	

LULC dynamics analysis result shows that EBLUS is stable than other LUSs and the land covers that are exchanging over years and the quantity of internal trade off and flow matrixes of different LULC categories are indicators of the dynamics (Table 4.2). The “from to” analysis shows that the estimated area that was changed to or gained from each LULC classes (Mekuria, 2005). In 1930s more than 20% of Gurage Mountain landscape were covered with natural forests and primarily oriented to subsistence agriculture (Woldetsadik, 2004) and since then the forests have been decreasing and the removal has been particularly rapid from 1991 to 1992 because of the political system change in the country (Bekalu and Feleke, 1996).

According to Charles et al., (2016) and Bewket and Teferi (2009) expansions of subsistence crop production and deforestation have been the common forms of transitions and dynamics. Similar trends of transitions occurred in Meki river watershed, which was manifested by a high increase in bareland and cultivated land while a fast and sharp decrease in grass land and plantation forests with considerable decrease in natural forest cover and bush land cover. The virtuous thing in the watershed was the continuous expansion of EBLUS and increased approximately 46% over the past twenty years (CSA, 1995–2017); while yield has been reported to increase twelve fold (James S Borrell, et al, 2020). Similarly, there was an increase in EBLUS over the last thirty years by 11.2% in Meki river watershed which gained from all other LUSs (Table 4.2).

According to Derege et al., 2012; Abraham, 2006; Legesse et al., 2004 and Bekele, 2003; the highlands of Meki river watershed are highly cultivated and the deforestation rate was growing every year, so that the sediment yield to the lakes from the feder rivers is substantially expected to be high.

An abundant livestock population has played its part in the loss of vegetation and grass cover through overgrazing of range lands (Derege et al., 2012; Ayenew, 2004; Legesse et al., 2004). During 1973–2006, considerable change in land use and land cover took place in the Ethiopian CRV. Spatial analysis showed that the areas of water bodies, forest, and woodland decreased, whereas the areas of land classified as intensively cultivated, mixed cultivation/woodland and degraded land increased. Degraded land increased mainly at the expense of cultivated lands (intensive and mixed cultivation) and cultivated land increased at the cost of woodland and forest (Derege et al., 2012).

The most direct negative consequence of the increasing area of land degradation is the decreasing productive capacity of cultivated land, which causes food scarcity across the CRV. Food shortages and food aid reliance are becoming common (Derege et al., 2012). The major causes of LULC change and land degradation in the Ethiopian CRV are growth in human population and livestock in a region of limited natural resources, unsustainable and/or poor farming techniques, a land tenure system that discourages land conservation, and poverty (Derege et al., 2012).

Hence, Meki river watershed was practicing a significant land use system change and dyamics from forest and grass land use systems to EBLUS, cultivated land use system and bare/eroded landscape/built-up LUS. The increase in EBLUS has a positive implication to prevent soil erosion and conserves soil, which contributes to the sustainability of water bodies and the farming system particularly in steep slopes (Zerfu, et al., 2018; Shigeta 1990).

4.2. State and trends of Soil erosion rate in Meki river watershed

4.2.1. State and trends of Soil erosion rate in different land use land covers

The result of this research shows that the upper catchments of the watershed are facing sever degradation irrespective of the land use systems which is evidenced by the high increase in soil loss in the forest land cover from 14.5 t ha-1yr-1 to 25.94 t ha-1yr-1, in EBLUS from 17 t ha-1yr-1 to 22.65 t ha-1yr-1, in cultivated land from 26 t ha-1yr-1 to 27.15 t ha-1yr-1, in grass land use system from 25 to 27 t ha-1yr-1, in eucalyptus plantation from 28.5 t ha-1yr-1 to 31.17 t ha-1yr-1 and in bush & khatland from 32 t ha-1yr-1 to 40.5 t ha-1yr-1 but there is a decrease in soil loss in bare soil and eroded landscape/built-up from 69.2 t ha-1yr-1 to 64.4 t ha-1yr-1 in 1987 and 2017 respectively as shown in Table 4.3.

Based on regression analysis, the annual average soil loss of the watershed increased from 25 t ha-1yr-1 (SD = 71.22) to 30.1 (SD = 89.3) for 1987 and 2017 respectively. Meshesha et al. (2012) also reported annual soil loss of 31 t ha-1yr-1 in 1973 and 56 t ha-1 in 2006 in the Central Rift Valley of Ethiopia which is attributed to conversion of forests or woodlands to croplands.

SCRP (1996) and Hurni (1989) underlines that rapid population increase, deforestation, over cultivation, expansion of cultivated land at the expense of lands under communal use rights (grazing and forests), cultivation of marginal and steep lands, overgrazing, and other social, economic and political factors have been believed to be the driving force to soil degradation which is an evidence for this research result. Bewket and Teferi (2009) also expresses that the conversions of marginal areas and forests to cultivated land have apparently contributed to the existing high rate of soil erosion and land degradation in the highlands of Ethiopia.

In both years the annual average values were beyond the permissible limit of soil loss for Ethiopian highlands as reported by Kebede et al. (2015) as the 'tolerable' range of soil loss for the central rift valley as less than 10 t ha−1yr−1 and Hurni (1993) expressed the range as 6 t ha−1yr−1 to 10 t ha−1yr−1 (Table 2.1). The rate found in this study was more than the tolerable limit mentioned in both cases (Table 4.3) but the lowest level of loss is recorded in the EBLUS in 2017 analysis (Figure 4-5) which was visualized from the shift of high soil loss distribution from enset growing zone to the non-enset growing one.

Table 4.3: The soil loss change in land covers (1987 to 2017)

Class_Name	Soil Loss 1987 (t ha-1yr-1)		Soil Loss 2017 (t ha-1yr-1)	
	Mean	**SD**	**Mean**	**SD**
Grassland	25	83	27	90
Forest and Natural vegetation	14.5	57	25.94	124.2
Eucalyptus plantation	28.5	72	31.17	88
EBLUS	17	61	22.65	68
Cultivated land	26	44	27.15	44
Bush and Khatland	32	70	40.22	78.3
Bare soil and eroded landscape/built-up	69.2	175.25	64.4	120.65

The dominant factor for the retarded soil loss in the EBLUS was the protective nature of the land use system through long leaves with good leaf area index (LAI) to dissipate the energy of rain drop although the slope gradient was high in the enset growing portion of the watershed and according to Kebede et al., (2015), the perennial crop such as 'Enset' based agroforestry contributed to arrest soil movement in these areas.

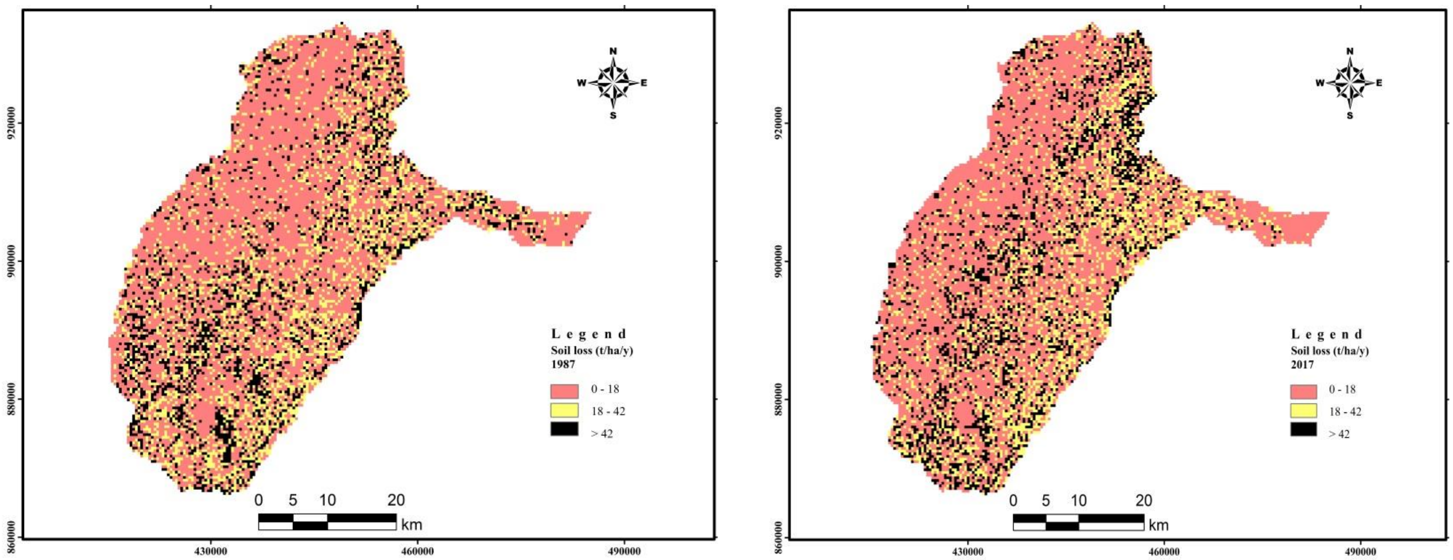

Figure 4-5: Soil loss (ton ha^{-1}year^{-1}) in 1987 and in 2017 respectively

A pairwise comparison of soil loss from each land use system indicated that a significant amount of sediment have been kept in-situ dueto expansion and enhancement of EBLUS in the watershed which saved 11.426 t ha-1yr-1 relative to other land use systems. If the whole watershed is covered by EBLUS (scenario 1), a significant amount of soil (2,411,332.3 t yr-1) would be saved from marching downstream to lake Ziway from 2110.4 sq.km of area of land which was under threat of siltation so that EBLUS will contribute for sustainability of the lake (Zerfu, et al, 2018; Shigeta 1990).

The highest soil loss was verified in the bare soil and eroded landscape/built-up areas in 1987 than the recent years because of the new construction activities and extraction of materials were ongoing without giving due attention to the environmental components and current awareness is growing concerning the environmental problems of construction activities. The soil loss in 2017 showed higher in bare soil and eroded landscape/built-up areas than other land uses systems which were attributed to construction activities in the newly established urban settings.

Bush lands were one of the leading soil loss zones due to overgrazing and annual mass burning activities of those bushes on the upper zone of the watershed (Zerfu, et al., 2018; Shigeta 1990). Based on the farmer’s response, they were burning the bushes and forests to get fire wood easily and to avoid wild animal attack on their crop, cattle and themselves.

Observation during field visit (transect walk) and information from elders of upper zone of the watershed, eucalyptus on steep slope can aggravate the movement of soil downward due to absence of root fiber to hold the soil in-situ which is manifested by high value of soil loss in eucalyptus land use system followed by cultivated land use system which are temporarily covered by annual crops during high rainfall season while it has high record at the onset of rainfall which brings its soil loss higher than soil loss from forest and EBLUS.

Alemu et al. (2018), found bathymetric differencing of lake Ziway as 3.13 t ha-1yr-1 sediment was accumulating that is attributed to the existence of outlet to Bulbula river, floodplain depositions and sand mining from the tributary rivers especially Meki river before entering to the lake. The other reason may be attributed to EBLUS which was not considered in former studies that generated the lowest soil loss in 2017 as shown in Figure 4-6.

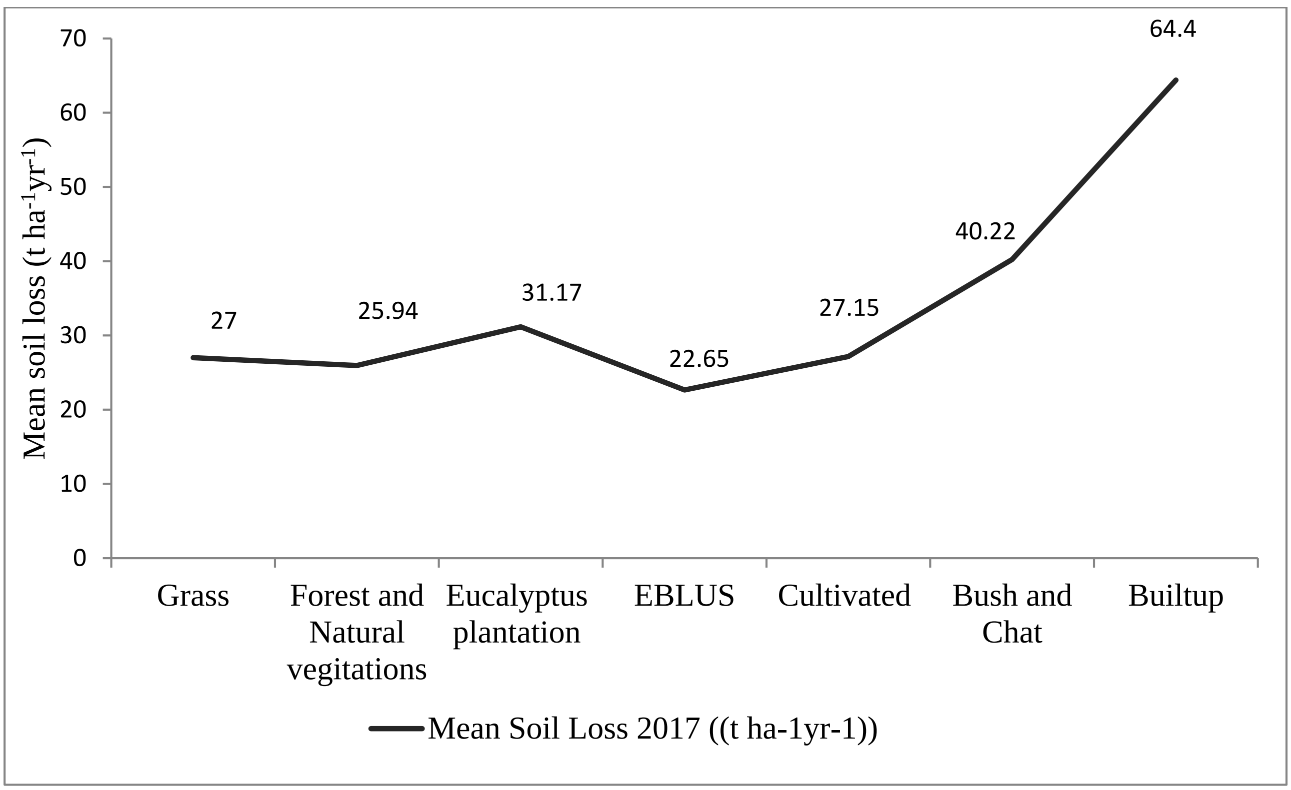

Figure 4-6: Mean Soil loss curve in 2017 for different land use systems

4.2.2. State and trends of Soil erosion rate in Sub-watershed

Soil loss is evaluated for 34 sub-watersheds over the last 30 years (1987 and 2017) against the national standard range of 2 to 18 t ha-1yr-1 (Hurni, 1985) and currently only six sub-watersheds (W3080, W3260, W3300, W3460, W3690 and W3730) out of 34 sub-watersheds (17.65%) are nearest or below the standard line which shows almost majority of the area in the watershed are suffering from soil loss risk as shown in Figure 4-7.

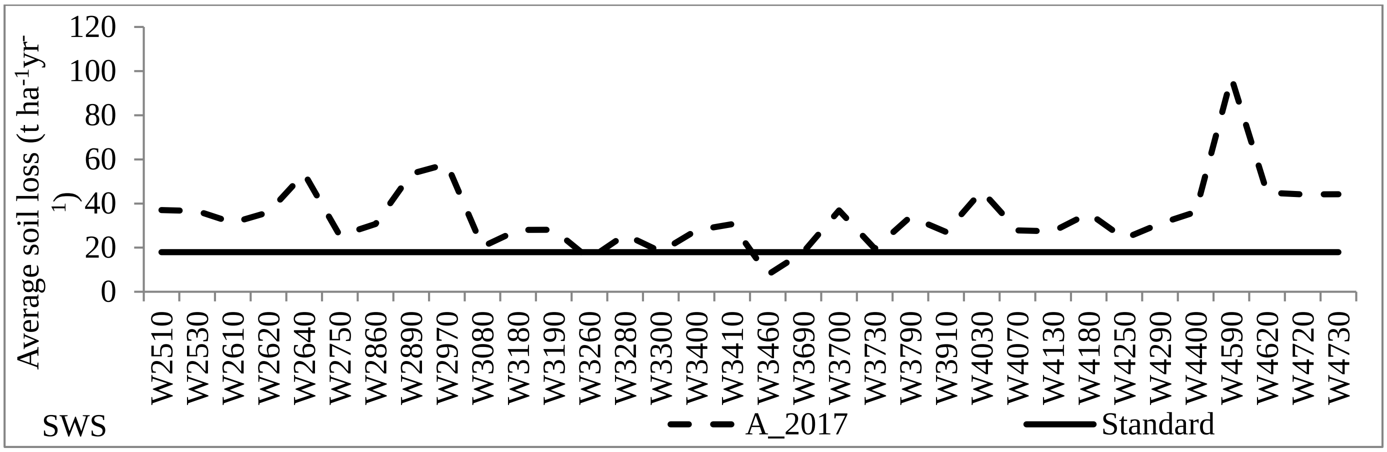

Figure 4-7: Evaluation of mean soil loss from sub-watersheds with respect to national standard

The range of soil loss rate in the central rift valley should not be beyond its formation rate of 10 t ha-1yr-1 as shown in Table 2.1.

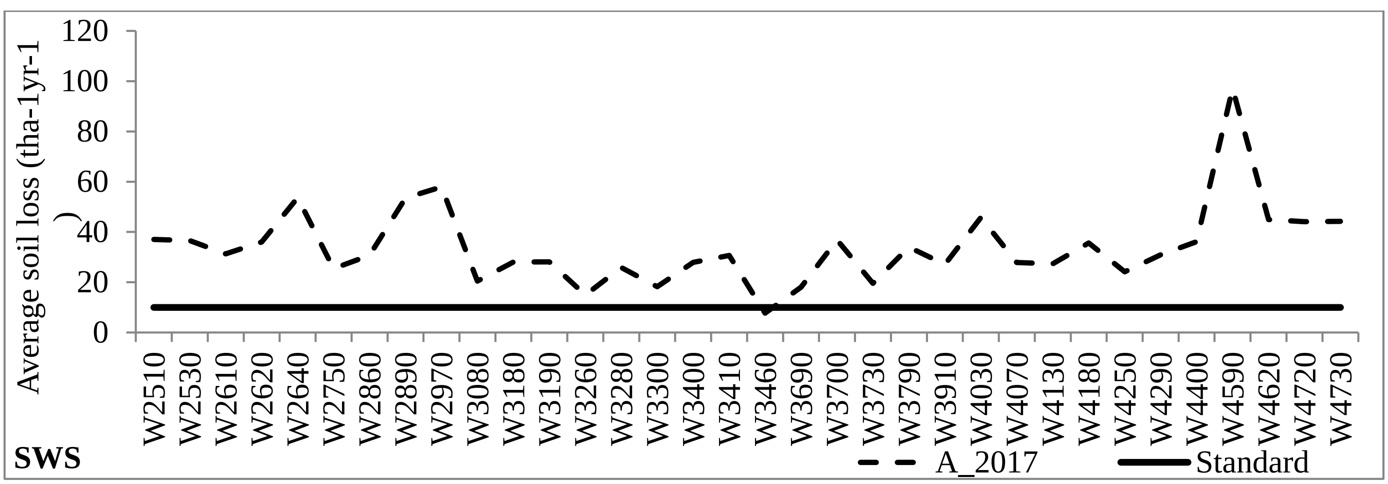

Figure 4-8: Evaluation of mean soil loss from sub-watersheds with respect to Rift valley limits

Comparison of soil loss from sub-watersheds with the standard in the central rift valley given in Table 2.1, only two sub-watersheds (W3260 and W3460) (5.88%) are nearest or below the standard line that shows a terrible soil loss risks that threatens the annual crop production and the productivity of the land impacting the local farmers' food security (Kebede et al., 2015; Brevik, 2013; Pimentel and Burgess 2013) in the Meki river watershed as shown in Figure 4-8.

Recently, erosion manifested in all parts of the watershed but more pronounced in the middle zone because of intensive cultivation practice without conservation measures and also overgrazing of grasslands as shown in Figure 4-9.

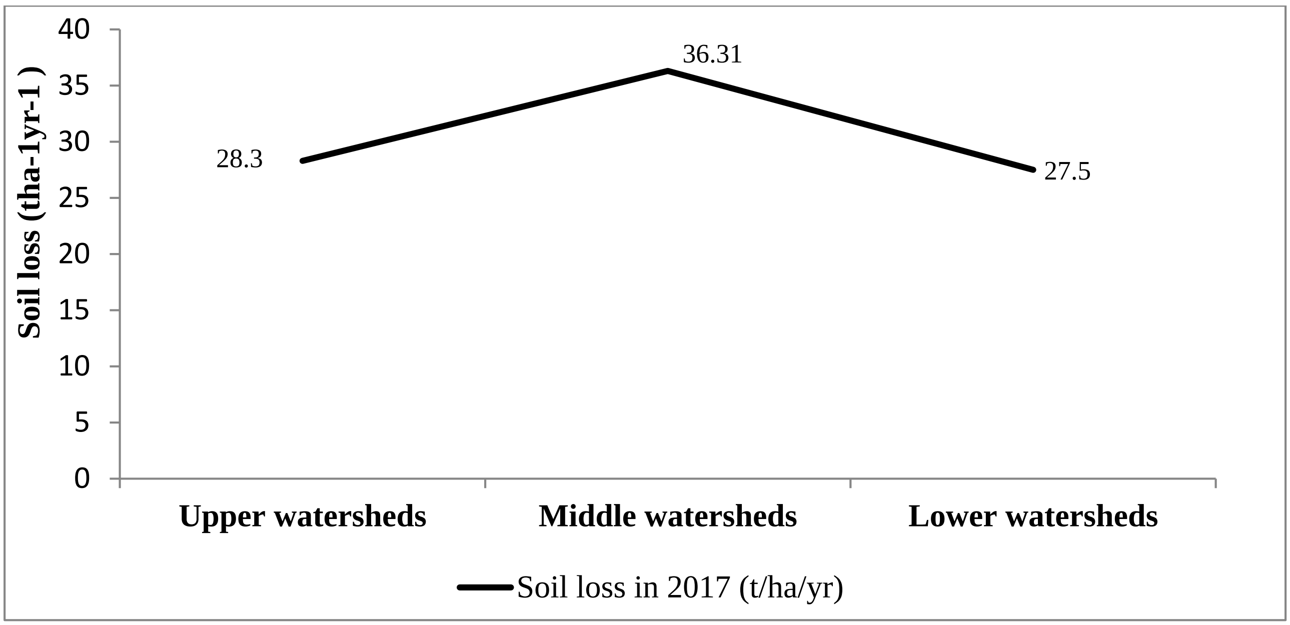

Figure 4-9: Zone based soil loss in Meki river watershed

Considering the mean soil loss values of Non-enset growing region of the watershed (the lower watershed with that of middle watershed) and comparing it with the upper enset growing portion of the watershed, there is a noticeable difference in soil loss as shown in Figure 4-10.

Based on the soil loss in 2017, the algebraic difference of Non-enset growing and enset growing zones were evaluated as 1.405t ha-1yr-1 so that 296,509.9 tons of soils have been saved from Meki river watershed every year marching down to Lake Ziway due to EBLUS which implies that EBLUS can contribute to the sustainability and life of the Lake.

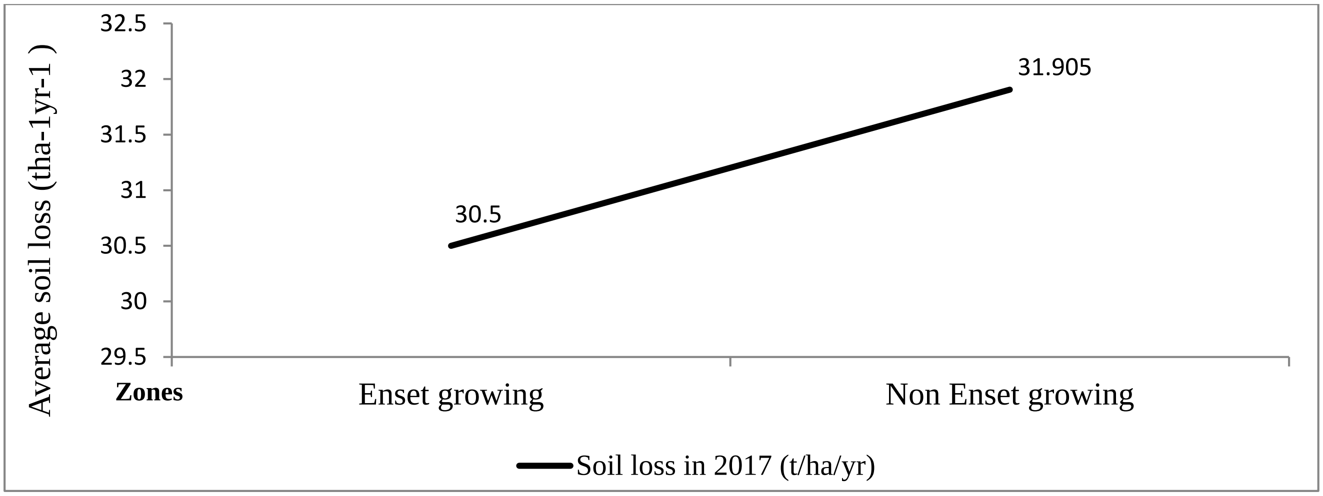

Figure 4-10: EBLUS and its contribution to reduce soil erosion in Meki river watershed

Therefore, the expansion of EBLUS will contribute for the ecological sustainability of the surrounding in addition to its social, economic, food security, environmental and microclimatic prominence and also it can reduce the soil erosion risk and contributes in the sustainability of water bodies especially lake Ziway by reducing sedimentation problem.

4.2.3. Soil erosion severity class for management priority

The estimated annual mean soil loss rates erosion risk classes and ranges of soil loss rates were adopted following the FAO soil description guidelines (FAO, 2006), other similar studies from different locations and expertise judgment (Kebede Wolka et al., 2015), with some modification to suit the local condition of Meki river watershed as shown in Table 4.4. Accordingly, the annual soil loss Range adopted (t ha-1yr-1) for Meki river watershed to suit the topographical, land cover and soil condition of the watershed sothat it will be used for further modeling and management purposes in the similar featured watersheds of Ethiopia.

Bearing in mind the range taken by Kebede et al. (2015) is in the central rift valley, including the very low range, and modifying the ranges to fit with the standards stated in Hurni (1985) for highlands of Ethiopia (18 t ha-1yr-1) and for cultivated land (42 t ha-1yr-1), the adopted ranges are given as Very low (<5), Low (5-10), Moderate (10-18), High (18-30), Very high (30-42), Severe (42-80) and Very sever (>80) and hence, the result of Meki river watershed is presented in the sub-watershed basis as shown in Table 4.5.

Table 4.4: Annual soil loss Range and severity class adoption

Severity class	Annual soil loss Range (t ha-1yr-1) (Bewket and Teferi, 2009)	Annual soil loss Range (t ha-1yr-1) (Kebede Wolka et al., 2015)	Annual soil loss Range (t ha-1yr-1) (Habtamu et al., 2020)	Annual soil loss Range (t ha-1yr-1) (Asnake and Amare, 2019)	Annual soil loss Range (t ha-1yr-1) (A.Kavian, 2017)	Annual soil loss Range adopted (t ha-1yr-1)
Very low	-	-	-	<5	0-5	<5
Low	<12	0-10	0-10	5-15	5-25	5-10
Moderate	12-25	10-20	10-20	15-30	25-50	10-18
High	25-50	20-30	20-30	-	50-80	18-30
Very high	50-80	30-45	30-50	-	>80	30-42
Severe	80-125	45-60	>50	30-50		42-80
Very sever	>125	60-80	-	>50		>80
Extremely Sever	-	80-85.64	-	-		

Table 4.5: Annual soil loss rate and severity class

Severity class	Soil loss (t ha-1yr-1)	Priority class	Sub-watersheds	Area (ha)	Percent
Low	5-10	VI	W3460	4627.5	2.2
Moderate	10-18	V	W3260	3115.8	1.48
High	18-30	IV	W2750,W3080,W3180,W3190, W3280,W3300,W3400,W3690, W3730,W3910,W4070,W4130 &W4250	89988.9	42.64
Very high	30-42	III	W2510,W2530,W2610,W2620, W2860,W3410,W3700,W3790, W4180,W4290&W4400	67907.2	32.18
Severe	42-80	II	W2640,W2890,W2970,W4030, W4620,W4720&W4730	43531.5	20.6
Very sever	>80	I	W4590	1868.2	0.9

Spatial distribution of severity and its priority class is mapped for priority of soil and water conservation programs to be held based of the severity order as shown in Figure 4-11. As the largest part of the valley (80%) is found in relatively gentle to flat topography, most of the degraded areas are found in gentle to moderate slope area (Derege et al., 2012).

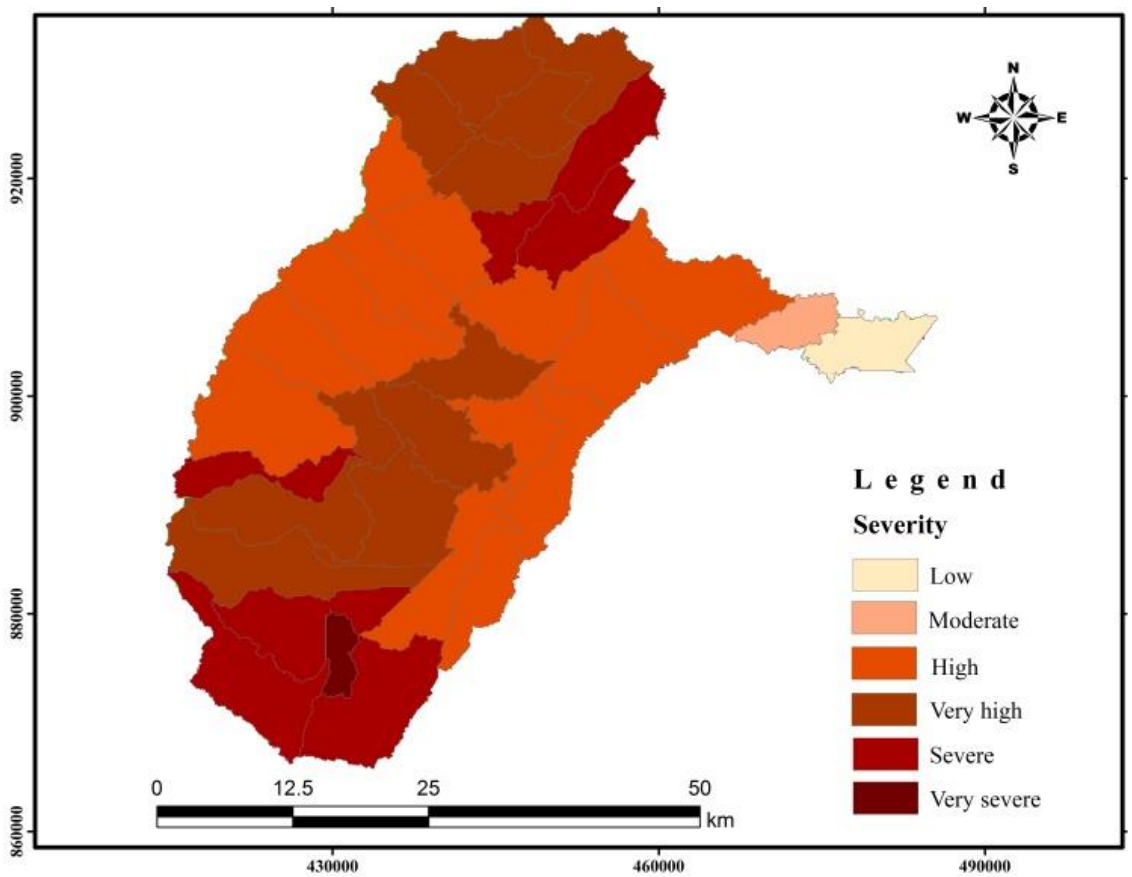

Figure 4-11: Spatial distribution of severity and its priority class

The distribution map shows that very low soil loss is spatially well distributed on the Enset growing portion of the watershed but, the mean of both Enset growing zone of the watershed (30.5 t ha-1yr-1) and non-Enset growing zone of the watershed (31.905 t ha-1yr-1) falls in the same severity class (very high) and priority class III. Hence, although the effect of topography is very high in Enset growing zone of the watershed, the soil loss is modified by the presence of vegitation cover, especially EBLUS that could contribute to arrest soil movement in these areas (Kebede et al., 2015).

4.2.4. *Evaluation of impact of EBLUS on sediment load*

Although observed sediment data is not available for Meki river for calibration and validation, the contributions of EBLUS on the amount of sediment load (modelled with flow) after analyzing the four scenarios and the individual rates of impacts of EBLUS on the generation of sediment load in the watershed for the years 1987 and 2017 were computed (Table 4.6).

Table 4.6: Annual sediment load (t ha-1yr-1) in different scenarios

SWS	Area (Km2)	1987		2017	
		WOEBLUS	WEBLUS	WOEBLUS	WEBLUS
		Sediment (t $ha^{-1}yr^{-1}$)	Sediment (t $ha^{-1}yr^{-1}$)	Sediment (t $ha^{-1}yr^{-1}$)	Sediment (t $ha^{-1}yr^{-1}$)
W2510	54.6332	0.82	0.64	1.08	0.63
W2530	60.4529	1.22	1.19	1.22	1.19
W2610	48.3344	1.29	0.96	1.29	0.96
W2620	49.8624	0.52	0.46	0.53	0.46
W2640	55.4568	1.38	0.87	1.38	0.87
W2750	35.1565	0	0	0	0
W2860	58.1634	3.02	1.80	3.02	1.80
W2890	28.0548	0	0	0	0
W2970	54.7446	2.57	2.56	2.57	2.56
W3080	61.8334	1.54	1.53	1.54	1.53
W3180	107.544	1.67	1.73	1.73	1.72
W3190	89.6239	2.90	2.50	2.90	2.50
W3260	31.1576	1.23	1.00	1.27	1.00
W3280	70.0151	0.78	1.22	1.25	1.22
W3300	58.7668	7.15	6.42	7.17	6.42
W3400	82.4782	0.52	0.36	0.53	0.36
W3410	54.6073	1.80	1.24	1.87	1.24
W3460	46.2753	0	0	0	0
W3690	66.2208	3.04	2.99	3.05	2.99
W3700	27.2959	7.44	7.58	7.45	7.57
W3730	43.9288	7.71	7.61	7.94	7.61
W3790	68.7512	0	0	0	0
W3910	106.091	7.69	7.42	7.73	7.53
W4030	41.9423	12.15	11.21	12.08	11.21

SWS	Area (Km2)	1987		2017	
		WOEBLUS	WEBLUS	WOEBLUS	WEBLUS
		Sediment (t $ha^{-1}yr^{-1}$)	Sediment (t $ha^{-1}yr^{-1}$)	Sediment (t $ha^{-1}yr^{-1}$)	Sediment (t $ha^{-1}yr^{-1}$)
W4070	66.125	3.51	3.16	3.50	3.10
W4130	65.7365	6.53	6.20	6.52	6.20
W4180	80.704	2.34	2.32	2.32	2.32
W4250	46.3686	0.97	0.97	0.97	0.97
W4290	95.7803	0.39	0.39	0.39	0.39
W4400	80.4865	2.01	2.01	2.01	2.01
W4590	18.6824	13.15	13.24	13.24	13.24
W4620	74.9025	5.09	5.09	5.09	5.09
W4720	93.856	0	0	0	0
W4730	86.358	0.15	0.07	0.14	0.10
Designation (Average)		S1 = 2.9584	S2 = 2.786	S3 = 2.99311	S4 = 2.788

The sediment load simulated with flow was used to get the statistical contribution of EBLUS relative to other LUSs. There was an increase in the average sediment load from 2.9584 t $ha^{-1}yr^{-1}$ to 2.99311 by S3 - S1 = 0.0347 t $ha^{-1}yr^{-1}$ (Jang *et al*., 2015) resulted from the effects of LULC changes with out considering EBLUS as a separate LUS (EBLUS as a cultivated land use system) and an increase in the sediment load from 2.786 t $ha^{-1}yr^{-1}$ to 2.788 t $ha^{-1}yr^{-1}$ by S4 - S2 = 0.002414 t $ha^{-1}yr^{-1}$ were attributed to the EBLUS changes (considering EBLUS as a separate land use system). The contribution of EBLUS was evaluated as ((S4 - S2) – (S3 - S1)) = -0.03231 t $ha^{-1}yr^{-1}$ (Jang *et al*., 2015). 93.048% of an increase (0.0347 t $ha^{-1}yr^{-1}$) was arrested due to EBLUS (Table 4.7). Therefore, the result showed EBLUS has an implication to reduce the sediment load generated the watershed by 93.048% as compared to cultivated LUS (Table 4.7).

Table 4.7: Impact matrix of EBLUS on sediment load in different scenarios

Years	Scenarios	1987		2017		Sediment (t $ha^{-1}yr^{-1}$)	Change	Impact
		WEBLUS	**WOEBLUS**	**WEBLUS**	**WOEBLUS**			
1987	**WEBLUS**	0	-0.17	-0.0024	-0.21	2.786	0.0024	**0.03231**
	WOEBLUS	0.17	0	0.17	-0.035	2.9584		
2017	**WEBLUS**	0.0024	-0.17	0	-0.21	2.788		
	WOEBLUS	0.21	0.035	0.21	0	2.99311	0.0347	**93.048**

According to Haregeweyn *et al.,* 2015a, the poor availability and reliability of SY data for Ethiopian rivers remains a major bottleneck for a better understanding of the dynamics and drivers of SY variability in the region and that was manifested in this research for calibration of the result.

According to Alemu *et al.* (2018), the bathymetric differencing of Lake Ziway indicates that the sediment was accumulating at a rate of 3.13 t $ha^{-1}yr^{-1}$. Considering EBLUS, the average sediment accumulated in 2017 is 2.788 t $ha^{-1}yr^{-1}$ that may express the value simulated is nearest to the bathymetrically measured value but Lake Ziway receives sediment from two rivers (Meki and Katar) that the accumulation of 2.788 t $ha^{-1}yr^{-1}$ sediment only from Meki river is logical. Aman and Brook (2021) and Kebede et al., (2015) reported an average and minimum sediment of 11 and 0.34 t ha-1yr-1 respectively in Meki watershed. The sediment yield in the NEGZ (4030, 3300, 3700, 3730, 4590) is higher than the EGZ (2510, 2530, 2610, 2640) of the watershed (Figure 4-12) and hence, expansion of Enset-Based land use system can reduce the sediment load and contribute in the sustainability of Lake Ziway by reducing sedimentation problem.

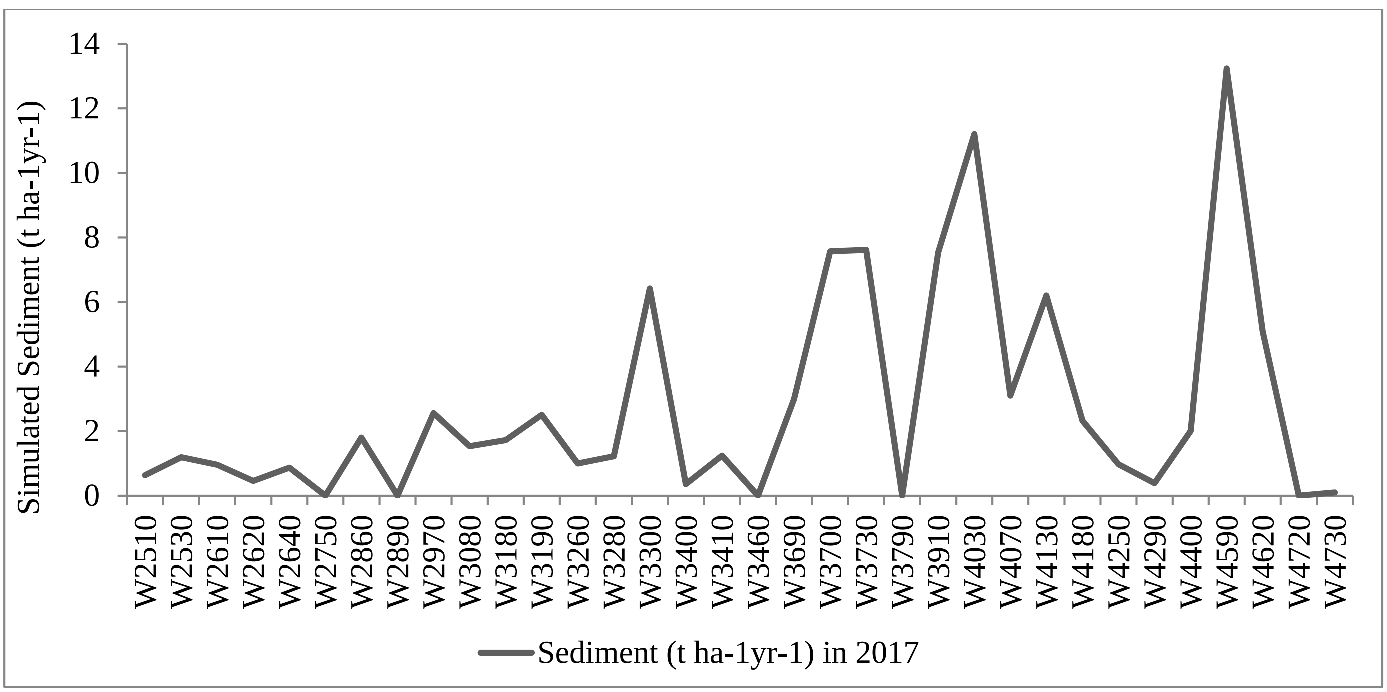

Figure 4-12: Sediment load for sub-watersheds in Meki River Watershed

4.3. State of infiltration rate of the soil under different land use systems

Infiltration rate of the soil is an important variable to understand and predict a range of soil processes (Yimer, et al., 2009). In order to understand such processes, field data on infiltration rate of the soil under different land use systems (LUSs) in Meki river watershed were collected, summarized and presented in Table 4.8.

High infiltration rate was measured in the forests LUS (mean 12.9675 mmhr-1) followed by EBLUS (mean 12.8125 mmhr-1) with a lower record in cultivated LUS (10.375 mmhr-1). Similarly, Ibeje (2018) reported that the mean steady state infiltration rates of farm lands are lower than that of forest land that shows the infiltration rate of the soil is under the influence of LULCC (Ibeje, 2018).

EBLUS is one of the prominent component in Meki river watershed and it improved the infiltration rate of the soil by increasing the organic matter content of the soil through litter fall and pseudo stem cover falls (Mesfin et al., 2017) and also the 2 to 3 meters long root fiber measured in the field helped to enhance the presence of void spaces of the soil to transmit rain water easily to the ground water system.

The presence of wide leaves in EBLUS protected the direct impact of the rain drop and permited more through fall which reduced the speed of the rain drop and gave more time to increase the recharge and reduce erosion (Alemu et al., 2020; Kebede et al., 2015). Hence, EBLUS can improve the infiltration rate of the soil that makes EBLUS as essential LUS in water resources and watershed management.

Although statistically not significant, the Upper zone of the watershed shows higher mean infiltration rate (11.0125 mmhr-1) than the Middle zone (10.92625 mmhr-1) of the watershed that shows the presence of more forest LUS and EBLUS in the Upper zone than the middle zone of the watershed which enhanced infiltration rate of the soil (Yimer, et al., 2009; Oliver, et al., 2006).

Table 4.8: Mean infiltration rate of land uses

	Mean Infiltration Rate (mm/Hour)				Basic infiltration rate (mm/hour) (Oliver et al., 2006)
Land Use	Soil Texture	Zone			
		Upper	Middle	Mean infiltration rate of LUSs	
Cultivated	Sandy Loam		19.125	10.375	20 to 30
	Silt Loam	12	13.9625		10 to 20
	Clay Loam	7.2125	5.825		5 to 10
	Clay		4.125		1 to 5
Bare/eroded landscape/Built up	Sandy Loam		8.75	7.0625	20 to 30
	Silt Loam	7.0625	10		10 to 20
	Clay Loam		5.5		5 to 10
	Clay		4		1 to 5
Grass land & planted forest	Sandy Loam		19.25	11.1875	20 to 30
	Silt Loam	15.8625	9.95		10 to 20
	Clay Loam	8.6	7.9625		5 to 10
	Clay		5.5		1 to 5
EBLUS	Sandy Loam		22.55	12.8125	20 to 30
	Silt Loam	12.625	17.025		10 to 20
	Clay Loam	10.875	9.375		5 to 10
	Clay		4.425		1 to 5
Natural Forest	Sandy Loam		22.625	12.9675	20 to 30
	Silt Loam	15.25	15.5		10 to 20
	Clay Loam	9.625	10.3475		5 to 10
	Clay		4.4575		1 to 5
Average		11.0125	10.92625		

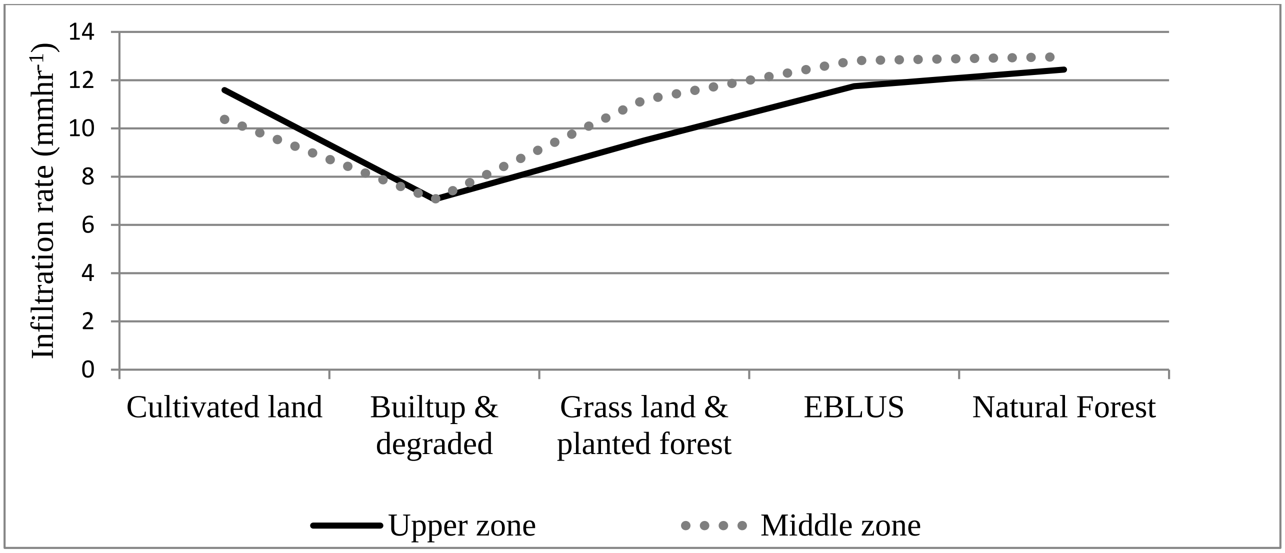

Figure 4-13: Vegetation zone based infiltration rate of the soil (mmhr-1)

There was a significant difference between infiltration rates at different land use systems at 5% significance level (α = 0.05) with a p-value of 0.0094 (<α) due to a low value in the Bare LUS and cultivated LUS and a high value in Forests LUS and EBLUS and a non-significance difference was observed among vegetation zones with p-value of 0.443 (>α) (Table 4.9).

Table 4.9: Analysis of variance for vegetation zones and land use systems

Source of Variation	**SS**	**df**	**MS**	**F**	**P-value**	**F crit**
Land use systems	40.16	4	10.04	16.52	0.009	6.39
Vegetation zone	0.44	1	0.44	0.72	0.44	7.71
Error	2.43	4	0.61			
Total	43.04	9				

Therefore, a high mean infiltration rate in Forests LUS and EBLUS shows that there is an improvement in hydrological parameters and as stated by Yimer et al., (2009) and Oliver et al., (2006), the improvement in infiltration rate has a huge contribution in runoff reduction and alleviation of sedimentation problems to water bodies which have a direct influence on water resources and watershed management in Meki river watershed.

4.4. Determination of Curve number matrix for EBLUS

The CN of EBLUS interpolated for each HSG with their respective infiltration rate and Carbon stock relative to other LUSs (Table 4.10). Carbon stock was modified by growth period (more than 5 years) (Mesfin *et al.*, 2017), stages of growth and energy production of EBLUS that presses the double counting of carbon stock. Hence, infiltration rate of the soil powers 85% of the CN while 15% of the CN of LUSs was influenced by carbon stock which was computed as:

Table 4.10: Curve Number Interpolation for EBLUS

Curve Number of EBLUS	Hydrologic Soil Group (HSG)				Curve Number of EBLUS	Hydrologic Soil Group (HSG)			
Parameter 1 (Infiltration rate)	**A**	**B**	**C**	**D**	**Parameter 2 (Carbon stock)**	**A**	**B**	**C**	**D**
$\mathbf{EI1} = \frac{BA*IB}{IE}$	42.4	46.9	49.6	50.7	$\mathrm{ESq1} = \frac{BA*SqB}{SqE}$	0.13	0.15	0.154	0.16
$\mathbf{EI2} = \frac{FA*IF}{IE}$	36.4	60.7	73.9	80	$\mathrm{ESq2} = \frac{FA*SqF}{SqE}$	21.3	35.5	43.18	46.73
$\mathbf{EI3} = \frac{GA*IG}{IE}$	42.8	60.3	69	73.4	$\mathrm{ESq3} = \frac{GA*SqG}{SqE}$	5.3	7.46	8.54	9.075
$\mathbf{EI4} = \frac{CA*IC}{IE}$	54.3	63.2	68.8	72.1	$\mathrm{ESq4} = \frac{CA*SqC}{SqE}$	17.3	20.1	21.94	22.97
Cumulative CN of EBLUS at different HSG						**A**	**B**	**C**	**D**
$\mathbf{E} = \frac{0.85*\sum_{i=1}^{4} EIi+0.15*\sum_{i=1}^{4} ESqi}{4}$						**39**	**51.5**	**58.3**	**61.6**

Therefore, finally the general formula developed through regorous simple linear regression model of the two parameters for EBLUS that was given as Eqn.4-1:

$$\mathbf{E} = \frac{0.85*\sum_{i=1}^{n} \mathrm{EIi}+0.15*\sum_{i=1}^{n} \mathrm{ESqi}}{n} \tag{4-1}$$

<u>Where:</u>

- EIi = Infiltration based Curve number of EBLUS relative to i LUS
- ESqi = Carbon stock based Curve number of EBLUS relative to i LUS

Therefore, the new lookup table for all LUSs including EBLUS with a CN matrix of 39, 51.5, 58.3 and 61.6 for HSG of A, B, C and D respectively was prepared and fed to HEC-GeoHMS together with that of the union of LUSs and soil information in order to generate the new CN grid (Merwed, 2012) that can be used for further surface runoff modeling (Vaezi, et al., 2010). CN of EBLUS was lower than other LUSs for HSG B, C and D while it was preceded by Natural forest for HSG A that shows EBLUS can be best for soils with poor infiltration rate like HSG of D as shown in Table 4.11.

Asimilar method of interpolation was used in Mohammed Reza Pahlavan-Rad, et al., 2020 that used simple (multiple linear regressions) model to link covariates that include curve number and infiltration rate that found the mean measured soil water infiltration in the study area was 13.6 mm h^{-1} and low infiltration rate (Brouwer et al, 1985) is likely because of low soil organic matter. Stewart, *et al.*, 2002 and Mitchell, 2005, used geostatistics (generalized linear regression techniques (kriging) of unknown values. Hence, simple linear regression based estimation and prediction has been done in this research to interpolate the CN matrix of EBLUS relative to other LUSs and presented in Table 4.11.

Table 4.11: New look-up table for CN of different LUSs including EBLUS

Land Cover/Land Use	**Hydrologic Soil Group (HSG)**			
	A	**B**	**C**	**D**
Open Water	100	100	100	100
Bare/eroded landscape/Builtup LUS	77	85	90	92
Natural Forest LUS	36	60	73	79
Grasslands & plantation LUS	49	69	79	84
Cultivated LUS	67	78	85	89
EBLUS	**39**	**51.5**	**58.3**	**61.6**

Hence, the new CN matrix of the Meki river watershed was generated from the new lookup table including EBLUS (2017) and mapped as shown in Figure 4-14. This CN grid could be used in different models of rainfall-runoff modeling purposes and also researchers and runoff flow simulators.

Finally, a formula was developed and presented in Equation 25 that will contribute to the scientific community as a new hydrological model to be used by future scientists working in those enset growing areas with similar watershed features.

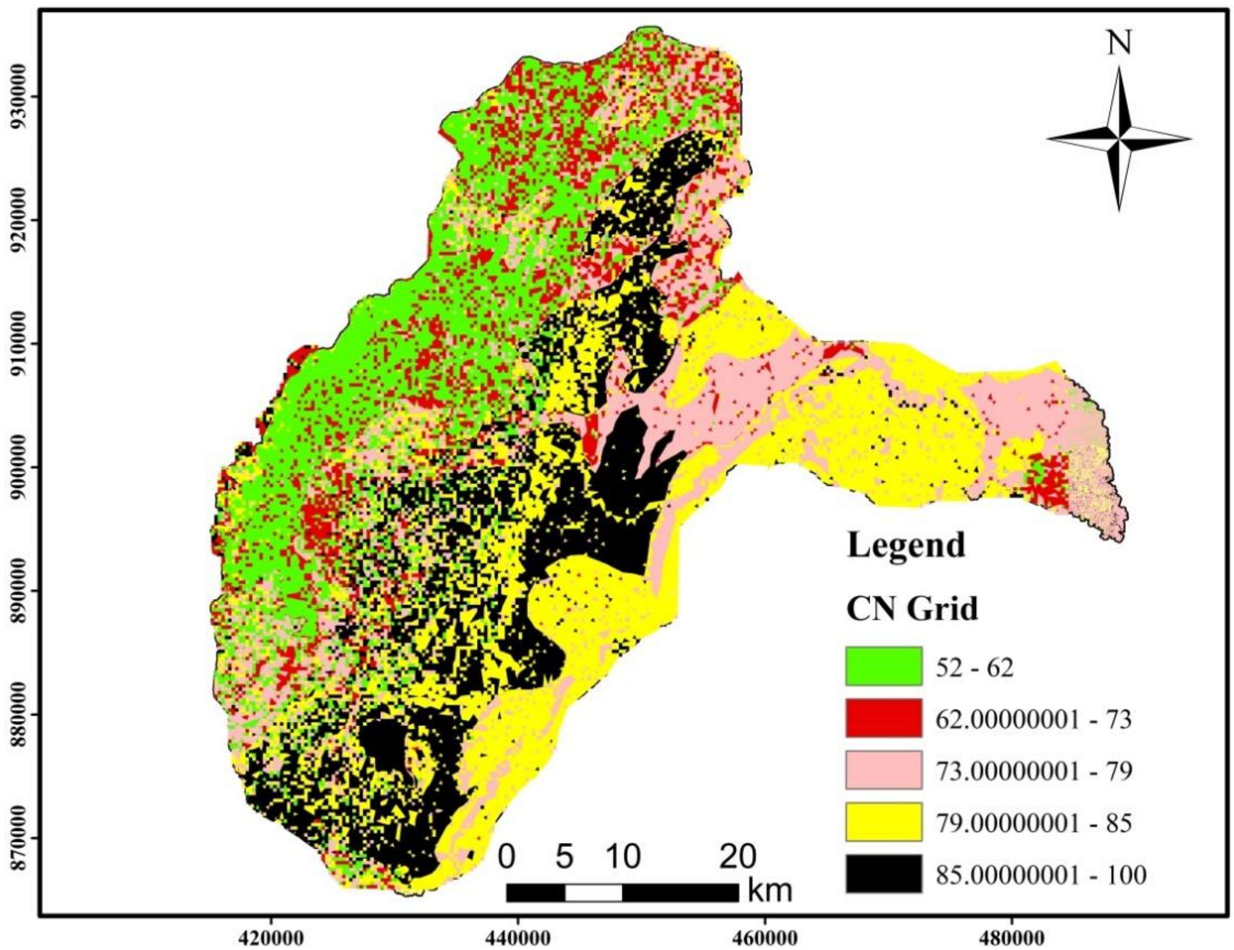

Figure 4-14: CN grid of Meki river watershed

4.5. Evaluating the impact of EBLUS on magnitude of surface runoff, water resources and watershed management

4.5.1. Model parameters of Meki river watershed and relative evaluation of rainfall

4.5.1.1. Curve number and nominal parameters used in HEC-HMS model

The nominal curve number grids for the four senarios were generated (EBLUS as a Cultivated LUS and EBLUS as a separate LUS in the years 2017 and 1987) as shown in Figure 4-15.

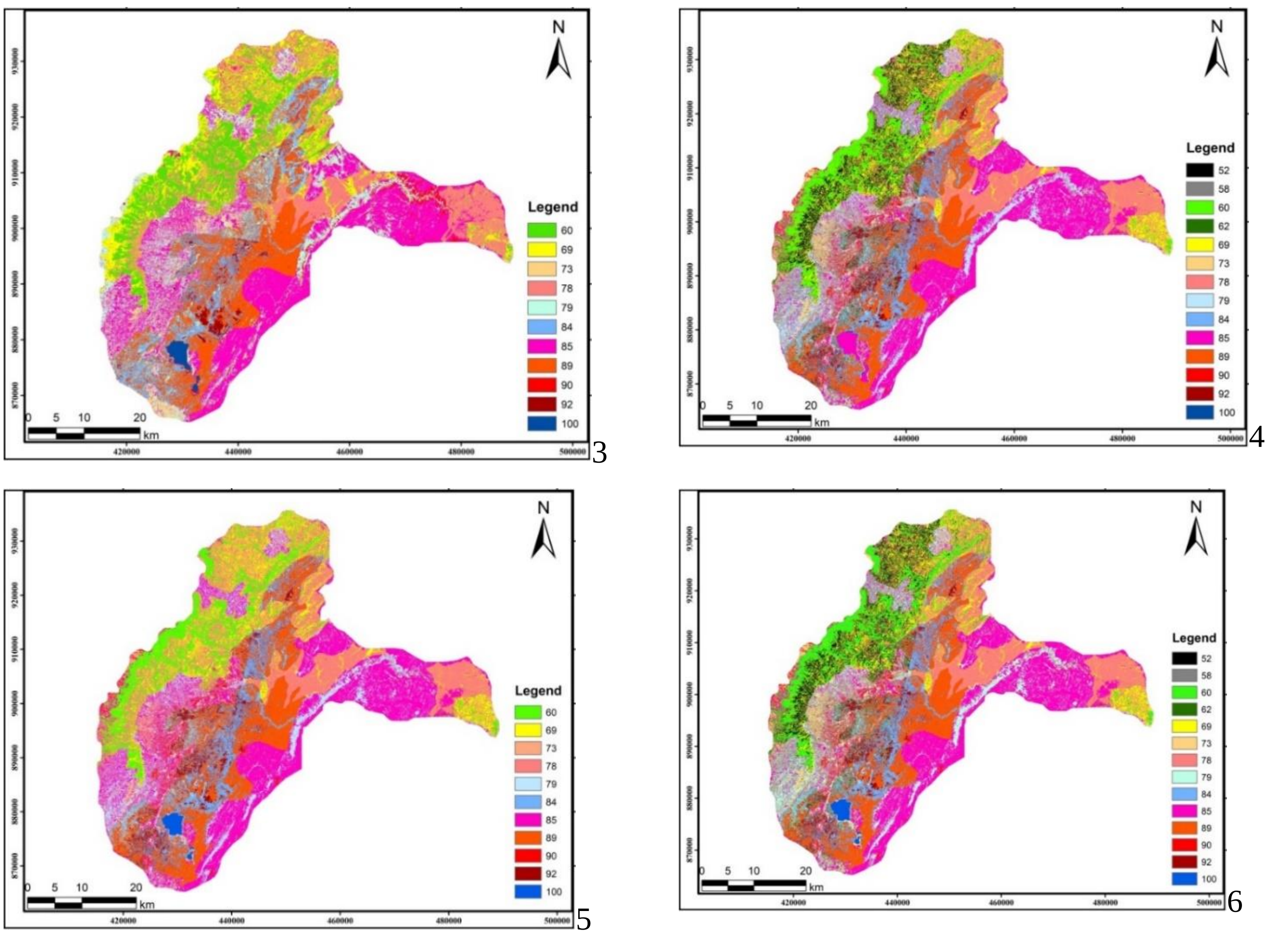

Figure 4-15: Curve Number grids of four scenarios (1987 and 2017)

[3] EBLUS considered as a Cultivated LUS in 1987 – BAU scenario
[4] EBLUS is considered as a separate LUS in 1987 – New scenario1
[5] EBLUS considered as a Cultivated LUS in 2017 – BAU scenario
[6] EBLUS considered as a separate LUS in 2017 – New scenario2

HEC-GeoHMS, Geostatistical tools and ArcGIS 10.1 were employed to generate the model parameters (CN, lag time, initial abstraction, initial discharge, recession constant, Muskinham K and x) of each of the 34 sub-watersheds and reaches pre-delineated in Meki river watershed using hydro DEM, merged features of LULC and soil data, and CNLookUp table input datasets (Mewded et al., 2021) that considered EBLUS as a separate land use system (Table 4.12).

Table 4.12: Model parameter for impact valuation of EBLUS on magnitude of surface runoff

SWS[7]	Area	1987		2017		SWS	Area	1987		2017	
	(Km2)	CN-A[8]	CN-B[9]	CN-A	CN-B		(Km2)	CN-A	CN-B	CN-A	CN-B
W2510	54.63	73.7	72.7	74.15	72.7	**W3690**	66.22	70.6	65.5	72.3	65.5
W2530	60.45	72	63.85	73	63.85	**W3700**	27.3	85	81.83	85.8	81.3
W2610	48.33	71	62.4	70.1	62.4	**W3730**	43.93	88	88.13	88.14	88.13
W2620	49.86	74.1	71.67	74.1	71.7	**W3790**	68.75	86.5	85.5	86.9	85.5
W2640	55.46	80	79.7	80	79.7	**W3910**	106.09	75	68.02	75.2	68.02
W2750	35.16	74.32	65.7	74.32	65.7	**W4030**	41.94	75.6	69.11	76.83	69.11
W2860	58.16	77.1	73.23	77.1	73.23	**W4070**	66.13	85	84.8	84.8	84.8
W2890	28.05	77.5	76.8	77.5	76.8	**W4130**	65.74	86	85.5	85.5	85.5
W2970	54.74	80.3	80.12	80.3	80.12	**W4180**	80.70	80.4	74.26	80.14	74
W3080	61.83	72.7	66	72.7	66	**W4250**	46.37	84.2	84.25	84.25	84.25
W3180	107.54	81.15	81.14	81.15	81.14	**W4290**	95.78	82.7	76.6	82.2	76.6
W3190	89.62	71.11	64.92	71.11	65	**W4400**	80.49	87	85.47	86.84	85.5
W3260	31.16	83.5	83.5	83.5	83.5	**W4590**	18.68	90.9	85.44	89.4	89
W3280	70.02	82.7	83.86	84.1	83.9	**W4620**	74.90	86.6	83.85	87	85
W3300	58.77	68.6	62.86	70.4	62.9	**W4720**	93.86	85.53	85.1	85.6	85
W3400	82.48	79.7	80.17	80.17	80.2	**W4730**	86.36	83.6	82.64	85.8	82.7
W3410	54.61	79	82.3	83.7	82.3	**Average**		**79.74**	**76.54**	**80.11**	**76.93**
W3460	46.28	80	65.5	79.5	74.5						

7 Sub-watersheds

8 Enset Based Land Use System (EBLUS) as a Cultivated land use system – scenario1

9 EBLUS as a separate land use system – scenario 2

The CN, lag time, initial abstraction, initial discharge, recession constant, and Muskinham K and x values representing the entire watershed were the initial input (Nominal) model parameters for HEC-HMS modeling (Calibration and validation) as shown in Table 4.13.

Table 4.13: Nominal model parameters of Meki river watershed (2017)

SWS	CN	LT	IA	ID	RC	SWS	CN	LT	IA	ID	RC
W2530	63.8	73.72	35.30	2.24	0.8	**W3700**	81.3	213.18	15.35	1.02	0.8
W2510	72.6	185.54	22.06	2.02	0.8	**W3790**	85.5	403.22	11.12	2.56	0.8
W2620	71.7	123.35	18.32	1.845	0.8	**W4720**	85	260.46	9.86	4.74	0.8
W2610	62.4	75.51	37.01	1.79	0.8	**W4730**	82.7	300.25	14.33	4.36	0.8
W2860	73	140.24	23.24	2.15	0.8	**W4590**	89	302.48	9.86	0.94	0.8
W2750	65.7	85.39	34.85	1.3	0.8	**W4620**	85	237.72	12.60	3.78	0.8
W3080	66	114.81	15.09	2.3	0.8	**W4290**	76.6	242.34	19.95	4.83	0.8
W2890	76.8	221.94	20.95	1.04	0.8	**W4180**	74	202.50	21.93	4.07	0.8
W2640	79.7	250.58	14.66	2.05	0.8	**W4400**	85.5	623.19	12.32	4.06	0.8
W2970	80	181.70	14.66	2.03	0.8	**W4130**	85.5	940.00	9.11	2.45	0.8
W3280	83.9	227.3	12.62	2.6	0.8	**W4250**	84.25	346.01	9.60	2.34	0.8
W3190	65	188.94	34.72	3.33	0.8	**W3730**	88.13	466.42	9.46	1.64	0.8
W3300	62.9	132.37	38.17	2.2	0.8	**W4070**	84.8	1027.07	11.67	2.46	0.8
W3410	82.3	307.47	19.82	2.03	0.8	**W3400**	80.17	263.55	14.20	3.07	0.8
W3910	68.02	154.19	28.58	3.95	0.8	**W3180**	81.14	290.99	12.62	4	0.8
W4030	69.11	163.74	28.45	1.56	0.8	**W3260**	83.5	352.53	11.83	1.16	0.8
W3690	65.5	116.42	29.81	2.46	0.8	**W3460**	74.5	875.48	14.08	1.72	0.8

4.5.1.2. Final optimized model parameters used in HEC-HMS model

The final optimized model parameters are presented in Table D.3 and it describes that the curve number (CN II), Lag time, initial abstruction, initial discharge, RC kept constant (0.01), K and x computed after manual and automatic optimization processes.

4.5.2. HEC-HMS modeling

Sensitivity analysis

The sensitivity result shows that curve number (CN2), Muskingham K, Recession Constant, Initial Discharge, Initial Abstruction, Lag Time and Muskingham X were found to be sensitive parameters for simulated volume and peak flow during the calibration period in their order of sensitivity for Meki river watershed (Table D.2 of Appendix 4, Table 4.14 and Table 4.15).

Table 4.14: Parameters evaluation for sensitivity ranking interms of percent volume change

Elements	Parameter	-50%	-40%	-20%	0%	10%	20%	40%	50%
SWS[10]	**CN**	-7.431	-4.46	-2.23	0	0.645	2.29	9	12
SWS	**IA**	0.196	0.154	0.0987	0	-0.06	-0.156	-0.195	-0.1982
SWS	**LT**	0.0899	0.092	0.104	0	-0.09	-0.155	-0.224	-0.226
Reach	**MK**	-1.532	-1.24	-0.641	0	0.313	0.412	0.951	1.234
Reach	**MX**	-0.047	-0.05	-0.038	0	0.353	0.412	0.4765	0.47667
SWS	**ID**	0.196	0.194	0.16	0	-0.1	-0.131	-0.193	-0.1982

Table 4.15: Sensitivity ranking of parameters

Parameters	Minimum of Percent Volume Change	Slope	Sensitivity rank
Curve Number	-7.431	5.225	1
Initial Abstruction	-0.198230764	-0.063	4
Lag Time	-0.226	-0.0494	5
Muskingham K	-1.532	0.4071	2
Muskingham X	-0.046642533	0.0746	6
Initial Discharge	-0.198230764	-0.0628	3

CN is one of the major critical parameter that is directly related to LULC and soil characteristics (Alemu, *et al.*, 2018). Hence, it was considered in the evaluation of impact of EBLUS on surface runoff. It is followed by Muskingham K and the influence of base flow initial discharge was high while the Muskingham x's influence was very low as it was evident from Elizabeth (1994). Despite the high sensitivity of flow volume to recession constant, it was independent of land use impacts (Bitew *et al.*, 2019). Therefore, base flow recession constant was not considered (kept constant).

[10] Sub-Watersheds

Calibration and validation of HEC-HMS model

HEC-HMS model is capable of simulating rainfall-runoff relation for dendritic watershed in space and time and it has been used successfully in different parts of the world river basins for catchment modeling (Sintayehu, 2013). The selection of rainfall-runoff simulation time step is a critical step for hydrologic modelling and model calibration and validation and it depends on many factors, such as rainfall characteristics, watershed properties and availability and completeness of rainfall and stream monitoring data (Bitew et al., 2019; Chu and Steinman, 2009). Similarly, in this research the consistency of rainfall with the observed flow was used to select the calibration and validation time step. Hence, calibration was performed to adjust baseline (Nominal) parameters (CN, MK, ID, IA, LT, and Mx) and the automated calibration was done to minimize the objective function value (PWRMSE) for optimized parameters.

The manual and optimization trials calibration of the HEC-HMS parameters was conducted using the observed stream flow data from Meki guaging station for the period 1985 to 2010. The goodness of fit was evaluated using hydrograph visualization and calculated statistics value of the estimated and observed stream flows as shown in Figure 4-16.

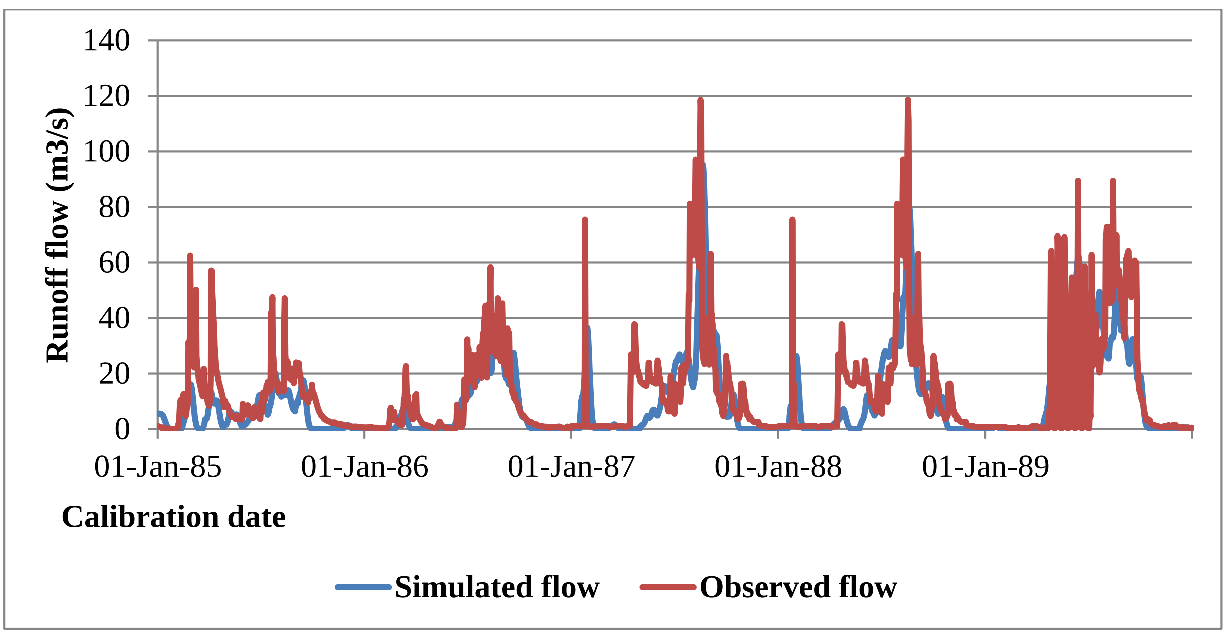

Figure 4-16: Calibration of HEC-HMS model (01 Jan 1985 to 31 Dec 1989)

The comparison of the observed river stream flow to the simulated runoff in this study shows a close (very good) (Moriasi *et al*., 2007 and Mewded *et al*., 2021) agreement between the two (NSE=76.25) as shown in Table 4.16. The parameters were optimized to obtain a closer result of the simulated flow to the observed stream flow. The graph in Figure 4-16 shows that the observed flow pattern resembled well with the simulated outlet stream flow.

Model validation used similar input parameters as determined by the calibration and the model was executed for the validation period from 1990 to 1994 with the calibrated parameters to check the ability of the model to accurately calculate the stream flow at Meki river watershed. Similar to the calibration, the validation comparison of hydrograph as well as the estimated and observed statistical values of stream flow shows good (Moriasi *et al*., 2007 and Mewded *et al*., 2021) (NSE=62) agreement between the simulated and observed stream flow in terms of the peak value and the rising and recession of the stream flow (Figure 4-17).

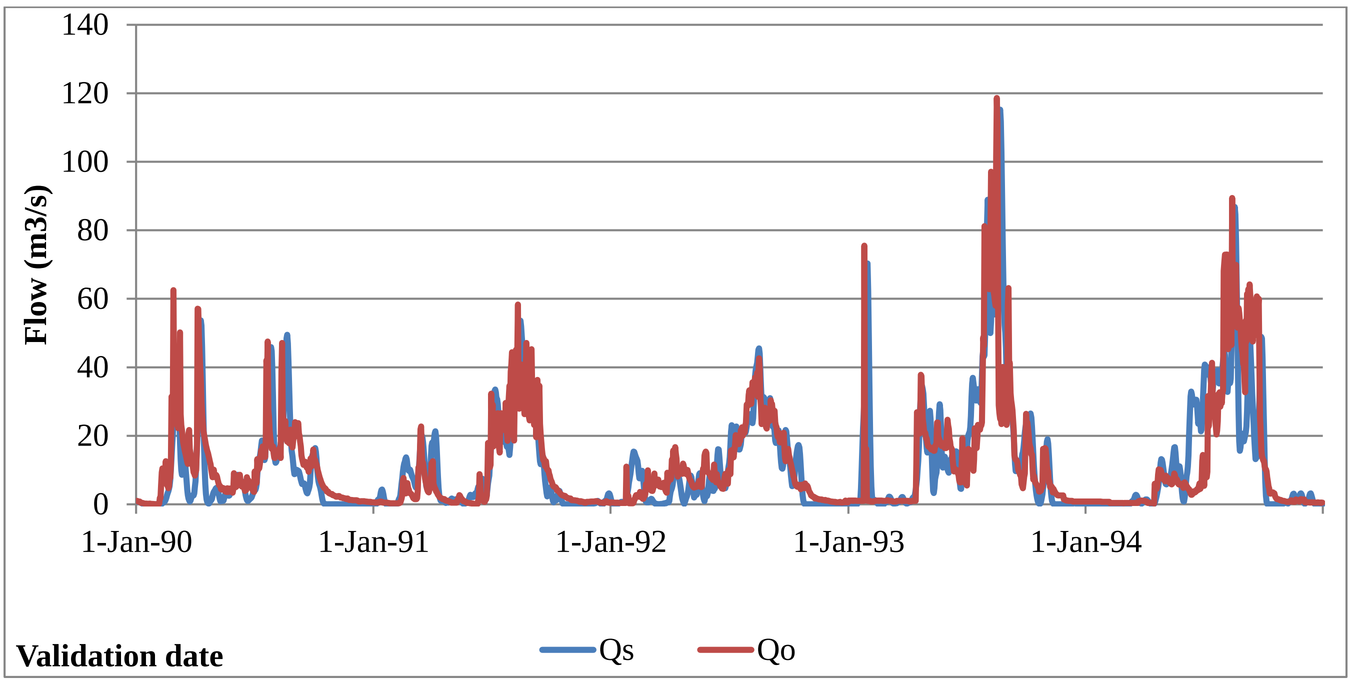

Figure 4-17: Validation of HEC-HMS model (01 Jan 1990 to 31 Dec 1994)

The manual and automatic calibration at the outlet of Meki river watershed shows that the model peak flow caches the observed peak flow both for calibration (before and after) and validation (before and after) respectively as shown in Figure D-3 and Figure D-4 of Appendix 4.

Calibration (NSE=76.25) and validation (NSE=62) results (Table 4.16) confirmed that the adequacy of the HEC-HMS model for rainfall-runoff simulation in Meki river watershed. This result agrees with the findings of Tassew et al., 2019; Tefera 2017; Mewded et al., 2021; and Yilma 2007 that ensured the applicability of the HEC-HMS model at various spatio-temporal scales in Ethiopia for various purposes such as water availability assessment. In general the HEC-HMS model performed well for stream flow estimation.

Table 4.16: Model performance measurements during runoff simulation

Performance parameters			1985-1989	1990-1994	Best range	Remark
Peak Flow (M3/S)	**Simulated**	**BOP**	173.5	236		
		AOP	116.4	139.7		
	Observed		118.6	139.6		
Total Volume (Million m3)	**Simulated**	**BOP**	3586.86	4046.90		
		AOP	2160.03	1584.27		
	Observed		1964.86	1581.08		
NSE (%)		**BOP**	-1.357	-5.172	>0.5	
		AOP	76.25	62	>0.5	Adequate
RMSE StdDev		**BOP**	1.5	2.5	<1	
		AOP	0.9	0.9	<1	Adequate
Percent Bias		**BOP**	9.37	156	±10	
		AOP	9.97	0.25	±10	Adequate
Time of Peak		**BOP**	18-Aug-87	18-Aug-93		
		AOP	20-Aug-87	22-Aug-93		
Time of Peak		**Observed**	17-Aug-87	15-Aug-93		
Objective Function			RMSE	RMSE		
BOP =	Before Optimization		**AOP =**	After Optimization		
NSE =	Nash-Satclife [11]		**RMSE=**	Root Mean Square Error		

In this study, the performance (NSE ratings), RMSE StdDev[12] and Percent Bias[13] (Bitew et al., 2019; and Mewded et al., 2021) were assigned for calibration and validation periods as shown in Table 4.16 and found adequate.

[11] very good for 0.75 < NSE ≤ 1.0; good for values 0.65 < NSE ≤ 0.75; satisfactory for 0.50 < NSE ≤ 0.65 and unsatisfactory for NSE ≤ 0.50 (Moriasi *et al*., 2007 and Mewded *et al*., 2021)
[12] RMSE StdDev best at ≤1 (Mewded *et al*., 2021)
[13] Percent Bias best at ±10% the positive values indicate model underestimation bias, and the negative values indicate model overestimation bias (Bitew *et al.*, 2019)

Estimation of long term monthly and annual average Stream flow at MRWS outlet

From the calibrated and validated stream flow of the HEC-HMS model results of MRWS outlet, the long term mean monthly and average annual stream flow of the catchment has been estimated as shown in Table 4.17 and Table 4.18 respectively.

Table 4.17: Long term Average monthly stream flow at MRWS outlet

Month	Calibration Period (1985-1989)		Validation period (1990-1994)	
	Long term Average of Calibrated flow (m3/s)	Long term Average of observed flow (m3/s)	Long term Average of Validated flow (m3/s)	Long term Average of observed flow (m3/s)
Jan	3.21	2.28	0.93	3.93
Feb	3.15	2.99	0.41	5.35
Mar	1.57	6.09	3.32	7.07
Apr	3.31	11.31	1.65	7.63
May	4.37	10.63	1.66	6.95
Jun	13.71	10.26	8.29	7.23
Jul	23.19	22.16	23.94	17.35
Aug	35.48	46.53	29.44	25.79
Sep	20.05	25.02	19.44	16.52
Oct	3.81	7.73	3.06	13.7
Nov	0.042	2.73	0.18	5.57
Dec	0.17	0.81	0.16	2.66

Graphically, the calibrated long term monthly peak flow resembles to the long term monthly observed flow as shown in Figure 4-18 but it under estimates the simulated flow although the performance parameter scores adequate. Similarly the validated long term monthly peak flow resembles to the long term monthly observed flow as shown in Figure 4-19 but it over estimates the simulated flow although the performance parameter scores adequate. The difference in the under estimation and over estimation attributed to the poor relationship between the observed flow with the precipitation in all gauging stations of the watershed as shown in Appendix 4.

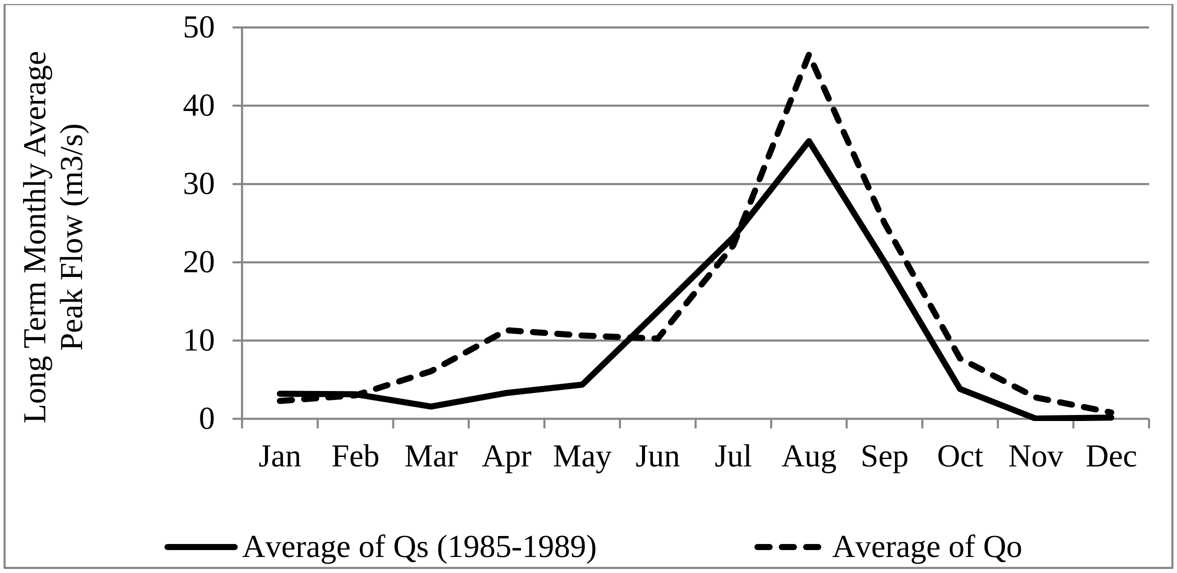

Figure 4-18: Long term monthly average peak flow for calibration period (1985-1989)

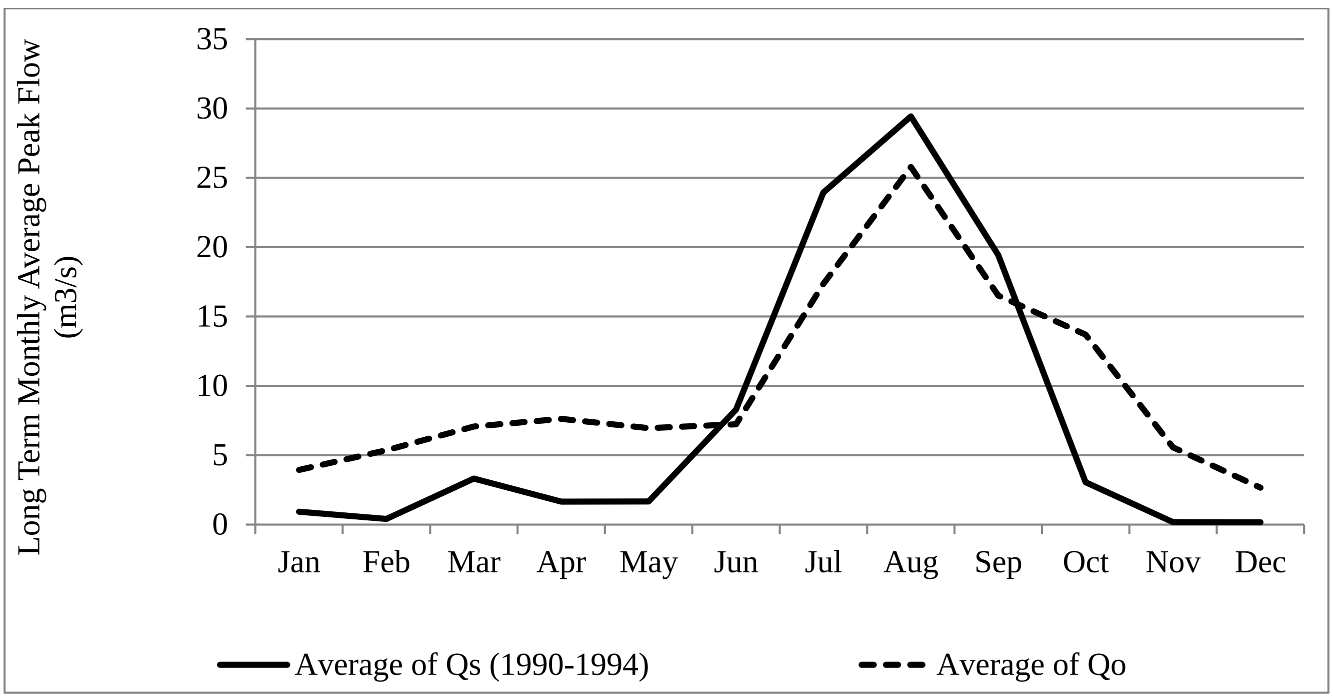

Figure 4-19: Long term monthly average peak flow for validation period (1990-1994)

The long term annual average stream flow for both calibration and validateion is presented in Table 4.18 that shows the under and over estimations respectively. Validated flow has shown a good long term annual average (LTAA) with the observed than the calibrated one.

Table 4.18: Long term Average Annual stream flow at Meki river watershed outlet

Year	Calibration Period (1985-1989)		Year	Validation period (1990-1994)	
	Average of Calibrated (m3/s)	Average of observed (m3/s)		Average of Validated (m3/s)	Average of observed (m3/s)
1985	5.015	10.48	**1990**	8.34	10.48
1986	6.50	8.59	**1991**	8.97	8.59
1987	11.57	14.26	**1992**	9.01	9.67
1988	10.42	14.23	**1993**	16.99	14.26
1989	13.42	14.69	**1994**	12.71	13.01
LTAA	9.38	12.45		11.20	11.20

4.5.3. Impact of EBLUS on magnitude of surface runoff

The performance of the model satisfies the modeling requirements of HEC-HMS (Table 4.16) despite the poor quality of observed flow at the gauging station (outlet) of MRWS (Alemu, et al., 2018). The long term monthly (Table 4.17) and the long term annual (Table 4.18) flow for both calibration and validation periods shows that there is a nearest value to the observed flow sothat we can consider the model for further analysis of the watershed. Accordingly, impact of EBLUS on magnitude of surface runoff was evaluated on the sub-watershed basis (Table 4.19).

Table 4.19: Calibrated annual surface runoff in different scenarios

SWS	Area (Km2)	1987				2017			
		EBLUS as a Cultivated LUS		EBLUS as a separate LUS		EBLUS as a Cultivated LUS		EBLUS as a separate LUS	
		P[14] (m^3/s)	V[15] (Mil m3)	P (m^3/s)	V (Mil m3)	P (m^3/s)	V (Mil m3)	P (m^3/s)	V (Mil m3)
W2510	54.6332	3.6	6.93	3.6	6.85	3.7	6.97	3.6	6.84
W2530	60.4529	3.9	7.26	3.5	6.52	3.9	7.35	3.5	6.52
W2610	48.3344	3.1	5.71	2.8	5.08	3	5.64	2.8	5.08
W2620	49.8624	3.3	6.42	3.3	6.23	3.3	6.42	3.3	6.24

[14] Peak flow
[15] Flow Volume

SWS	Area (Km2)	1987				2017			
		EBLUS as a Cultivated LUS		EBLUS as a separate LUS		EBLUS as a Cultivated LUS		EBLUS as a separate LUS	
		P[14] (m^3/s)	V[15] (Mil m3)	P (m^3/s)	V (Mil m3)	P (m^3/s)	V (Mil m3)	P (m^3/s)	V (Mil m3)
W2640	55.4568	4	7.71	4	7.68	4	7.705	4	7.68
W2750	35.1565	2.3	4.35	2.1	3.9	2.3	4.35	2.1	3.9
W2860	58.1634	4	7.66	3.8	7.32	4	7.66	3.8	7.3
W2890	28.0548	1.9	3.74	1.9	3.71	1.9	3.74	1.9	3.71
W2970	54.7446	3.9	7.63	3.9	7.62	3.9	7.63	3.9	7.61
W3080	61.8334	4.1	7.89	3.8	7.24	4.1	7.89	3.8	7.24
W3180	107.5441	7.8	15.19	7.8	15.19	7.8	15.19	7.8	15.19
W3190	89.6239	5.7	10.65	5.3	9.81	5.7	10.65	5.3	9.83
W3260	31.1576	2.3	4.52	2.3	4.52	2.3	4.52	2.3	4.52
W3280	70.0151	5.2	10.06	5.2	10.18	5.2	10.21	5.2	10.19
W3300	58.7668	3.6	6.7	3.4	6.2	3.7	6.86	3.4	6.2
W3400	82.4782	5.9	11.42	5.9	11.48	5.9	11.48	5.9	11.48
W3410	54.6073	3.8	7.4	4	7.67	4	7.79	4	7.67
W3460	46.2753	3.3	6.43	2.8	5.39	3.3	6.39	3.1	6.04
W3690	66.2208	4.2	7.92	4	7.41	4.3	8.1	4	7.41
W3700	27.2959	2	3.99	2	3.86	2.1	4.03	2	3.84
W3730	43.9288	3.4	6.71	3.4	6.72	3.4	6.72	3.4	6.72
W3790	68.7512	5.3	10.31	5.2	10.2	5.3	10.35	5.2	10.2
W3910	106.0911	7.1	13.43	6.6	12.31	7.1	13.46	6.6	12.31
W4030	41.9423	2.8	5.35	2.6	4.94	2.9	5.43	2.6	4.94
W4070	66.125	5	9.75	5	9.73	5	9.73	5	9.73
W4130	65.7365	5	9.85	5	9.8	5	9.8	5	9.8
W4180	80.704	5.8	11.04	5.4	10.3	5.7	11.01	5.4	10.27
W4250	46.3686	3.5	6.82	3.5	6.82	3.5	6.82	3.5	6.82
W4290	95.7803	7	13.5	6.6	12.62	7	13.43	6.6	12.62

SWS	Area (Km2)	1987				2017			
		EBLUS as a Cultivated LUS		**EBLUS as a separate LUS**		**EBLUS as a Cultivated LUS**		**EBLUS as a separate LUS**	
		P[14] (m^3/s)	**V[15] (Mil m3)**	**P (m^3/s)**	**V (Mil m3)**	**P (m^3/s)**	**V (Mil m3)**	**P (m^3/s)**	**V (Mil m3)**
W4400	80.4865	6.2	12.09	6.1	11.9	6.2	12.07	6.1	11.91
W4590	18.68236	1.5	2.94	1.4	2.78	1.5	2.89	1.5	2.88
W4620	74.9025	5.7	11.2	5.6	10.89	5.7	11.24	5.6	11.02
W4720	93.856	7.1	13.98	7.1	13.92	7.1	13.99	7.1	13.9
W4730	86.358	6.4	12.47	6.3	12.34	6.5	12.75	6.3	12.35
Average		4.403	8.5	4.271	7.98	4.421	8.54	4.282	8.23

The contributions of EBLUS on magnitude of surface runoff was determined after analyzing the four scenarios and the impacts of EBLUS on the generation of surface runoff in the watershed for the period 1987–2017 were calculated based on Table 4.19. Peak flow (m3/s) and flow volume (mm) for the four scenarios (EBLUS as a Cultivated LUS and EBLUS as a separate LUS in 1987 and 2017) was analysed as impact matrix using MS-Excel and the analysis result is shown in Table 4.20.

Table 4.20: Impact Matrix for EBLUS on magnitude of surface runoff

	Scenarios	Simulated annual Average runoff (Qi) (mm)	Change [16] (2017-1987) (mm)	Impact of EBLUS
1987	**WEBLUS[17]**	Q1 = 132.193	Q3 – Q1 = 0.4856	
	WOEBLUS[18]	Q2 = 137.032	Q4 – Q2 = 0.5494	**0.064mm**
2017	**WEBLUS**	Q3 = 132.679		
	WOEBLUS	Q4 = 137.582	((Q4–Q2)–(Q3–Q1))/ (Q4-Q2) =	**11.62%**

[16] Changes in a scenario relative to the other scenarios
[17] With EBLUS (Considering EBLUS as a separate LUS)
[18] Without EBLUS (Considering EBLUS as a Cultivated LUS)

The average of simulated runoff volume (mm) was used to get the statistical contribution of EBLUS relative to other land use systems. There was an increase in the average surface runoff by 0.5494mm (Q4-Q2) resulted from the effects of LULC changes (WOEBLUS) while considering expansion of cultivated land rather than EBLUS and also there was an increase in the average surface runoff by 0.4856mm (Q3-Q1) was attributed to the expansion of EBLUS (WEBLUS).

The contribution of EBLUS was evaluated as 0.064mm ((Q4-Q2)-(Q3-Q1)) relative to cultivated LUS and based on the formula ((Q4-Q2)-(Q3-Q1))/ (Q4-Q2) in Mewded *et al.*, 2021 and 11.62% of an increase was arrested due to EBLUS (Table 4.20). Therefore, the result showed EBLUS has an implication to increase infiltration rate of the soil and reducing the magnitude of surface runoff unlike cultivated land use system.

According to Mewded *et al.*, 2021; Elias *et al.*, 2019 and Dinka *et al.*, 2019, expansion of cultivated land use system increases surface runoff by decreasing infiltration, disturbing the soil structure and reducing surface roughness, eventually increasing surface runoff. Decrease in plantation decreases the canopy cover causing reduced interception, loss of permeability (due to exposure of soil particles to raindrop impacts), and decreased surface roughness that reduces interception and infiltration to increase surface runoff (Mewded *et al.,* 2021; Elias *et al.,* 2019 and Dinka *et al.*, 2019). Simiarly, the result shows that the increase in enset cover also improves the infiltration capacity of the soil and decrease in the surface runoff.

The simulated data was extracted for upper, middle and lower zone of the watershed and the mean values of each zone recorded as shown in Figure 4-20. The lower sub-watersheds shows very high generation capacity despite the topography was suitable for high infiltration rate while the upper sub-watersheds where most of EBLUS found showed the lowest response for runoff generation against the topographical steepness of the area that indicated contribution of EBLUS was high in MRWS despite the area coverage of EBLUS was very low (only 10%).

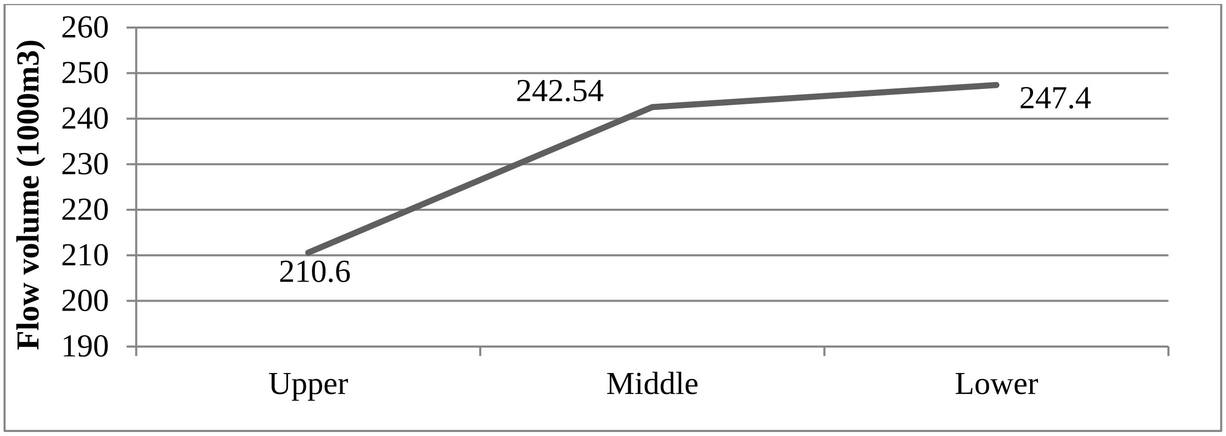

Figure 4-20: Zonal mean flow of Meki river watershed

Base flow in Meki river watershed is insignificant (alpha > 0.5) in almost all sub-watersheds (Cunderlik and Simonovik, 2004 and Jeevika and Jagritee, 2018). Since the contribution of base flow to the recession limb of the hydrograph in Meki river watershed is insignificant (alpha > 0.5), the contribution of EBLUS couldnot be detected at this level of study.

4.5.4. Impact of EBLUS on water resources and watershed management

The increase in EBLUS area coverage by11.2% while the transition to the other LUS is not significant in the Meki river watershed enables EBLUS to play a significant role in the stability and resilience of the water resources system in the watershed.

The lowest soil loss (22.65t ha-1yr-1) in 2017 recorded in EBLUS and it reduced the sediment load from the watershed by 0.0347t ha-1or 93.048% as compared to the change on other LUSs. Therefore, EBLUS shows a relevant implication to save soil from water erosion by reducing the truction power of the rain drop and it contributes in the protection of water bodies (Lake Ziway) from sedimentation problem (Mewded *et al.*, 2021; Elias *et al.*, 2019 and Dinka *et al.*, 2019).

According to Elias et al., 2019, plantation increases infiltration capacity of the soil and the same result was found in this research that the higher mean infiltration rate was observed in EBLUS, it improved the average CN of the whole watershed and reduced the magnitude of surface runoff by 11.62% that improves the water availability in the watershed. Therefore, EBLUS has a huge role in water resources and watershed management.

5. Conclusion and Recommendation

5.1. Conclusions

Meki river watershed (MRWS) is dominantly covered by cultivated LUS (41.5%) and followed by Bush and Khat LUSs (25.6%). EBLUS, Forest and plantations LUSs, bare/ built up LUSs and water bodies including wetland comprised of 10.65%, 14.14%, 7.4% and 0.75% of the watershed respectively. The upper part of MRWS is covered by Erica, Enset and natural forest LUSs, while the middle and lower altitudes of the watershed is dominantly covered by culivated LUSs.

The EBLUS is characterized as a sustainable LUS, but it is subjected to change. The expansion of open-field food crops (Teff, Wheat, maize, pepper, potato, etc) and of monocultural cash crops (khat) causes not only a gradual loss of species diversity and tree biomass, but also a decrease in the perennial crops and native tree species. EBLUS is considered to play a significant role in the stability and resilience of the system. It is dominantly practiced on the upper zone of MRWS that shows an increase in area coverage (11.2%) over the last 30 years.

GIS based RUSLE is used to model soil loss in MRWS. 82.35% and 94.12% of the sub-watersheds are experiencing high to very severe soil erosion risks beyond the tolerable soil loss level of 18 t ha-1yr-1 and 10 t ha-1yr-1 respectively which threatens crop production and productivity of the land impacting local farmers' food security.

The lowest soil loss from EBLUS (22.65t ha-1yr-1) is recorded in 2017 even lower than forest LUS (25.94 t ha-1yr-1). Soil loss in Enset growing zone (30.5 t ha-1yr-1) are less than that of the non-Enset growing zones of the watershed (31.905 t ha-1yr-1) despite the steep slopes of the Enset growing zone which can arrest 296,509.9 tons of soil every year from marching down to Lake Ziway and contributes for the sustainability and life of water bodies.

EBLUS has a significant implication to reduce the sediment load generated from the watershed by 0.0347tonnes/ha or 93.048% as compared to other land use systems. The sediment yield in the NEGZ is higher than the EGZ of the watershed. It can also be used as a basic input data for further hydrological investigation for adjacent ungauged catchments by transferring the required calibrated parameters through regionalization or other techniques.

Although statistically not significant, the Upper (enset growing) zone of the watershed has higher mean infiltration rate (11.0125mmhr-1) than the Middle (non-enset growing) zone (10.92625mmhr-1) of the watershed. The high mean infiltration rate at the upper zone showed the presence of more forest LUS and EBLUS than the middle zone of the watershed which enhanced infiltration and water holding capacity of the soil.

EBLUS improved the average CN from 81.72 to 78.21 for the whole watershed and a significant volume of water is expected to infiltrate due to the presence of EBLUS. The CN grid was developed for MRWS which can be used as an input for different modeling research purposes concerning surface runoff generation capacity of the area. In order to increase the performance of models in simulating the runoff, it is better to develop the local and regional curve number of the catchment instead of using the tabulated standardized CN values and to identify regional valid unit hydrographs.

The sensitivity result shows that the SCS runoff curve number (CN2), Recession Constant, Muskingham K, Initial Discharge, Initial Abstraction, Lag Time and Muskingham X were found to be sensitive parameters for simulated volume and peak flow during the calibration period (1991) in their order of sensitivity for MRWS. Calibration (NSE=75.9%, RMSE StdDev=0.5, Percent Bias =6.69, and R square=97%) and validation (NSE=62%, RMSE StdDev=0.5, Percent Bias =-1.31, and R square=97%) results confirmed that the adequacy of the HEC-HMS model for rainfall-runoff simulation despite the poor quality of observed flow at the outlet of MRWS.

11.62% (0.064mm) of surface runoff was infiltrated due to EBLUS. Regarding the zonal distribution of surface runoff flow volume, the lower sub-watersheds have very high surface runoff generation capacity (Mean = 247.4mm) despite the topography was suitable for high infiltration rate while the upper sub-watersheds showed the lowest response for surface runoff generation against the topographical steepness of the area (Mean = 210.6mm). The middle zone of the watershed showed moderate runoff (Mean = 242.54mm) that indicates the contribution of EBLUS is high in MRWS despite the area coverage of EBLUS was very low (only 10%). The contribution of base flow to the recession limb of the hydrograph in MRWS is insignificant (alpha > 0.5), the contribution of EBLUS could not be detected at this level of study.

Generally, the result showed that EBLUS has a significant implication to decrease the truction power of rainfall, increasing the canopy cover of the watershed, reduce the soil loss, increase infiltration rate of the soil, reduce the magnitude of surface runoff and reduce the sediment load that in turn contribute in the sustainability of Lake Ziway and ensure water availability in the watershed. Therefore, EBLUS can contribute to: Ground water recharge, Ecological sustainability (Lake Ziway), Water resources conservation and ensure water availability in the watershed and Watershed management in Meki river watershed.

5.2. Recommendation

In the Short term (<2years): Initiate the extension program to the expansive production and processing of EBLUS which can help the production of sufficient inputs to the industries to be established in the area, Integration of new crops into the existing multi-storey system of EBLUS and increase area coverage of EBLUS.

In the Medium term (2-5years): Prepare separate land use policy to EBLUS and incorporating other fruit as an agro-forestry to it will create harmony to the existing ecology, start watershed management based on priority and additional study of adaptability range, Climate change impact, industrial implication and others.

In the Long term (>5years): Watershed management (Soil and water conservation activities) in the upper watersheds in addition to expanding EBLUS and expanding EBLUS to the drought prone part of our country.

Generally, the presence of EBLUS brought several ecological and hydrological benefits as it is discussed and hence, expanding it requires a policy change and awareness creation to the community for the market based production of shade loving agroforestry trees like coffee and cassava under the Enset cultivation and decision makers should intervene in enhancement of EBLUS. Therefore, crafting separate land use policy considering such a multipurpose agroforestry system and incorporating fruit production to the system is mandatory and also creating conducive environment to the extension program that the upper part of the watershed can produce sufficient inputs or raw material to the industries to be established in the watershed.

Reference

Abebe, T., Wiersum, K.F. and Bongers, F. (2010). Spatial and temporal variation in crop diversity in agroforestry homegardens of Southern Ethiopia. Agroforestry Systems 78: 309-322.

Abebe, T., Wiersum, K.F., Bongers, F. and Sterck, F. (2006). Diversity and dynamics in homegardens of Southern Ethiopia. In: Kumar B.M. and Nair P.K.R. (eds.) Tropical homegardens: a time-tested example of sustainable agroforestry. Springer Science, Dordrecht, the Netherlands, pp. 87-103.

Abraham LZ. (2006). Climate change impact on Lake Ziway watershed availability Ethiopia. MSc Thesis. University of Applied Sciences Cologne.

Addis, HK & Klik, A (2015). 'Predicting the spatial distribution of soil erodibility factor using USLE nomograph in an agricultural watershed, Ethiopia', International Soil and Water Conservation Research, vol. 3, no. 4, pp. 282-90.

Admasu Tsegaye and Struik P.C., (2003). Growth, radiation use efficiency and yield potential of enset (Ensete ventricosum) at different sites in southern Ethiopia. Ann. appl. Biol., 142, 71-81.

Admasu, T. (2007). Effect of repetitive transplanting & leafe pruning on growth and dry matter partitioning of Enset. Agronomy, 6(1), 45-52.

Alemu Beyene, Sebsebe Demisew, Mekuria Argaw, Azage Gebreyohannes (2020). Enset-Based land use land cover change detection and its impact on soil erosion in Meki river watershed, Lake Ziway Sub-Basin, Central Rift Valley of Ethiopia, International Journal of Environmental Systems Research / *Environ Syst Res* **9,** 37. https://doi.org/10.1186/s40068-020-00198-x.

Alemu Beyene, Sebsebe Demisew, Mekuria Argaw, Azage Gebreyohannes (2022). Effects of enset-based land use system on infiltration rate and curve number of the soil in Meki river watershed, Lake Ziway Sub-Basin, Central Rift Valley of Ethiopia. International Journal of Sustainable Water Resources Management, Springer. https://doi.org/10.1007/s40899-022-00667-4.

Alemu O. Aga, Bayou Chane and Assefa M. Melesse (2018). Soil Erosion Modelling and Risk Assessment in Data Scarce Rift Valley Lake Regions, Ethiopia, Water 2018, 10, 1684; doi:10.3390/w10111684 www.mdpi.com/journal/water

Aman Bunta and Brook Abate (2021). Runoff and Sediment Yield Modeling of Meki River Watershed Using SWAT Model in Rift Valley Lakes Basin, Ethiopia, American Journal of Civil Engineering. Vol. 9, No. 5, 2021, pp. 155-166. doi: 10.11648/j.ajce.20210905.12.

Ambachew Zerfu, Gebre, S., Berecha, G., *(*2018). Assessment of spatial distribution of enset plant diversity and enset bacteria wilt using geostatistical techniques in Yem special district, Southern Ethiopia. *Environ Syst Res* **7,** 23. https://doi.org/10.1186/s40068-018-0126-9.

Ambika K., (2012). Studying the impact of different land use changes in the hydrological cycle of a watershed. Tropical resource institute, yale school of forestry and environmental studies, Jiangxi province, China.

Anderson, J., Hardy, E., Roach, J., Witmer, R., (1976). A Land-Use and Land-Cover Classification System for use with Remote Sensor Data. US Geological Survey Professional Paper 964, Washington, DC.

Andrew A, Millward E, Mersey J. (1999). Adapting the RUSLE to model soil erosion potential in a mountainous tropical watershed. Catena. 38:109–129.

Angima SD, Stott DE, O'Neill MK, Ong CK, Weesies GA. (2003). Soil erosion prediction using RUSLE for central Kenyan highland conditions. Agric Ecosyst Environ. 97:1029–1049.

Anita S., Haile B., Tesfaye S., Abebe Y., Amaldegn A. and Tabogie E. (1996). Enset Farming Systems in Southern Region, Ethiopia. Report on a Rapid Rural Appraisal in Gurage, Hadiya and Sidama Zones, University of Florida. Deutsche Gesellschaft for Technische Zusammenarbeit (GTZ), 83.

Antonio Paz González, Cleide Aparecida de Abreu, Ana Maria Tarquis, and Eduardo Medina-Roldán (2014). Impacts of Land Use Changes on Soil Properties and Processes. The Scientific World Journal Volume 2014, Article ID 831975, http://dx.doi.org/10.1155/2014/831975.

Argaw M, Teketay D, Olsson M., (1999). Soil seed flora, germination and regeneration pattern of woody species in Acacia woodland of the Rift Valley in Ethiopia. Journal of Arid Environments 43: 411–414.

Asnake Yimam Yesuph and Amare Bantider Dagnew (2019). Soil erosion mapping and severity analysis based on RUSLE model and local perception in the Beshillo Catchment of the Blue Nile Basin, Ethiopia. Environmental Systems Research, 8 (17).

Ataollah Kavian, Samaneh Hoseinpoor Sabet, Karim Solaimani & Behnoosh Jafari (2017) Simulating the effects of land use changes on soil erosion using RUSLE model, Geocarto International, 32:1, 97-111, DOI: 10.1080/10106049.2015.1130083

Ayalew D, Dercon S, Gautam M. (2005). Property rights in a very poor country: tenure insecurity and investment in Ethiopia. WPS-021: Global Poverty Research Group (GPRG).

Ayenew T. (2004). Environmental implications of changes in the levels of lakes in the Ethiopian Rift Since 1970. Regional Environmental Change 4: 12–204.

Azene Bekele, Ann Birnie and Bo Tenqnas (1993). Useful trees and shrubs for ETHIOPIA. Identification, Propagation and Management for Agricultural and Pastoral Communities, Regional Soil Conservation Unit/SIDA Technical Handbook No.5.

Baker RED, Simmonds NW (1953). The genus Ensete in Africa. Kew Bulletin 8: 405–416.

Banasik, K & Walling, D (1996). 'Predicting sedimentgraphs for a small agricultural catchment', Hydrology Research, vol. 27, no. 4, pp. 275-94.

Barbora, B., & Jaroslava, B. (2014). Effect of various compost doses on the soil infiltration capacity.

Bekalu, M., Feleke, D., (1996). Ethiopian Village Studies: Imdibir Haya Gasha, Gurage. Addis Ababa University and Oxford University, Addis Ababa and Oxford.

Bekele M. (2003). Forest property rights, the role of the state, and institutional exigency: the Ethiopian experience. PhD Thesis. Department of Rural Development Studies, Swedish University of Agricultural Sciences, Uppsala.

Benneh, G., Morgan, W. B., and Uitto, J. I. (1996). Sustaining the Future, Economic, Social, and Environmental Change in Sub-Saharan Africa, United Nations University Press, Tokyo, Japan.

Bennett, JP 1974, 'Concepts of mathematical modeling of sediment yield', Water resources research, vol. 10, no. 3, pp. 485-92.

Beven, K.J. and Binley, A., (1992). The Future of Distributed Models: Model Calibration and Uncertainty Prediction. Hydrological Processes, 6: 279-298.

Beven, K.J., (2001). Rainfall-Runoff Modelling: The Primer. Wiley, New York.

Bewket W. and Teferi E. (2009). Assessment of Soil Erosion Hazard and Prioritization for Treatment At The Watershed Level: Case Study in the Chemoga Watershed, Blue Nile Basin, Ethiopia, LAND DEGRADATION & DEVELOPMENT, Wiley InterScience (www.interscience.wiley.com) DOI: 10.1002/ldr.944, John Wiley & Sons, Ltd.

Bicknell, B.R., J.C. Imhoff, J.L. Kittle, A.S. Donigian, and R.C. Johanson. (2001). Hydrologic simulation program-FORTRAN. User‘s manual, v.11, Athens, GA., USEPA.

Bill Sharfenberg, M. B. (2018). Hydrologic Modeling System HEC-HMS user’s manual US Army corps of Engineers, USA.

Birkhead, A.; James, C. (2002). Muskingum river routing with dynamic bank storage. J. Hydrol., 264, 113–132.

Birmeta G, Nybom H, Bekele E (2002). RAPD analysis of genetic diversity among clones of the Ethiopian crop plant Ensete ventricosum. Euphytica 124: 315 – 325.

Bitew G. Tassew, Mulugeta A. Belete and K. Miegel (2019). Application of HEC-HMS Model for Flow Simulation in the Lake Tana Basin: The Case of Gilgel Abay Catchment, Upper Blue Nile Basin, Ethiopia. Journa of Hydrology; doi:10.3390/hydrology601002. www.mdpi.com/journal/hydrology

Blanco, H & Lal, R (2008). Principles of soil conservation and management, vol. 167169, Springer New York.

Borah, D.K. and Bera, M. (2004). Watershed scale hydrologic and nonpoint source pollution models: review of applications. Transactions of the ASAE. Vol. 47(3): 789−803

Borrell J.S., Mark Goodwin, Guy Blomme, Kim Jacobsen, Abebe M. Wendawek, Dawd Gashu, Ermias Lulekal, Zemede Asfaw, Sebsebe Demissew and Paul Wilkin (2020). Enset-based agricultural systems in Ethiopia: A systematic review of production trends, agronomy, processing and the wider food security applications of a neglected banana relative. Plants, People, Planet. 2020;00:1–17. https ://doi.org/10.1002/ppp3.10084.

Brandt SA, Spring A, Hiebsch C, et al (1997). The “Tree Against Hunger”: enset-based agricultural system in Ethiopia. Washington, DC: American Association for the Advancement of Science.

Brevik EC (2013). The potential impact of climate change on soil properties and processes and corresponding influence on food security. Agriculture 3(3):398–417.

BRIDGE, W. P. (1992). The lesion nematode pratylenchus goodeyi, an important pest of Ensete in Ethiopia. Tropical pest management, 38(3), 325-326.

Burch, G., Bath, R., Moore, I., & O’Loughlin, E. (1987). A comparative hydrological behavior of forested and cleared catchments in south eastern Australia. Journal of Hydrology, 90, 19-42.

Castro Filho, C., Lourenco, A., Guimaraes, M. D. F. and Fonseca, I. C. B. (2002). Aggregate Stability under Different Soil Management Systems in a Red Latosol in the State of Parana, Brazil. Soil Tillage Res.,65: 45–51.

Charles Hernick, Arianne Neigh, Amare Worku, Fikadu Getachew, Kathleen Hurley, Emily Wasley (2016). Tropical Forest and Biodiversity (FAA 118/119) Assessment, USAID Ethiopia, the Cadmus Group, Inc. www.cadmusgroup.com.

Chen, C. R., Condron, L. M., Davis, M. R.and Sherlock, R. R. (2000). Effects of Afforestation on Phosphorus and Biological Properties in a New Zealand Grassland Soil.Plant Soil, 220: 151–163.

Chow, V. T., R.Maidment, D., & Mays, L. W. (1988). APPLIED HYDROLOGY. New York St. Louis San Francisco Auckland Bogota Caracas Lisbon London Madrid Mexico City Milan Montreal New Delhi San Juan Singapore Sydney Tokyo Toronto: McGraw-Hill, Inc.

Chu, X.; Steinman, A. (2009). Event and continuous hydrologic modeling with HEC-HMS. J. Irrig. Drain. E-Asce., 135, 119–124.

Coleman, B. (2014). Effects of changes to rainfall estimates due to climate change on runoff.

Congalton RG, Green K (1999). Assessing the accuracy of remote sensed data. Remote Sens Environ 37:35–46

Crowe AS, Schwartz FW (1985). Application of a lake-watershed model for the determination of water balance. J Hydrol 81:1–26

Cunderlik, J.M. and Simonovik, S.P. (2004). Assessment of Water Resources Risk and Vulnerability to Changing Climate Conditions. Available at: http://www.eng.uwo.ca/research/iclr/fids/publications/cfcas-climate/reports/report%20IV.pdf.

DeFries, R., Eshleman, K.N., (2004). Land-use change and hydrologic processes: a major focus for the future. Hydrol. Proc. 18, 2183–2186.

Deng, L., Zhu, G., Tang, Z., Shangguan, Z. (2016). Global patterns of the effects of land-use changes on soil carbon stocks. Glob. Ecol. Conserv. 5:127–138. https://doi.org/10.1016/J.GECCO.2015.12.004.

Derege Tsegaye Meshesha, A. Tsunekawa and M. Tsubo (2012). Continuing Land Degradation: Cause–Effect in Ethiopia's Central Rift Valley, Land Degrad. Develop. 23: 130–143 (2012). DOI: 10.1002/ldr.1061

Dinka MO, Klik A (2019) Effect of land use-land cover change on the regimes of surface runoff- The case of lake Basaka catchment (Ethiopia). Environ Monit Assess 191:278

Elfert , S., & Bormann, H. (2010). Simulated impact of past and possible future land use changes on the hydrological response of the Northern German lowland 'Hunte' catchment. J.HYDROL, 383, 245– 255.

Elias E, Seifu W, Tesfaye B, Girmay W (2019) Impact of land use/ cover changes on lake ecosystem of ethiopia central rift valley. Cogent Food Agric 5:1–20

Elias, A. A. (2011). Soil Nutrient Evaluation under Different Land Use Types in the Smallholder Farming Systems of Jimma Zone, Ethiopia. International Journal of Agricultural Research, 6(9), 707-713.

Elizabeth M.Show. (1994). Hydrology in practice 3rd edition.

Engdasew Feleke, Engdawork Assefa, Tesfaye Zeleke and Alemu Beyene (2020). Characterization Of Salt Affected Soils and Identification of Salinity Sources in Irrigated Soils: The Case of Small Scale Irrigation Schemes in Adami Tulu Jido Kombolcha and Ziway Dugda Districts in the Central Rift Valley of Ethiopia. Ethiop. J. Biol. Sci. 19(1): 81–102, 2020. ISSN: 1819-8678. The Biological Society of Ethiopia.

ENMA (2017). Ethiopian National Meteorology Agency data analysis, Addis Ababa, Ethiopia

Ermias Teferi, Woldeamlak Bewket, S.Uhlenbrooka, J.Wenninger (2013). Understanding recent land use and land cover dynamics in the source region of the Upper Blue Nile, Ethiopia: Spatially explicit statistical modeling of systematic transitions, Agriculture, Ecosystems and Environment 165 98– 117 journal home page: www.elsevier.com/locate/agee

Ethiopian Minister of Water and Energy (2013). Strategic agenda for adaptation to urban water-mediated impacts of climate change in Addis Ababa, Federal Democratic Republic of Ethiopia.

Ethiopian Road Authority (ERA) (2013). Drainage Design Manual, Addis Ababa, Ethiopia.

Fan, J. and Gijbels, I. (1996). Local Polynomial Modelling and Its Applications, Chapman & Hall. London.

FAO (2006). Guidelines for soil description, FAO, Rome

FAO, (2007). State of the world's forests. http://www.fao.org/docrep/009/a0773e/a0773e00.HTM Accessed on15 Dec 2009.

FAO, CAS, IIASA, JRC & ISRIC. (2003). The Harmonized World Soil Database (HWSD) Viewer.

Feddema, J., Oleson, K., Bonan, G., Mearns, L., Buja, L., Meehl, G., et al. (2005). The importance of land-cover change in simulating future climates. SCIENCE, 310(5754), 1674-1678.

Feldman, A. (2000). Hydrologic Modeling System HEC-HMS Technical Reference Manual, USArmy corps of Engineers, USA.

Fetta Negash (2019). Diversity and indigenous management of enset (ensetventricosum (welw.) cheesman) landraces in Gurage, southern Ethiopia.

Fleming, & Brauer (2016). Hydrologic Modeling System HEC-HMS Quick Start Guide, US Army Corps of Engineers, Institute of Water Resources, Hydrologic Engineering Center, 609 Second Street, Davis CA 95616-4687.

Foody GM (2002). Status of land cover classification accuracy assessment. Remote Sens Environ 80:185–201

García-Ruiz, JM (2010). 'The effects of land uses on soil erosion in Spain: a review', Catena, vol. 81, no. 1, pp. 1-11.

Gardner, W. R. (1958). Some steady-state solutions of unsaturated moisture flow equations with application to evaporation from a water table. IN: Soil Science 85: 228-232. 51.

Garedew E., Mats S., Ulf S., Bruce M., (2009). Land-use and land-cover dynamics in the central Rift Valley of Ethiopia. Environmental Management 44: 683–694.

Gebrejewergs Aredehey, Atinkut Mezgebu & Atkilt Girma | (2020) The effectsof land use land cover change on hydrological flow in Giba catchment, Tigray, Ethiopia, Cogent Environmental Science, 6:1, 1785780, DOI: 10.1080/23311843.2020.1785780

Ghaffari, G., Keesstra, S., Ghodousi, J., & Ahmadi, H. (2010). SWAT-simulated hydrological impact of land-use change in the Zanjanrood Basin, Northwest Iran. HYDROL PROCESS, 24(7), 892-903.

Godfray, H.C.J., Beddington, J.R., Crute, I.R., Haddad, L., Lawrence, D., Muir, J.F., Pretty, J., Robinson, S., Thomas, S.M. and Toulmin, C. (2010). Food security: the challenge of feeding 9 billion people. Science 327: 812-818.

Gupta, H.V., Kling, H., Yilmaz, K.K., and Martinez, G.F. (2009). Decomposition of the mean squared error and NSE performance criteria: Implications for improving hydrological modelling. J. Hydrol. 2009, 377, 80–91.

Habtamu Atoma, K.V.Suryabhagavan, M.Balakrishnan (2020). Soil erosion assessment using RUSLE model and GIS in Huluka watershed, Central Ethiopia, Sustainable Water Resources Management (2020) 6:12 https://doi.org/10.1007/s40899-020-00365-z, Springer Nature Switzerland

Hajigholizadeh, M, Melesse, AM & Fuentes, HR (2018). 'Erosion and sediment transport modelling in shallow waters: A review on approaches, models and applications', International journal of environmental research and public health, vol. 15, no. 3, p. 518.

Halwatura, D & Najim, M (2013). 'Application of the HEC-HMS model for runoff simulation in a tropical catchment', Environmental modelling & software, vol. 46, pp. 155-62.

Hamby, D. (1994). A review of techniques for parameter sensitivity analysis of environmental models. Environ. Monit. Assess. 1994, 32, 135–154.

Hawkins, R.H. (1993). Asymptotic determination of runoff curve numbers from data. J. Irrig. Drain. Eng., 119, 334–345.

Herweg, K., and Ludi, E., (1999). The performance of selected soil and water conservation measures: Case studies from Ethiopia and Eritrea.

Hickey, R (2000). 'Slope angle and slope length solutions for GIS', Cartography, vol. 29, no. 1, pp. 1-8.

Hoerl, A.E. and Kennard, R.W. (1970). Ridge regression: biased estimation for nonorthogonal problems, Technometrics, 12, 55-67.

Holden, E. and Linnerud, K. (2007). The sustainable development area: Satisfying basic needs and safeguarding ecological sustainability. Sustainable Development 15: 174-187.

Hoogerbrugge, I.D. and Fresco, L.O. (1993). Homegarden systems: agricultural characteristics and challenges. Gatekeeper Series No. 39. International Institute for Environment and Development, London, UK.

Houghton J.T., (1995). Climatic Change 1994: Radiative forcing of climatic change and an evaluation of IPCC IS92 Emission Scenarios. Intergovernmental panel on climate change. Cambridge University press, Cambridge, UK.

Hurni, H. (1993). Land Degradation, famine and resource scenarios in Ethiopia. In World Soil Erosion and Conservation, ed. D. Pimentel. Cambridge University press, Cambridge.

Hurni, H., (1985). Soil conservation manual for Ethiopia. Ministry of agriculture, Addis Ababa

Hurni, H., (1986). Degradation & conservation of the soil resources in the Ethiopian highlands

Ibeje A.O., J. a. (2018). Impact of land use on infiltration. World journal of Engineering Research and Technology, 4 (6), 95 -102.

Iliasse Khaddor and AdilHafidiAlaoui (2014). Production of a Curve Number map for Hydrological simulation - Case study: Kalaya Watershed located in Northern Morocco. International Journal of Innovation and Applied Studies. ISSN 2028-9324 Vol. 9 No. 4 Dec. 2014, pp. 1691-1699 © 2014 Innovative Space of Scientific Research Journals http://www.ijias.issr-journals.org/

ITT Industries, Inc. (2006). Environmental Visual Images, 4990 Pearl East Circle Boulder, CO 80301, USA. 3307869900, envi@RSInc.com, http://www.RSInc.com/envi.

Jackson, R., & Lijalem, Z. (2007). Calibration and Validation of SWAT Hydrological model for Meki river watershed.

James Harrison 1, K. A. (2014). A Draft Genome Sequence for Ensete ventricosum, the Drought-Tolerant “Tree Against Hunger”. Agronomy, 4, 13-33.

James K. Searcy and Clayton H. Hardison (1960). Double-Mass Curves, Manual of Hydrology: Part 1: General Surface-Water Techniques, Methods and practices of the Geological Survey.

James S Borrell, Manosh K Biswas, Mark Goodwin, Guy Blomme, Trude Schwarzacher, J S (Pat) Heslop-Harrison, Abebe M Wendawek, Admas Berhanu, Simon Kallow, Steven Janssens, Ermias L Molla, Aaron P Davis, Feleke Woldeyes, Kathy Willis, Sebsebe Demissew, Paul Wilkin (2019). Enset in Ethiopia: a poorly characterized but resilient starch staple. Annals of Botany, Volume 123, Issue 5, 11 April 2019, Pages 747–766, https://doi.org/10.1093/aob/mcy214

Jang Pak, Kervi Ramos, Matthew Fleming, William Scharffenberg, and Stanford Gibson (2015). Sensitivity Analysis for Sediment Transport In The Hydrologic Modeling System (HEC-HMS)

Jansen H, Hengsdijk H, Legesse D, Ayenew T, Hellegers P, Spliethoff P., (2007). Land and water resource assessment in the Ethiopia central rift valley. Alterra-rapport 1587, Alterra, Wageningen.

Jeevika Khadka and Jagritee Bhaukajee (2018). Rainfall-Runoff Simulation and Modelling Using HEC-HMS and HEC-RAS Models: Case Studies from Nepal and Sweden, TVVR-18/5009, ISSN 1101-9824, Lund 2018, www.tvrl.lth.se, Lund University , Box 118, 22100 Lund, Sweden

Jerzy , R., Anna , R.-P., & Jan , R. (2014). The Effect of Land Use Change on Transformation of Relief and Modification of Soils in Undulating Loess Area of East Poland. Scientific World Journal, 2014(341804).

Jetten, V., Henkens, E., and De Jong, S., (1988). The Universal Soil Loss Equation. Version 1.0, release 1.0, distributed. Department of Physical Geography, Utrecht University, The Netherlands

Jin, H., Liang, R., Wang, Y., and Tumula, P. (2015). Flood-runoff in semi-arid and sub-humid regions, a case study: A simulation of jianghe watershed in northern China. Water 2015, 7, 5155–5172.

Jin, X.; Xu, C.Y.; Zhang, Q.; Chen, Y.D. (2009). Regionalization study of a conceptual hydrological model in Dongjiang basin, south China. Quat. Int., 208, 129–137.

Julien, PY (2010). Erosion and sedimentation, Cambridge university press.

Juraj M. Cunderlik and Slobodan P. Simonovic (2004). Caibration, Verification and Sensitivity analysis of the HEC-HMS Hydrologic Model, CFCAS project: Assessment of Water Resources Risk and Vulnerability to Changing Climatic Conditions.

Kassa Tadele 2009). Watershed Hydrological Responses to Changes in Land Use and Land Cover, and Management Practices at Hare Watershed, Ethiopia, Universität Siegen, Fakultät Bauingenieurwesen Research Institute for water and Environment, PhD Desertation.

Kayet, N. and K. A. (2018). Evaluation of soil loss estimation using the RUSLE model and SCS-CN method in hillslope mining areas. International Soil and Water Conservation Research.

Kebede Wolka, Habitamu Tadesse, Efrem Garedew and Fantaw Yimer (2015). Soil erosion risk assessment in the Chaleleka wetland watershed, Central Rift Valley of Ethiopia, Environmental Systems Research (2015) 4:5, DOI 10.1186/s40068-015-0030-5.

Kim, H., and Maeng, S.J. (2019). Development of flood alert application in Mushim stream watershed Korea. Int. J. Disast. Risk Re. 2017, 21, 11–26.

Kocyigit, R. and Demirci, S. (2012). Long-term changes of aggregateassociated and labile soil organic carbon and nitrogen after conversion from forest to grassland and cropland in northern Turkey, Land Degrad. Dev., 23, 475–482.

Koneti S, Sunkara SL, Roy PS (2018). Hydrological modeling with respect to impact of land-use and land-cover change on the runoff dynamics in Godavari river basin using the HEC-HMS model. ISPRS Int J Geo Inf 7(206):1–17.

Kumar, B.M. and Nair P.K.R. (eds.) (2006). Tropical homegardens. A time-tested example of sustainable agroforestry. Springer, Dordrecht, the Netherlands.

Lal, R. (1988). Soil degradation and the future of agriculture in sub-Saharan Africa, J. Soil Water Conserv., 43, 444–451.

Lal, R. (2003). Cropping Systems and Soil Quality. J. Crop Prod., 8(1/2): 33-52.

Legesse D, Vallet-coulomb C, Gasse F. (2004). Analysis of hydrological response of a tropical terminal lake, Lake Abiyata (Main Ethiopian Rift Valley) to changes in climate and human activities. Hydrological Process 18: 487–504.

Legesse D. and Ayenew T. (2006). Effect of improper water and land resource utilization on the central main Ethiopian rift valley lakes. Quaternary International 148: 8–18.

Liu BY, Nearing MA, Shi PJ. (2000). Slope length effects on soil loss for steep slopes. Soil Sci Soc Am J. 64:1759–1763.

Lock JM (1993). Musaceae. In: Polehill RM (ed.) Flora of Tropical East Africa: prepared at the Royal Botanic Gardens/Kew with assistance from the East African Herbarium. Rotterdam: A.A. Balkema on behalf of the East African Governments.

Loveland, T., Sohl, T., Stehman, S., Gallant, A., Sayler, K., Napton, D., (2002). A Strategy for Estimating the Rates of Recent United States Land-Cover Changes. Photogrammetric Engineering and Remote Sensing 68, 1091 – 1099).

Lu D, Weng Q (2007). A survey of image classification methods and techniques for improving classification performance. Int J Remote Sens 28:823–870

Lu, D., Mausel, P., Brondizio, E. And Moran, E., (2003). Change Detection Techniques

Lulseged Tamene and Paul, L., (2008). Soil erosion studies in northern Ethiopia. pp.73-100. In: Ademola,K., Braimch, A., and Paul, L. (eds): Land Use and Soil Resources, Springer Netherlands. The Netherlands.

M. Fleming and T. Brauer (2018). Hydrologic Modeling System HEC-HMS Quick Start Guide, US Army Corps of Engineers, Institute of Water Resources, Hydrologic Engineering Center, 609 Second Street, Davis CA 95616-4687.

Majidi, A., Shahedi, K., (2012). Simulation of rainfall-runoff process using Green-Ampt method and HEC-HMS model (Case study: AbnamaWatershed, Iran). J. Hydraul. Eng. 2012, 1, 5–9.

Mallick J, Alashker Y, Mohammad SA, Ahmed M, Hasan MA. (2014). Risk assessment of soil erosion in semi-arid mountainous watershed in Saudi Arabia by RUSLE model coupled with remote sensing and GIS. Geocarto Int.29:915–940.

Matson, P.A., Parton, W.J., Power, A.G. and Swift, M.J. (2002). Agricultural intensification and ecosystem properties. Science 277: 504.

Mberu BU. (2006). Internal migration and house hold living condition in Ethiopia. Demographic Research 14: 509–540.

Mbow, C., Van Noordwijk, M., Luedeling, E., Neufeldt, H., Minang, A., & Kowero, G. (2014). Agroforestry solutions to address food security and climate change challenges in Africa. Curr. Opin. Environ. Sustain. 6:61–67. https://doi.org/10.1016/.

McCarthy, G.T. (1938). The unit hydrograph and flood routing. In Proceedings of the Conference of North Atlantic Division, Washington, WA, USA,.

McCuen RH (1982). A guide to hydrologic analysis using SCS methods. Prentice-Hall, Englewood Cliffs

McGraw-Hill (2003). Surface runoff - Sci-Tech Dictionary. Dictionary of Scientific and Technical Terms.

Mekuria Argaw (2005). Forest Conversion-Soil Degradation-Farmers' Perception nexus: Implications for sustainable land use in the southwest of Ethiopia. Ecology and Development Series, No. 26, 2005.

Mengesha Zerihun, Mohammed S. Mohammedyasin, Demeke Sewnet, Anwar A. Adem, Mindesilew Lakew (2018). Assessment of soil erosion using RUSLE, GIS and remote sensing in NW Ethiopia, Geodrs, doi:10.1016/j.geodrs.

Merritt, W., Letcher, R., and Jakemna, A. (2003). A review of erosion and sediment transport models. Environmental Modelling and Software 2003;18(8-9): 761-799.

Merritt, WS, Letcher, RA & Jakeman, AJ (2003). 'A review of erosion and sediment transport models', Environmental modelling & software, vol. 18, no. 8-9, pp. 761-99.

Merriam, C. F., (1937). A comprehensive study of the rainfall on the Susquehanna valley: Am. Geophys. Union Trans., pt. 2, p. 471-476.

Merwade, V. (2012). Creating SCS Curve Number Grid using HEC-Geo-HMS. School of Civil Engineering, Purdue University. vmerwade@purdue.edu, 1-26.

Mesfin, M. M., & Arjen, Y. H. (2016). Four billion people facing severe water scarcity. American Association for Advancement of Science.

Mesfin, S., Christine, F., & Kumlachew, Y. (2018). Plant diversity analysis for conservation of Afromontane vegetation in socio-ecological mountain landscape of Gurage, South Central Ethiopia. International Journal of Biodiversity and Conservation, 10(4), 161-171.

Mesfin, S., Osamu, S., Christine, F., & Kumelachew, Y. (2017). Quantification and mapping of the supply of and demand for carbon storage and sequestration service in woody biomass and soil to mitigate climate change in the socio-ecological environment table 5 of pp 349.

Mezgebu Mewded, Adane Abebe, Seifu Tilahun and Zeleke Agide (2021). Impact of land use and land cover change on the magnitude of surface runoff in the endorheic Hayk Lake basin, Ethiopia

Michael Doughery. (2002). Gendered Scripts and Declining Soil Fertility in Southern Ethiopia.

Mitchell, Andy (2005). The ESRI Guide to GIS Analysis, Volume 2. ESRI Press.

Mitchell, J., and Bubnezer, G., (1980). Soil loss estimation. In M.J. Kirkby and R.P.C. Morgan (eds.) Soil Erosion. John Wiley and Sons, Chichester, England. pp.17-62

Mohammad Reza Pahlavan-Rad, Khodadad Dahmardeh, Mojtaba Hadizadeh, Gholamali Keykha, Nader Mohammadnia, Mojtaba Gangali, Mehdi Keikha, Naser Davatgar, Colby Brungard (2020). Prediction of soil water infiltration using multiple linear regression and random forest in a dry flood plain, eastern Iran, CATENA, Volume194, 104715, ISSN0341- 8162, https://doi.org/10.1016/j.catena.2020.104715.

Mohawesh Y., Taimeh A., and Ziadat F. (2015). Effects of land use changes and soil conservation intervention on soil properties as indicators for land degradation under a Mediterranean climate

Morgan, R., (1995). Soil Erosion and Conservation.Edinburgh: Addison-Wesley Longman.

Morgan, RPC (2009). Soil erosion and conservation, John Wiley & Sons.

Moriasi DN, Arnold JG, Van Liew MW et al (2007). Model evaluation guidelines for systematic quantification of accuracy in watershed simulations. Trans ASABE 50:885–900

MOWIE (2013). Strategic agenda for adaptation to urban water-mediated impacts of climate change in Addis Ababa, Federal Democratic Republic of Ethiopia. Addis Ababa.

Najim, M.M.M., Babelb, M.S., Loofb, R. AGNPS (2006). Model Assessment for a Mixed Forested Watershed in Thailand. ScienceAsia 2006, 32, 53–61.

Nash, J.E. and Sutcliffe, J.V. (1970). River flow forecasting through conceptual models part I—A discussion of principles. J. Hydrol. 1970, 10, 282–290.

Nearing, M, Jetten, V, Baffaut, C, Cerdan, O, Couturier, A, Hernandez, M, Le Bissonnais, Y, Nichols, M, Nunes, J & Renschler, C (2005). 'Modeling response of soil erosion and runoff to changes in precipitation and cover', Catena, vol. 61, no. 2-3, pp. 131-54.

Negash, A. (2001). Diversity and conservation of enset (Ensete ventricosum Welw. Cheesman) and its relation to household food and livelihood security in South-western Ethiopia. PhD dissertation, Wageningen University, the Netherlands.

Neher, D. (1992). Ecological sustainability in agricultural systems: Definition and measurement. Journal of Sustainable Agriculture 2: 51-61.

Nejadhashemi1 A. P., Wardynski1 B. J., and Munoz J. D. (2011). Evaluating the impacts of land use changes on hydrologic responses in the agricultural regions of Michigan and Wisconsin. Hydrol. Earth Syst. Sci. Discuss., 8, 3421–3468, 2011. www.hydrol-earth-syst-sci-discuss.net/8/3421/2011/, doi:10.5194/hessd-8-3421-2011.

Neter, J., Wasserman, W., Kutner, M.H., (1990). Applied Statistical Models; Richard D. Irwin, Inc.: Burr Ridge, IL, USA.

Netting, R.M.C. and Stone, M.P. (1996). Agrodiversity on a farming frontier: Kofyar smallholders on the Benue plains of Central Nigeria. Africa 66: 52-69.

Nunes, AN, De Almeida, AC & Coelho, CO (2011). 'Impacts of land use and cover type on runoff and soil erosion in a marginal area of Portugal', Applied Geography, vol. 31, no. 2, pp. 687-99.

Nyssen, J., Clymans, W., Descheemaeker, K., Poesen, J., Vandecasteele, I., Vanmaercke, M., Zenebe, A., Van Camp, M., Haile, M., Haregeweyn, N., Moeyersons, J., Martens, K., Gebreyohannes, T., Deckers, J., & Walraevens, K. (2010). Impact of soil and water conservation measures on catchment hydrological response - a case in north Ethiopia. Hydrological Processes, 24(13), 1880–1895. https://doi.org/10.1002/hyp.7628.

Nyssen, J., Habtamu , T., Mulugeta, L., Amanuel, Z., Nigussie , H., & Mitiku , H. (2008). Spatial and temporal variation of soil organic carbon stocks in a lake retreat area of the Ethiopian Rift Valley. Geoderma, 146 , 261–268.

Ojiem, J.O., De Ridder, N., Vanlauwe, B. and Giller, K.E. (2006). Socio-ecological niche: a conceptual framework for integration of legumes in smallholder farming systems. International Journal of Agricultural Sustainability 4: 79-93.

Okirya Martin, Albert Rugumayo and Janka Ovcharovichova (2012). Application of Hec-Hms/Ras and GIS Tools in Flood Modeling: A Case Study for River Sironko, UGANDA. GLOBAL Journal of engineering, design & technology.

Oliver B., Niels A. W., Hogler F., and Reinhard F. H. (2006). Water infiltration and hydraulic conductivity in sandy cambisols: impacts of forest transformation on soil hydrological properties.

Ouyang D, Bartholic J. (2001). Web-based GIS application for soil erosion prediction. Proceeding of an international symposium soil erosion research for the 21th century; Jan 3–5; Honolulu, HI.

Padoch, C. and Pinedo-Vasquez, M. (2010). Saving swidden to save biodiversity. Biotropica 42: 550-552.

Pak, J, Fleming, M, Scharffenberg, W & Ely, P (2008). 'Soil erosion and sediment yield modeling with the hydrologic modeling system (HEC-HMS)', in World Environmental and Water Resources Congress 2008: Ahupua'A, pp. 1-10.

Pak, J, Ramos, K, Fleming, M, Scharffenberg, W & Gibson, S (2015). 'Sensitivity analysis for sediment transport in the hydrologic modeling system (HEC-HMS)', in Proc., Joint Federal Interagency Conf.

Pak, JH, Fleming, M, Scharffenberg, W, Gibson, S & Brauer, T (2015). 'Modeling surface soil erosion and sediment transport processes in the Upper North Bosque River Watershed, Texas', Journal of Hydrologic Engineering, vol. 20, no. 12, p. 04015034.

Pak, JH, Kou, Z, Kwon, HJ & Lee, JJ (2009). 'Predicting Debris Yield From Burned Watersheds: Comparison of Statistical and Artificial Neural Network Models 1', JAWRA Journal of the American Water Resources Association, vol. 45, no. 1, pp. 210-23.

Pal M, Mather PM (2003). An assessment of the effectiveness of decision tree methods for land cover classification. Remote Sens Environ 86:554–565

Perfecto, I., Vandermeer, J. and Wright, E.L. (2009). Nature’s matrix: linking agriculture, conservation and food sovereignty. Earthscan Ltd., London, UK.

Petroviˇc, F (2021). Hydrological Impacts of Climate Change and Land Use. Water 2021, 13, 799. https:// doi.org/10.3390/w13060799

Peyre, A., Guidal, A., Wiersum, K.F. and Bongers, F. (2006). Homegarden dynamics in Kerala, India. In: Kumar B.M. and Nair P.K.R.(eds.) Tropical homegardens: a time-tested example of sustainable agroforestry. Springer Science, Dordrecht, the Netherlands, pp. 87-103.

Pimentel D, Burgess M (2013). Soil erosion threatens food production. Agriculture 3(3):443–463

Pimentel, D, Harvey, C, Resosudarmo, P, Sinclair, K, Kurz, D, McNair, M, Crist, S, Shpritz, L, Fitton, L & Saffouri, R (1995). 'Environmental and economic costs of soil erosion and conservation benefits', Science, vol. 267, no. 5201, pp. 1117-23.

Pretty, J.N., Morison, J.I.L. and Hine, R.E. (2003). Reducing food poverty by increasing agricultural sustainability in developing countries. Agriculture, Ecosystems and Environment 95: 217-234.

Putra, S. S. (2013). Reservoir Sabo works Solutions in Limboto Lake Sedimentations. Procedia Environmental Sciences, 17, 230-239.

Qiu, Y., Jia, Y., Zhao, J., Wang, X., Bennett, J., & Zhou, Z. (2010). Valuation of flood reductions in the Yellow River Basin under land use change. J WATER RES PL-ASCE, 136(1), 106-115.

Quideau, S. A., Anderson, M. A., Graham, R. C., Chadwick, O. A. and Trumbore, S. E. (2000). Soil Organic Matter Processes: Characterization by 13C NMR and 14C Measurements. For. Ecol. Manage., 138: 19–27.

Rahmato D. (1989). Famine and survival strategies: a case study from North- East, food and famine. Monograph No. 1, Institute of Development Research. Addis Ababa: Addis Ababa University.

Ramakrishnan, D. B. (2009). SCS-CN and GIS-based approach for identifying potential water harvesting sites in the Kali Watershed, Mahi River Basin, India. Journal of earth system science, 118(4), 355-368.

Ramesh H. (2016). Assessment of soil erosion by RUSLE model using remote sensing and GIS - A case study of Nethravathi Basin. Geoscience Frontiers, Elsevier, 7(6), 953-961.

Remo, J., Pinter, N., & Heine, R. (2010). The use of retro- and scenario-modeling to assess effects of 100 + years river of engineering and land-cover change on Middle and Lower Mississippi River flood stages. J HYDROL, 376(3-4), 403-416.

Reza Kabiri (2014). Simulation of Runoff using Modified SCS-CN Method using GIS System, Case Study: Klang Watershed in Malaysia. Research Journal of Environmental Sciences, 8: 178-192.

Rezaei N., Roozitalab M. H., and Ramezanpour H. (2012). Effect of Land Use Change on Soil Properties and Clay Mineralogy of Forest Soils Developed in the Caspian Sea Region of Iran. J. Agr. Sci. Tech. Vol. 14: 1617-1624

Riezebos, H. T. and Loerts, A. C. (1998). Influence of Land use change and tillage practice on soil organic matter in southern Brazil and eastern Paraguay, Soil Till. Res., 49, 271–275.

Roose, E., (1986). Runoff and erosion before and after clearing depending on the type of crop in West Africa. In: R. Lal and P.A. Sanches (eds.), Land clearing and development in the tropics, A.A. Balkema, Rotterdam.

Saha, S., (1996). Integrated use of Remote Sensing and GIS for Soil Erosion Hazard Modeling-A Case Study.http://www.gisdevelopment.net/aars/acrs/1996/ss/ss1005.

Scharffenberg, W. E. (2010). Hydrologic modeling system (HEC-HMS): Physically-based simulation components. . Paper presented at the Proceedings of the 2nd Joint Federal Interagency Conference.

Schilling, K., Jha, M., Zhang, Y., Gassman, P., & Wolter, C. (2008). Impact of land use and land cover change on the water balance of a large agricultural watershed: Historical effects and future directions. WATER RESOUR RES 44, doi:10.1029/2007WR006644.

Scholten W. 2007. Agricultural development and water use in the central rift valley of Ethiopia: a rapid appraisal. Internship Report. University of Twente.

Schwärzel, K. & J. Punzel (2007). Hood-Infiltrometer: New type of tension infiltrometer. Soil Sci. Soc .Am.J. 71:1438-1447.

Shi ZH, Cai CF, Ding SW, Wang TW, Chow TL. (2004). Soil conservation planning at the small watershed level using RUSLE with GIS: a case study in the Three Gorge Area of China. Catena. 55:33–48.

Shiferaw Feleke, R. L. (2003). Determinants of Food Security in Southern Ethiopia . American Agricultural Economics Association Meetings in Montreal, Canada, 1-29.

Shigeta M (1990). Folk in situ conservation of ensete (Ensete ventricosum (Welw) Cheesman): towards the interpretation of indigenous agricultural science of the Ari, Southwestern Ethiopia. Afr Study Monogr 10(3):93–107

Shyam, R., Chauhan, H.S. and Sharma, J.S. (1994). Optimal operation scheduling model for a canal system. *Agricultural Water Management* 26: 213–225.

Singh, V. P. (1995). Computer models of watershed hydrology, V. P. Singh, ed., Water Resources Publications, Littleton, Colo., 1–22.

Singh, V.P. and D.A Woolhiser. (2002). Mathematical modelling of watershed hydrology. J. Hydrol. Eng., 7(4):270-292.

Sintayehu Legesse Gebre (2013). Application of the HEC-HMS Model for Runoff Simulation of Upper Blue Nile River Basin

Smith, C. K., de Assis, O. F., Gholz, H. L. and Baima, A. (2002). Soil Carbon Stocks after Forest Conversion to Tree Plantations in Lowland Amazonia, Brazil. For. Ecol.Manage., 164: 257–263.

Soil Conservation Research Project (SCRP) (1996). Soil erosion hazard assessment for land evaluation. Research Report, SCRP, Addis Ababa.

Spring A, Hiebsch C, Tabogie E, Weldmichael G (1996) Enset needs assessment project phase I Report. Awassa, Ethiopia.

Stewart A., Chris Brunsdon, and Martin Charlton (2002). Geographically Weighted Regression: the analysis of spatially varying relationships. John Wiley & Sons.

Subramanya, K. (2008). Engineering Hydrology. 3rd edn, Tata McGray-Hill Publishing Company, New Delhi.

Sun, W, Shao, Q, Liu, J & Zhai, J (2014). 'Assessing the effects of land use and topography on soil erosion on the Loess Plateau in China', Catena, vol. 121, pp. 151-63.

Swift, M.J. and Ingram, J.S.I. (eds.) (1996). Effects of global change on multi-species agroecosystems. Global Change and Terrestrial Ecosystems, Report no. 13, GCTE Activity 3.4, GCTE Focus 3 Office, Wallingford, UK.

Tadesse G. (2001). Land degradation: a challenge to Ethiopia. Environmental Management 27: 815–824.

Tassew BG, Belete MA, Miegel K (2019) Application of HECHMS model for flow simulation in the lake Tana basin: the case of Gilgel Abay catchment, upper Blue Nile basin, Ethiopia. Hydrology 6:1–17

Tefera AH (2017) Application of water balance model simulation for water resource assessment in upper Blue Nile of north Ethiopia using HEC-HMS by GIS and remote sensing: case of Beles river basin. Int J Hydrol 1:222–227

Tesfahunegn, G. B. (2013). Soil quality indicators response to land use and soil management systems in northern Ethiopia's catchment, Land Degrad. Dev., doi:10.1002/ldr.2245, online first.

Tesfaye and Bongers (2012). Land-use dynamics in enset-based agroforestry homegardens in Ethiopia, Forest-people interfaces: Understanding community forestry and biocultural diversity, DOI 10.3920/978-90-8686-749-3_4.

Tesfaye B, Lüdders P (2003). Diversity and distribution patterns of enset landraces in Sidama, Southern Ethiopia. Genetic Resources and Crop Evolution 50: 359–371.

Tesfaye, A., Negatu,W., Brouwer, R., van der Zaag, P. (2014). Understanding soil conservation decision of farmers in the Gedeb watershed, Ethiopia, Land Degrad. Dev., 25, 71–79, doi:10.1002/ldr.2187.

Tewolde, M.H.; Smithers, J. (2006). Flood routing in ungauged catchments using Muskingum methods. Water SA, 32, 379–388.

Thalita Costa de Moraes, Vitor Juste dos Santos Maria Lúcia Calijuri, and Fillipe Tamiozzo Pereira Torres (2017). Effects on runoff caused by changes in land cover in a Brazilian southeast basin: evaluation by HEC-HMS and HEC-GEOHMS

Tilahun A. & Robert D. (2006). Improved Decision-Making for Achieving Triple Benefits of Food Security, Income and Environmental Services through Modeling Cropping Systems in the Ethiopian Highlands. African Highlands Initiative (AHI) working paper number 20.

Tilman, D., Cassman, K.G., Matson, P.A., Naylor, R. and Polasky, S. (2002). Agricultural sustainability and intensive production practices. Nature 418: 671-677.

Treitz, P. & Rogan, J., (2003). Remote Sensing for Mapping and Monitoring Land-Cover and Land – Use Change-An Introduction

Tu, J. (2009). Combined impact of climate and land use changes on stream flow and water quality in eastern Massachusetts, USA. J HYDROL, 379, 268-283.

Uhlenbrook, S., (2007). Biofuel and water cycle dynamics: what are the related challenges for hydrological processes research? Hydrol. Proc. 21, 3647–3650.

Uloro Y. & Mengel K. (2014). Response of Enset (Ensetventricosum W.) to mineral fertilizers in southwest Ethiopia,. SUdanlage 35390 Giessen, Germany: Institute of Plant Nutrition of the Justus Liebig University.

United States Department of Agriculture, Natural Resources Conservation Service (USDA-NRCS) (1986). "Urban Hydrology for Small Watersheds"; Technical Release 55, United States

Department of Agriculture, Natural Resources Conservation Services, Conservation Engineering Division, Washington, DC, USA.

USACE (2016A), Hydrologic modeling system HEC-HMS, user's manual, version 4.2, USACE-HEC Davis, CA.

USACE (2016b). Hydrologic modeling system HEC-HMS: User's manual, Hydrologic Engineering Center Davis, CA.

USDA S (1972). National Engineering Handbook, Section4-Hydrology. Washington, USA

Vaezi A. R., Bahrami H. A., Sadeghi S. H. R., and Mahdian M. H. (2010). Modeling relationship between runoff and soil properties in dry-farming lands, NW Iran. Hydrology and Earth System Sciences (HESS), 7, 2577–2607.

Van Remortel, RD, Maichle, RW & Hickey, RJ (2004). 'Computing the LS factor for the Revised Universal Soil Loss Equation through array-based slope processing of digital elevation data using a C++ executable', Computers & geosciences, vol. 30, no. 9-10, pp. 1043-53.

Vaze, J., Jordan, P., Beecham, R., Frost, A. and Summerell, G. (2012). Guidelines for rainfall-runoff modelling. Australian Government Department of Innovation, Industry, science and Research.

Wakindiki, I. I. C. and Ben-Hur, M. (2002). Indigenous soil and water conservation techniques: effect on runoff, erosion, and crop yields under semiarid conditions, Aust. J. Soil Res., 40, 367–379.

Wang Y, Woonsup C, Brian MD (2005). Long-term impacts of land use change on non-point source pollutant loads for the St. Louis metropolitan area, USA. Environ Manage 35:194–205

Wang, G., Liu, J., Kubota, J., & Chen, L. (2007). Effects of land-use changes on hydrological processes in themiddle basin of the Heihe River, northwest China. HYDROL PROCESS, 21, 1370 -1382.

Wang, Q., Wang, S., and Yu, X. (2011). Decline of soil fertility during forest conversion of secondary forest to Chinese fir plantations in subtropical China, Land Degrad. Dev., 22, 444–452.

Ward, P., Renssen, H., Aerts, J., van Balen, R., & Vandenberghe, J. (2008). Strong increases in flood frequency and discharge of the River Meuse over the late Holocene: impacts of long-term anthropogenic land use change and climate variability. HYDROL EARTH SYST SC., 12(1), 159-175.

Westphal E. (1975). Agricultural Systems in Ethiopia. Wageningen.: Center for Agricultural Publishing and Documentation.

Wischmeier, W., and Smith D., (1978). Predicting rainfall erosion losses: a guide to conservation planning. Agricultural Handbook, No. 587. Science and Education Administration, US Department of Agriculture, Washington, DC, USA. 58 pp.

Woldetsadik, M., (2004). Impacts of population pressure on land use/land cover change, agricultural system and income diversification in West Gurage land, Ethiopia. Norwegian J. Geogr. 58 (46). https://doi.org/10.1080/00291950410004357.

Wooding, R. A. (1968). Steady infiltration from a shallow circular pond. IN: Water Resources Research 4. 1259-1273.

Wuest, SB, Williams, JD & Gollany, HT (2006). 'Tillage and perennial grass effects on ponded infiltration for seven semi-arid loess soils', Journal of soil and water conservation, vol. 61, no. 4, pp. 218-23.

Yakir H., and Morin E. (2011). Hydrologic response of a semi-arid watershed to spatial and temporal characteristics of convective rain cells. Hydrol. Earth Syst. Sci., 15, 393–404, 2011. www.hydrol-earth-syst-sci.net/15/393/2011/doi:10.5194/hess-15-393-2011.

Yan, Xin. (2009). Linear regression analysis: theory and computing. Published by World Scientific Publishing Co. Pte. Ltd. 5 Toh Tuck Link, Singapore 596224.

Yang, CT (1996). 'Sediment transport: theory and practice'.

Yilma H, Moges SA (2007) Application of semi-distributed conceptual hydrological model for flow forecasting on upland catchments of Blue Nile river basin- A case study of Gilgel Abbay catchment. Catchment Lake Res 200:155–170.

Yimer F., Messing I., Ledin S., Abdelkadir A. (2008). Effects of different land use types on infiltration rate in a catchment in the highlands of Ethiopia. Soil Use and Management, 24, 344–349.

Yimer, F. and Abdelkadir, A. (2011). Soil property changes following conversion of acacia woodland into grazing and farmlands in the Rift Valley area of Ethiopia, Land Degrad. Dev., 22, 425–431.

Yirmaga, M. T. (2013). Improving the Indigenous Processing of Kocho, an Ethiopian Traditional Fermented Food. Nutrition & Food Sciences, 3(1), 1-6.

Yueqing X, Ding L, Jian P. (2011). Land use change and soil erosion in the Maotiao River watershed of Guizhou Province. J Geogr Sci. 21:1138–1152.

Zehetner, F., & Miller, W. (2006). Erodibility and runoff-infiltration characteristics of volcanic ash soils along an altitudinal climosequence in the Ecuadorian Andes, Catena. Catena, 65, 201-213.

Zeiger, M., & Fohrer, N. (2009). Impact of organic farming systems on runoff formation processes-A long-term sequential rainfall experiment, Soil Till. Res. Soil Tillage, 102, 45-54.

Zelelew, D.G. (2017). Spatial mapping and testing the applicability of the curve number method for ungauged catchments in Northern Ethiopia. J. Soil Water Conserv., 5, 293–301.

Zhang, H, Wei, J, Yang, Q, Baartman, JE, Gai, L, Yang, X, Li, S, Yu, J, Ritsema, CJ & Geissen, V (2017). 'An improved method for calculating slope length (λ) and the LS parameters of the Revised Universal Soil Loss Equation for large watersheds', Geoderma, vol. 308, pp. 36-45.

A. Appendix 1: Land use land cover classification and dynamics analysis

Table A.1: Satellite image data collected from different sources

Year	Sensor	No. of bands	Date of acquisition	Path/Row	Land sat Mission	Resolution (m)	Image Source
1987	TM	7	01-01-87	168/054-169/054 & 168/055-169/055	5	30	USGS
2017	ETM+	12	01-01-17	168/054-169/054 & 168/055-169/055	7	15m PAN / 30	USGS
Topographic map			23-10-17				EGSIA
SRTM DEM			10-01-17			30	USGS

Table A.2: Land use land cover dynamics in Meki river watershed

Class name	Bare land	Grass land	Forest and Natural vegetation	EBLUS	Eucalyptus plantation	Cultivated land	Bush and Khat land	Total
Bare land	0	2320.7	67.21	-3.03	3103	122	301	6046.25
Grass land	-2320.7	0	24.72	-1134	-642.13	-132.53	-100	-4183.45
Forest and Natural vegetation	-67.21	-24.72	0	-232.8	435.23	-776.4	-135.28	-801.18
EBLUS	3.03	1134	232.8	0	461.2	25	342	2198.03
Eucalyptus plantation	-3103	642.13	-435.23	-461.2	0	167.59	-198.24	-3387.97
Cultivated land	-122	132.53	776.4	-25	-167.59	0	266.9	861.24
Bush and Khat land	-301	100	135.28	-342	198.24	-266.9	0	-558.59

CORRELATION MATRIX

Table A.3: Statistics of individual layers for 1987

Layer	1	2	3	4	5	6
1	1.00000	0.98944	0.96837	0.94552	0.92598	0.92394
2	0.98944	1.00000	0.99110	0.95794	0.94513	0.94248
3	0.96837	0.99110	1.00000	0.95784	0.95979	0.95541
4	0.94552	0.95794	0.95784	1.00000	0.96425	0.92934
5	0.92598	0.94513	0.95979	0.96425	1.00000	0.98380
6	0.92394	0.94248	0.95541	0.92934	0.98380	1.00000

Table A.4: Statistics of individual layers for 2017

Layer	1	2	3	4	5	6
1	1.00000	0.98727	0.97190	0.89599	0.86478	0.87838
2	0.98727	1.00000	0.98520	0.90702	0.87268	0.88510
3	0.97190	0.98520	1.00000	0.90856	0.89079	0.90821
4	0.89599	0.90702	0.90856	1.00000	0.91656	0.88205
5	0.86478	0.87268	0.89079	0.91656	1.00000	0.97651
6	0.87838	0.88510	0.90821	0.88205	0.97651	1.00000

Accuracy assessment analysis (ENVI 4.3)

Table A.5: Accuracy of classification for 1987 image

Class	Prod. Acc. (Percent)	User Acc. (Percent)
Forest and Natural vegetation	99.97	97.00
Eucalyptus plantation	91.50	99.89
EBLUS	95.27	99.70
Bush and Khat land	98.43	99.06
Bare land / Settlement	96.63	99.86
Cultivated land	82.80	89.83
Grass land	82.70	80.11

Table A.6: Accuracy of classification for 2017 image

Class	Prod. Acc. (Percent)	User Acc. (Percent)
Forest and Natural vegetation	95.52	98.67
Eucalyptus plantation	97.30	95.80
EBLUS	96.76	96.05
Bush and Khat land	95.31	95.72
Bare land / Settlement	95.80	95.27
Cultivated land	86.15	85.30
Grass land	86.12	84.01

B. Appendix 2: Soil erosion modeling

a. Soil erosion modeling Framework

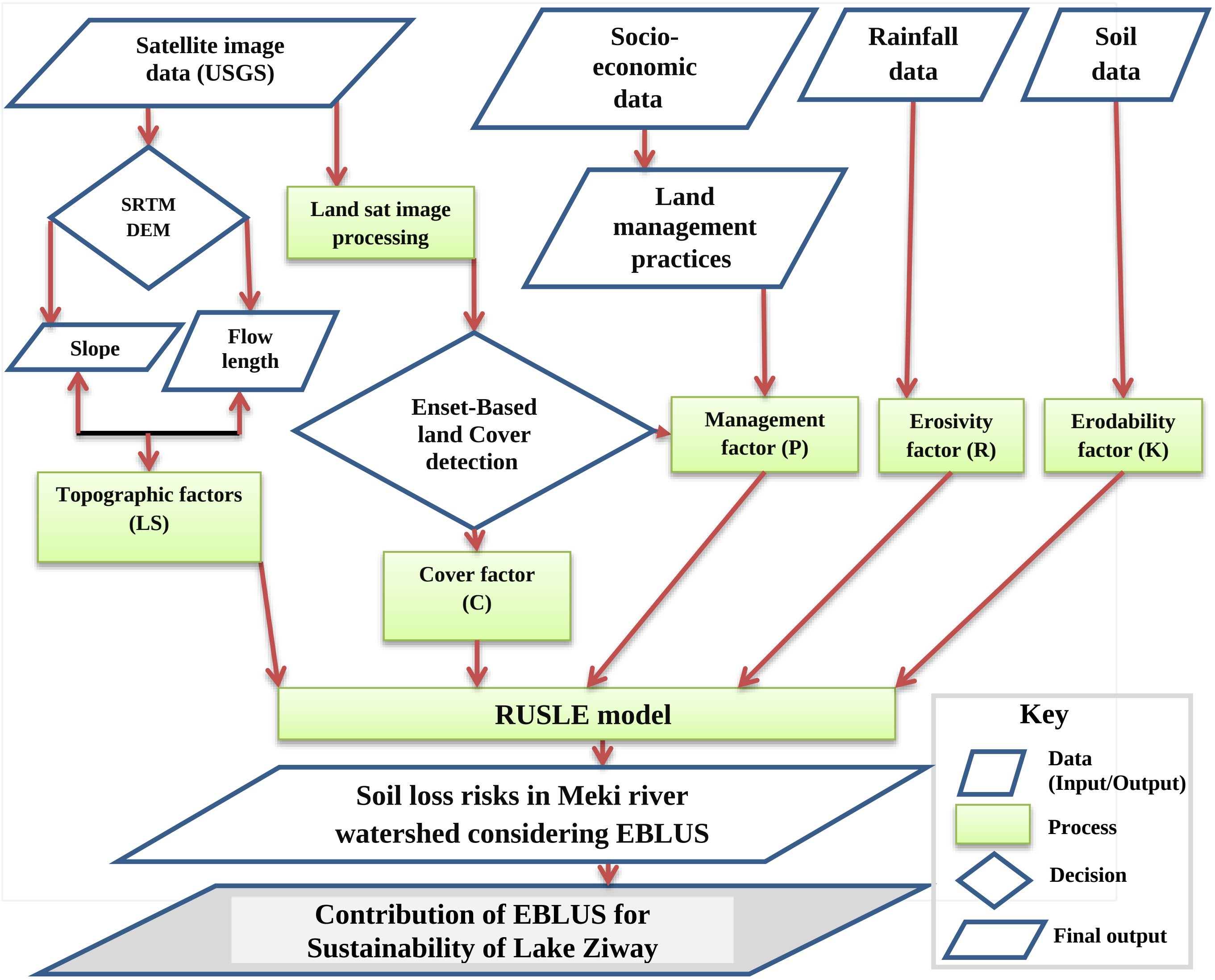

Figure B-1: RUSLE model flow diagram

b. Sub-watershed based soil erosion factors analyzed

Table B.1: Sub-watershed based soil erosion factors and soil loss in Meki river watershed

Zone	SWS	R	C	LS	K	P	A_2017	A_1987	Standard1	Standard2
U	W2510	548.9	0.1004	3.7	0.231	0.918	37.044	26.8515	10	18
U	W2530	563.73	0.038	5.924	0.24441	0.795	36.611	26	10	18
U	W2610	575	0.0374	7	0.25	0.728	31.2813	37.772	10	18
U	W2620	551.65	0.074	4.58	0.224	0.8582	36.02	17.23	10	18
M	W2640	535.5	0.159	2.99	0.218	0.966	53.672	31.5	10	18
U	W2750	584.205	0.03221	6.5	0.23	0.7363	25.445	21.22	10	18
U	W2860	556.52	0.091	5.267	0.2105	0.832	30.73	14.1434	10	18
M	W2890	550.45	0.149	3.704	0.21	0.9124	53.52	19.7325	10	18
M	W2970	533.72	0.1555	2.852	0.2041	0.974	57.9413	33	10	18
U	W3080	570.4	0.049	6.923	0.234	0.761	20.446	11.77	10	18
L	W3180	503.31	0.145	1.751	0.2324	0.99	28.034	29.39	10	18
U	W3190	599.41	0.0511	7.15	0.2363	0.7512	28.1	26.73	10	18
L	W3260	487	0.1461	1	0.2132	1	14.911	26.5	10	18
M	W3280	538.431	0.159	1.78	0.186	0.9834	25.9	19.18344	10	18
U	W3300	583.872	0.033	7.2	0.245	0.72	18.2	12.122	10	18
L	W3400	511.793	0.1442	1.71	0.232	0.998	27.9044	31.403	10	18
M	W3410	555.421	0.18	1.67	0.1834	0.97	30.64	16.57	10	18
L	W3460	484.45	0.1653	0.513	0.2	1	7.73325	13.1	10	18
U	W3690	624.61	0.039	7.42	0.232	0.74	18.07	10.5	10	18
M	W3700	601.352	0.1765	2.63	0.16143	0.925	36.8635	32.69	10	18
M	W3730	537.281	0.17	1.351	0.15223	0.996	19.55	17.12	10	18
M	W3790	566.42	0.2	1.784	0.16	0.97	33.96	24.29	10	18
U	W3910	643.73	0.0751	6	0.22	0.781	27.1	20.78	10	18
U	W4030	651.571	0.121	5.6	0.22	0.793	45.76	37.0215	10	18
L	W4070	523.04	0.15	1.64	0.199	1	27.831	35	10	18
M	W4130	572	0.1601	1.77	0.18	1	27.3734	31.7	10	18
U	W4180	642.114	0.121	4.544	0.19622	0.855	35.6	42.22	10	18
L	W4250	555.53	0.144	1.7	0.196	1	24.1651	30.43	10	18
U	W4290	654.815	0.094	3.53	0.19	0.885	30.884	39.54	10	18
M	W4400	588.35	0.19	2	0.153	0.97	36.15	29.11	10	18
M	W4590	633.33	0.39	2.644	0.197	0.96	97.11	66.66	10	18
M	W4620	647.1	0.24	2.5	0.16331	0.96	44.935	34.101	10	18
L	W4720	619.71	0.16	2.425	0.181	0.99	44.11	44.754	10	18
M	W4730	674.3	0.17	3.26	0.165	0.95	44.21	29.4104	10	18

Note:

Standard 1: refers to the soil loss standard for Central Riftvalley

Standard 2: refers to the national soil loss standard

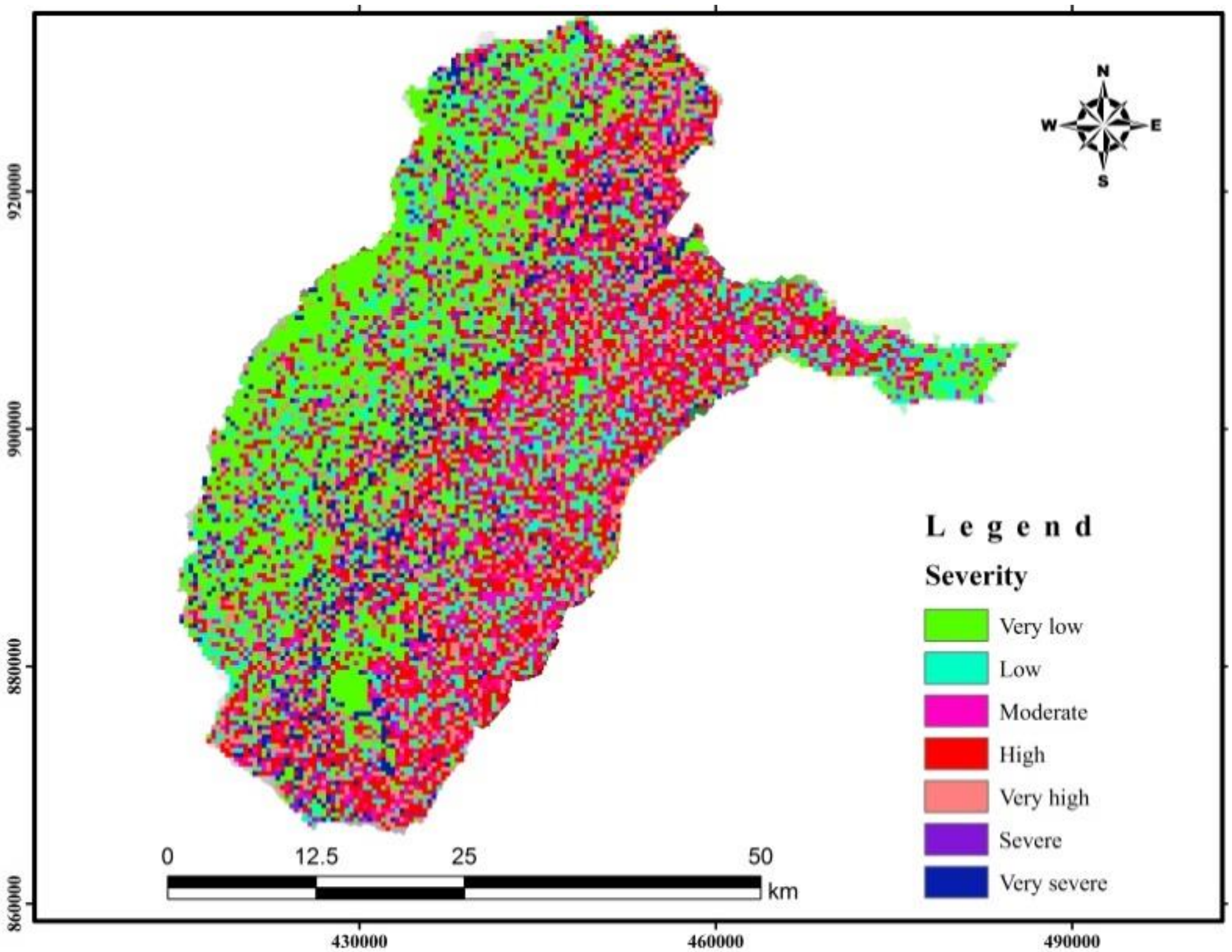

Figure B-2: Spatial distribution of severity and its priority class

Table B.2: Regression analysis result for 1987 and 2017 soil losses

ANOVA							
	df	***SS***	***MS***	***F***	***Significance F***	**R Square**	**Standard Error**
Regression	1	1888.975	1888.97	91.27	0.000213	0.95	4.55
Residual	5	103.48	20.7				
Total	6	1992.45					

c. RUSLE input factors estimation table and standards

Table B.3: RUSLE input factors estimation table

R: Rainfall Erosivity								
Rainfall (mm)	100	200	400	800	1200	1600	2000	2400
Factor (R)	48	104	217	441	665	890	1115	1340
K: Soil Erodibility								
Soil Colour	Black	Brown	Red	Yellow				
Factor (K)	0.15	0.2	0.25	0.3				
L: Slope Length								
Length (m)	5	10	20	40	80	160	240	320
Factor L	0.5	0.7	1	1.4	1.9	2.7	3.2	3.8
S: Slope Gradient								
Slope (%)	5	10	15	20	30	40	50	60
Factor (S)	0.4	1	1.6	2.2	3	3.8	4.3	4.8
C: Land Cover Factor								
Cover	factor	Cover	factor	Cover	factor	Cover	factor	
Dense forest	0.001	Dense grass	0.01	Other forest	0.02	Degraded grass	0.05	
Badlands soft	0.04	Badlands hard	0.05	Fallow Hard	0.05	Fallow Ploughed	0.6	
Sorghum, Maize	0.1	Ethiopian Teff	0.25	Cereals	0.18	Continuous fallow	1	
Pulses	0.15							
P: Management								
Land Management	Factor P	Land Management	Factor P	Land Management	Factor P	Land Management	Factor P	
Ploughing up and Down	1	Ploughing on contour	0.9	Intercropping	0.8	Dense Intercropping	0.7	
Strip Cropping	0.6	Applying Mulch	0.5	Stone Cover (40%)	0.8	Stone Cover (80%)	0.8	
Source: Source Mekuria (2005); Hellden (1987); Hurni (1985)								

Table B.4: Zonal Variability of soil formation rates (Sources Hurni, 1993)

Zone	Soil Formation Rates (tons/ha/year)
Gonder, Rift Valley	6-10
Gojam, Arsi Regions	10-14
Welega, Kefa, Shewa	18-22
Gemo Gofa	10-14
Kenya border	6-10

C. Appendix 3: Curve number Modeling

a. Curve number modeling Framework

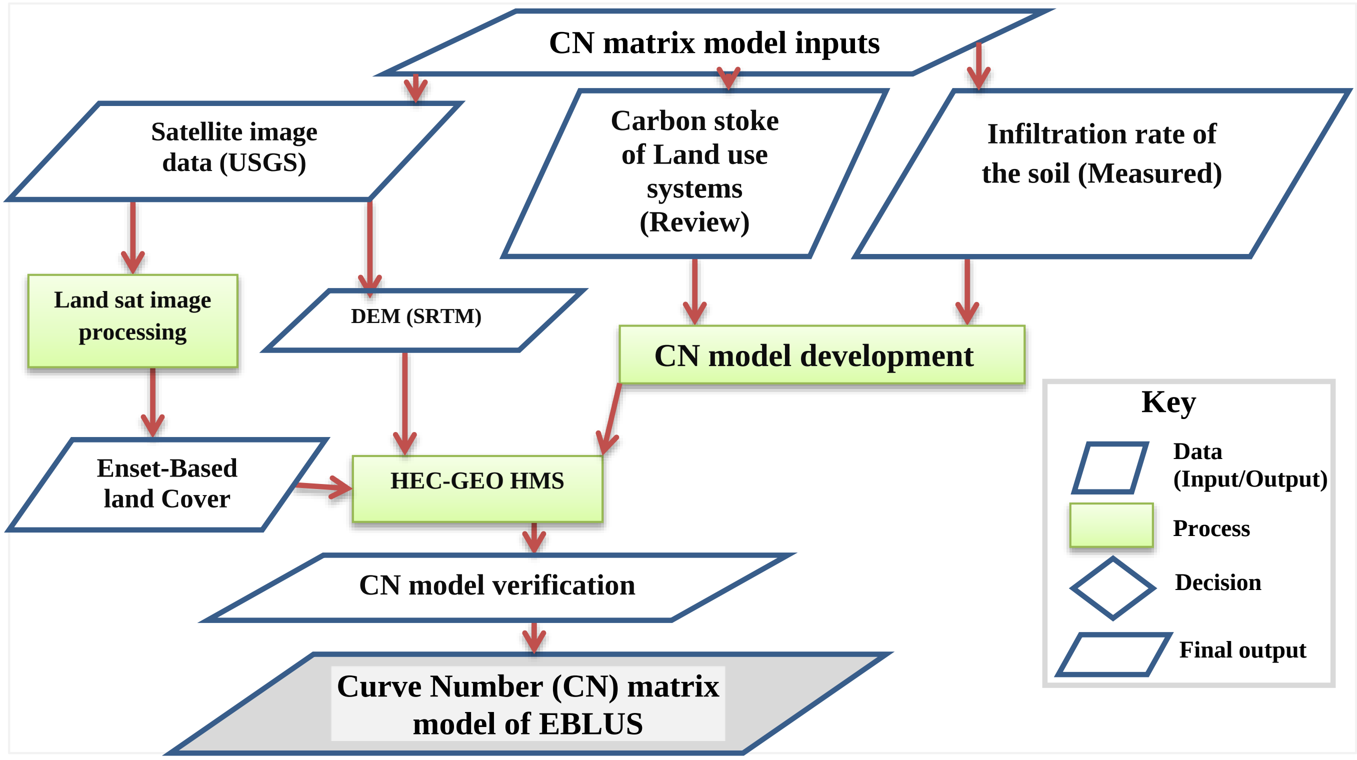

Figure C-1: CN matrix model flow diagram

b. Field measurement of infiltration rate

The samling points were described separately as shown in Table C.1.

Table C.1: Sampling points and their descriptions

No.	x	y	Sampling Zone	Sampling Zone description
1	438141	898964	CZ11	Cutivated land in vegitation zone 1 and soil type 1
2	440906	904908	CZ12	Cutivated land in vegitation zone 1 and soil type 2
3	445744	910437	CZ13	Cutivated land in vegitation zone 1 and soil type 3
4	453347	915967	CZ14	Cutivated land in vegitation zone 1 and soil type 4
5	454038	915828	CZ21	Cutivated land in vegitation zone 2 and soil type 1

No.	x	y	Sampling Zone	Sampling Zone description
6	445744	908087	CZ22	Cutivated land in vegitation zone 2 and soil type 2
7	443809	903940	CZ23	Cutivated land in vegitation zone 2 and soil type 3
8	443809	900208	CZ24	Cutivated land in vegitation zone 2 and soil type 4
9	450444	913893	BZ11	Bare land in vegitation zone 1 and soil type 1
10	445606	903940	BZ12	Bare land in vegitation zone 1 and soil type 2
11	438003	894540	BZ13	Bare land in vegitation zone 1 and soil type 3
12	433303	891223	BZ14	Bare land in vegitation zone 1 and soil type 4
13	438141	874773	BZ21	Bare land in vegitation zone 2 and soil type 1
14	444777	898411	BZ22	Bare land in vegitation zone 2 and soil type 2
15	429709	895646	BZ23	Bare land in vegitation zone 2 and soil type 3
16	430815	903664	BZ24	Bare land in vegitation zone 2 and soil type 4
17	453485	916934	GZ11	Grass land in vegitation zone 1 and soil type 1
18	444085	909055	GZ12	Grass land in vegitation zone 1 and soil type 2
19	438279	905184	GZ13	Grass land in vegitation zone 1 and soil type 3
20	432335	895231	GZ14	Grass land in vegitation zone 1 and soil type 4
21	429847	887352	GZ21	Grass land in vegitation zone 2 and soil type 1
22	437312	876431	GZ22	Grass land in vegitation zone 2 and soil type 2
23	435653	887490	GZ23	Grass land in vegitation zone 2 and soil type 3
24	435100	895231	GZ24	Grass land in vegitation zone 2 and soil type 4
25	425700	883481	EZ11	EBLUS in vegitation zone 1 and soil type 1
26	425147	891223	EZ12	EBLUS in vegitation zone 1 and soil type 2
27	426806	898411	EZ13	EBLUS in vegitation zone 1 and soil type 3
28	429571	903940	EZ14	EBLUS in vegitation zone 1 and soil type 4
29	431091	906152	EZ21	EBLUS in vegitation zone 2 and soil type 1
30	439247	915414	EZ22	EBLUS in vegitation zone 2 and soil type 2
31	448371	924814	EZ23	EBLUS in vegitation zone 2 and soil type 3
32	453071	925920	EZ24	EBLUS in vegitation zone 2 and soil type 4
33	439385	928408	NZ11	Natural vegitation (Forest) land in vegitation zone 1 and soil type 1

No.	x	y	Sampling Zone	Sampling Zone description
34	455835	932278	NZ12	Natural vegitation (Forest) land in vegitation zone 1 and soil type 2
35	432888	915414	NZ13	Natural vegitation (Forest) land in vegitation zone 1 and soil type 3
36	422382	906428	NZ14	Natural vegitation (Forest) land in vegitation zone 1 and soil type 4
37	419065	890946	NZ21	Natural vegitation (Forest) land in vegitation zone 2 and soil type 1
38	422106	875602	NZ22	Natural vegitation (Forest) land in vegitation zone 2 and soil type 2
39	431091	867446	NZ23	Natural vegitation (Forest) land in vegitation zone 2 and soil type 3
40	429847	875187	NZ24	Natural vegitation (Forest) land in vegitation zone 2 and soil type 4

Table C.2: Field measurement results of infiltration rate (Amozi meter)

Average Infiltration Rate (IR) (mm/Hour)													
		Agroecology										**Average infiltration (mm/hour)**	**Basic infiltration rate (mm/hour) (Oliver, Niels, Hogler, & Reinhard, 2006)**
Land Use	**Soil Texture, Type**	**Afro-alpine (Ericacious) (>3000)**					**Dry Afro-montane (1800-3000masl)**						
	Replication	**1**	**2**	**3**	**4**	**Av.**	**1**	**2**	**3**	**4**	**Av.**		
Cultivated LUS	Sandy Loam						22	16.9	19.1	18.5	19.13	10.375	20 to 30
	Silt Loam	11	14.5	10.2	12.3	12	13	11.5	13.2	18.2	13.96		10 to 20
	Clay Loam	6	5.5	9	8.35	7.21	6	4.6	6.7	6	5.83		5 to 10
	Clay						2.5	3	5	6	4.13		1 to 5
Builtup& degraded LUS	Sandy Loam						7.9	10.8	8.6	7.7	8.75	7.0625	20 to 30
	Silt Loam	7.65	8.25	6.55	5.8	7.06	7	11	12	10	10		10 to 20
	Clay Loam						4.2	4.7	6.1	7	5.5		5 to 10
	Clay						5	3	4	4	4		1 to 5
Grass land& planted forest LUS	Sandy Loam						19.6	18.2	18.2	21	19.25	11.1875	20 to 30
	Silt Loam	11.2	13.25	22	17	15.86	11	11	10	7.8	9.95		10 to 20
	Clay Loam	7.7	10	9.2	7.5	8.6	6.2	8.9	7.25	9.5	7.96		5 to 10
	Clay						6	6.9	5	4.1	5.5		1 to 5
EBLUS	Sandy Loam						22	21.6	26.5	20.1	22.55	12.8125	20 to 30
	Silt Loam	15.5	11.5	9.75	13.75	12.63	15.9	18.5	18.2	15.5	17.03		10 to 20
	Clay Loam	11	11.3	11.2	10	10.88	8.6	9.2	11	8.7	9.38		5 to 10
	Clay						5.5	2.7	3.5	6	4.43		1 to 5
Natural Forest LUS	Sandy Loam						23	21	26	20.5	22.63	12.9675	20 to 30
	Silt Loam	17.3	18.3	13.1	12.3	15.25	16.5	14	18	13.5	15.5		10 to 20
	Clay Loam	12.2	6.8	11	8.5	9.63	14	9.8	10	7.59	10.35		5 to 10
	Clay						4.7	5	4.48	3.65	4.46		1 to 5

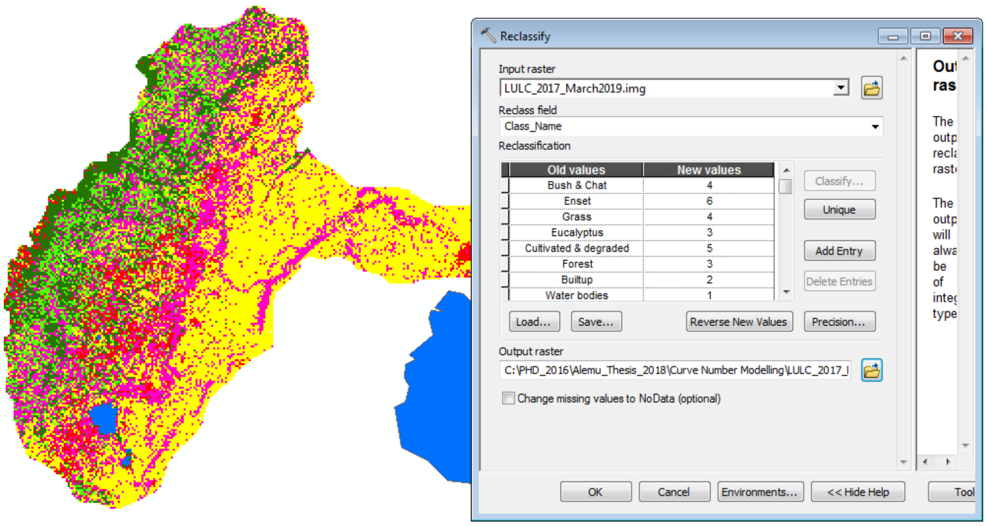

Figure C-2: Reclassification window with assigned new values

Hydrological soil group can be derived from soil properties as shown in Table C.3

Table C.3: Hydrological soil group (HSG) derived from soil properties (ERA, 2013, Modified from USDA 1986 and NEH-4 1997 lookup tables)

HSG	USDA soil texture class	Soil content	Property
A	1,2,3	Sand, loamy sand or sandy loam types of soils	Low runoff potential and high infiltration rates even when thoroughly wetted; consist chiefly of deep, well to excessively drained sands or gravels
B	4,5,6	Silt, loam or silt	Moderate infiltration rate and consist of soils chiefly with moderately fine to moderately coarse textures
C	7	Sandy clay loam	Low infiltration rates when thoroughly wetted and consist chiefly of soils with moderately fine to fine structure
D	8,9,10,11,12	Clay loam, silty clay loam, sandy clay, silty clay or clay	Highest runoff potential, very low infiltration rates when thoroughly wetted and consist chiefly of clay soils
0	0	Water bodies	N/A
-1	13	Permanent ice/snow	N/A

Table C.4: Sub-watershed based CN of EBLUS in the upper and middle zones

Sub-watershed	CN	S	IA	Zone
W2510	73.16	93.1843	18.6369	U19
W2530	64.18	141.762	28.3524	U18
W2620	71.79	157.269	31.4539	U17
W2610	61.76	125.501	25.1002	U16
W2860	73.21	130.674	26.1347	U15
W2750	66.93	148.983	29.7965	U14
W3080	66.03	138.946	27.7891	U13
W3300	63.03	26.2295	5.2459	U12
W3190	64.64	136.169	27.2338	U11
W3690	65.1	118.981	23.7962	U10
W3700	82.85	113.956	22.7912	U9
W3910	68.1	88.1336	17.6267	U8
W4030	69.03	76.9878	15.3976	U7
W4180	74.24	53.2828	10.6566	U6
W4290	76.74	43.7028	8.74055	U5
W4620	85.32	42.2099	8.44198	U4
W4590	90.64	99.8097	19.9619	U3
W4730	82.66	92.9471	18.5894	U2
W4720	85.75	65.7784	13.1557	U1
W4250	84.33	62.5898	12.518	M9
W4130	85.53	76.9446	15.3889	M8
W4400	85.4	49.2474	9.84947	M7
W3790	85.71	54.2524	10.8505	M6
W3410	82.4	42.3482	8.46963	M5
W3280	83.76	43.4239	8.68478	M4
W2890	76.75	47.1977	9.43954	M3
W2970	80.23	42.9718	8.59436	M2
W2640	79.43	47.3049	9.46097	M1

Table C.5: Harmonized world soil database (HWSD) extracted for Meki river watershed

Soil Mapping Unit	16982	16903	16807	16654	16855		
Dominant Soil Group	**FL - Fluvisols**	**AN – Andosols**	**PH - Phaeozems**	**LP - Leptosols**	**VR - Vertisols**		
Sequence	1	1	1	1	1	2	3
Share in Soil Mapping Unit (%)	100	80	100	90	40	40	10
Database ID	17567	17385	17178	16795	17276	17277	17278
Soil Unit Symbol (FAO 90)	FLe	ANz	PHl	LPq	VRe	NTu	LVx
Soil unit Name (FAO 90)	Eutric Fluvisols	Vitric Andosols	Luvic Phaeozems	Lithic Leptosols	Eutric Vertisols	Humic Nitisols	Chromic Luvisols
Topsoil Texture	Medium	Medium	Medium	Medium	Fine	Fine	Medium
Reference Soil Depth (cm)	100	100	100	10	100	100	100
Drainage class (0-0.5% slope)	Moderately Well	Moderately Well	Moderately Well	Imperfectly	Poor	Moderately Well	Moderately Well
AWC (mm)	150	150	150	15	125	150	150
Gelic Properties	No	No	No	No	No	No	No
Vertic Properties	No	No	No	No	Yes	No	No
Petric Properties	No	No	No	No	No	No	No
Topsoil Sand Fraction (%)	44	61	32	43	21	24	51
Topsoil Silt Fraction (%)	33	32	36	29	25	27	22
Topsoil Clay Fraction (%)	23	7	32	28	54	49	27
Topsoil USDA Texture Classification	loam	sandy loam	clay loam	clay loam	clay (light)	clay (light)	sandy clay loam
Topsoil Reference Bulk Density (kg/dm3)	1.39	1.6	1.32	1.36	1.22	1.24	1.38
Topsoil Bulk Density (kg/dm3)	1.33	0.97	1.28	1.31	1.51	1.18	1.45

Topsoil Gravel Content (%)	1	1	1	32	1	1	1
Topsoil Organic Carbon (% weight)	0.73	3.43	1.71	0.39	1.07	2.45	0.63
Topsoil pH (H2O)	7	5.8	6.2	7.5	6.9	5.3	6.4
Topsoil CEC (clay) (cmol/kg)	50	70	50	51	68	21	31
Topsoil CEC (soil) (cmol/kg)	14	17	22	16	40	20	10
Topsoil Base Saturation (%)	91	45	85	100	100	27	85
Topsoil TEB (cmol/kg)	12.7	7.7	18.7	16	40	5.4	8.5
Topsoil Calcium Carbonate (% weight)	0.8	0	0	3.1	0.4	0	0
Topsoil Gypsum (% weight)	0.1	0	0	0.1	0.1	0	0
Topsoil Sodicity (ESP) (%)	2	1	1	1	1	1	2
Topsoil Salinity (ECe) (dS/m)	0.1	0	0	0.4	0.3	0	0
Database ID	17567	17385	17178	16795	17276	17277	17278
Subsoil Sand Fraction (%)	46	68	28	-	20	18	45
Subsoil Silt Fraction (%)	31	26	33	-	24	21	21
Subsoil Clay Fraction (%)	23	6	39	-	56	61	34
Subsoil USDA Texture Classification	loam	sandy loam	clay loam	-	clay (light)	clay(heavy)	clay loam
Subsoil Reference Bulk Density (kg/dm3)	1.39	1.63	1.28	-	1.21	1.2	1.33
Subsoil Bulk Density (kg/dm3)	1.4	1	1.37	-	1.58	1.25	1.5

Subsoil Gravel Content (%)	1	1	1	-	1	1	1
Subsoil Organic Carbon (% weight)	0.32	1.48	0.71	-	0.56	0.96	0.35
Subsoil pH (H2O)	7.3	6.1	6.8	-	7.5	5.4	6.5
Subsoil CEC (clay) (cmol/kg)	49	131	58	-	70	16	31
Subsoil CEC (soil) (cmol/kg)	13	13	25	-	41	20	12
Subsoil Base Saturation (%)	94	75	95	-	100	29	84
Subsoil TEB (cmol/kg)	12.2	9.8	23.8	-	41	5.8	10.1
Subsoil Calcium Carbonate (% weight)	1.8	0	0.4	-	1.4	0	0.1
Subsoil Gypsum (% weight)	0.1	0	0.1	-	0.1	0	0
Subsoil Sodicity (ESP) (%)	2	2	2	-	2	1	1
Subsoil Salinity (ECe) (dS/m)	0.1	0	0.1	-	0.3	0	0

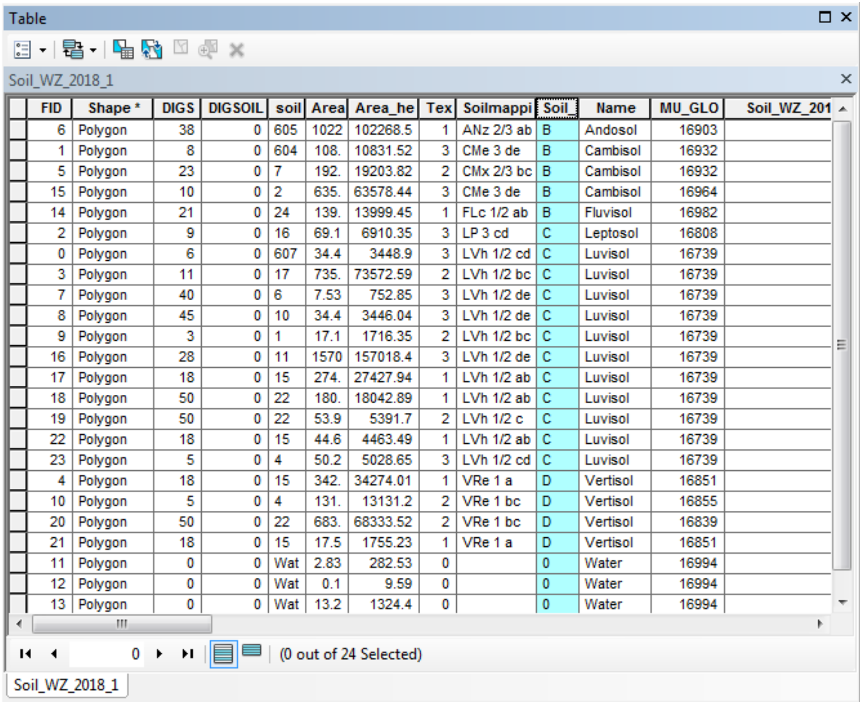

Table

Soil_WZ_2018_1

FID	Shape *	DIGS	DIGSOIL	soil	Area	Area_he	Tex	Soilmappi	Soil_	Name	MU_GLO	Soil_WZ_201
6	Polygon	38	0	605	1022	102268.5	1	ANz 2/3 ab	B	Andosol	16903	
1	Polygon	8	0	604	108.	10831.52	3	CMe 3 de	B	Cambisol	16932	
5	Polygon	23	0	7	192.	19203.82	2	CMx 2/3 bc	B	Cambisol	16932	
15	Polygon	10	0	2	635.	63578.44	3	CMe 3 de	B	Cambisol	16964	
14	Polygon	21	0	24	139.	13999.45	1	FLc 1/2 ab	B	Fluvisol	16982	
2	Polygon	9	0	16	69.1	6910.35	3	LP 3 cd	C	Leptosol	16808	
0	Polygon	6	0	607	34.4	3448.9	3	LVh 1/2 cd	C	Luvisol	16739	
3	Polygon	11	0	17	735.	73572.59	2	LVh 1/2 bc	C	Luvisol	16739	
7	Polygon	40	0	6	7.53	752.85	3	LVh 1/2 de	C	Luvisol	16739	
8	Polygon	45	0	10	34.4	3446.04	3	LVh 1/2 de	C	Luvisol	16739	
9	Polygon	3	0	1	17.1	1716.35	2	LVh 1/2 bc	C	Luvisol	16739	
16	Polygon	28	0	11	1570	157018.4	3	LVh 1/2 de	C	Luvisol	16739	
17	Polygon	18	0	15	274.	27427.94	1	LVh 1/2 ab	C	Luvisol	16739	
18	Polygon	50	0	22	180.	18042.89	1	LVh 1/2 ab	C	Luvisol	16739	
19	Polygon	50	0	22	53.9	5391.7	2	LVh 1/2 c	C	Luvisol	16739	
22	Polygon	18	0	15	44.6	4463.49	1	LVh 1/2 ab	C	Luvisol	16739	
23	Polygon	5	0	4	50.2	5028.65	3	LVh 1/2 cd	C	Luvisol	16739	
4	Polygon	18	0	15	342.	34274.01	1	VRe 1 a	D	Vertisol	16851	
10	Polygon	5	0	4	131.	13131.2	2	VRe 1 bc	D	Vertisol	16855	
20	Polygon	50	0	22	683.	68333.52	2	VRe 1 bc	D	Vertisol	16839	
21	Polygon	18	0	15	17.5	1755.23	1	VRe 1 a	D	Vertisol	16851	
11	Polygon	0	0	Wat	2.83	282.53	0		0	Water	16994	
12	Polygon	0	0	Wat	0.1	9.59	0		0	Water	16994	
13	Polygon	0	0	Wat	13.2	1324.4	0		0	Water	16994	

0 (0 out of 24 Selected)

Soil_WZ_2018_1

Figure C-3: Hydrologic soil group (HSG) assignment

Table C.6: Standard curve number matrix assignment for different hydrologic soil groups

Name	MU_GLOBAL	PctA	PctB	PctC	PctD
Luvisol	16739	0	0	100	0
Cambisol	16932	0	100	0	0
Leptosol	16808	0	0	100	0
Vertisol	16851	0	0	0	100
Andosol	16903	0	100	0	0
Fluvisol	16982	0	100	0	0

Table

Meki_Soil_LU

Are	Text	Soilm	Name	FID_lulc_	FID_Soil_W	MU_GLOBA	HSG	HYDROID	PctA	PctB	PctC	PctD
0	0			0	-999	16739	C	2	0	0	0	0
0	0			1	-999	16739	C	2	0	0	0	0
0	0			2	-999	16739	C	2	0	0	0	0
0	0			4	-999	16739	C	2	0	0	0	0
0	0			6	-999	16739	C	2	0	0	0	0
0	0			7	-999	16739	C	2	0	0	0	0
0	0			10	-999	16739	C	2	0	0	0	0
0	0			11	-999	16739	C	2	0	0	0	0
0	0			14	-999	16739	C	2	0	0	0	0
0	0			15	-999	16739	C	2	0	0	0	0
0	0			16	-999	16739	C	2	0	0	0	0
0	0			19	-999	16739	C	2	0	0	0	0
0	0			22	-999	16739	C	2	0	0	0	0
0	0			23	-999	16739	C	2	0	0	0	0
0	0			24	-999	16739	C	2	0	0	0	0
0	0			25	-999	16739	C	2	0	0	0	0
0	0			32	-999	16739	C	2	0	0	0	0
0	0			33	-999	16739	C	2	0	0	0	0
0	0			46	-999	16739	C	2	0	0	0	0
0	0			47	-999	16739	C	2	0	0	0	0
0	0			48	-999	16739	C	2	0	0	0	0
0	0			49	-999	16739	C	2	0	0	0	0

0 (0 out of 9219 Selected)

Meki_Soil_LU

Figure C-4: Nearest neighbor value assignment of hydrological and soil characteristics for slivers

Table

cnlookup

Rowid	OBJEC	FIEL	LUVALUE	DESCRIPTION	A	B	C	D
1	0	0	1	Water bodies	100	100	100	100
3	0	0	2	Builtup	77	85	90	92
5	0	0	3	Eucalyptus/Forest	36	60	73	79
7	0	0	4	Bush & Chat/Grass	49	69	79	84
9	0	0	5	Cultivated & degraded	67	78	85	89
11	0	0	6	Enset	39	52	58	62

1 (0 out of 6 Selected)

cnlookup | LULC_2017_March2019Recl.img

Figure C-5: Lookup table considering Enset-Based land use system

Table

CNLookup_NoEnset

OID	OBJECTID	FIELD1	LUVALUE	DESCRIPTIO	A	B	C	D
1	0	0	5	Cultivated & degraded	67	78	85	89
4	0	0	4	Bush & Chat/Grass	49	69	79	84
3	0	0	3	Eucalyptus/Forest	36	60	73	79
2	0	0	2	Builtup	77	85	90	92
5	0	0	1	Water bodies	10	10	10	10

1 (1 out of 6 Selected)

CNLookup_NoEnset

Figure C-6: Lookup table without considering Enset-Based land use system

D. Appendix 4: Surface runoff modeling

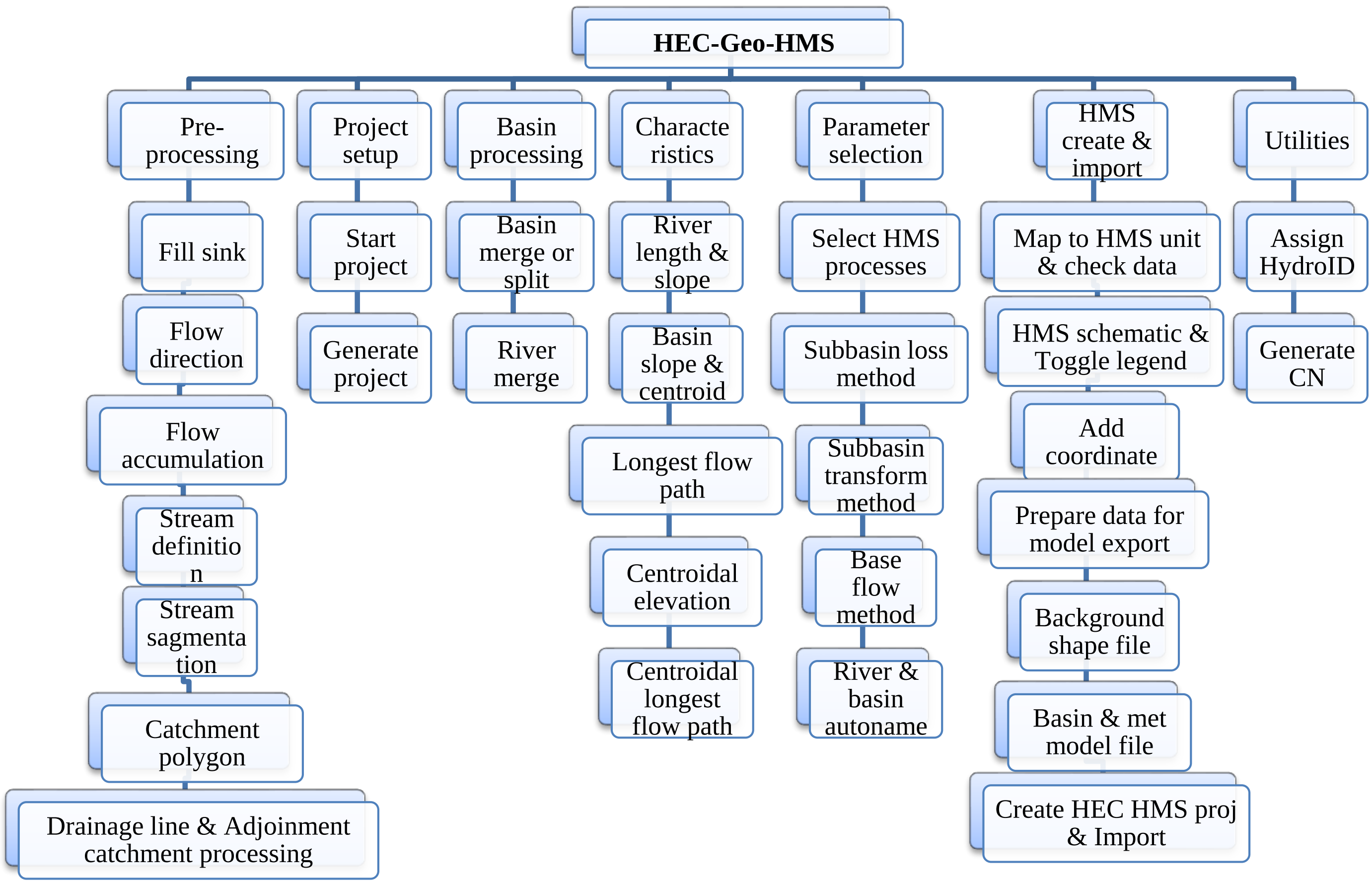

Figure D-1: Flowcharts of HEC-GeoHMS Model

a. Surface runoff modeling Framework

Table D.1: Comparison of simulation years for calibration and validation

	1985-1989	1990-1994	1995-1999	2000-2004	Best Range
Peak flow simulated (m3/s)	173.5.5	236	168.8	117.6	
Nash	-1.357	-5.172	-7.809	-1.522	>0.50
Pbias	82.58	156	225.37	77.57	10%
RMSEStdDev	1.5	2.5	3	1.6	<1
Peak flow observed (m3/s)	118.6	139.6	55.1	64.2	
Peak time of simulation	18-Aug-87	18-Aug-93	22-Jul-96	26-Jun-01	
Peak time of observed	17-Aug-87	15-Aug-93	21-Aug-96	14-Jul-01	
Remark	1	3	4	2	

Table D.2: Sensitivity assessment of parameters in Meki river watershed

A. Curve number assessment values for sub-watersheds

CN	-20%	-15%	-10%	-5%	0	5%	10%	15%	20%
W2530	47.2	50.15	53.1	56.05	59	61.95	64.9	67.85	70.8
W2510	55.776	59.262	62.748	66.234	69.72	73.206	76.692	80.178	83.664
W2620	58.8	62.475	66.15	69.825	73.5	77.175	80.85	84.525	88.2
W2610	46.28	49.1725	52.065	54.9575	57.85	60.7425	63.635	66.5275	69.42
W2860	54.888	58.3185	61.749	65.1795	68.61	72.0405	75.471	78.9015	82.332
W2750	47.448	50.4135	53.379	56.3445	59.31	62.2755	65.241	68.2065	71.172
W3080	61.68	65.535	69.39	73.245	77.1	80.955	84.81	88.665	92.52
W2890	56.64	60.18	63.72	67.26	70.8	74.34	77.88	81.42	84.96
W2640	62.08	65.96	69.84	73.72	77.6	81.48	85.36	89.24	93.12
W2970	62.08	65.96	69.84	73.72	77.6	81.48	85.36	89.24	93.12
W3280	64.08	68.085	72.09	76.095	80.1	84.105	88.11	92.115	96.12
W3190	47.52	50.49	53.46	56.43	59.4	62.37	65.34	68.31	71.28
W3300	45.68	48.535	51.39	54.245	57.1	59.955	62.81	65.665	68.52
W3410	57.544	61.1405	64.737	68.3335	71.93	75.5265	79.123	82.7195	86.316
W3910	51.2	54.4	57.6	60.8	64	67.2	70.4	73.6	76.8
W4030	51.28	54.485	57.69	60.895	64.1	67.305	70.51	73.715	76.92
W3690	50.416	53.567	56.718	59.869	63.02	66.171	69.322	72.473	75.624
W3700	61.44	65.28	69.12	72.96	76.8	80.64	84.48	88.32	92.16
W3790	65.632	69.734	73.836	77.938	82.04	86.142	90.244	94.346	98.448
W4720	66.992	71.179	75.366	79.553	83.74	87.927	92.114	96.301	100.488
W4730	62.4	66.3	70.2	74.1	78	81.9	85.8	89.7	93.6
W4590	66.992	71.179	75.366	79.553	83.74	87.927	92.114	96.301	100.488
W4620	64.104	68.1105	72.117	76.1235	80.13	84.1365	88.143	92.1495	96.156
W4290	57.44	61.03	64.62	68.21	71.8	75.39	78.98	82.57	86.16
W4180	55.88	59.3725	62.865	66.3575	69.85	73.3425	76.835	80.3275	83.82
W4400	64.384	68.408	72.432	76.456	80.48	84.504	88.528	92.552	96.576
W4130	67.84	72.08	76.32	80.56	84.8	89.04	93.28	97.52	101.76
W4250	67.288	71.4935	75.699	79.9045	84.11	88.3155	92.521	96.7265	100.932
W3730	67.44	71.655	75.87	80.085	84.3	88.515	92.73	96.945	101.16
W4070	65.056	69.122	73.188	77.254	81.32	85.386	89.452	93.518	97.584
W3400	62.528	66.436	70.344	74.252	78.16	82.068	85.976	89.884	93.792
W3180	64.08	68.085	72.09	76.095	80.1	84.105	88.11	92.115	96.12
W3260	64.888	68.9435	72.999	77.0545	81.11	85.1655	89.221	93.2765	97.332
W3460	62.64	66.555	70.47	74.385	78.3	82.215	86.13	90.045	93.96

B. Lag time manual calibration values for sub-watersheds

LT	-20%	-15%	-10%	-5%	0	5%	10%	15%	20%
W2530	58.97909	62.66528	66.35148	70.03767	73.72386	77.41005	81.09625	84.78244	88.46863
W2510	148.4343	157.7114	166.9886	176.2657	185.5429	194.82	204.0972	213.3743	222.6514
W2620	98.68069	104.8482	111.0158	117.1833	123.3509	129.5184	135.686	141.8535	148.021
W2610	60.41077	64.18645	67.96212	71.7378	75.51347	79.28914	83.06482	86.84049	90.61616
W2860	112.1896	119.2015	126.2134	133.2252	140.2371	147.2489	154.2608	161.2726	168.2845
W2750	68.31263	72.58217	76.85171	81.12125	85.39079	89.66033	93.92987	98.19941	102.469
W3080	91.8473	97.58775	103.3282	109.0687	114.8091	120.5496	126.29	132.0305	137.7709
W2890	177.5515	188.6485	199.7454	210.8424	221.9394	233.0363	244.1333	255.2303	266.3272
W2640	200.4616	212.9905	225.5193	238.0482	250.577	263.1059	275.6347	288.1636	300.6924
W2970	145.362	154.4472	163.5323	172.6174	181.7026	190.7877	199.8728	208.9579	218.0431
W3280	181.8398	193.2048	204.5698	215.9348	227.2997	238.6647	250.0297	261.3947	272.7597
W3190	151.1485	160.5953	170.0421	179.4889	188.9357	198.3825	207.8293	217.276	226.7228
W3300	105.8933	112.5116	119.13	125.7483	132.3666	138.985	145.6033	152.2216	158.84
W3410	245.9743	261.3477	276.7211	292.0945	307.4679	322.8413	338.2147	353.5881	368.9615
W3910	123.3519	131.0614	138.7709	146.4804	154.1899	161.8994	169.6089	177.3184	185.0279
W4030	130.9921	139.1791	147.3661	155.5531	163.7401	171.9271	180.1141	188.3011	196.4881
W3690	93.13858	98.95974	104.7809	110.6021	116.4232	122.2444	128.0655	133.8867	139.7079
W3700	170.5474	181.2066	191.8658	202.525	213.1843	223.8435	234.5027	245.1619	255.8211
W3790	322.5783	342.7394	362.9006	383.0617	403.2229	423.384	443.5452	463.7063	483.8674
W4720	208.3676	221.3905	234.4135	247.4365	260.4594	273.4824	286.5054	299.5284	312.5513
W4730	240.2005	255.213	270.2255	285.238	300.2506	315.2631	330.2756	345.2882	360.3007
W4590	241.9801	257.1039	272.2277	287.3514	302.4752	317.5989	332.7227	347.8465	362.9702
W4620	190.1747	202.0606	213.9465	225.8324	237.7183	249.6043	261.4902	273.3761	285.262
W4290	193.8705	205.9874	218.1043	230.2212	242.3381	254.455	266.5719	278.6888	290.8057
W4180	161.9959	172.1206	182.2454	192.3701	202.4949	212.6196	222.7443	232.8691	242.9938

W4400	498.5512	529.7106	560.8701	592.0295	623.189	654.3484	685.5079	716.6673	747.8268
W4130	752.001	799.001	846.0011	893.0012	940.0012	987.0013	1034.001	1081.001	1128.001
W4250	276.8112	294.1119	311.4126	328.7133	346.0139	363.3146	380.6153	397.916	415.2167
W3730	373.1331	396.4539	419.7748	443.0956	466.4164	489.7372	513.058	536.3789	559.6997
W4070	821.6541	873.0075	924.3609	975.7142	1027.068	1078.421	1129.774	1181.128	1232.481
W3400	210.8416	224.0192	237.1968	250.3744	263.552	276.7296	289.9072	303.0848	316.2624
W3180	232.7934	247.343	261.8925	276.4421	290.9917	305.5413	320.0909	334.6405	349.19
W3260	282.0201	299.6464	317.2726	334.8989	352.5251	370.1514	387.7776	405.4039	423.0301
W3460	700.382	744.1559	787.9297	831.7036	875.4775	919.2514	963.0252	1006.799	1050.573

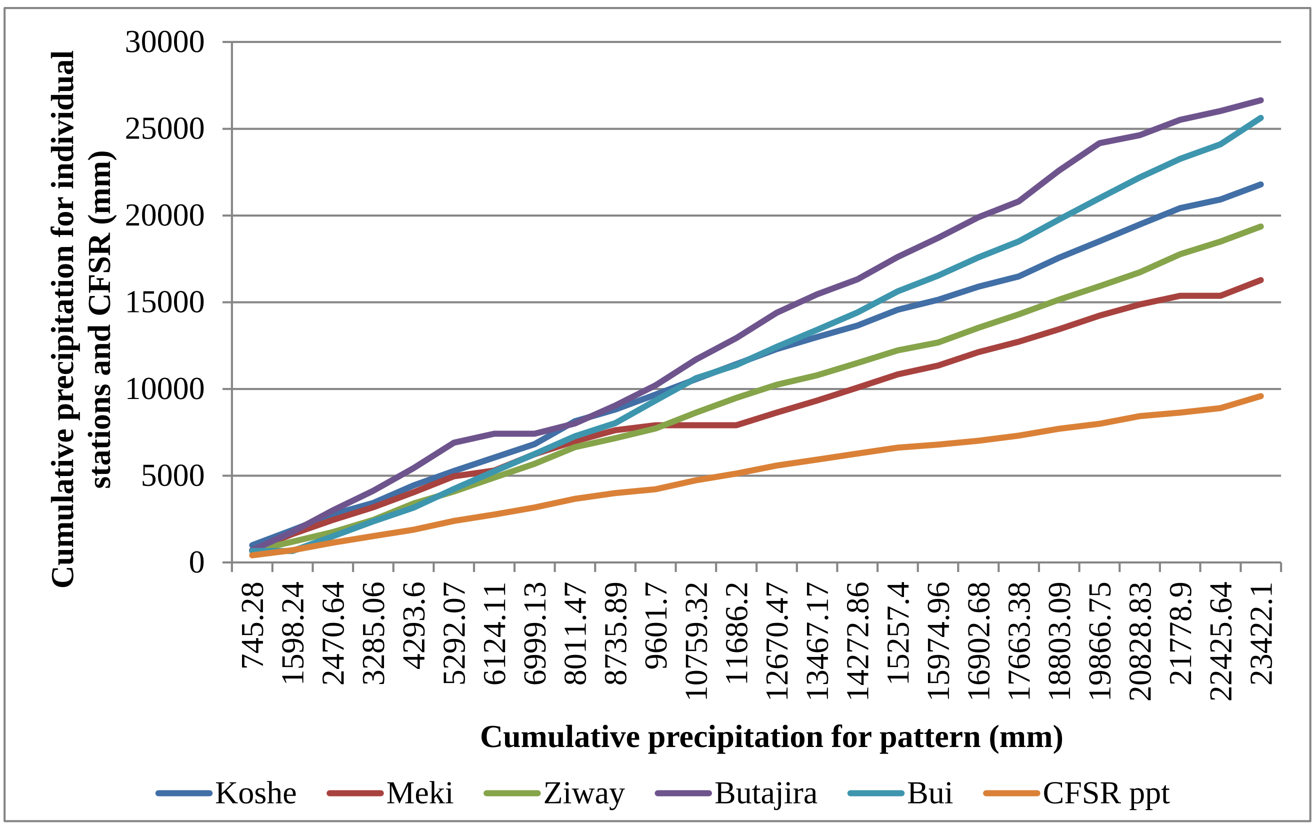

Figure D-2: Double mass curve of stations in the watershed

C. Sub-watershed based transform parameters in Meki river watershed

Worksheet for computation of time of travel according to TR-55 methodology											
Blue - GIS defined, Green - user specified, White and yellow - calculated, Red - final result											
Watershed Name	**W2510**	**W2530**	**W2610**	**W2620**	**W2640**	**W2750**	**W2860**	**W2890**	**W2970**	**W3080**	**W3180**
Watershed ID	**251**	**253**	**261**	**262**	**264**	**275**	**286**	**289**	**297**	**308**	**318**
Sheet Flow Characteristics											
Manning's Roughness Coefficient	0.25	0.25	0.25	0.25	0.25	0.25	0.25	0.25	0.25	0.25	0.25
Flow Length (ft)	100	100	100	100	100	99.9999	99.9999	100	99.9999	99.9999	99.9999
Land Slope (ft/ft)	0.1969	0.2297	0.3937	0.1312	0.6562	0.7546	-0.0984	0.1969	0.1969	0.3937	0.4593
Sheet Flow Tt (hr)	0.01	0.01	0.00	0.01	0.01	0.01	0.01	0.01	0.01	0.00	0.01
Shallow Concentrated Flow Characteristics											
Surface Description (1 - unpaved, 2 - paved)	1	1	1	1	1	1	1	1	1	1	1
Flow Length (ft)	14817	9647	12206	12606	14522	16049.993	15416.0468	16253.552	13114.2756	13738.0846	17101.184
Watercourse Slope (ft/ft)	0.0777	0.1122	0.1296	0.058	0.0438	0.1069	0.0536	0.0357	0.0368	0.2233	0.0875
Average Velocity - computed (ft/s)	4.50	5.40	5.81	3.89	3.38	5.28	3.74	3.05	3.10	7.62	4.77
Shallow Concentrated Flow Tt (hr)	0.92	0.50	0.58	0.90	1.19	0.85	1.15	1.48	1.18	0.50	1.00
Channel Flow Characterisitics											
Cross-sectional Flow Area (ft2)	20	20	20	20	20	20	20	20	20	20	20
Wetted Perimeter (ft)	20	20	20	20	20	20	20	20	20	20	20
Hydraulic Radius - computed (ft)	1.00	1.00	1.00	1.00	1.00	1.00	1.00	1.00	1.00	1.00	1.00
Channel Slope (ft/ft)	0.0305	0.0582	0.079	0.0371	0.0106	0.0758	0.0535	0.0051	0.0208	0.0369	0.0114
Manning's Roughness Coefficient	0.03	0.03	0.03	0.03	0.03	0.03	0.03	0.03	0.03	0.03	0.03
Average Velocity - computed (ft/s)	8.67	11.98	13.96	9.57	5.11	13.67	11.49	3.55	7.16	9.54	5.30
Flow Length (ft)	59209	26794	28165	33331	47900	22086.1816	40463.8079	24027.3689	40642.9238	42555.4613	65168.5285
Channel Flow Tt (hr)	1.90	0.62	0.56	0.97	2.60	0.45	0.98	1.88	1.58	1.24	3.41
Watershed Time of travel (hr)	**2.82**	**1.12**	**1.15**	**1.88**	**3.80**	**1.30**	**2.13**	**3.37**	**2.76**	**1.74**	**4.41**

Sheet Flow Characteristics																							
Manning's Roughness Coefficient	0.25	0.25	0.25	0.25	0.25	0.25	0.25	0.25	0.25	0.25	0.25	0.25	0.25	0.25	0.25	0.25	0.25	0.25	0.25	0.25	0.25	0.25	0.25
Flow Length (ft)	100	100	100	100	100	99.9999	99.9999	99.9999	100	100	99.9999	99.9999	99.9999	100	99.9999	99.9999	99.9999	99.9999	99.9999	99.9999	99.9999	99.9999	99.9999

Land Slope (ft/ft)	0.164	0.1312	0.3937	0.2625	0.5249	0.3937	0.1312	0.3937	0.2953	0.164	0.5249	0.3937	0.3609	0.164	0.2625	0.3937	0.0984	0.2297	0.8202	0.1969	0.3281	0.1312	0.1312
Sheet Flow Tt (hr)	0.000	0.002	0.001	0.000	0.001	0.001	0.002	0.000	0.001	0.02	0.01	0.00	0.01	0.01	0.01	0.01	0.01	0.01	0.01	0.01	0.02	0.01	0.01	0.01
Shallow Concentrated Flow Characteristics																							
Surface Description	1	1	1	1	1	1	1	1	1	1	1	1	1	1	1	1	1	1	1	1	1	1	1
Flow Length (ft)	13359.5756	21975.3642	20729.8565	13121.4348	17587.5885	22562.5205	24994.5346	16361.4633	12532.1934	20953.67	21078.85	12319.11	10694.46	15436.3	14929.64	20297.39	17312.78	15214.57	20216.9	15567.41	16005.3	13290.44	16693.18
Watercourse Slope (ft/ft)	0.1869	0.0131	0.06	0.2258	0.0653	0.0302	0.0066	0.165	0.0134	0.0096	0.0416	0.1888	0.108	0.0227	0.0176	0.0923	0.0174	0.0634	0.0508	0.0076	0.0924	0.0252	0.1099
Average Velocity - computed (ft/s)	6.98	1.85	3.95	7.67	4.12	2.80	1.31	6.55	1.87	1.58	3.29	7.01	5.30	2.43	2.14	4.90	2.13	4.06	3.64	1.41	4.90	2.56	5.35
Shallow Concentrated Flow Tt (hr)	0.53	3.31	1.46	0.48	1.18	2.24	5.30	0.69	1.86	3.68	1.78	0.49	0.56	1.76	1.94	1.15	2.26	1.04	1.54	3.07	0.91	1.44	0.87
Channel Flow Characterisitics																							
A (ft2)	20	20	20	20	20	20	20	20	20	20	20	20	20	20	20	20	20	20	20	20	20	20	20
P (ft)	20	20	20	20	20	20	20	20	20	20	20	20	20	20	20	20	20	20	20	20	20	20	20
R (ft)	1.00	1.00	1.00	1.00	1.00	1.00	1.00	1.00	1.00	1.00	1.00	1.00	1.00	1.00	1.00	1.00	1.00	1.00	1.00	1.00	1.00	1.00	1.00
S (ft/ft)	0.0387	0.002	0.0105	0.0462	0.0095	0.0073	0.0003	0.0441	0.0139	0.0023	0.006	0.0328	0.0406	0.0004	0.0007	0.04	0.0098	0.0407	0.0012	0.0035	0.0146	0.0082	0.0223

Manning's Roughness Coefficient	0.03	0.03	0.03	0.03	0.03	0.03	0.03	0.03	0.03	0.03	0.03	0.03	0.03	0.03	0.03	0.03	0.03	0.03	0.03	0.03	0.03	0.03	0.03
Average Velocity - computed (ft/s)	9.77	2.22	5.09	10.68	4.84	4.24	0.86	10.43	5.86	2.38	3.85	9.00	10.01	0.99	1.31	9.93	4.92	10.02	1.72	2.94	6.00	4.50	7.42
Flow Length (ft)	81978.1445	16278.2189	36403.5437	58806.2259	48940.7236	37020.8077	24676.1294	40196.1493	28799.5698	29026.73	59971.88	59845.21	69195.69	49340.71	58209.94	68583.49	52800.37	94922	48918.63	15958.11	58230.33	40557.99	98320.03
Channel Flow Tt (hr)	2.33	2.04	1.99	1.53	2.81	2.42	7.97	1.07	1.37	3.39	4.33	1.85	1.92	13.80	12.30	1.92	2.98	2.63	7.90	1.51	2.70	2.50	3.68
Watershed Time of travel (hr)	**2.87**	**5.36**	**3.45**	**2.01**	**4.00**	**4.67**	**13.29**	**1.77**	**3.24**	**7.08**	**6.12**	**2.34**	**2.49**	**15.57**	**14.26**	**3.07**	**5.26**	**3.68**	**9.45**	**4.60**	**3.61**	**3.96**	**4.55**

D. Base flow nominal model parameters with ratio to peak of 0.1

SWS	Expected flow	Initial discharge	SWS	Expected flow	Initial discharge
W2510	20.19	2.02	W3460	17.21	1.72
W2530	22.36	2.24	W3690	24.61	2.46
W2610	17.87	1.79	W3700	10.15	1.015
W2620	18.45	1.84	W3730	16.36	1.64
W2640	20.50	2.05	W3790	25.58	2.56
W2750	12.98	1.3	W3910	39.45	3.95
W2860	21.51	2.15	W4030	15.58	1.56
W2890	10.39	1.04	W4070	24.61	2.46
W2970	20.35	2.03	W4130	24.46	2.45
W3080	22.98	2.3	W4180	40.73	4.07
W3180	39.99	4	W4250	23.41	2.34
W3190	33.33	3.33	W4290	48.33	4.83
W3260	11.59	1.16	W4400	40.62	4.06
W3280	26.04	2.60	W4590	9.42	0.94
W3300	21.86	2.19	W4620	37.79	3.78
W3400	30.66	3.07	W4720	47.36	4.74
W3410	20.31	2.03	W4730	43.56	4.36

E. Base flow initial discharge values for sub-watersheds

	-20%	-15%	-10%	-5%	0	5%	10%	15%	20%
W2530	1.792	1.904	2.016	2.128	2.24	2.352	2.464	2.576	2.688
W2510	1.616	1.717	1.818	1.919	2.02	2.121	2.222	2.323	2.424
W2620	1.476	1.568	1.6605	1.75	1.845	1.937	2.03	2.122	2.214
W2610	1.432	1.5215	1.611	1.7005	1.79	1.8795	1.969	2.0585	2.148
W2860	1.72	1.8275	1.935	2.0425	2.15	2.2575	2.365	2.4725	2.58
W2750	1.04	1.105	1.17	1.235	1.3	1.365	1.43	1.495	1.56
W3080	1.84	1.955	2.07	2.185	2.3	2.415	2.53	2.645	2.76
W2890	0.832	0.884	0.936	0.988	1.04	1.092	1.144	1.196	1.248
W2640	1.64	1.7425	1.845	1.9475	2.05	2.1525	2.255	2.3575	2.46
W2970	1.624	1.7255	1.827	1.9285	2.03	2.1315	2.233	2.3345	2.436
W3280	2.08	2.21	2.34	2.47	2.6	2.73	2.86	2.99	3.12
W3190	2.664	2.8305	2.997	3.1635	3.33	3.4965	3.663	3.8295	3.996
W3300	1.76	1.87	1.98	2.09	2.2	2.31	2.42	2.53	2.64
W3410	1.624	1.7255	1.827	1.9285	2.03	2.1315	2.233	2.3345	2.436
W3910	3.16	3.3575	3.555	3.7525	3.95	4.1475	4.345	4.5425	4.74
W4030	1.248	1.326	1.404	1.482	1.56	1.638	1.716	1.794	1.872
W3690	1.968	2.091	2.214	2.337	2.46	2.583	2.706	2.829	2.952
W3700	0.816	0.867	0.918	0.969	1.02	1.071	1.122	1.173	1.224
W3790	2.048	2.176	2.304	2.432	2.56	2.688	2.816	2.944	3.072
W4720	3.792	4.029	4.266	4.503	4.74	4.977	5.214	5.451	5.688
W4730	3.488	3.706	3.924	4.142	4.36	4.578	4.796	5.014	5.232
W4590	0.7536	0.8007	0.8478	0.8949	0.942	0.9891	1.0362	1.0833	1.13
W4620	3.024	3.213	3.402	3.591	3.78	3.969	4.158	4.347	4.536
W4290	3.864	4.1055	4.347	4.5885	4.83	5.0715	5.313	5.5545	5.796
W4180	3.2584	3.462	3.6657	3.869	4.073	4.277	4.4803	4.68	4.89
W4400	3.248	3.451	3.654	3.857	4.06	4.263	4.466	4.669	4.872
W4130	1.96	2.0825	2.205	2.3275	2.45	2.5725	2.695	2.8175	2.94
W4250	1.872	1.989	2.106	2.223	2.34	2.457	2.574	2.691	2.808
W3730	1.312	1.394	1.476	1.558	1.64	1.722	1.804	1.886	1.968
W4070	1.968	2.091	2.214	2.337	2.46	2.583	2.706	2.829	2.952
W3400	2.456	2.6095	2.763	2.9165	3.07	3.2235	3.377	3.5305	3.684
W3180	3.2	3.4	3.6	3.8	4	4.2	4.4	4.6	4.8
W3260	0.928	0.986	1.044	1.102	1.16	1.218	1.276	1.334	1.392
W3460	1.376	1.462	1.548	1.634	1.72	1.806	1.892	1.978	2.064

F. Base flow recession constant values for sub-watersheds

	-20%	-15%	-10%	-5%	0	5%	10%	15%	20%
W2530	0.64	0.68	0.72	0.76	0.8	0.84	0.88	0.92	0.96
W2510	0.64	0.68	0.72	0.76	0.8	0.84	0.88	0.92	0.96
W2620	0.64	0.68	0.72	0.76	0.8	0.84	0.88	0.92	0.96
W2610	0.64	0.68	0.72	0.76	0.8	0.84	0.88	0.92	0.96
W2860	0.64	0.68	0.72	0.76	0.8	0.84	0.88	0.92	0.96
W2750	0.64	0.68	0.72	0.76	0.8	0.84	0.88	0.92	0.96
W3080	0.64	0.68	0.72	0.76	0.8	0.84	0.88	0.92	0.96
W2890	0.64	0.68	0.72	0.76	0.8	0.84	0.88	0.92	0.96
W2640	0.64	0.68	0.72	0.76	0.8	0.84	0.88	0.92	0.96
W2970	0.64	0.68	0.72	0.76	0.8	0.84	0.88	0.92	0.96
W3280	0.64	0.68	0.72	0.76	0.8	0.84	0.88	0.92	0.96
W3190	0.64	0.68	0.72	0.76	0.8	0.84	0.88	0.92	0.96
W3300	0.64	0.68	0.72	0.76	0.8	0.84	0.88	0.92	0.96
W3410	0.64	0.68	0.72	0.76	0.8	0.84	0.88	0.92	0.96
W3910	0.64	0.68	0.72	0.76	0.8	0.84	0.88	0.92	0.96
W4030	0.64	0.68	0.72	0.76	0.8	0.84	0.88	0.92	0.96
W3690	0.64	0.68	0.72	0.76	0.8	0.84	0.88	0.92	0.96
W3700	0.64	0.68	0.72	0.76	0.8	0.84	0.88	0.92	0.96
W3790	0.64	0.68	0.72	0.76	0.8	0.84	0.88	0.92	0.96
W4720	0.64	0.68	0.72	0.76	0.8	0.84	0.88	0.92	0.96
W4730	0.64	0.68	0.72	0.76	0.8	0.84	0.88	0.92	0.96
W4590	0.64	0.68	0.72	0.76	0.8	0.84	0.88	0.92	0.96
W4620	0.64	0.68	0.72	0.76	0.8	0.84	0.88	0.92	0.96
W4290	0.64	0.68	0.72	0.76	0.8	0.84	0.88	0.92	0.96
W4180	0.64	0.68	0.72	0.76	0.8	0.84	0.88	0.92	0.96
W4400	0.64	0.68	0.72	0.76	0.8	0.84	0.88	0.92	0.96
W4130	0.64	0.68	0.72	0.76	0.8	0.84	0.88	0.92	0.96
W4250	0.64	0.68	0.72	0.76	0.8	0.84	0.88	0.92	0.96
W3730	0.64	0.68	0.72	0.76	0.8	0.84	0.88	0.92	0.96
W4070	0.64	0.68	0.72	0.76	0.8	0.84	0.88	0.92	0.96
W3400	0.64	0.68	0.72	0.76	0.8	0.84	0.88	0.92	0.96
W3180	0.64	0.68	0.72	0.76	0.8	0.84	0.88	0.92	0.96
W3260	0.64	0.68	0.72	0.76	0.8	0.84	0.88	0.92	0.96
W3460	0.64	0.68	0.72	0.76	0.8	0.84	0.88	0.92	0.96

Table D.3: Final optimized parameters in HEC-HMS (K=2hrs and x=0.02)

SWS	IA	CN	Lag time	ID	RC	SWS	IA	CN	Lag time	ID	RC
W2530	11.91	4.48	73.72	0.02	0.01	**W3700**	5.18	5.83	213.18	0.01	0.01
W2510	7.44	5.29	185.54	0.02	0.01	**W3790**	3.75	6.23	403.22	0.03	0.01
W2620	6.18	5.58	123.35	0.02	0.01	**W4720**	3.33	6.36	260.46	0.05	0.01
W2610	12.49	4.4	75.51	0.02	0.01	**W4730**	4.83	5.92	300.25	0.04	0.01
W2860	7.84	5.21	140.24	0.02	0.01	**W4590**	3.33	6.36	302.48	0.01	0.01
W2750	11.76	4.5	85.39	0.01	0.01	**W4620**	4.25	6.08	237.72	0.04	0.01
W3080	5.09	5.85	114.81	0.02	0.01	**W4290**	6.73	5.45	242.34	0.05	0.01
W2890	7.1	5.38	221.94	0.01	0.01	**W4180**	7.4	5.3	202.49	0.04	0.01
W2640	4.96	5.89	250.58	0.02	0.01	**W4400**	4.16	6.11	623.19	0.04	0.01
W2970	4.95	5.9	181.7	0.02	0.01	**W4130**	3.07	6.44	940	0.02	0.01
W3280	4.26	6.08	227.3	0.03	0.01	**W4250**	3.24	6.39	346.02	0.02	0.01
W3190	11.71	4.51	188.94	0.03	0.01	**W3730**	3.19	6.4	466.42	0.02	0.01
W3300	12.87	4.34	132.37	0.02	0.01	**W4070**	3.94	6.17	1027.07	0.02	0.01
W3410	6.69	5.46	307.47	0.02	0.01	**W3400**	4.79	5.93	263.55	0.03	0.01
W3910	9.64	4.86	154.19	0.04	0.01	**W3180**	4.26	6.08	290.99	0.04	0.01
W4030	9.6	4.87	163.74	0.02	0.01	**W3260**	3.99	6.16	352.53	0.01	0.01
W3690	10.06	4.78	116.42	0.02	0.01	**W3460**	4.75	5.94	875.48	0.02	0.01

Table D.4: Gradation curves of Meki river watershed (Source: HWSD and field assessment)

Size	T1	T2	T3	T4	T5	M1	L1	L2
0.002	24	28	54	27	42	32	7	23
0.003	24	28	54	27	42	32	7	23
0.004	24	28	54	27	42	32	7	23
0.005	24	28	54	27	42	32	7	23
0.006	24	28	54	27	42	32	7	23
0.007	24	28	54	27	42	32	7	23
0.008	24	28	54	27	42	32	7	23
0.009	24	28	54	27	42	32	7	23
0.01	24	28	54	27	42	32	7	23
0.011	24	28	54	27	42	32	7	23
0.012	24	28	54	27	42	32	7	23
0.013	24	28	54	27	42	32	7	23
0.014	24	28	54	27	42	32	7	23
0.015	24	28	54	27	42	32	7	23
0.016	24	28	54	27	42	32	7	23
0.017	24	28	54	27	42	32	7	23
0.018	24	28	54	27	42	32	7	23

Size	**T1**	**T2**	**T3**	**T4**	**T5**	**M1**	**L1**	**L2**
0.019	24	28	54	27	42	32	7	23
0.02	24	28	54	27	42	32	7	23
0.021	24	28	54	27	42	32	7	23
0.022	24	28	54	27	42	32	7	23
0.023	24	28	54	27	42	32	7	23
0.024	24	28	54	27	42	32	7	23
0.025	24	28	54	27	42	32	7	23
0.026	24	28	54	27	42	32	7	23
0.027	24	28	54	27	42	32	7	23
0.028	24	28	54	27	42	32	7	23
0.029	24	28	54	27	42	32	7	23
0.03	24	28	54	27	42	32	7	23
0.031	24	28	54	27	42	32	7	23
0.032	24	28	54	27	42	32	7	23
0.033	24	28	54	27	42	32	7	23
0.034	24	28	54	27	42	32	7	23
0.035	24	28	54	27	42	32	7	23
0.036	24	28	54	27	42	32	7	23
0.037	24	28	54	27	42	32	7	23
0.038	24	28	54	27	42	32	7	23
0.039	24	28	54	27	42	32	7	23
0.04	55	57	79	49	70	68	39	56
0.041	55	57	79	49	70	68	39	56
0.042	55	57	79	49	70	68	39	56
0.043	55	57	79	49	70	68	39	56
0.044	55	57	79	49	70	68	39	56
0.045	55	57	79	49	70	68	39	56
0.046	55	57	79	49	70	68	39	56
0.047	55	57	79	49	70	68	39	56
0.048	55	57	79	49	70	68	39	56
0.049	55	57	79	49	70	68	39	56
0.05	55	57	79	49	70	68	39	56
0.051	55	57	79	49	70	68	39	56
0.052	55	57	79	49	70	68	39	56
0.053	55	57	79	49	70	68	39	56
0.054	55	57	79	49	70	68	39	56
0.055	55	57	79	49	70	68	39	56
0.056	55	57	79	49	70	68	39	56
0.057	55	57	79	49	70	68	39	56
0.058	55	57	79	49	70	68	39	56

Size	T1	T2	T3	T4	T5	M1	L1	L2
0.059	55	57	79	49	70	68	39	56
0.06	55	57	79	49	70	68	39	56
0.061	55	57	79	49	70	68	39	56
0.062	55	57	79	49	70	68	39	56
0.063	100	100	100	100	100	100	100	100
0.064	100	100	100	100	100	100	100	100
0.065	100	100	100	100	100	100	100	100
0.066	100	100	100	100	100	100	100	100
0.067	100	100	100	100	100	100	100	100
0.068	100	100	100	100	100	100	100	100
0.069	100	100	100	100	100	100	100	100
0.07	100	100	100	100	100	100	100	100
0.071	100	100	100	100	100	100	100	100
0.072	100	100	100	100	100	100	100	100
0.073	100	100	100	100	100	100	100	100
0.074	100	100	100	100	100	100	100	100
0.075	100	100	100	100	100	100	100	100
0.076	100	100	100	100	100	100	100	100
0.077	100	100	100	100	100	100	100	100
0.078	100	100	100	100	100	100	100	100
0.079	100	100	100	100	100	100	100	100
0.08	100	100	100	100	100	100	100	100
0.081	100	100	100	100	100	100	100	100
0.082	100	100	100	100	100	100	100	100
0.083	100	100	100	100	100	100	100	100
0.084	100	100	100	100	100	100	100	100
0.085	100	100	100	100	100	100	100	100
0.086	100	100	100	100	100	100	100	100
0.087	100	100	100	100	100	100	100	100
0.088	100	100	100	100	100	100	100	100
0.089	100	100	100	100	100	100	100	100
0.09	100	100	100	100	100	100	100	100
0.091	100	100	100	100	100	100	100	100
0.092	100	100	100	100	100	100	100	100
0.093	100	100	100	100	100	100	100	100
0.094	100	100	100	100	100	100	100	100
0.095	100	100	100	100	100	100	100	100
0.096	100	100	100	100	100	100	100	100
0.097	100	100	100	100	100	100	100	100
0.098	100	100	100	100	100	100	100	100

b. Data quality Assessment (Comparison of observed flow Vs average rainfall of the watershed)

Table D.5: Cumulative station precipitation for Mass curve computation

Year	Koshe	Meki	Ziway	Butajira	Bui	CFSR ppt	Average
1985	997	705.6	659.1	705.6	659.1	410.3008	745.28
1986	1866.7	1643.4	1200.3	1757.4	659.1	705.5285	1598.24
1987	2774.4	2447.4	1753.2	3005.3	1508.6	1144.08	2470.64
1988	3433.8	3176.2	2453.8	4129.8	2367.4	1519.275	3285.06
1989	4440.6	4046.4	3405.3	5441.3	3161.3	1890.515	4293.6
1990	5276.1	4967.7	4094.7	6906.8	4241	2395.246	5292.07
1991	6048.3	5303	4896.3	7420	5259.4	2763.292	6124.11
1992	6822.9	6237.6	5690.5	7420	6249	3173.07	6999.13
1993	8137.4	6987.4	6649.4	8014.8	7274.5	3669.429	8011.47
1994	8811.9	7626.2	7166.7	9046	8033.2	4001.353	8735.89
1995	9681.6	7907.6	7730.7	10214.8	9339.6	4220.628	9601.7
1996	10571.1	7907.6	8642.8	11698.6	10621.2	4741.301	10759.32
1997	11430.2	7907.6	9491.4	12938.9	11380.7	5128.486	11686.2
1998	12297.2	8635.5	10247.6	14398.8	12426.9	5589.405	12670.47
1999	12995.9	9330.6	10793.1	15453.2	13410.5	5924.88	13467.17
2000	13653.9	10082.1	11497.4	16318.8	14408.9	6283.616	14272.86
2001	14565.7	10841	12223.1	17610.3	15629.5	6621.678	15257.4
2002	15144.4	11352.6	12680.7	18709.1	16530.8	6798.664	15974.96
2003	15895	12126.2	13531.5	19896.9	17582.6	7020.371	16902.68
2004	16489.2	12727.3	14305.1	20810.3	18503.8	7315.987	17663.38
2005	17565.7	13448.9	15147.2	22593.9	19768.5	7704.959	18803.09
2006	18519.3	14228.3	15923.7	24166.2	20997.2	7998.144	19866.75
2007	19486.8	14878.7	16727.3	24631.2	22195.5	8433.606	20828.83
2008	20426.3	15372.9	17769.4	25515.5	23269.4	8642.942	21778.9
2009	20927.9	15372.9	18498.1	26020.2	24108	8899.243	22425.64
2010	21786.5	16279.5	19361.4	26642.5	25625.8	9593.704	23422.1

Table D.6: Flow versus rainfall consistency evaluation

Date	Flow	Imdibir ppt	Butajira ppt	Bui ppt	Koshe ppt	Meki ppt	Ziway ppt	Remark
30Mar1994	7.2948	0	0	0	0	0	0	No RF
31Mar1994	5.7782	0	0	0	0	0	0	No RF
01Apr1994	31.639	0	0	0	0	0	0	No RF
02Apr1994	45.292	0	0	0	0	0	0	No RF
03Apr1994	62.79	0	0	0	0	0	0	No RF
04Apr1994	6.719	0	0	0	0	0	0	No RF
11Apr1994	6.5426	0	0	0	0	0	0	No RF
12Apr1994	5.6526	0	0	0	0	0	0	No RF
13Apr1994	22.711	0	0	0	0	0	0	No RF
14Apr1994	52.951	0	0	0	0	0	0	No RF
15Apr1994	60.013	0	0	0	0	0	0	No RF
25Sep1994	10.609	0	0	0	0	0	0	No RF
26Sep1994	6.5664	0	0	0	0	0	0	No RF
27Sep1994	4.3362	0	0	0	0	0	0	No RF
28Sep1994	24.162	0	0	0	0	0	0	No RF
29Sep1994	51.969	0	0	0	0	0	0	No RF
30Sep1994	56.609	0	0	0	0	0	0	No RF
06Oct1994	0.885	0	0	0	0	0	0	No RF
07Oct1994	10.247	0	0	0	0	0	0	No RF
09Oct1994	5.5784	0	0	0	0	0	0	No RF
10Oct1994	32.182	0	0	0	0	0	0	No RF
11Oct1994	57.284	0	0	0	0	0	0	No RF
12Oct1994	60.013	0	0	0	0	0	0	No RF
19Oct1994	9.5598	0	0	0	0	0	0	No RF
20Oct1994	6.1762	0	0	0	0	0	0	No RF
21Oct1994	7.462	0	0	0	0	0	0	No RF
22Oct1994	28.976	0	0	0	0	0	0	No RF
23Oct1994	55.937	0	0	0	0	0	0	No RF
24Oct1994	41.934	0	0	0	0	0	0	No RF
30Oct1994	1.107	0	0	0	0	0	0	No RF
31Oct1994	10.308	0	0	0	0	0	0	No RF
01Nov1994	6.308	0	0	0	0	0	0	No RF
02Nov1994	7.5946	0	0	0	0	0	0	No RF
03Nov1994	32.729	0	0	0	0	0	0	No RF
04Nov1994	53.609	0	0	0	0	0	0	No RF
05Nov1994	25.397	0	0	0	0	0	0	No RF
10Apr1990	36.64	0	0	0	0	0	0	No RF
11Apr1990	30.03	0	0	0	0	0	0	No RF
04Mar1992	20.75	0	0	0	0	0	0	No RF
06Mar1992	8.899	0	0	0	0	0	0	No RF

c. Calibration and validation results

A. Manual calibrations of Curve number

Table D.7: Manual calibration of CN

Change	Peak flow	Volume	Nash	Pbias	RMSE	%Volume Change	Date of peak
-20%	194.9	8000.3	-47.799	884.49	7	-15.29	27-May-96
-15%	195.5	8033.56	-48.097	888.58	7	-5.46	27-May-96
-10%	195.9	8063.23	-48.357	892.22	7	-1.4	27-May-96
-5%	196.3	8089.92	-48.584	895.51	7	-0.99	27-May-96
0	196.5	8113.99	-48.8	898.47	7.1	-0.63	27-May-96
5%	196.7	8135.81	-48.957	901.15	7.1	-0.297	27-May-96
10%	196.9	8155.64	-49.108	903.59	7.1	0	27-May-96
15%	197	8174.13	-49.241	905.86	7.1	0.27	27-May-96
20%	197.1	8190.85	-49.357	907.92	7	0.51	27-May-96

B. Manual calibration of peak flow for lag time

Change	Peak flow	Volume	Nash	Pbias	RMSE	%Volume Change	Date of peak
-20%	199.1	8129.29	-48.997	900.35	7.1	0.18856321	27-May-96
-15%	198.55	8125.37	-48.943	899.865	7.1	0.140189968	27-May-96
-10%	198	8121.44	-48.889	899.38	7.1	0.091816726	27-May-96
-5%	197.25	8117.72	-48.8445	898.925	7.1	0.045908363	27-May-96
0	196.5	8113.99	-48.8	898.47	7.1	0	27-May-96
5%	195.8	8109.55	-48.723	897.92	7.1	-0.0547203	27-May-96
10%	195.1	8107.37	-48.687	897.65	7	-0.08158748	27-May-96
15%	194.3	8103.25	-48.631	897.15	7	-0.13236398	27-May-96
20%	193.7	8103.88	-48.634	897.22	7	-0.12459961	15-Oct-97
30%	193.2	8095.4	-48.527	896.18	7	-0.22911046	21-Oct-97
50%	193.3	8082.99	-48.373	894.65	7	-0.38205618	20-Oct-97
ST/0.29	172.4	7192.69	-37.434	785.17	6.2	-11.3544631	23-Oct-97
Observed values	139.6	813.24					25-Jun-98

C. Manual calibration of Muskingham K and x

Change K	**Peak flow**	**Volume**	**Nash**	**Pbias**	**RMSE**	**Date of peak**	Status
-40%	238	8052.26	-53.177	890.78	7.4	01-May-96	Stable
-20%	208.7	8087.7	-50.494	895.16	7.2	15-Oct-97	Stable
-15%	206.6	8095.33	-50.0315	896.11	7.15	15-Oct-97	Stable
-10%	204.5	8102.95	-49.569	897.06	7.1	15-Oct-97	Stable
-5%	200.2	8109.21	-49.164	897.85	7.1	15-Oct-97	Stable
0	196.5	8113.99	-48.8	898.47	7.1	27-May-96	Unstable
5%	193.8	8117.31	-48.42	898.9	7	27-May-96	Unstable
10%	193	8119.15	-48.069	899.16	7	13-Nov-97	Unstable
15%	196.7	8119.49	-47.424	899.23	7	13-Nov-97	Unstable
20%	199.2	8118.36	-47.381	899.12	7	13-Nov-97	Unstable
Observed values	139.6	813.24				25-Jun-98	

Change x	**Peak flow**	**Volume**	**Nash**	**Pbias**	**RMSE**	**Date of peak**
-20%	208.7	8087.7	-50.494	895.16	7.2	15-Oct-97
-15%	206.6	8095.33	-50.0315	896.11	7.15	15-Oct-97
-10%	204.5	8102.95	-49.569	897.06	7.1	15-Oct-97
-5%	200.2	8109.21	-49.164	897.85	7.1	15-Oct-97
0	196.5	8113.99	-48.8	898.47	7.1	27-May-96
5%	193.8	8117.31	-48.42	898.9	7	27-May-96
10%	193	8119.15	-48.069	899.16	7	13-Nov-97
15%	196.7	8119.49	-47.424	899.23	7	13-Nov-97
20%	199.2	8118.36	-47.381	899.12	7	13-Nov-97

D. Manual calibration of base flow initial discharge and recession constant

Change ID	**Peak flow**	**Volume**	**Nash**	**Pbias**	**RMSE**	**Date of peak**	**%Volume Change**
-20%	196.5	8073.92	-48.531	893.41	7	27-May-96	-0.5
-15%	196.5	8083.94	-48.5905	894.68	7	27-May-96	-0.37
-10%	196.5	8093.96	-48.65	895.94	7	27-May-96	-0.25
-5%	196.5	8103.98	-48.725	897.21	7.1	27-May-96	-0.12
0	196.5	8113.99	-48.8	898.47	7.1	27-May-96	0
5%	194.75	8116.57	-48.4345	898.82	7	27-May-96	0.032
10%	193	8119.15	-48.069	899.16	7	13-Nov-97	0.06
15%	194.75	8136.61	-48.5835	901.34	7	13-Nov-97	0.28
20%	196.5	8154.06	-49.098	903.52	7.1	27-May-96	0.49

Change RC	Peak flow	Volume	Nash	Pbias	RMSE	%Volume Change
-20%	189.1	7609.59	-42.681	836.42	6.6	-6.22
-15%	190.55	7714.25	-43.931	849.295	6.7	-4.93
-10%	192	7818.9	-45.181	862.17	6.8	-3.64
-5%	194.25	7966.45	-46.9905	880.32	7.1	-1.82
0	196.5	8113.99	-48.8	898.47	7.1	0
5%	201	8381.69	-52.117	931.395	7.3	3.3
10%	205.5	8649.39	-55.434	964.32	7.5	6.6
15%	218.75	9383.18	-64.7555	1054.585	8.1	15.64
20%	232	10117	-74.077	1144.85	8.7	24.69

Table D.8: Calibrated Average monthly flow (m3/s) before optimization (BOP) and after optimization (AOP)

Months	Average of Calibrated flow BOP	Average of Calibrated flow AOP	Average of Observed flow
Jan	8.964516129	3.558709677	2.282580645
Feb	4.694326241	2.880851064	3.263829787
Mar	4.106451613	1.5	5.980645161
Apr	10.90733333	3.384	11.48333333
May	16.38774194	4.400645161	10.83419355
Jun	37.36133333	14.11	9.906
Jul	60.62451613	23.40322581	23.57419355
Aug	73.34451613	35.61290323	45.95290323
Sep	47.20333333	19.44866667	24.44533333
Oct	7.241935484	3.501935484	7.50516129
Nov	0.317333333	0.050666667	2.522
Dec	0.256129032	0.16	0.789032258

Table D.9: Validated Average monthly flow (m3/s) BOP and AOP

Months	Average of Validated flow BOP	Average of Validated flow AOP	Average of Observed flow
Jan	1.979354839	0.929677419	4.080645161
Feb	2.812765957	0.412056738	5.224822695
Mar	8.992903226	3.369677419	7.129677419
Apr	9.761333333	1.688666667	7.648666667
May	7.429032258	1.621290323	7.062580645
Jun	50.98133333	8.642	7.424
Jul	74.81290323	24.5116129	18.10258065
Aug	85.43870968	29.32322581	25.29677419
Sep	53.07933333	18.87933333	16.10666667
Oct	9.647096774	2.741290323	13.73741935
Nov	0.772	0.18	5.312
Dec	0.481290323	0.161290323	2.580645161

Table D.10: Summary of calibrated and validated surface runoff

Hydrologic elements	Drainage area (Km2)	Summary of Calibrated results (1985-1989)		Summary of Validated results (1990-1994)	
		Peak Discharge (m3/s)	**Time of peak**	**Peak Discharge (m3/s)**	**Time of peak**
J644	779.7055	41	13Aug1987, 00:00	56.5	15Aug1993, 00:00
J647	1925.41356	95.1	18Aug1987, 00:00	130	17Aug1993, 00:00
J650	530.76966	33.1	13Aug1987, 00:00	43.4	15Aug1993, 00:00
J653	148.3907	11.5	10Aug1987, 00:00	11.7	14Aug1993, 00:00
J656	576.7075	33.8	13Aug1987, 00:00	44.8	15Aug1993, 00:00
J659	2064.11526	94.7	20Aug1987, 00:00	127.6	18Aug1993, 00:00
J662	642.87476	39.3	13Aug1987, 00:00	51.6	15Aug1993, 00:00
J665	369.57916	25.3	13Aug1987, 00:00	32.2	15Aug1993, 00:00
J670	2032.95766	94.7	19Aug1987, 00:00	129	17Aug1993, 00:00
J673	80.704	7.1	10Aug1987, 00:00	7.2	14Aug1993, 00:00
J676	396.491	23.7	13Aug1987, 00:00	30.5	15Aug1993, 00:00
J681	1842.93536	95.5	15Aug1987, 00:00	132.1	16Aug1993, 00:00
J684	110.2014	8.3	10Aug1987, 00:00	10.2	14Aug1993, 00:00
J687	148.0334	12.3	10Aug1987, 00:00	12.4	14Aug1993, 00:00
J692	271.4463	16.4	13Aug1987, 00:00	21.2	15Aug1993, 00:00
J697	35.1565	2.7	10Aug1987, 00:00	2.8	14Aug1993, 00:00
J700	310.3013	19.6	13Aug1987, 00:00	25.1	15Aug1993, 00:00
J703	66.2208	5.4	10Aug1987, 00:00	5.5	14Aug1993, 00:00
J706	1776.81036	96.4	14Aug1987, 00:00	130.8	15Aug1993, 00:00
J709	55.4568	5.3	10Aug1987, 00:00	5.3	14Aug1993, 00:00
J712	241.5501	16.1	08Aug1988, 00:00	20.4	14Aug1993, 00:00
J715	164.9485	11	10Aug1987, 00:00	13.9	14Aug1993, 00:00
J718	48.3344	3.7	10Aug1987, 00:00	3.8	14Aug1993, 00:00
J721	86.358	8.3	10Aug1987, 00:00	8.3	14Aug1993, 00:00
J724	93.856	9.5	10Aug1987, 00:00	9.4	14Aug1993, 00:00
J727	60.4529	4.7	10Aug1987, 00:00	4.8	14Aug1993, 00:00
J730	115.0861	8	10Aug1987, 00:00	9.6	14Aug1993, 00:00
J733	273.79886	19.8	09Aug1988, 00:00	25.8	14Aug1993, 00:00
J736	198.89636	16.4	08Aug1988, 00:00	19.3	14Aug1993, 00:00
J738	60.4529	4.1	08Aug1988, 00:00	4.7	14Aug1993, 00:00
J742	48.3344	3.2	08Aug1988, 00:00	3.7	14Aug1993, 00:00
J744	213.2829	13.6	11Aug1987, 00:00	17.3	14Aug1993, 00:00
J747	213.2829	13.2	12Aug1987, 00:00	16.9	15Aug1993, 00:00
J750	35.1565	2.4	08Aug1988, 00:00	2.8	14Aug1993, 00:00
J752	35.1565	2.2	09Aug1988, 00:00	2.8	14Aug1993, 00:00
J754	55.4568	4.5	08Aug1988, 00:00	5.2	14Aug1993, 00:00

Hydrologic elements	**Drainage area (Km2)**	**Summary of Calibrated results (1985-1989)**		**Summary of Validated results (1990-1994)**	
		Peak Discharge (m3/s)	**Time of peak**	**Peak Discharge (m3/s)**	**Time of peak**
J756	35.1565	2.1	09Aug1988, 00:00	2.7	15Aug1993, 00:00
J758	55.4568	4.2	11Aug1987, 00:00	5.3	14Aug1993, 00:00
J761	35.1565	2.1	10Aug1988, 00:00	2.7	15Aug1993, 00:00
J763	35.1565	2	13Aug1987, 00:00	2.7	15Aug1993, 00:00
J767	1925.41356	94.3	18Aug1987, 00:00	130.2	17Aug1993, 00:00
J768	1925.41356	93.7	19Aug1987, 00:00	129.6	17Aug1993, 00:00
J772	506.6924	30.1	13Aug1987, 00:00	40.1	15Aug1993, 00:00
J776	506.6924	29.5	13Aug1987, 00:00	39.8	15Aug1993, 00:00
J778	1842.93536	94.1	17Aug1987, 00:00	128.9	16Aug1993, 00:00
J781	1842.93536	94.5	16Aug1987, 00:00	131.3	16Aug1993, 00:00
J783	2064.11526	94.2	20Aug1987, 00:00	128.2	18Aug1993, 00:00
J786	1842.93536	95.3	16Aug1987, 00:00	132.4	16Aug1993, 00:00
J788	576.7075	32.9	14Aug1987, 00:00	44.5	15Aug1993, 00:00
J790	576.7075	32.7	14Aug1987, 00:00	43.4	15Aug1993, 00:00
J792	148.3907	9.9	08Aug1988, 00:00	11.6	14Aug1993, 00:00
J797	1776.81036	95.5	15Aug1987, 00:00	129.6	16Aug1993, 00:00
J800	779.7055	40.8	14Aug1987, 00:00	56	15Aug1993, 00:00
J803	148.0334	10.6	08Aug1988, 00:00	12.3	14Aug1993, 00:00
J805	1090.0068	58.7	14Aug1987, 00:00	79.3	15Aug1993, 00:00
J808	310.3013	19	13Aug1987, 00:00	25.1	15Aug1993, 00:00
J812	241.5501	15.2	12Aug1987, 00:00	19.7	15Aug1993, 00:00
J814	241.5501	15.8	09Aug1988, 00:00	19.8	14Aug1993, 00:00
J817	642.87476	37.9	14Aug1987, 00:00	51.2	15Aug1993, 00:00
J820	450.28316	28.6	14Aug1987, 00:00	38.1	15Aug1993, 00:00
J822	450.28316	28.8	13Aug1987, 00:00	38.4	15Aug1993, 00:00
J824	450.28316	29.4	13Aug1987, 00:00	38.6	15Aug1993, 00:00
J828	273.79886	19.5	12Aug1987, 00:00	25.2	15Aug1993, 00:00
J831	198.89636	15.8	11Aug1987, 00:00	19.5	14Aug1993, 00:00
Outlet1	2110.39056	95.1	20Aug1987, 00:00	128	17Aug1993, 00:00
Reach-1	530.76966	32.2	14Aug1987, 00:00	42.8	15Aug1993, 00:00
Reach-2	110.2014	7.8	11Aug1987, 00:00	9.7	14Aug1993, 00:00
R1000	1842.93536	94.1	17Aug1987, 00:00	128.9	16Aug1993, 00:00
R1020	2064.11526	94	21Aug1987, 00:00	127.9	18Aug1993, 00:00
R1030	2064.11526	94.2	20Aug1987, 00:00	128.2	18Aug1993, 00:00
R1060	1842.93536	94.5	16Aug1987, 00:00	131.3	16Aug1993, 00:00
R1070	576.7075	32.9	14Aug1987, 00:00	44.5	15Aug1993, 00:00
R1100	576.7075	32.7	14Aug1987, 00:00	43.4	15Aug1993, 00:00
R1110	148.3907	9.9	08Aug1988, 00:00	11.6	14Aug1993, 00:00

Hydrologic elements	Drainage area (Km2)	Summary of Calibrated results (1985-1989)		Summary of Validated results (1990-1994)	
		Peak Discharge (m3/s)	**Time of peak**	**Peak Discharge (m3/s)**	**Time of peak**
R1140	1842.93536	95.3	16Aug1987, 00:00	132.4	16Aug1993, 00:00
R1230	148.3907	9.3	09Aug1988, 00:00	11.6	14Aug1993, 00:00
R1240	576.7075	32.2	15Aug1987, 00:00	42.9	16Aug1993, 00:00
R1260	1776.81036	94.6	15Aug1987, 00:00	130.3	16Aug1993, 00:00
R1320	1776.81036	95.5	15Aug1987, 00:00	129.6	16Aug1993, 00:00
R1330	779.7055	40.8	14Aug1987, 00:00	56	15Aug1993, 00:00
R1360	66.2208	4.7	08Aug1988, 00:00	5.4	14Aug1993, 00:00
R1370	148.0334	9.8	09Aug1988, 00:00	12.4	14Aug1993, 00:00
R1400	779.7055	40.1	14Aug1987, 00:00	54.8	15Aug1993, 00:00
R1410	1090.0068	57.8	15Aug1987, 00:00	78.1	16Aug1993, 00:00
R1440	310.3013	18.6	14Aug1987, 00:00	24.4	15Aug1993, 00:00
R1460	148.0334	10.6	08Aug1988, 00:00	12.3	14Aug1993, 00:00
R1470	310.3013	19	13Aug1987, 00:00	25.1	15Aug1993, 00:00
R150	60.4529	4.1	08Aug1988, 00:00	4.7	14Aug1993, 00:00
R1520	241.5501	14.9	13Aug1987, 00:00	19.8	15Aug1993, 00:00
R1570	241.5501	15.2	12Aug1987, 00:00	19.7	15Aug1993, 00:00
R1590	241.5501	15.8	09Aug1988, 00:00	19.8	14Aug1993, 00:00
R1610	642.87476	37.5	14Aug1987, 00:00	50.4	15Aug1993, 00:00
R170	60.4529	3.8	09Aug1988, 00:00	4.8	14Aug1993, 00:00
R1710	642.87476	37.9	14Aug1987, 00:00	51.2	15Aug1993, 00:00
R1820	450.28316	28.5	14Aug1987, 00:00	37.3	15Aug1993, 00:00
R1840	450.28316	28.6	14Aug1987, 00:00	38.1	15Aug1993, 00:00
R1860	450.28316	28.8	13Aug1987, 00:00	38.4	15Aug1993, 00:00
R1920	369.57916	24.7	13Aug1987, 00:00	32.4	15Aug1993, 00:00
R1950	80.704	6.1	08Aug1988, 00:00	7.1	14Aug1993, 00:00
R2020	273.79886	19.4	13Aug1987, 00:00	25.4	15Aug1993, 00:00
R2030	273.79886	19.5	12Aug1987, 00:00	25.2	15Aug1993, 00:00
R2060	198.89636	15.1	12Aug1987, 00:00	18.5	14Aug1993, 00:00
R2100	198.89636	15.8	11Aug1987, 00:00	19.5	14Aug1993, 00:00
R2130	86.358	7	08Aug1988, 00:00	8.2	14Aug1993, 00:00
R2220	93.856	8	08Aug1988, 00:00	9.3	14Aug1993, 00:00
R260	115.0861	7.4	11Aug1987, 00:00	9.3	14Aug1993, 00:00
R270	48.3344	3.2	08Aug1988, 00:00	3.7	14Aug1993, 00:00
R290	48.3344	3	09Aug1988, 00:00	3.8	14Aug1993, 00:00
R300	164.9485	10.7	11Aug1987, 00:00	13.5	14Aug1993, 00:00
R330	213.2829	13.2	12Aug1987, 00:00	16.9	15Aug1993, 00:00
R400	213.2829	12.9	13Aug1987, 00:00	17.2	15Aug1993, 00:00
R410	35.1565	2.4	08Aug1988, 00:00	2.8	14Aug1993, 00:00

Hydrologic elements	Drainage area (Km2)	Summary of Calibrated results (1985-1989)		Summary of Validated results (1990-1994)	
		Peak Discharge (m3/s)	Time of peak	Peak Discharge (m3/s)	Time of peak
R430	35.1565	2.2	09Aug1988, 00:00	2.8	14Aug1993, 00:00
R450	55.4568	4.5	08Aug1988, 00:00	5.2	14Aug1993, 00:00
R470	35.1565	2.1	09Aug1988, 00:00	2.7	15Aug1993, 00:00
R490	55.4568	4.2	11Aug1987, 00:00	5.3	14Aug1993, 00:00
R510	55.4568	4.1	12Aug1987, 00:00	5	15Aug1993, 00:00
R540	35.1565	2.1	10Aug1988, 00:00	2.7	15Aug1993, 00:00
R590	35.1565	2	13Aug1987, 00:00	2.7	15Aug1993, 00:00
R600	35.1565	2	14Aug1987, 00:00	2.6	15Aug1993, 00:00
R610	271.4463	16.1	13Aug1987, 00:00	21.3	15Aug1993, 00:00
R680	1925.41356	93.7	19Aug1987, 00:00	129.6	17Aug1993, 00:00
R710	1925.41356	93.2	19Aug1987, 00:00	128.3	17Aug1993, 00:00
R770	1925.41356	94.3	18Aug1987, 00:00	130.2	17Aug1993, 00:00
R790	396.491	22.8	13Aug1987, 00:00	30.5	15Aug1993, 00:00
R810	2032.95766	94.3	20Aug1987, 00:00	127.5	18Aug1993, 00:00
R830	506.6924	29.5	13Aug1987, 00:00	39.8	15Aug1993, 00:00
R870	1842.93536	93.2	18Aug1987, 00:00	129.5	17Aug1993, 00:00
R890	506.6924	29.4	14Aug1987, 00:00	39.5	15Aug1993, 00:00
W2510	54.6332	4.8	10Aug1987, 00:00	4.9	14Aug1993, 00:00
W2530	60.4529	4.7	10Aug1987, 00:00	4.8	14Aug1993, 00:00
W2610	48.3344	3.7	10Aug1987, 00:00	3.8	14Aug1993, 00:00
W2620	49.8624	4.6	10Aug1987, 00:00	4.6	14Aug1993, 00:00
W2640	55.4568	5.3	10Aug1987, 00:00	5.3	14Aug1993, 00:00
W2750	35.1565	2.7	10Aug1987, 00:00	2.8	14Aug1993, 00:00
W2860	58.1634	5.1	10Aug1987, 00:00	5.1	14Aug1993, 00:00
W2890	28.0548	2.5	10Aug1987, 00:00	2.5	14Aug1993, 00:00
W2970	54.7446	5.2	10Aug1987, 00:00	5.2	14Aug1993, 00:00
W3080	61.8334	5.9	10Aug1987, 00:00	5.9	14Aug1993, 00:00
W3180	107.5441	10.5	10Aug1987, 00:00	10.5	14Aug1993, 00:00
W3190	89.6239	7	10Aug1987, 00:00	7.1	14Aug1993, 00:00
W3260	31.1576	3.1	10Aug1987, 00:00	3.1	14Aug1993, 00:00
W3280	70.0151	6.8	10Aug1987, 00:00	6.8	14Aug1993, 00:00
W3300	58.7668	4.4	10Aug1987, 00:00	4.5	14Aug1993, 00:00
W3400	82.4782	7.9	10Aug1987, 00:00	7.9	14Aug1993, 00:00
W3410	54.6073	4.9	10Aug1987, 00:00	5	14Aug1993, 00:00
W3460	46.2753	4.5	10Aug1987, 00:00	4.4	14Aug1993, 00:00
W3690	66.2208	5.4	10Aug1987, 00:00	5.5	14Aug1993, 00:00
W3700	27.2959	2.6	10Aug1987, 00:00	2.6	14Aug1993, 00:00
W3730	43.9288	4.5	10Aug1987, 00:00	4.4	14Aug1993, 00:00

Hydrologic elements	Drainage area (Km2)	Summary of Calibrated results (1985-1989)		Summary of Validated results (1990-1994)	
		Peak Discharge (m3/s)	Time of peak	Peak Discharge (m3/s)	Time of peak
W3790	68.7512	6.8	10Aug1987, 00:00	6.8	14Aug1993, 00:00
W3910	106.0911	8.8	10Aug1987, 00:00	8.9	14Aug1993, 00:00
W4030	41.9423	3.5	10Aug1987, 00:00	3.5	14Aug1993, 00:00
W4070	66.125	6.5	10Aug1987, 00:00	6.5	14Aug1993, 00:00
W4130	65.7365	6.7	10Aug1987, 00:00	6.6	14Aug1993, 00:00
W4180	80.704	7.1	10Aug1987, 00:00	7.2	14Aug1993, 00:00
W4250	46.3686	4.7	10Aug1987, 00:00	4.6	14Aug1993, 00:00
W4290	95.7803	8.7	10Aug1987, 00:00	8.7	14Aug1993, 00:00
W4400	80.4865	7.9	10Aug1987, 00:00	7.9	14Aug1993, 00:00
W4590	18.68236	1.9	10Aug1987, 00:00	1.9	14Aug1993, 00:00
W4620	74.9025	7.3	10Aug1987, 00:00	7.3	14Aug1993, 00:00
W4720	93.856	9.5	10Aug1987, 00:00	9.4	14Aug1993, 00:00
W4730	86.358	8.3	10Aug1987, 00:00	8.3	14Aug1993, 00:00

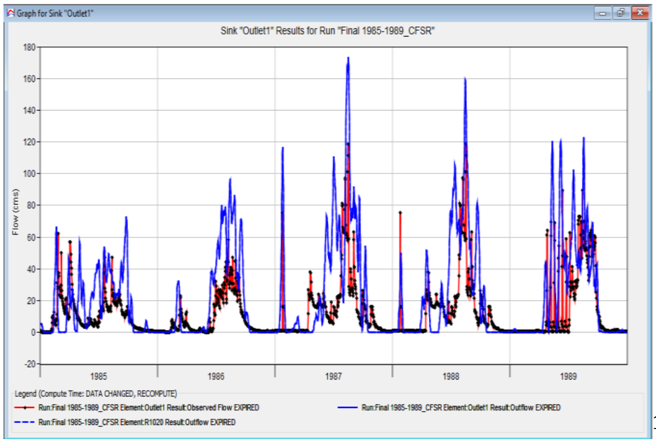

[19]

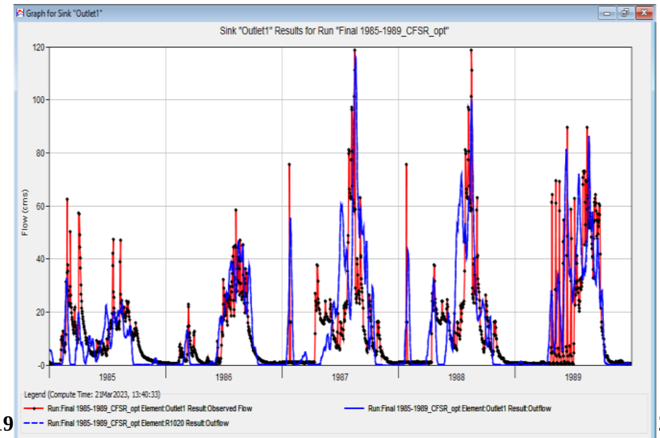

[20]

Figure D-3: Calibration of HEC-HMS model (01 Jan 1985 to 31 Dec 1989)

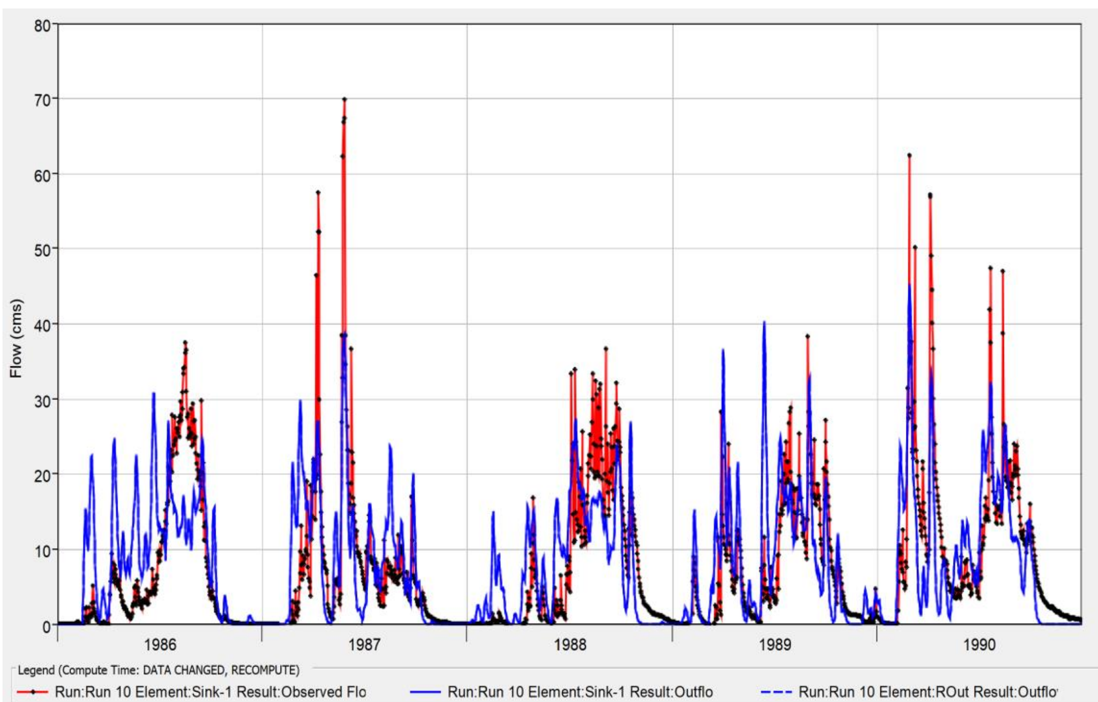

Figure D-4: Validation of HEC-HMS model (01 Jan 1990 to 31 Dec 1994)

[19] Calibration before optimization
[20] Calibration after optimization
[21] Validation after optimization

Table D.11: Observed flow and precipitation data used in Meki river watershed study

Year	Average of Koshe	Average of Meki	Average of Bui	Average of Ziway	Average of Butajira	Average of Average (Thieson polygon)	Average flow of Meki river
1985	2.731506849	1.933150685		1.805753425		1.316679452	5.502717352
1986	2.382739726	2.569315068	0	1.499168975	2.881643836	1.919753425	5.748419178
1987	2.486849315	2.202739726	2.32739726	1.514794521	3.41890411	2.306139726	6.863493151
1988	1.801639344	1.991256831	2.346448087	1.91420765	3.072404372	2.216437158	7.257486339
1989	3.005373134	2.384109589	2.175068493	2.621212121	3.593150685	2.701838356	6.953482192
1990	2.29532967	2.524109589	2.982596685	1.888767123	4.015068493	2.681293151	10.47398356
1991	2.115616438	1.025382263	3.021958457	2.196164384	2.899435028	1.798183562	8.592093151
1992	2.305357143	2.617927171	2.726170799	2.169945355		1.905513661	9.671203005
1993	3.611263736	2.054246575	2.963872832	2.627123288	2.779439252	2.428676712	14.26695342
1994	1.853021978	1.750136986	2.095856354	1.417260274	2.825205479	1.932956164	13.01944918
1995	2.382739726	1.162809917	3.598898072	1.545205479	3.202191781	2.088641096	7.069019406
1996	2.443681319		3.579888268	2.492076503	4.054098361	2.325486339	9.06879276
1997	2.35369863		2.260416667	2.324931507	3.398082192	1.925164384	5.905071233
1998	2.375342466	2.179341317	2.874175824	2.071780822	3.999726027	2.593591781	15.83196164
1999	1.914246575	2.271568627	2.702197802	1.494520548	2.888767123	2.106243836	7.445043836
2000	1.964179104	2.053278689	2.727868852	1.92431694	2.365027322	2.150051913	3.772508197
2001	2.72994012	2.079178082	3.353296703	2.015833333	3.548076923	2.585553425	9.017484384
2002	1.585479452	1.401643836	2.469315068	1.278212291	3.010410959	1.864183562	6.001792922
2003	2.056438356	2.302380952	2.937988827	2.330958904	3.254246575	2.5124	7.095861644
2004	1.623497268	1.642349727	2.516939891	2.113661202	2.495628415	2.073898907	8.20322623
2005	2.949315068	1.982417582	3.493646409	2.307123288	4.886575342	2.991213699	7.841725114
2006	2.61260274	2.147107438	3.384848485	2.133241758	4.307671233	2.80949863	8.811522511
2007	2.650684932	1.947305389	3.283013699	2.201643836	3.079470199	2.127268493	11.30082822
2008	2.581043956	2.025409836	2.942191781	2.84726776	2.555780347	2.36618306	6.746961703
2009	1.501796407		2.297534247	2.029805014	1.382739726	1.345090411	7.546681849
2010	2.570658683	2.483835616	4.544311377	2.466571429	1.891489362	2.530235616	8.924274873
2011	1.138235294	1.695820896	3.151506849	1.906232295	3.468115942	1.742065753	
2012	1.96090535	3.462445415	1.98715847	0	3.448484848	1.306830601	
2013	2.403296703	1.951497006	2.580821918	2.298019802	5.130541872	2.15409863	
2014	4.019444444	2.351780822	3.174485597	2.189548023	4.236538462	2.582405479	
2015	1.474863388	1.814693878	2.056410256	1.713919414	1.330181818	1.183342466	
2016	1.924043716	2.429927007	2.890123457	2.809489051	0.96358209	1.738806011	
2017	1.181137725	3.168292683	2.937086093	2.133233533	0.44358209	1.389136986	

Table D.12: GPS points for land cover classification

x	Y	LC	X	Y	LC	x	y	LC	x	y	LC
431282	898148	T	430897	901249	F	430971	900904	G	8.897	38.77	1
432516	899517	R	430915	901171	C	430862	901175	C	8.86	38.81	12
432056	899989	F	430948	901115	C	430834	901207	C	8.86	38.81	13
432007	900043	F	430935	901062	G	430765	901288	F	8.86	38.81	14
431173	901828	AF	430915	901014	RI	430731	901272	F	8.1	38.246	3360
430911	902339	AF	430960	900932	RI	430640	901212	F	8.052	38.49	20meter
430788	902540	AF	430998	900821	G	430593	901188	G	8.04	38.73	AJK
430740	902615	AF	430981	900707	G	430401	900975	G	8.381	39.01	Awash
430408	904267	C	430965	900651	B	430364	900968	G	8.15	38.3	Beyene
430352	904374	C	430909	900664	G	430353	900950	C	8.12	38.373	bir_hen
430335	904418	C	430898	900605	G	430357	900868	C	8.115	38.21	Bozhebar
430341	904465	C	430896	900581	C	430323	900893	C	8.32	38.55	bui1
430337	904511	C	430903	900529	C	430250	900891	C	8.34	38.56	Buicult
430297	904601	C	430899	900421	C	430225	900877	G	8.21	38.35	buyema erica4
430291	904429	G	430823	900392	C	430200	900871	G	8.195	38.362	buyema2enset
430332	904350	G	430844	900368	G	430183	900883	C	8.144	38.38	buyema3enset
430362	904302	G	430856	900343	G	430101	900873	C	8.165	38.37	buyemaenset2
430364	904246	G	430691	900177	AF	430015	900874	RI	8.205	38.113	cheza gebeya
430431	903916	C	430733	900138	AF	429916	900885	RI	8.18	38.45	china camp
430499	903750	C	430770	900068	C	429855	900878	RI	8.24	38.077	degraded1
430550	903621	C	430961	899765	C	429786	900925	F	8.114	38.78	dugda2
430604	903476	C	431019	899665	C	429738	900931	F	8.225	38.88	Dugdaw
430641	903380	B	431021	899655	AF	429700	900953	F	8.06	38.48	ensenotown
430641	903378	B	431051	899474	AF	429669	900986	C	8.064	38.474	esenotown
430748	902750	C	430964	899331	AF	429622	901012	C	8.234	38.482	gogeti1
430745	902513	C	430988	899277	AF	429629	900961	C	8.146	38.3	goiban1
430761	902441	AF	430963	899187	C	429598	900887	E	8.2	38.46	j4
430780	902378	AF	431019	899028	C	429527	900908	G	8.36	38.57	j6
430770	902355	C	429434	899868		429312	900925	F	7.977	38.72	jido2
430747	902345	C	429375	899672	T	429347	900931	G	8.165	38.43	jole mazoria
430747	902326	AF	430175	898826	T	429458	900726	E	8.177	38.44	jole1
430767	902267	AF	430649	898305	S	429319	900780	E	8.204	38.46	jole2
430739	902249	AF	430916	898022	T	429224	900859	E	8.225	38.47	jole3
430684	902217	C	430924	898039	T	428784	901313	E	8.252	38.49	kela1
430617	902163	C	431044	898295	T	428786	901366	G	8.258	38.5	kela2
430662	902035	C	430986	898320	S	428760	901382	G	8.3	38.53	kela3
430646	901970	C	430912	900788	G	428746	901369	E	8.27	38.513	kela4
430735	901592	F	430868	900959	S	428737	901356	E	8.27	38.514	kella1
430769	901550	F	430880	901001	S	428747	901242	E	8.01	38.6	Koshecult

426507	902054	F	431073	900957	G	428742	901265	E	8.01	38.59	koshecult1
426503	902028	F	426698	901479	G	428817	901283	C	8.011	38.58	koshecult2
426502	901999	F	426740	901464	C	428910	901298	E	8.014	38.57	koshecult3
426485	901978	RO	426888	901439	F	428915	901307	E	8.015	38.55	koshecult6
426474	901887	DV	426945	901376	G	428908	901362	C	8.042	38.5	koshecult7
426516	901840	F	426955	901351	G	429016	901065	C	8.015	38.53	koshetown
426546	901828	C	426998	901312	E	429033	900999	C	9.084	38.76	Koso
426565	901828	C	426966	901322	E	427317	901102	Elc	8.3	38.6	lab1 sodo
426591	901814	C	427240	901152	G	426299	901707	G	8.4	38.6	lab2 sodo
426664	901787	C	427285	901192	F	426287	901670	G	8.6	38.64	Lemen
426715	901779	C	427313	901209	F	426356	901792	G	8.6	38.6	lemen2
426733	901743	G	427316	901169	F	426336	901806	G	8.2	38.84	Meki
426767	901740	F	427313	901159	G	426354	901825	G	8.15	38.82	Mekiriver
426790	901731	F	427328	901144	G	426373	901829	F	8.1	38.3	meskan1
426826	901738	G	427333	901143	C	426369	901839	F	8.1	38.5	mixed1
426861	901733	G	427342	901036	E	426380	901845	F	8.14	38.44	mixed2
426924	901717	G	427373	901015	E	426390	901854	F	8.14	38.43	mixed3
426963	901710	G	427339	901000	E	426401	901892	RO	8.13	38.42	mixed4
427010	901720	G	427539	901008	E	426424	901898	G	8.13	38.41	mixed6
427400	901940	G	427567	900078	C	426413	901988	G	8.13	38.4	mixed7
427321	901904	F	427620	900833	C	426404	901988	G	8.13	38.39	mixed8
427295	901830	C	427681	900779	C	426387	902009	RO	8.25	38.08	Mohor Aklil
427304	901853	E	427810	900659	S	426422	902032	RO	8.35	38.57	sampling 1
426140	901713	G	427872	900574	C	426427	902073	F	8.27	38.51	selfhelp river
426136	901773	F	427955	900532	F	426424	902104	F	8.41	38.62	Suten
425828	902011	G	428007	900482	C	426415	902135	F	8.53	38.63	Tere
425826	902040	G	428034	900458	C	426453	902197	F	8.1	38.2	Terega
425711	902247	F	428078	900425	C	426435	902229	F	8.44	38.61	Tiya
425696	902243	F	428172	900339	C	426399	902288	F	8.11	38.37	But Bus stn
425623	902243	G	428316	900250	C	426363	902238	F	8.16	38.43	welenshu1
425635	902220	G	428379	900226	E	426368	902248	F	8.11	38.36	yetebon1
425753	902016	E	428583	900121	C	426373	902263	F	7.94	38.69	zewaytokoshe
426003	901840	E	428608	900094	F	426387	902302	F	7.9	38.7	ziway bus stn
426415	901635	G	428710	900062	F	426393	902278	F	7.94	38.73	ziway lake
426466	901635	G	428726	900019	C	426419	902259	F	7.94	38.66	ziway2
426492	901627	G	428905	899955	C	426450	902252	F	7.94	38.65	ziway2bush
426515	901616	Q	428980	899892	C	426479	902232	F	7.94	38.65	ziwaybush2
426598	901614	C	429042	899890	C	426542	902162	G	7.95	38.63	ziwaybush3
426631	901582	C	429280	899764	G	426537	902135	G	7.99	38.63	ziwaybush5
426646	901539	C	425639	902270	G	426542	902078	G	7.98	38.63	ziwaycult1
426662	901488	C	425600	902346	F_CL	426524	902066	G	7.99	38.62	ziwaycult2

424705	903540	SH	425565	902421	F	424724	904563	G	425238	905239	D
424652	903549	G	425519	902414	F	424759	904571	G	425236	905246	D
424658	903610	B	425481	902323	F	424788	904615	G	425257	905248	D
424671	903615	G	425445	902441	F	424779	904657	G	425270	905259	B
424679	903651	G	425371	902542	F	424842	904767	G	425301	905285	B
424656	903693	E	425353	902672	G	424874	904776	E	425407	905424	G_E
424668	903732	E	425299	902737	C	424875	904794	F	425633	905536	G_E
424680	903740	E	425301	902782	E	424870	904813	F	425681	905554	G
424706	903773	F	425198	902821	E	424895	904848	G	425709	905569	G
424716	903829	G	425169	902827	F	424913	904897	G	425729	905606	G
424763	903910	E	425137	902855	F	424959	904912	C	425769	905623	G
424772	903917	E	425097	902928	C	424948	904942	C	425772	905649	F
424785	903929	E	425029	902964	F	424969	904968	F	425773	905687	F
424792	903937	E	424984	903042	F	424966	904974	F	425781	905713	F
424706	903985	F	424955	903063	F	425987	906583	E	425827	905773	F
424601	904177	E	425013	903130	F	425983	906814	D	425909	905697	F
424632	904210	F	424987	903134	F	426000	906879	D	425913	905673	F
424581	904199	E	424973	903123	F	425991	906850	D	425922	905632	E
424578	904210	E	424951	903174	F	425938	906823	D	425925	905618	E
424497	904241	G	424982	903222	C	425932	906799	D	425918	905600	E
424481	904266	G	424960	903240	F	425917	906810	D	425905	905583	E
424386	904263	E	424947	903241	F	425889	906805	D	425887	905533	E
424381	904257	E	424926	903271	F	425872	906797	D	425865	905514	E
424381	904258	E	424816	903355	E	425852	906758	G	425845	905503	C
424411	904298	F	424818	903355	SH	425860	906695	G	425859	905447	C
424375	904312	F	424799	903393	F_SH	425909	906640	F_E	425860	905414	C
424416	904317	F	424817	903419	F_SH	425911	906608	F_E	425888	905341	F_G
424476	904378	G	424824	903436	F_SH	425937	906570	F	425896	905327	F_G
424471	904405	G	424853	903430	F_SH	425921	906548	F	425898	905337	F_G
424478	904415	G	424881	903401	F_SH	425917	906418	F	425889	905339	F_G
424477	904348	Fp	424894	903401	F_SH	425919	906367	F	425863	905331	F_G
424515	904259	Fp	424906	903405	F_SH	425910	906324	F_G	425656	905115	E
424530	904295	Fp	424900	903424	F_SH	425914	906294	F	425641	905129	E
424566	904339	Fp	424889	903436	G	425914	906241	F	425631	905127	E
424587	904363	Fp	424900	903470	G	425909	906168	F_E	425670	905107	E
424593	904399	Fp	424878	903471	G	425889	906149	F	425648	905012	F
424608	904412	Fp	424845	903524	F	425929	905939	E	425588	904978	F
424626	904433	G	424838	903508	F_G	425907	905930	E	425364	904811	F
424666	904496	G	424799	903513	F_G	425918	905630	F?	425260	904666	F
424698	904551	G	424757	903530	F_G	425933	905619	F?	425256	904635	F
423155	903848	F	423516	903397	G	426278	903222	C	425261	904641	F

423384	903975	F	424208	903529	G	432075	899021	E	425279	904645	F
423486	903359	G	430956	898016	G	429653	898192	C	425291	904630	F
423520	903398	G	425807	901657	W	432439	898217	C_FP	425308	904618	F
425845	904015	D	430769	897631	D	431149	897176	T	425321	904600	F
425856	904033	D	430802	897544	D	431248	897147	T	425341	904570	G
425871	904041	D	430778	897473	D	431416	897120	T	425366	904565	G
425886	904028	D	430761	897427	D	431601	897130	T	425355	904535	G
425880	903997	D	430728	897321	D	431929	897370	T	425335	904487	C
426014	903888	F	430863	897262	T	430529	897955	T	425350	904455	C
426067	903762	F	430983	897228	T	430681	897887	T	425361	904426	C
425969	905546	F?	426138	905722	F_G	425224	905144	F_D	425325	904438	G
425997	905566	F	426151	905758	F_G	425203	905146	D	425286	904438	G
426012	905604	F	426099	905789	F_G	425183	905103	D	425277	904405	G
426033	905705	F	426080	905800	F_G	425180	905149	D	425304	904403	G
426050	905667	F	426082	905828	F_G	425124	905132	D	425347	904419	G
426091	905723	F	426104	905837	F_G	425102	905127	D	425388	904409	G
426097	905735	F	426101	905848	F_G	425083	905134	F	425432	904398	G
426130	905633	E	425996	905845	F_G	425010	905141	G	425506	904333	E
426253	905615	F	425712	905503	F_G	425025	905189	G	425522	904317	E
426301	905377	F	425673	905518	G	425110	905180	G	425536	904299	E
426238	905647	E	425662	905505	G	425125	905209	G	425554	904318	E
426220	905668	E	425653	905484	G	425139	905239	G	425703	904184	G
426211	905654	E	425627	905464	G	425165	905275	G	425723	904198	G
426160	905691	E	425234	905182	F	425206	905216	G	425736	904183	G
426124	905708	F_G	425234	905142	F	425234	905223	D	425729	904147	G

E. Appendix 5: Questionnaire

PART I. LAND MANAGEMENT AND SOIL DEGRADATION

Section A: History of the land units

1. What was the land cover of the area 30 – 40 years ago, 20 – 30 years ago & 20 years up to now respectively?

a. Forest

b. Cultivated

c. Grazing land

d. Wetland(water logged)

e. Others specify_______________________________

Section B: Soil Erosion/Sedimentation and Protection

1. Is there any soil erosion or sedimentation problem in your area? Yes ----------1, go to

2. Why didn't you take measures? ____________________.

It is costly=1; High labor demanding=2; I don't know how=3; Other reasons (specify)=4

3. Was there a similar problem 5 years ago? Yes ---1, No ---2; 10 years ago? Yes ----1, No ----2. 20 years ago? Yes----1, No---2; 30 years ago? Yes---1, No---2.

4. Do you think the problem is a result of deforestation in your village? Yes ----------1, No -------------2.

5. What do you think will happen to your farm in the next 5-10 years if you don't take protection measures?_________________.

I will loss portion of my land by erosion=1; Productivity will decrease as a result of top soil

erosion=2; Nothing more will happen=3; I don't know=4; others (specify)=5

6. Do you discuss soil erosion problems with your neighbors, local authorities, extension

agents or other community members? Yes ------------1, No ----------2.

7. Have you ever participated in any soil conservation work initiated by the above mentioned agents? Yes -----------1, No ------------2.

Dedicated

To

My extremely positive, innocent, loving, very kind, hard worker, supportive, committed, caring and best mentor

Azage Gebreyohannes Gebremariam (PhD)